TECHNISCHE UNIVERSITÄT MÜNCHEN

Lehrstuhl für Organische Chemie II

Protein target identification and characterization of photo-cross-linkable small molecules

Jürgen Franz Eirich

Vollständiger Abdruck der von der Fakultät für Chemie der Technischen Universität München zur Erlangung des akademischen Grades eines

Doktors der Naturwissenschaften

genehmigten Dissertation.

Vorsitzender:	Univ.-Prof. Dr. Johannes Buchner
Prüfer der Dissertation:	1. Univ.-Prof. Dr. Stephan A. Sieber
	2. TUM Junior Fellow Dr. Sabine Schneider

Die Dissertation wurde am 26.11.2013 bei der Technischen Universität München eingereicht und durch die Fakultät für Chemie am 08.01.2014 angenommen.

Stefan: "Sag mal, hast du nicht auch manchmal das Gefühl, du kommst hier nie weg?"
Kai: "Wieso? Ist doch nett hier."

Lammbock

Danksagung

Zunächst möchte ich mich bei Stephan Sieber für die hervorragenden Arbeitsbedingungen, das entgegengebrachte Vertrauen und die große Freiheit bei Planung und Durchführung von Experimenten bedanken, so wie die Möglichkeit ständig eigene Ideen entwickeln und umsetzen zu können.

Den Mitgliedern der Prüfungskommission danke ich für die Bemühungen bei der Bewertung meiner Arbeit.

Mein Dank gilt auch zahlreichen Kooperationspartnern, vor allem aber den Mitgliedern der FOR 1406: Danke Simone Braig, Stephan Zahler und Angelika Vollmar für interessante Gespräche und aufschlussreiche Daten aus der „biologischen Ecke“. Herzlichen Dank auch an Jens Burkhart, Judith Hoffmann (geborene Peter), Phil Servatius, Angelika Ullrich und Uli Kazmaier, die mit der Synthese vieler Verbindungen – oft auch „auf Wunsch“ – viele Experimente überhaupt erst ermöglicht haben.

Vielen Dank an Mona Wolff und Katja Bäuml, die durch das Übernehmen der vielen „Kleinigkeit“ den Laboralltag sehr viel angenehmer gemacht haben. (Es gib immer ein Gel mehr, als man bestellt hat und die Orbi ist kalibriert, auch wenn sie nicht läuft ;))

Ich danke der fast nicht zu überblickenden Zahl an Forschungspraktikantinnen (und Praktikanten) für die tatkräftige Unterstützung bei der täglichen Laborarbeit.

Ich danke allen Kolleginnen und Kollegen im Arbeitskreis für die hervorragende Atmosphäre. Besonderer Dank gilt Matt für die zahlreichen Ratschläge, die nur ein weiser, alter Mann geben kann, Philipp dafür, dass er meinen Abzug aus dem Dornröschenschlaf erweckt hat und Lena für das Stimmungsaufhellen in Labor C.

Ich danke Herrn Lehmann für diverse Duelle im Klugsch…en. Danke Wolfi – Du bist die menschgewordene IMDb ;). Danke Märri für die Schublade und die vielen, spannenden Fakten aus dem Leben einer holländischen Kartoffel. Danke Franjo und Roman für die tägliche Extradosis Bayern. Danke Johannes K. und Jan für täglich neue Grenzüberschreitungen im Bereich Humor und Max dafür, dass er den Witz dann auch erklärt. Danke Georg für den Ansporn, täglich noch eine Tasse Kaffee mehr zu trinken.

Ich danke meinen Freunden aus der „alten Heimat“ und denen von beiden Enden der U6 – „Home is, where the heart is!“ – für die zahlreichen Möglichkeiten der Zerstreuung. (Schon sonderbar, wie man vor lauter Grillen, Fußball- und Serienabenden, Boarden und Biertrinken doch noch zum Arbeiten kommt…)

Ich danke meiner Familie und Kathrin für die Unterstützung in all den Jahren…

Table Of Contents

Parts of this thesis have been published in international journals:

Chapter 1: Unraveling the protein targets of vancomycin in living *S. aureus* and *E. faecalis* cells

J. Am. Chem. Soc., 2011, 133 (31), pp 12144–12153

DOI: 10.1021/ja2039979

Chapter 2: Pretubulysin derived probes as novel tools for monitoring the microtubule network *via* Activity-Based Protein Profiling and Fluorescence Microscopy

Mol. BioSyst., 2012,8, 2067-2075

DOI: 10.1039/C2MB25144B

Zusammenfassung

Die Identifizierung und Charakterisierung von Proteinen aus komplexen Proben stellt zur Zeit eine der großen Herausforderungen der Proteomik dar. Diese Fragestellungen können in vielen verschiedenen Zusammenhängen, auch für Proteine von geringer Abundanz, untersucht werden. Funktionsweisen und die Zugehörigkeiten zu bestimmten Zellkompartimenten oder posttranslationale Modifikationen können bestimmt werden. Die Chemische Proteomik untersucht dabei neben der Interaktion mit anderen Proteinen auch Metaboliten, Kofaktoren oder wirkstoffähnliche Moleküle als potentielle Bindungspartner. Das aktivitäts- und affinitäts-basierte Protein-Profiling stellt für diese Untersuchungen passende Verbindungen als Werkzeuge zur Verfügung.

In dieser Arbeit sollen die Proteinbindepartner kleiner Moleküle unterschiedlicher Herkunft identifiziert werden. Um einen möglichst aufschlussreichen Eindruck über biologisch relevante Interaktionen zu erhalten, wurden die Versuche in lebenden Zellen durchgeführt. Da die Ursprungssubstanzen keine intrinsische Fähigkeit besitzen, selbst kovalent mit Proteinen zu reagieren, wurden sie semisynthetisch mit einem Photoquervernetzer und einer bio-orthogonalen Reportergruppe modifiziert oder es wurden Sonden totalsynthetisch aufgebaut. Quervernetzer und Reporter wurden dabei so eingeführt, dass nur minimale Veränderungen am Grundgerüst der Ausgangsverbindungen vorgenommen wurden.

Das Glycopeptid-Antibiotikum Vancomycin bindet das D-Ala-D-Ala-Motiv der bakteriellen Zellwand. Aus diesem Naturstoff wurden Photosonden hergestellt und benutzt um deren Bindung an Proteine in lebenden Bakterien zu untersuchen. Die Interaktion des Antibiotikums mit einem potentiellen Ziel wurde in einem *in vitro* Enzymassay bestätigt.

Pretubulysin ist ein höchst zytotoxischer Sekundärmetabolit, der aus Myxobakterien isoliert werden kann. Es wurden Photosonden synthetisiert, die auf diesem potenten Naturstoff basieren. Dazu wurde eine bereits etablierte Totalsynthese mit entsprechend funktionalisierten Vorstufen durchgeführt. Mit den so generierten Sonden war es möglich, Tubulin als Zielstruktur der Ursprungsverbindung im komplexen Proteom lebender Zellen durch Massenspektrometrie und Fluoreszenzmikroskopie zu verifizieren. Für beide Techniken konnte die gleiche Sonde verwendet werden.

In einem *screening* wurde eine neue, potente Stoffklasse „T8-01 – T8-20“ zur Chemosensibilisierung von Krebszellen gefunden. Um deren molekularen Wirkmechanismus aufzuklären, wurde basierend auf ihrem gemeinsamen Strukturmotiv eine Photosonde entwickelt. Sie sollte den zu Beginn gefundenen Verbindungen möglichst nahe kommen. Die Interaktion dieser neuen Substanzklasse mit ihrem Zielprotein wurde *in vitro* untersucht.

Die Proteinziele verschiedener Sonden konnten in intakten humanen und bakteriellen Zellen markiert und per Massenspektrometrie identifiziert werden. Diese Treffer wurden durch die Markierung der isolierten Proteine verifiziert werden. Die Interaktionen wurden eingehend untersucht und die Inhibition der Ziele konnte in spezifischen *in vitro* Funktionsstudien gezeigt werden.

Summary

The identification and characterization of proteins in complex samples is the major question in current proteomics. These issues can be addressed in many different contexts. Functions and sub cellular locations or post-translational modifications of proteins can be determined. Besides the interactions with other proteins, the field of chemical proteomics studies also metabolites, co-factors or drug like molecules as potential binding partners. Activity and affinity-based protein profiling provide a suitable tool box for these investigations.

In this thesis the protein targets of small molecules from different origins were identified. To draw the most conclusive picture of biologically relevant interactions these studies were conducted in intact living cells. All parental compounds had no intrinsic ability to bind covalently to proteins. Therefore either the mother compounds were modified semi-synthetically with a photo-cross-linker and a bio-orthogonal reporter tag or the probe molecules were build up by total synthesis. The cross-linker and the reporter were integrated with only minor changes to the original scaffold.

The glycopeptide antibiotic vancomycin is described to bind the D-Ala-D-Ala motif of bacterial cell walls. Photo probes were derived from this compound and used to study protein targets in living bacteria. The interaction of the antibiotic and one of its potential targets was confirmed in an *in vitro* enzymatic assay and could be related to a phenotype yielding from a genetic knock out of the target enzyme.

Pretubulysin is a highly cytotoxic secondary metabolite originating from myxobacteria. Photo probes based on this potent natural product were synthesized. Modified precursors were fed into the already existing total synthesis strategy. It was possible to verify tubulin as a target of the small molecule in the complex proteome of living cells by a mass spectrometry-based approach and by fluorescent microscopy. The same probe could be used in both techniques.

The T8 family represents a potent structural scaffold for new chemo sensitizing compounds. A photo probe derived from these molecules was designed to investigate their molecular mode of action. The probe should mimic the initial screening hits as close as possible. The interaction of this newly discovered compound class with their protein target was investigated *in vitro*. Further studies can be conducted to investigate this interaction *in vivo*.

The protein targets of different probes could be labeled in intact human or bacterial cells and be identified by mass spectrometry. The hits could be verified by the labeling of the isolated proteins. These interactions were further characterized and the inhibition of the targets could be shown in specific *in vitro* studies such as functional assays.

Abbreviations

%	percent
°C	degree celcius
Å	Ångström, 10^{-10} m
ABC	ATP binding cassette
ABP	Activity-Based Probe
ABPP	Activity-Based Protein Profiling
AfBP	Affinity-Based Probe
AfBPP	Affinity-Based Protein Profiling
Ac	acetyl
Ala	alanine
Amp	ampicillin
APS	ammonium persulfate
Atl	autolysin
ATP	adenosine triphosphate
att	*attachment*
Bcl2	B-cell lymphoma 2
BH3	Bcl-2 Homology domain 3
BHB	brain heart infusion broth
bp	base pairs
BP	benzophenone
Boc	di-tert-butyl dicarbonate
BSA	bovine serum albumin
Cbz	carboxybenzyl
CC	click chemistry
C_q	quantification cycle
CuAAc	Copper-catalyzed Alkyne Azide Cycloadditions
Da	Dalton
DCM	Dichloromethane
DIC	*N*,*N*'-diisopropylcarbodiimide
DIPEA	*N*,*N*-diisopropylethylamine
DMAP	4-(dimethylamino)-pyridine
DMEM	Dulbecco's Modified Eagle Medium
DMF	dimethylformamid
DMSO	dimethylsulfoxide
DNA	deoxyribonucleic acid
DOC	deoxycholate
Dpg	3,5-dihydroxyphenylglycine
EC_{50}	half maximal effective concentration
EDTA	ethylendiaminetetraacetate
ER	endoplasmic reticulum
ESI	electrospray ionisation
et al.	*et alii*
EtBr	ethidium bromide
EtOAc	ethylacetate

FBS	fetal calf serum
FCS	fetal bovine serum
fd	*functional domain*
fl	full length
fwd	forward
g	gram
g	gravity of Earth
Glu	glutamate
Glu*N*Ac	*N*-acetylglucosamine
Gly	glycine
GRP	Glucose Regulated Protein
h	hour(s)
HBTU	O-benzotriazole-*N*,*N*,*N*',*N*'-tetramethyluroniumhexafluorophosphate
HeLa	"Henrietta Lacks"
His	histidine
HOBt	hydroxybenzotriazole
Hpg	4-hydroxyphenylglycine
HPLC	high-performance liquid chromatography
HR	high resolution
Hz	Hertz, s^{-1}
hν	Planck constant x phase speed
IAP	Inhibitor of Apoptosis Protein
IC_{50}	half maximal inhibitory concentration
ICAT	Isotope-Coded Affinity Tags
IHF	Integration Host Factor
iHex	iso-hexane
Ile	isoleucine
iPr	iso-Propyl
iTRAQ	isobaric Tags for Relative and Absolute Quantification
k	Kilo, 10^3
Kan	kanamycin
k_{cat}	rate constant
K_I	dissociation constant
K_M	Michaelis constant
L	liter
Lac	lactate
LB	*lysogeny broth*
LC	liquid chromatography
LR	low resolution
Lys	lysine
M	molar
MDA-MB	M.D. Anderson - metastatic breast
Mep	*N*-methylpipecolic acid
mg	milligram
Mhz	megahertz
MIC	minimal inhibitory concentration
min	minute(s)

mL	milliliter
mM	millimolar
mmol	millimol
MRSA	methicillin-resistent *Staphyloccus aureus*
MS	mass spectrometry
mTRAQ	mass differential Tags for Relative and Absolute Quantification
MTT	3-(4,5-dimethylthiazol-2-yl)-2,5-diphenyltetrazolium bromide
MurNAc	*N*-acetylmuramine acid
NHS	*N*-hydroxysuccinimide
nm	nanometer
NMR	nuclear magnetic resonance
NP	nonyl phenoxypolyethoxylethanol
OD	optical density
OPFP	O-pentafluorophenyl ester
p	Pico, 10^{-12}
PAGE	polyacrylamide gel electrophoresis
pB-Phe	p-benzoyl-phenylalanine
pB-Tup	p-benzoyl-tubuphenylalanine
PBP	Penicillin-binding protein
PBS	phosphate buffered saline
PCR	polymerase chain reaction
PDI	Protein Disulfide Isomerase
PG	peptidoglycan
pH	*Potentia Hydrogenii*
ppm	parts per million
PT	pretubulysin
PyBOP	benzotriazole-1-yl-oxy-tripyrrolidinophosphoniumhexafluorophosphate
rev	reverse
R_f	retention factor
RhN_3	rhodamin azide
RNA	ribonucleic acid
rpm	rounds per minute
RPMI	Roswell Park Memorial Institute medium
RT	retention time
SAR	structure activity relationship
SDS	sodium dodecylsulfate
SILAC	Stable-Isotope Labeling by Amino acids in Cell culture
SPAAC	Strain Promoted Alkyne Azide Cycloaddition
TAE	Tris, acetate, EDTA
TBTA	Tris[1-benzyl-1H-1,2,3-triazol-4-yl)-methyl]amine
tBu	tertiary butyl-
TCEP	tris(2-carboxyethyl)phosphine
TEA	triethylamine
tert	tertiary butyl-
TFA	trifluoracetic acid
TLC	thin layer chromatography

T_M	melting temperature
TMT	Tandem Mass Tags
Tup	tubuphenylalanine
Tut	tubutyrosine
Tuv	tubuvaline
UDP	uraciltriphosphate
UPR	Unfolded Protein Response
UV	ultra violett
VRE	vancomycin-resistent enterococci
VRSA	vancomycin-resistent *Staphylococcus aureus*
XIAP	X-linked Inhibitor of Apoptosis Protein
µL	mikroliter
µM	mikromolar

Introduction: Chemical Proteomics

Proteomics

The identification and characterization of proteins in complex samples is the major question in current proteomics. These issues can be addressed in many different contexts and are even more challenging when the proteins of interest are of low abundance. Either whole or sub proteomes can be examined, functions and sub cellular locations can be assigned or posttranslational modifications and interaction partners of proteins can be determined.[1-5] Besides the interactions with other proteins, that can also be metabolites, cofactors, or drug like molecule. These studies are part of the field of chemical proteomics.[6-9] A conceptual workflow is depicted in Scheme 1. To successfully isolate proteins from biological samples by small molecule interactions it is crucial to keep the proteins in their native, functional state. As some of them do not tolerate the transfer from their cellular context to lysates, it is an ongoing challenge to reveal physiologically relevant small molecule–protein interactions. Nevertheless, the vast majority of chemical proteomics studies is conducted in lysates.[10-13]

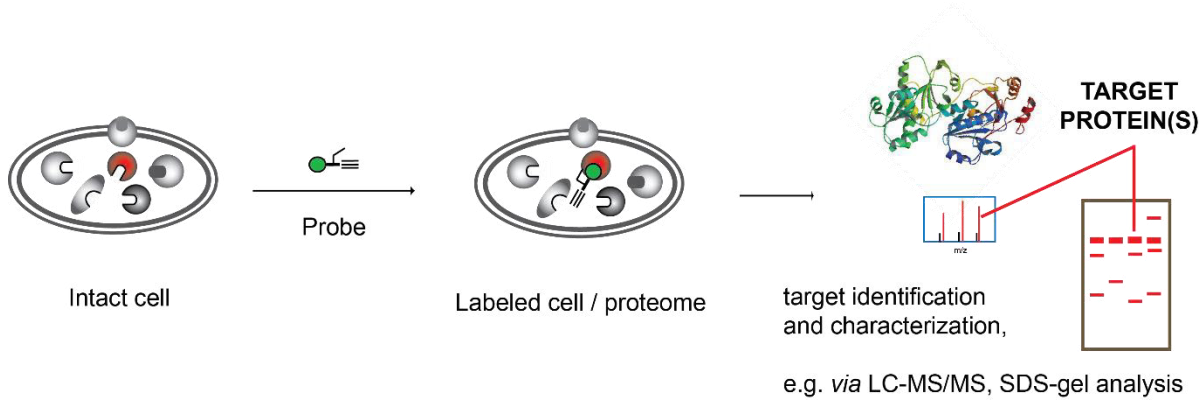

Scheme 1: Conceptual representation of a chemical proteomics workflow for target identification and characterization. (LC: Liquid Chromatography, MS: Mass Spectrometry, SDS: Sodium Dodecyl Sulfate) Exemplary crystal structure of protein disulfide isomerase (4EL1). [14]

For these affinity pull down strategies probes with distinct functionalities are required. A selectivity function that facilitates the equilibrium-driven affinity interaction with the target proteins and a sorting function or a direct linkage to a solid support are needed.[15] The Interactions between the immobilized bait and its prey are non-covalent and therefore reversible. This affects the actual protein isolation procedure with respect to buffer conditions and washing stringency, influencing the background caused by unspecific protein binding. These parameters must be adjusted carefully as low-affinity interactions between small molecules and their target proteins may be hard to detect with this

method. Virtually any structural element can be used as selectivity function when the connection point to the resin is chosen with sensible respect to the binding characteristics.

Activity- and affinity-based protein profiling

Activity-Based Protein Profiling (ABPP) has developed as a powerful methodology in the context of chemical proteomics and provides a big tool box to investigate the cellular localization and activity of proteins in space and time by the use of irreversibly binding small molecules.[16-19] These Activity-Based Probes (ABPs) can be of various origins and are often derived from enzyme substrates or mechanism-based (suicide) inhibitors.[20-24]

These molecules show diverse structures and can represent compounds like synthetic cofactor or substrate analogs.[25] As a consequence various processes such as methylation[26,27], palmitoylation[28], acetylation[29], glycosylation[30], phosphorylation[31,32], or farnesylation[33,34] and a broad spectrum of enzyme classes can be addressed.[35-44] In ABPP experiments the comparison of the expression or activity of a certain enzyme (class) in different cell lines and tissues is also possible even in a quantitative manner.[45,46]

An ABPP probe can be dissected into three moieties as depicted in Scheme 2: The small molecule has an entity that is responsible for its selectivity towards the protein binding partner. In addition there is a reactive unit needed for covalent binding of probe and protein. As a third part an analytical handle or reporter tag is needed. A clear structure–activity relation has to be known or made up for the small molecule probe to make sure that the attachment of additional functionalities does not perturb the original interactions of the compound and its targets.

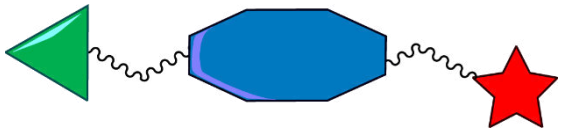

reactive moiety	selectivity group	reporter tag
fluororphosphonate, lactone, *Michael*-acceptor	natural product, cofactor, substrate	dye, biotin, alkine, azide

Scheme 2: Schematic representation of a small molecule probe for ABPP and examples for the included structural elements.

Classic ABPs are capable of direct reaction in a covalent manner with amino acids of the active site of enzymes.[15,47,48] The compounds are potent electrophiles and often derived from known inhibitors of

enzymes or enzyme classes. The covalent linkage of small molecule and protein is achieved in intact, living cells and also facilitates harsher conditions in downstream applications.

Capture compounds or Affinity Based Probes (AfBPs) are related to activity-based probes but lack an intrinsic reactivity that can form a covalent bond with proteins. A different mode of linkage is therefore facilitated:[49] Photo affinity ligands in general have evolved as valuable compounds in the field of chemical biology for many years.[50] Various applications in drug discovery and drug development have been shown.[51,52] These compounds can provide valuable insights into the structure and function of biological macromolecules as they can be derived from or mimic ligands of receptors or substrates of enzymes. Target identification of biologically active compounds, the determination of the selectivity and affinity of ligand–target complexes, or the three-dimensional mapping of ligand binding sites are possible applications.[53] To create a photo affinity probe, a non-covalent binding moiety is equipped with a photo reactive group. This can be either attached to an existing molecule *via* semi-synthesis or integrated into the underlying scaffold by building up the photo probe from scratch.

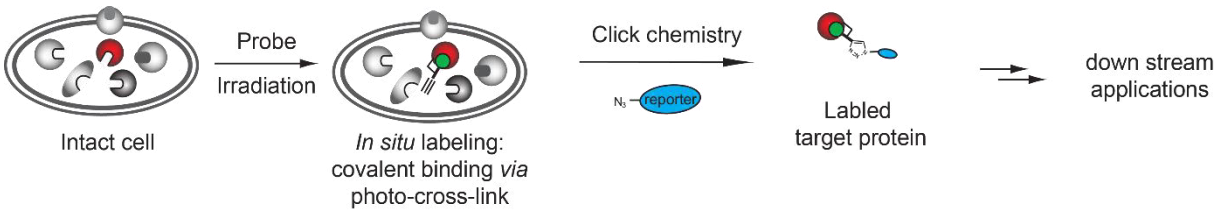

Scheme 3: Schematic work flow for in situ *labeling with an affinity-based photo probe in intact cells.*

When delivered to cells the probes first accomplish a non-covalent, affinity-mediated binding with their target proteins *in situ* as shown in Scheme 3. In a second step, the binding partners are trapped *via* a covalent bond formation between the probe and its binding parterns through the reactivity function by a photo-activated cross-link. This enables the detection of weak, but still specific interactions. Almost any small molecule can be used as selectivity function. The proteins are isolated on the basis of their affinities to this unit and independent of their abundance in the original biological sample.[54] Different photo reactive affinity-based probes have been used to study multiple enzyme classes including metalloproteases,[35-38] galectins,[39-41] histone deacetylases,[42,43] and methionine amino-peptidases[44]. In AfBPP experiments, the cross-linking yields can strongly vary.[49,55,56]

The reporter functions used for the identification and isolation of the targeted proteins in chemical biology have undergone significant advances within the past decades, due to the use of several bio-orthogonal reactions and ligation techniques.[23,42,57,58] To investigate the small molecule–protein

interactions in intact cells, probes have to be membrane-permeable. This goal is achieved by the use of molecules containing a small functional group, such as an alkyne or azide moiety. These functional groups hardly react with functionalities present in the biological system. However they enable a chemical ligation later on in the workflow. The actual analytical handle can be attached to the probe after the target recognition and covalent binding which is either facilitated by the intrinsic reactivity of the probe or a (photo) cross-linking reaction.[59-64]

The commonly used photo-cross-linkers as well as tags and ligation strategies are discussed in detail in later chapters (pages 5-8).

The identification of a specific biological target can give insight into the proteome of a living cell or even represent a suitable starting point for the better understanding of a certain disease and an entry for drug development.[65-68]

To gain even deeper insight into the proteome, to make quantitative statements and to determine binding constants[69,70], workflows in chemical proteomics can be extended with quantitative mass spectrometry (MS) techniques[71-77] such as Stable-Isotope Labeling by Amino acids in Cell culture (SILAC)[78-81] or dimethyl labeling[82-86], that are based on different isotopic labels.

Quantitative mass spectrometry in target fishing

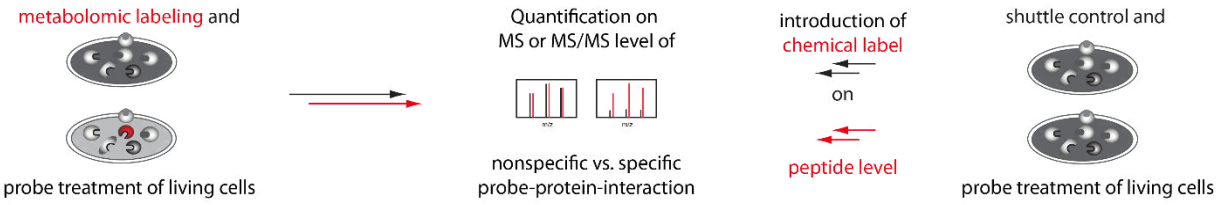

Scheme 4: Illustration of introduction and application of isotope labels and quantitative MS to enhance target identification.

Quantitative MS techniques can be divided into two main groups with respect to the way these labels are incorporated into proteins or peptides: metabolic and chemical labeling strategies (Scheme 4).[87-90]

Metabolic labeling is usually achieved by SILAC.[78-80] This approach can be used to address a variety of questions, not only protein expression analysis in general[91-95], but also the assignment of drug targets[81] or the quantification of protein phosphorylation in different stages of the cell cycle[96,97]. Metabolic labeling exhibits the advantage that samples of different states can be pooled early in the workflow. Quantification errors due to sample handling can be reduced by this measure. The technique is widely used in cell lines.[98,99] It can be employed to label whole organisms[100-102], in a limited way by spiking a

reference as internal standard to tissue samples[103,104] and was recently shown to work with bacteria as well.[105,106]

A broad variety of chemical labeling strategies is known. They can be further dissected into isobaric and isotopic labels.[107-111]

For target identification, Isotope-Coded Affinity Tags (ICAT)[112] couple active and inactive compounds (as controls) to beads.[113] Isobaric Tags for Relative and Absolute Quantification (iTRAQ)[114] were used for a variety of applications including the profiling of kinases.[10] Variations of these chemical labeling strategies were described, such as mass differential Tags for Relative and Absolute Quantification (mTRAQ)[109], Tandem Mass Tags (TMT)[115] and stable isotope dimethyl labeling[82-86].

In general, these chemical labeling strategies can be applied to a wider range of sample types. A drawback lies in the fact that the labels are mainly introduced on the peptide level. The quantification is based on modifications that are integrated later in the proteomic workflow what makes them prone to more variations and less accuracy.[116]

The actual quantification *via* MS can occur on different stages: SILAC and dimethyl labels are quantified at the MS level by comparing the ion intensities of the shifted peptide multiplets. Isobaric chemical labels utilize the MS^2 (or MS^3) level for quantification.

Chemistry

Some of the proteomic approaches described before rely on a profound knowledge of chemical reactions they take advantage of.

Photo reactive groups

Aliphatic[117] and aromatic diazirines[118-121], benzophenones[122] and aromatic (tetrafluoro) azides[123] have been widely used as photo reactive groups for different applications. Upon irradiation with UV light a highly reactive intermediate, a carbene, a diradical, or a nitrene respectively, is formed as shown in Scheme 5 on page 6. This intermediate then can form a covalent bond between the target protein and the ligand-derived photo probe. The point of attachment depends on the functional group used as cross-linker.

Each of these groups possesses distinct properties yielding in certain advantages and disadvantages when used as cross-linker for proteomic studies.[65,124,125]

Unsubstituted aryl azides have their maximum absorption at a wavelength below 300 nm. Irradiation with UVB light (280 – 315 nm) can result in substantial damage to the biological system. They are rather

prone to side reactions. Nitro-substituted derivatives can be irradiated with light of longer wavelength (350 nm). That leaves the biological system untouched. The motif is relatively small and can be easily prepared and incorporated into the ligand of choice.[123,126]

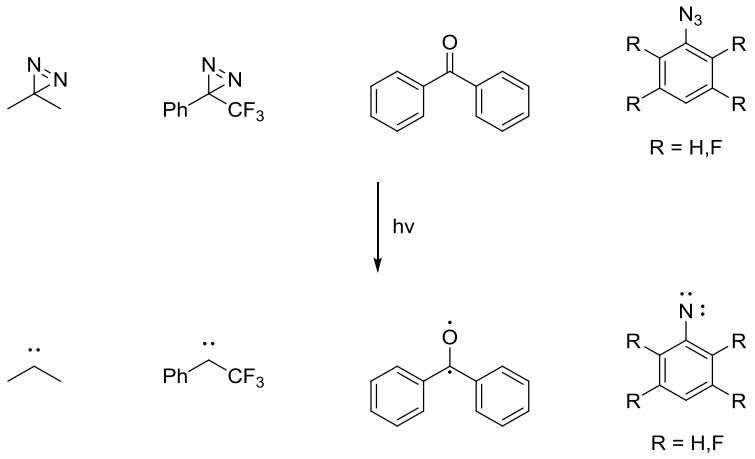

Scheme 5: Structures of cross-linkers and corresponding reactive species obtained after UV irradiation (hv).

Diazirines absorb most efficiently at 350 – 380 nm. During irradiation at this range of the light spectrum no significant damage to the biological system is expected. These compounds are stable to a wide range of chemical conditions but their longer synthesis can be a drawback. The intermediates formed up on irradiation are prone to rearrangements.[127-130]

Benzophenones are excited at 350 – 360 nm. The actual photo activation is reversible. This leads to a high cross-linking yield. The functional group is bulky and hydrophobic but it is commercially available as a broad variety of differentially functionalized building blocks.[131,132]

Reporter tags Reporter groups, such as radioactive isotopes (e.g., ^{125}I, ^{3}H), biotin, different epitope (or affinity) tags (e.g., His_6, FLAG), or fluorophores used to be incorporated directly into the structure of probes. They show different properties: Radioactive tags are advantageous as they are small in size and can easily be detected with high sensitivity. However, they require special handling and can undergo fast degradation. Biotin allows easy enrichment and isolation of the labeled target but is in competition with the naturally occurring biotinylation of other proteins. Peptidic tags and fluorophores facilitate an easy detection of the tagged proteins. They can be relatively large in size, and may negatively affect the biological activity by sterically disrupting key interactions between the probe and its target(s). These tags can cause cell impermeability of the small molecule due to the introduction of features like a charge.[133]

To address those disadvantages a variety of strategies has emerged to minimize the effect of the reporter moiety on binding and reactivity properties of a probe. Therefore either a terminal alkyne or an aliphatic azide as a clickable handle can be used. Bio-orthogonal reactions discussed in the following chapter[134-141] are then used to attach a functionalized tag of choice selectively to the biomolecule labeled by the probe.

These chemically modifiable reporter tags have a reduced influence on the ligand-protein interaction as they are relatively small in comparison to most of the groups mentioned before. They are easy to install and hardly react with biomolecules on their own. A variety of poly-functional reporters can be introduced, using these handles.

Bio-orthogonal ligation reactions

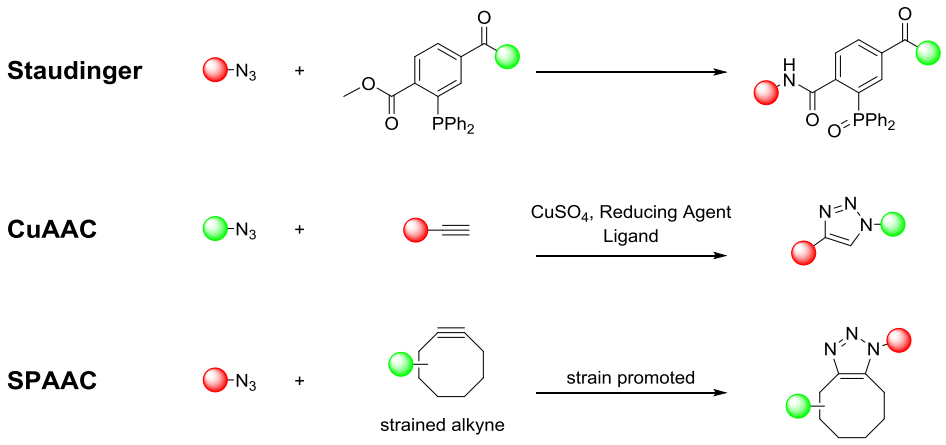

Scheme 6: Schematic representation of selected bio-orthogonal conjugation reactions, preferred functionalization of probe/protein (red dot) and of reporter (green dot) indicated.

The attachment of molecular modifications onto proteins for various applications is a central challenge in chemical proteomics. A lot of bio-orthogonal ligation reactions have been established in the recent years to address this issue. The most commonly used ones are summarized in Scheme 6. These reactions have to proceed with high selectivity in a complex mixture containing a vast number of different functionalities. A high degree of robustness combined with elevated yields and mild reaction conditions are favorable.

The *Staudinger* ligation[142] relies on an azide–phosphine conjugation and was shown to have numerous applications in chemical biology.[134,143-145]

The *Huisgen* 1,3-dipolar cycloaddition either copper catalyzed[135-141] or in other variants is widely used for a broad spectrum of studies.[146,147] The conversion of an alkyne and an azide to the correspondingly

substituted 1,2,3-triazole proceeds rapidly with high chemoselectivity and reliability. Drawbacks of Copper-catalyzed Alkyne Azide Cycloadditions (CuAAC) are the toxicity and denaturing effects of the copper(I) species needed as catalyst.[148] To address this issue and to increase biocompatibility customized Cu-chelating ligands were developed. Highly water-soluble *tris*-(triazolyl-methyl)amines enhance the rate of the cycloaddition and thereby the working concentration of copper(I) can be lowered.[140,149-154] The labeling of surface exposed azide functionalized sugars on live cells is one of the examples for the use of these tuned ligands.[150,155] Another concept to solve the problem arising from the toxicity of copper is to increase the local concentration of the metal at the reaction site *via* its coordination by a chelating substrate.[156] A copper-free, biocompatible azide–alkyne addition can be achieved by the use of strained alkyne substrates based on cyclooctyne scaffolds (SPAAC: Strain Promoted Alkyne Azide Cycloaddition).[147,157-164]

Inverse *Diels–Alder* ([4+2] D.A.) reactions of tetrazines and strained alkynes or alkenes as shown in Scheme 7 display both bioorthogonality and high reaction rates. They proceed without the need of any catalyst with only nitrogen as a side product. Only few applications in bioorganic chemistry have been published so far. Major drawbacks of these cycloaddition reactions are the limited synthetic availability and relatively large size of the reactive groups, e.g. in comparison to the established alkyne–azide systems.[165-170]

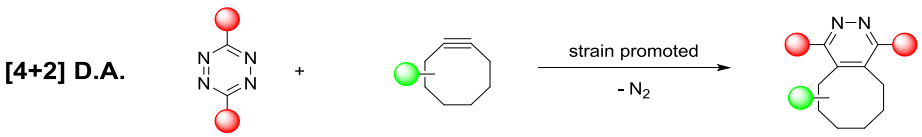

Scheme 7: Diels-Alder *conjugation reaction.*

Aim of this Thesis

The aim of this thesis was to identify the protein targets of small molecules from different origins. To draw the most conclusive picture the labeling studies were conducted in intact living cells wherever possible. All parental compounds used had no intrinsic ability to bind covalently to proteins. Therefore either the original compounds were modified semi-synthetically with a photo-cross-linker and a reporter tag or the probe molecules were build up by total synthesis. The interaction of probe and target was studied in detail.

The glycopeptide antibiotic vancomycin is described to bind the D-Ala-D-Ala motif of bacterial cell walls. Three photo probes were derived from this compound and used to study its protein targets in living bacteria. Pretubulysin is a highly cytotoxic secondary metabolite originating from myxobacteria. Photo probes based on this potent natural product were synthesized by and used to confirm tubulin as their cellular target. The T8 family represents a potent structural scaffold for chemo sensitizing compounds. A photo probe derived from these molecules was designed to investigate their molecular mode of action. The interaction of this newly discovered compound class with their protein target was investigated *in vitro*.

Chapter 1: Unraveling the protein targets of vancomycin in living *S. aureus* and *E. faecalis* cells

Jürgen Eirich, Ronald Orth, and Stephan A. Sieber

Published in

J. Am. Chem. Soc., 2011, 133 (31), pp 12144–12153

DOI: 10.1021/ja2039979

Publication Date (Web): July 7, 2011

Abstract Vancomycin is a potent glycolpeptide antibiotic that has evolved to specifically bind to the D-Ala-D-Ala dipeptide termini of nascent peptidoglycan. Although this mode of action is well established, several studies indicate that vancomycin and analogues exploit non-canonical target sites. In order to address all vancomycin targets in clinically relevant *S. aureus* and *E. faecalis* strains we developed a series of small molecule photoaffinity probes based on vancomycin. Proteomic profiling revealed the specific labeling of two previously unknown vancomycin targets that are likely to contribute to its antibiotic activity. The specific inhibition of the major staphylococcal autolysin Atl confirms previous observations that vancomycin alters *S. aureus* cell morphology by interaction with the autolytic machinery. Moreover, in *E. faecalis* the vancomycin photoprobe specifically binds to an ABC transporter protein, which likely impedes the uptake of essential nutrients such as sugars and peptides. The labeling of these two prominent membrane targets in living cells reveals a so far unexplored mode of vancomycin binding and inhibition that could allow a rational design of variants with improved activity.

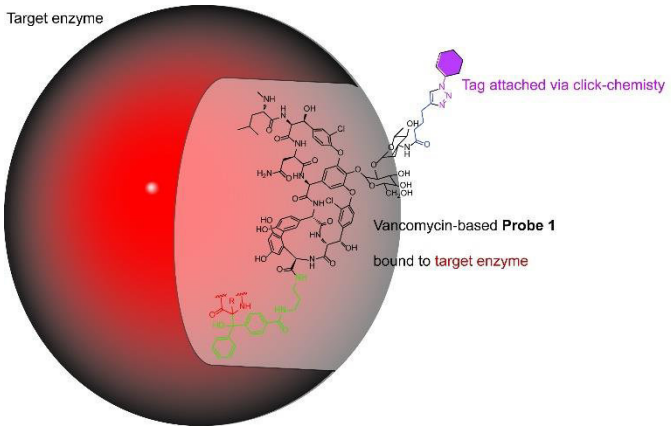

Introduction Vancomycin is a potent glycopeptide antibiotic that specifically binds to the D-Ala-D-Ala dipeptide termini of nascent peptidoglycan. The molecule forms a series of hydrogen bonds with the peptide backbone that block its further processing by penicillin binding proteins (PBPs) and thus the final steps of peptidoglycan and cell wall biosynthesis.[171-173] Although vancomycin was kept as an antibiotic of last resort, resistances to this unique mechanism of action have been observed which currently limit its application as a drug to treat serious methicillin-resistant Gram-positive infections. One prominent form of resistance, observed in enterococcal strains, redesigns cell wall biosynthesis to incorporate D-Ala-D-Lac (lactate) depsipeptide termini which significantly reduces vancomycin binding due to a lack of a crucial hydrogen bond.[171] Multiresistant *S. aureus* (MRSA e.g. Mu50 strain) have also

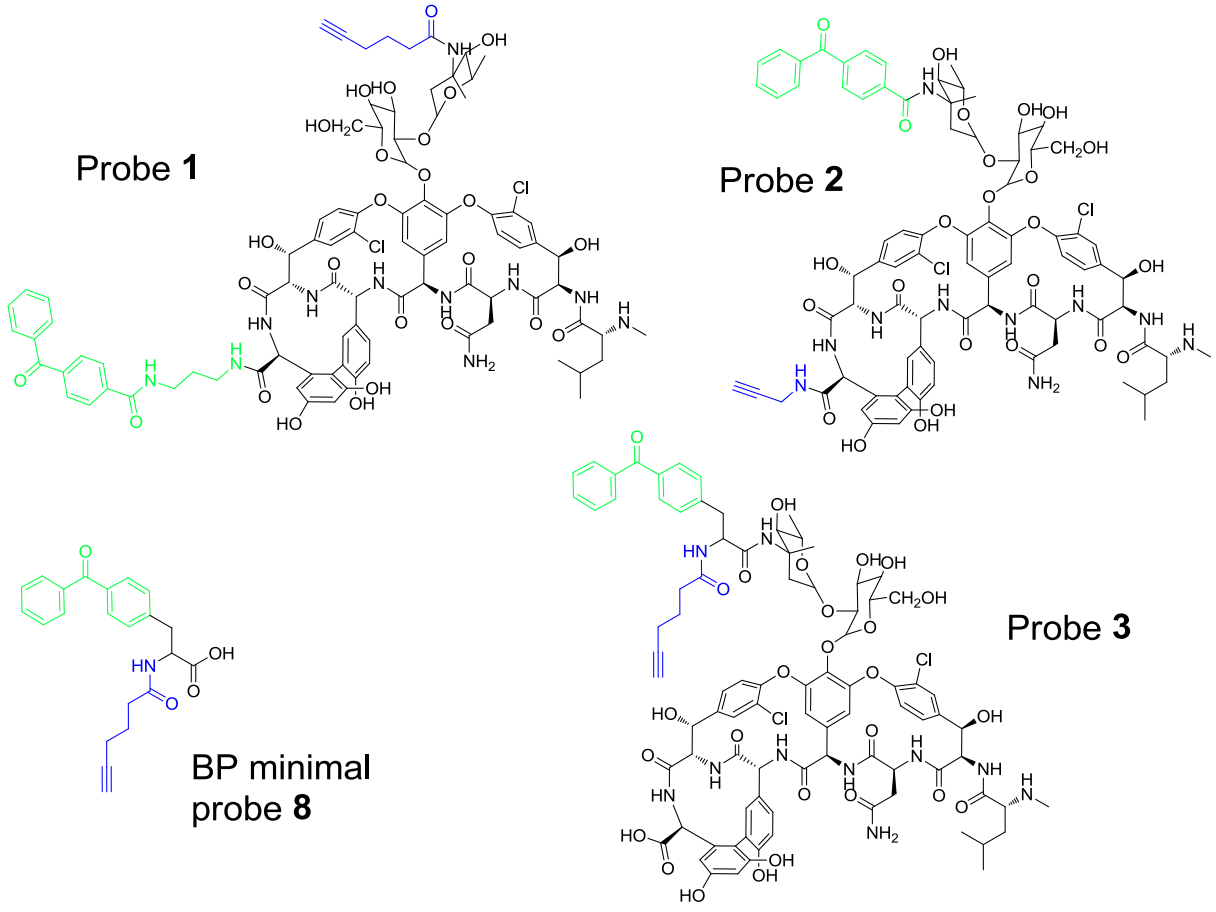

*Figure 1: Structures of vancomycin derived probes **1** - **3** and a benzophenone minimal probe (BP) carrying the photocrosslinker (green) and the alkyne handle (blue) on different positions.*

been reported to display reduced susceptibilities to vancomycin.[174,175] One important feature of these cells is a thickened cell wall that is rich in muropeptide components which retain intact D-Ala-D-Ala binding sites and therefore sequester substantial amounts of vancomycin distant to the cell wall

biosynthesis site.[174-179] The binding to muropeptides further leads to an inhibition of the *S. aureus* autolytic system by blocking the access of staphylococcal hydrolases to the cell wall substrate that is relevant for cell wall turnover, cell division and cell separation.[175,177,180] Vancomycin-treated *S. aureus* cells therefore display a lack of daughter cell separation leading to multicellular clusters. In addition, several other modes of vancomycin or vancomycin analogue action have been reported indicating that the complex structure of this compound class is suitable to interact with other targets than just D-Ala-D-Ala dipeptides. Studies by *Kahne et al.* revealed the transglycosylase domain of PBP1b as a specific binding site for a chlorobiphenyl-subsituted vancomycin derivative that leads to inhibition of transglycosylation and therefore exerts a potent antibiotic effect even against vancomycin resistant enterococcal strains (VRE).[181] Affinity chromatography further verified the direct interaction of immobilized vancomycin derivatives with this enzyme and other enzymes in cell lysates.[181,182] Moreover, recent investigations with biotinylated vancomycin photoprobes indicate that vancomycin binds to VanSsc kinase and induces the expression of resistance genes in *E. faecalis*.[183] Although this study was carried out in *E. coli* lysates and not in VRE the labeling of the whole proteome indicated the specific interaction with several other proteins that remained unexplored.

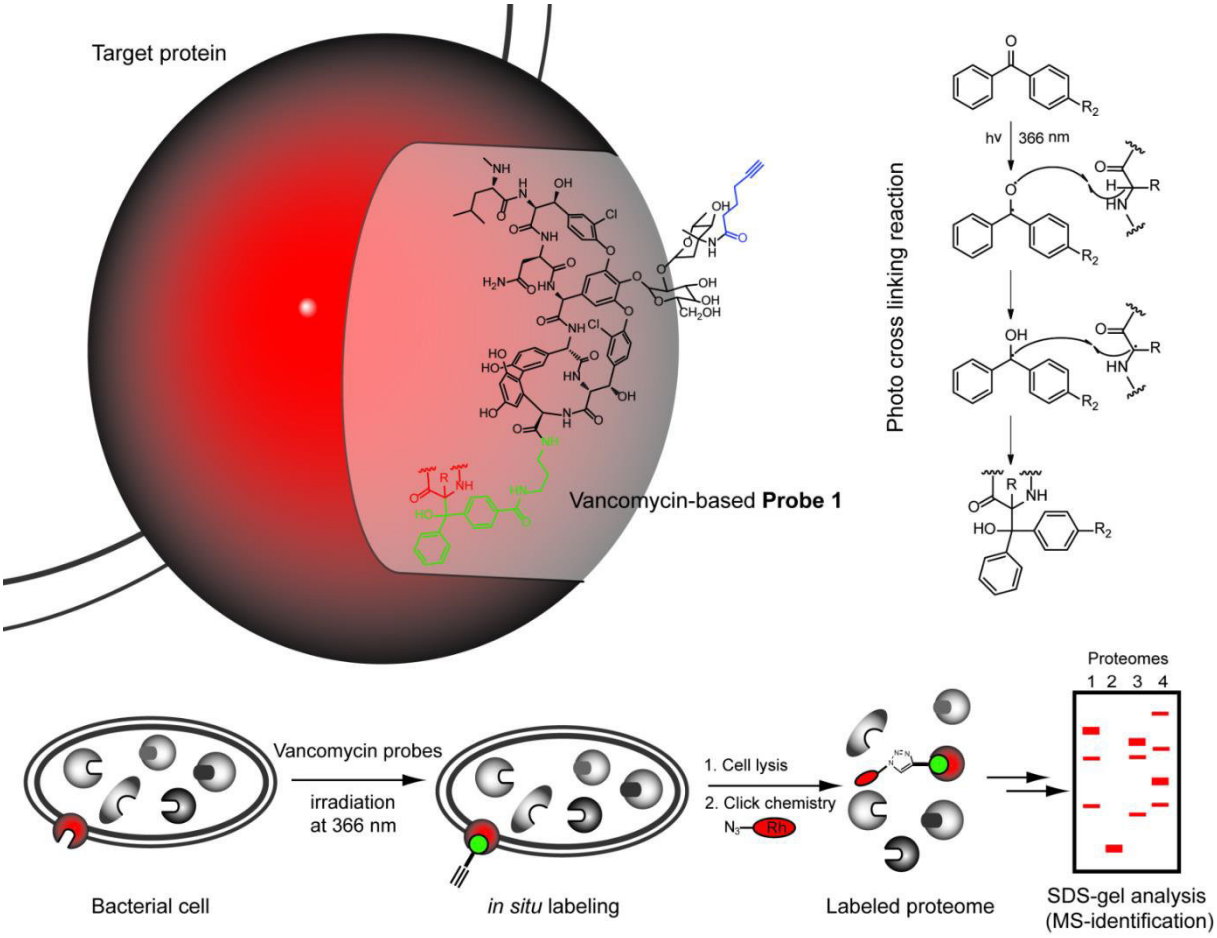

Figure 2: The vancomycin-derived probes are covalently attached to the amino acid backbone of their target proteins via *a benzophenone moiety as a photo activatable crosslinker. The alkyne group of the probes allows the identification of labeled enzymes by the introduction of a fluorescent tag via click chemistry after cell lysis and SDS-gel electrophoresis.*

Although useful for the evaluation of compound selectivity, profiling of cell lysates can cause artificial labeling effects due to induced protein degradation and corresponding changes in enzyme activities as well as the unrestricted access of molecules to cytosolic proteins.[184-186] We here introduce a novel generation of vancomycin photoprobes that are capable of labeling protein targets in living bacterial cells that are crucial for vancomycin activity.

The *in situ* profiling of *S. aureus* (SA), methicillin resistant *S. aureus* (MRSA), vancomycin susceptible *E. faecalis* (VSE) as well as vancomycin resistant *E. faecalis* (VRE) reveals the specific labeling of two previously unknown vancomycin targets that are likely to contribute to its antibacterial activity. In *S. aureus*, the inhibition of the major staphylococcal autolysin Atl confirms previous observations that vancomycin alters *S. aureus* cell morphology.[175,176,180] We here demonstrate that this is not solely done by blocking the access of autolysin to their sequestered peptidoglycan substrate but rather by a direct inhibition of the Atl activity. Moreover, in VSE and VRE vancomycin specifically binds to an ABC transporter protein, which likely impedes the uptake of essential nutrients such as sugars and peptides. The labeling of these two prominent membrane targets in living cells reveals a so far unexplored mode of vancomycin binding and inhibition that could allow a rational design of variants with improved activity.

Results and Discussion

The design of vancomycin-based affinity probes has to fulfill several prerequisites: Firstly, we required a synthetic strategy that introduces modifications at easy entry points such as the *C*-terminal carboxylic acid as well as the free amine of the vancosamine sugar. Secondly, the corresponding probes should be detached from any bulky marker that would affect its interaction with targets during life cell labeling.[187-189] We therefore designed and synthesized three

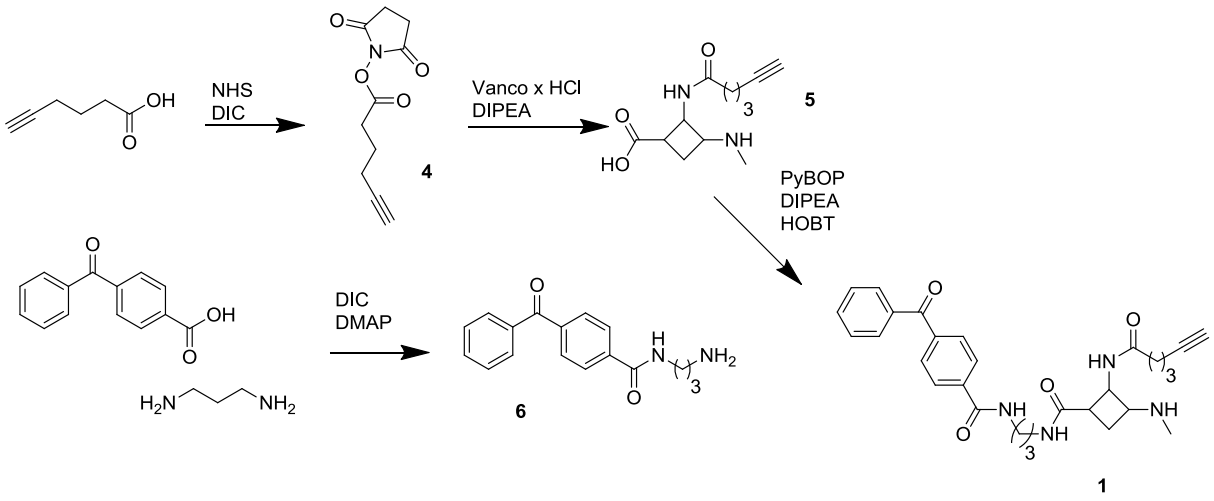

*Scheme 1: Synthetic strategy leading to probe **1**. The Vancomycin glycopeptide core is depicted as a square in **5** and probe **1**. Its peptide backbone runs as a horizontal diagonal (free carboxy terminus left, methylated amino terminus right). The disaccharide is located on the top edge.*

different probe scaffolds that contain a benzophenone photocrosslinker and a small alkyne handle (Figure 1). The alkyne serves as a benign tag for the modification with marker azides after live cell labeling *via* the Huisgen/Sharpless/Meldal click chemistry (CC) reaction (Figure 2).[136,139,141,184] The benzophenone is necessary to establish a covalent bond between the probe scaffold and the target enzyme which is required for visualization, enrichment and isolation of the labeled proteins. Activation of hexynoic acid *via* an NHS ester allowed a specific amide bond formation at the free amine of the vancosamine sugar moiety (Scheme 1).[190-195] Subsequently, the free *C*-terminal carboxylic acid was modified with a benzophenone amide under standard peptide coupling conditions (probe **1**). We utilized closely related synthetic procedures to introduce another probe (probe **2**) with the opposite decoration (benzophenone at vancosamine sugar and alkyne at *C*-terminal carboxylic acid) as well as one probe (probe **3**) in which both functionalities are attached to the vancosamine sugar (Figure 1).

*Table 1: MIC values (µM) for vancomycin hydrochloride and the probes **1 – 3**.*

Strain	Vancomycin x HCl	Probe **1**	Probe **2**	Probe **3**
S. aureus Mu50	1.3	2.5	2.5	1.3
S. aureus NCTC 8325	1.3	1.3	2.5	2.5
E. faecalis OG1RF (VSE)	2.5	1.3	2.5	< 0.6
E. faecalis V583 (VRE)	5	2.5	5	2.5

To test if and how the structural modifications influence the antibiotic potency of all vancomycin probes we determined their individual minimal inhibitory concentrations (MIC) against *S. aureus*, MRSA, VSE and VRE (Table 1). Unmodified vancomycin displayed potent activities against *S. aureus*, MRSA and VSE. As expected a drop in potency was observed for VRE. All three probes show comparable activities against *S. aureus* and slightly improved MICs against VSE and VRE (probes **1** and **3**) compared to unmodified vancomycin. Interestingly, the MIC of probe 3 in VSE drops below 0.6 µM, making it at least 4 fold more potent than vancomycin itself. These intriguing results indicate that the new probes exhibit all suitable traits for successful proteomic tools to unravel vancomycin protein targets.[192]

To evaluate labeling properties of the vancomycin probes we first tested conditions with bacterial lysates and finally optimized probe concentration and time of irradiation with the pathogenic strains VRE and MRSA *in situ* (Supporting Figure S1, Figure 3 A, B and C). The cells were treated with various concentrations of probes and irradiated at 366 nm for different durations. Subsequently, bacteria were lysed, rhodamine azide was attached to the probe scaffold under CC conditions and labeled proteins were visualized *via* fluorescent SDS gel analysis. A proteome incubation with 1 µM of probe and an irradiation time of 1 h turned out to be optimal in order to achieve saturated target labeling (Figure 3C). *In situ* labeling of staphylococcal proteomes revealed that all three probes labeled a protein in the

membrane with an apparent molecular mass of about 65 kDa (Figure 3B). Labeling of enteroccocal cells with all probes under *in situ* conditions revealed labeling of a single protein band with a molecular weight of about 40 kDa (Figure 3A). As there were no observed differences between *S. aureus* and MRSA as well as VSE and VRE, the labeled proteins likely do not represent resistance-associated targets

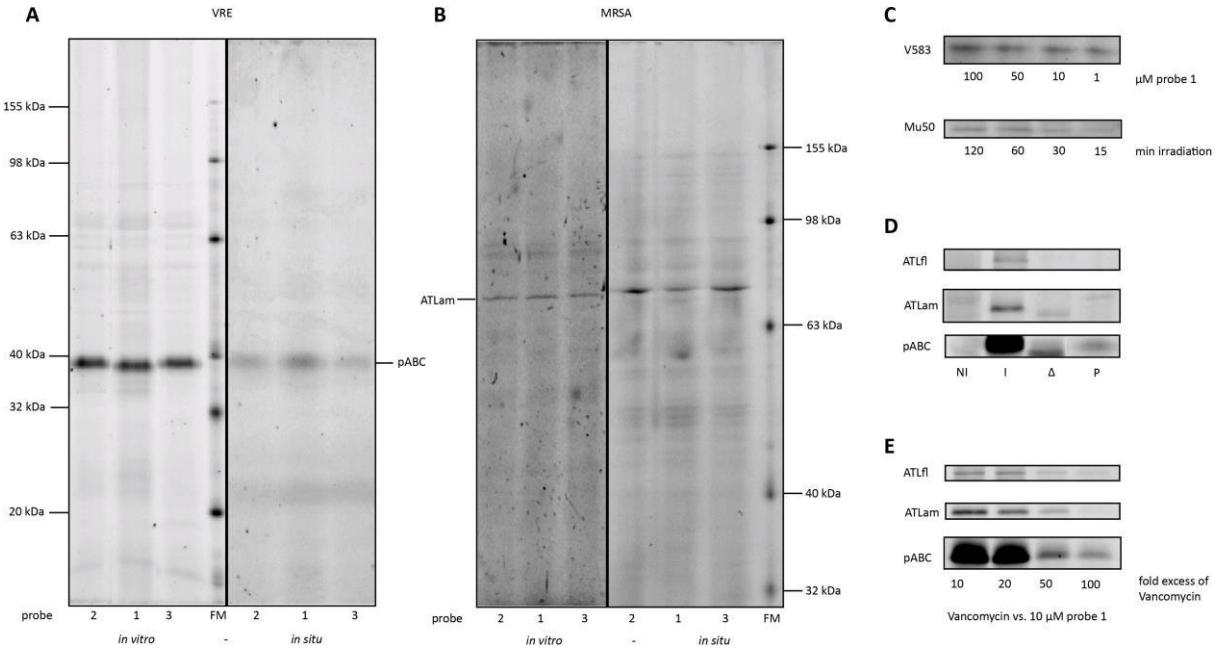

*Figure 3: Labeling of bacterial pathogens by vancomycin-based probes **1**, **2** and **3**. Membrane proteins of VRE (A) and MRSA (B) after in vitro (left) and* in situ *(right) labeling. (C) Time and concentration dependent labeling in VRE and MRSA. (D) Recombinantly expressed ATLfl, ATLam and pABC. NI = before induction, I = induced, Δ = heat control, P = protein in the proteome. (E) Competitive, concentration-dependent displacement of probe **1** by unmodified vancomycin in labeling experiments with overexpressed target proteins.*

but rather general interaction partners of vancomycin. All three probes exhibited the same protein target preferences, which indicates that protein labeling is driven solely by the scaffold and not by the attached modifications. We therefore conducted all subsequent studies with probe **1** as a representative example.

To unravel the identity of these two proteins we performed a quantitative proteome analysis by attaching a trifunctional rhodamine-biotin azide tag under CC conditions for the visualization, enrichment and identification of proteins by SDS-gel electrophoresis and mass spectrometry.[196] Analysis of the peptide fragments by the SEQUEST algorithm revealed strong hits for the bifunctional autolysin (ATL) in case of MRSA and a peptide ABC transporter (pABC) in case of VSE (Supporting Table S1). The MS results were independently confirmed by the recombinant overexpression of both target proteins in *E. coli* and subsequent labeling with probe **1** (Figure 3D). ATL was cloned and expressed in full length (ATLfl) as well as in a shorter version with its amidase domain (ATLam), which

was sufficient for successful probe interaction. Labeling occurred only with the native, folded proteins and not with heat-treated unfolded proteins emphasizing a specific interaction with the probes (Figure 3D). Moreover, these proteins were not labeled by a benzophenone-alkyne control peptide (Figure 1) which shows that target binding is not mediated by the photocrosslinker but solely by the vancomycin scaffold (Supporting Figure S2).[197] Unmodified vancomycin competed for ATLfl, ATLam and pABC labeling with probe **1**, which further emphasizes a direct and selective interaction of the unmodified natural product with these proteins (Figure 3E, Supporting Figure S3). Interestingly, these interactions are likely to contribute to vancomycin antibiotic activity since both targets are important for bacteria to maintain their cell wall (ATL) and import nutrition (pABC).

In order to maintain cell integrity, viability, division and growth, peptidogylcan must be continuously synthesized and degraded.[198] Peptidoglycan hydrolases are crucial for the degradation process and Atl represents the predominant hydrolase in staphylococci. Atl is a 147 kDa bifunctional enzyme with a 62 kDa *N*-acetylmuramyl-L-alanine amidase (am) and a 51 kDa endo-*N*-acetylglucosaminidase domain.[199] After translation, the Atl pro-peptide is cleaved into several processing intermediates that contain the two active domains together with different repeat units.[200,201] Since vancomycin probe incubation with SA and MRSA revealed a strong labeling of an Atl fragment of about 63 kDa it is most likely that vancomycin selectively interacts solely with the amidase unit of Atl. This was confirmed by protein overexpression where all three probes did not only label the full length (ATLfl) but also the recombinant amidase functional domain (ATLam) (Supporting Figure S2).

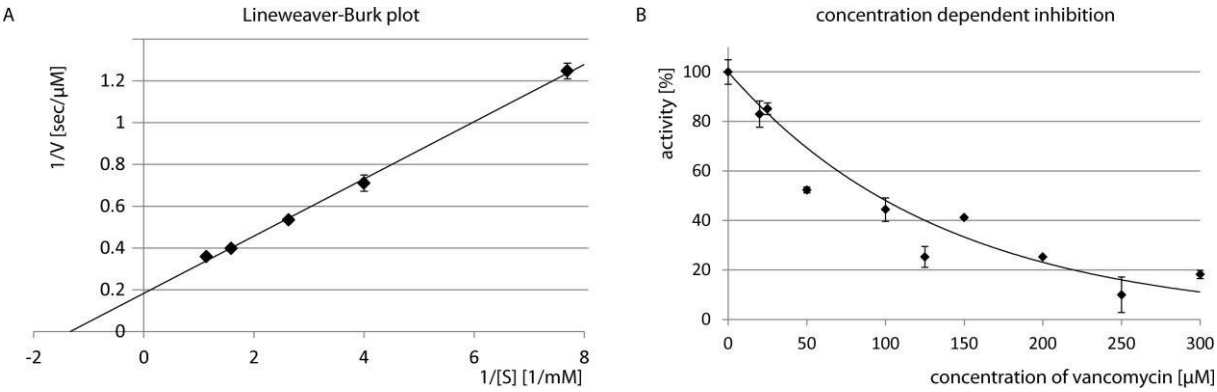

Figure 4: Interaction of vancomycin with ATLam via a peptidoglycan turnover assay. (A) Lineweaver-Burk plot for the degradation of peptidoglycan by ATLam to determine K_M and k_{cat} (B) Concentration dependent inhibition of ATLam by vancomycin.

Previous phenotypic characterization of a *S. aureus* Atl deletion mutant by *Götz et al.* demonstrated that mutant cells grow in large cell clusters which suggests that Atl is responsible for the splitting of the septum during cell division to allow the separation of daughter cells.[198] This mutation was not lethal

since a related Aaa amidase partially recovered the loss of Atl activity. A double mutation of both enzymes, however, significantly impaired bacterial growth.[202,203] In a different study by *Tomasz et al.* a similar atl phenotype of cell clustering was observed when sub-MIC concentrations of vancomycin were added to the culture medium of *S. aureus* which strongly suggests an inhibition of the autolytic process.[175,180] The authors suggest that this inhibtion is mediated by binding of vancomycin to muropeptides that sterically blocks access of all cell wall hydrolytic enzymes to the peptidoglycan substrate. Our results strongly emphasize that vancomycin also directly binds to the amidase unit of Atl and inhibits its enzymatic activity. This is further supported by an Atl activity assay in which recombinant ATLam was incubated with the natural peptidoglycan substrate. Atl degrades peptidoglycan, which can be photometrically followed at 600 nm. The dependence of the reaction rate on substrate concentration followed Michaelis-Menten kinetics with a K_M of 0.75 mM and a k_{cat} of 710 $^{s-1}$. Enzyme inhibition occured in a concentration dependent manner (Figure 4). Concentrations ranging from 75 nM to 300 µM of vancomycin show a slight to strong inhibition with an IC_{50} value of 95 µM and a K_I of 30 µM.

Taken together, our results show that vancomycin and corresponding probes directly target the Atl amidase domain in the presence and absence of peptidoglycan and also inhibit its activity. It is therefore most likely that this direct interaction further enhances the observed cell wall clustering phenotype that is caused by steric clashes with the autolytic machinery. This dual strategy of Atl amidase inhibition and limiting the access of all hydrolytic enzymes to their peptidoglycan substrates ensures a fine tuned regulation of autolysis that may allow a basal level of cell wall remodeling which is probably essential for bacterial survival. One additional function of the autolytic machinery is to trigger antibiotic induced cell degradation. Downregulation of autolysis provides *S. aureus* a unique advantage to survive low level vancomycin concentrations in its micro-environment.10 In addition, inhibition of the autolytic machinery increases the thickness of cell walls that further sequester vancomycin molecules and also limits the access of antibiotics to reach their cell wall biosynthesis targets. In fact, these changes in cell morphology and autolytic activity are observed among many strains of vacomycin resistant *S. aureus*.[174,178,179]

While Atl was the most prominent target in staphylococci, *E. faecalis* does not encode an amidase containing Atl, which accounts for the lack of its detection by our affinity probes. In contrast, probe labeling in living VRE and VSE revealed a peptide ABC transporter as the major proteome target. Peptide ABC transporters have a diverse array of functions in bacteria.[204,205] Some transporters are specialized for the import of essential nutrients such as sugars and peptides while others carry out the export of toxins or, in the case of virulent or drug resistant bacteria, antibiotics.[206] *E. faecalis* encodes a large number of sugar uptake systems such as ABC transporters that support bacteria to ferment

non-absorbed sugars in the gastrointestinal tract.[207] The ABC transporter identified here represents a so far uncharacterized protein that is most likely not involved in antibiotic resistance as it is present in both VRE and VSE strains.[208] This is supported by gene expression data that shows that there is no increased transcription upon incubation of bacteria with vancomycin (Supporting Table S2).

Conclusion

In conclusion, we unraveled the protein targets of vancomycin in living bacterial cells by a chemical proteomic strategy that utilizes affinity based photocrosslinking probes. Three functional vancomycin probes were designed and two unique structural modifications even exceeded the antibiotic potency of the unmodified natural product. It is well established that the binding of vancomycin to the D-Ala-D-Ala motif of nascent peptidoglycan and the corresponding inhibition of cell wall biosynthesis is the primary mode of action, which leads to autolysin triggered cell rupture and death. However, the direct inhibition of the Atl amidase domain represents a mode of action that causes massive defects in cell morphology and enhances the tolerance of *S. aureus* to low concentrations of vancomycin. This provides *S. aureus* with an efficient strategy to evade low vancomycin concentrations without acquiring resistance on the genetic level. The binding of vancomycin to Atl provides an intriguing perspective to design improved vancomycin inhibitors that exhibit lower affinity for this target and therefore increase antibacterial susceptibility in *S. aureus* and MRSA.

Experimental Section

General

All chemicals were of reagent grade or better and used without further purification. Chemicals and solvents were purchased from various commercial sources. For all reactions, only commercially available solvents of purissimum grade, dried over molecular sieves and stored under an argon atmosphere were used. Solvents for chromatography and workup purposes were generally of reagent grade and distilled before use. In all reactions, temperatures were measured externally. All NMR spectra of probe **1** and its precursor **5** were recorded with devices of the Bavarian NMR Center (for ^{1}H and ^{13}C spectra see Supporting Scheme S1). Other ^{1}H, ^{13}C and 2D NMR spectra were measured with Bruker Avance 250, Avance 360 or Avance 500 (in cases of **7** and probes **2** and **3** equipped with a CryoProbe) with B-ACS-60/120 auto samplers and referenced to the residual proton and carbon signal of the deuterated solvent, respectively. ESI mass spectra were recorded with Thermo LTQ Orbitrap XL or LTQ FT Ultra equipped with Dionex UltiMate 3000 Nano or Rapid Separation LC Systems. HPLC

analysis was accomplished with a Waters 2695 separations module, a X-Bridge BEH130 C_{18} column (4.6 mm x 100 mm) and a Waters 2996 PDA detector.

Synthetic strategy to vancomycin-based ABPP-probes The synthesis was based on commercially available vancomycin hydrochloride. Standard peptide coupling methods were used to modify the glycopeptide antibiotic as previously described.[192] Full characterization by NMR and HR-MS/MS was carried out for the probes.

Synthesis of 2,5-dioxopyrrolidin-1-yl hex-5-ynoate **4**.[190,195] *N*-Hydroxysuccinimide NHS (1.08 g, 9.35 mmol, 1.05 eq) and *N,N'*-diisopropylcarbodiimide (DIC) (1450 µL, 9.35 mmol, 1.05 eq) were added to a solution of 5-hexynoic acid (1.00 g, 984 µL, 8.92 mmol, 1 eq) in 40 mL CH_2Cl_2. The reaction was stirred for 16 h at rt. This mixture was washed with 30 mL H_2O three times and the combined inorganic phases were re-extracted with 30 mL DCM. The combined organic phases were washed with sat. NaCl, dried over Na_2SO_4 and the solvent was removed *in vacuo*. The crude product was purified by column chromatography (SiO_2, Ethylacetate:isoHexan = 2:3, R_f: 0.47) yielding 1.19 g of a yellow oil (64 %).

^{1}H NMR (360 MHz, $CDCl_3$, δ/ppm): 2.86 (s, 4H, 2x $NCOCH_2$), 2.79 (t, J = 7.4 Hz, 2H, $COCH_2$), 2.37 (td, J = 6.9, 2.6 Hz, 2H, $CqCH_2$), 2.03 (t, J = 2.6 Hz, 1H, CqCH), 1.98 (m, 2H $CH_2CH_2CH_2$).

^{13}C NMR (91 MHz, $CDCl_3$, δ/ppm): 169.0 (2 NC=O), 168.2 (1 OC=O), 82.4 (1 Cq), 69.8 (1 CH), 29.7 (1 CH_2), 25.6 (2 CH_2), 23.3 (1 CH_2), 17.6 (1 CH_2).

HR-ESI-MS, positive mode (m/z): 232.0591 $[M+Na]^+$ (calc.: 232.0580).

Synthesis of *N'*-hex-5-ynamide vancomycin 5.[193] Vancomycin hydrochloride (300 mg, 202 µmol, 1 eq) was dissolved in 2 mL DMF. *N,N'*-diisopropylethylamine (DIPEA) (176 µL, 1.0 mmol, 5 eq) and a solution of **4** (134 mg, 58 µL, 343 µmol, 1.7 eq) in 1 mL DMF were added. The reaction was stirred 24 h at rt and was subsequently poured into 30 mL ice cold Et_2O. The resulting precipitate was centrifuged at 10000 g at 4 °C for 15 min. The colorless supernatant was decanted and the pellet air-dried for 30 min. The residue was purified by HPLC yielding 135 mg of a colorless solid (43 %).

HPLC analysis, mobile phase (HPLC grade): A = water with 0.1% (v/v) TFA, B = acetonitrile with 0.1% (v/v) TFA. Gradient: T_0: B = 0%; T_{70}: B = 70%. Retention time: 18.0 min.

^{1}H NMR (600 MHz, d_6-DMSO, δ/ppm): 9.45 (s, 1H), 9.18 (s, 1H), 9.08 (s, 1H), 8.70 (d, J = 18.9 Hz, 1H), 8.57 (s, 1H), 7.89 – 7.79 (m, 1H), 7.68 (s, 1H), 7.52 (dd, J = 14.6, 8.4 Hz, 1H), 7.47 (s, 1H), 7.44 (d, J =

8.4 Hz, 1H), 7.32 (d, J = 8.4 Hz, 1H), 7.29 (d, J = 8.4 Hz, 1H), 7.17 – 7.13 (m, 1H), 7.05 (s, 1H), 6.99 (s, 1H), 6.77 (dd, J = 8.4, 2.0 Hz, 1H), 6.71 (d, J = 8.5 Hz, 2H), 6.68 (s, 1H), 6.58 (s, 1H), 6.40 (d, J = 6.6 Hz, 1H), 6.25 (d, J = 2.2 Hz, 1H), 5.98 (d, J = 6.5 Hz, 1H), 5.93 (s, 1H), 5.75 (d, J = 7.9 Hz, 1H), 5.67 (s, 1H), 5.60 (s, 1H), 5.35 (d, J = 5.0 Hz, 1H), 5.31 (dd, J = 6.7, 3.6 Hz, 1H), 5.28 (d, J = 7.7 Hz, 1H), 5.17 (s, 1H), 5.10 (d, J = 6.6 Hz, 1H), 5.08 (d, J = 5.1 Hz, 1H), 5.04 (d, J = 5.1 Hz, 1H), 4.92 (s, 1H), 4.69 – 4.63 (m, 1H), 4.43 (s, 1H), 4.42 (s, 1H), 4.32 (s, 1H), 4.18 (s, 1H), 4.05 (t, J = 5.4 Hz, 1H), 3.69 (d, J = 5.2 Hz, 1H), 3.53 (d, J = 8.1 Hz, 1H), 3.49 (d, J = 6.0 Hz, 1H), 3.44 (d, J = 6.3 Hz, 1H), 3.30 – 3.22 (m, 3H), 3.22 (s, 1H), 2.77 (t, J = 2.6 Hz, 2H), 2.63 – 2.60 (m, 1H), 2.28 – 2.21 (m, 5H), 2.16 – 2.06 (m, 4H), 1.97 (d, J = 13.0 Hz, 1H), 1.79 (d, J = 12.7 Hz, 1H), 1.70 – 1.51 (m, 2H), 1.40 (s, 3H), 1.10 (d, J = 6.3 Hz, 3H), 0.91 (d, J = 5.1 Hz, 3H), 0.86 (d, J = 5.6 Hz, 3H).

^{13}C NMR (151 MHz, d_6-DMSO, δ/ppm): 174.1, 172.6, 171.2, 170.8, 170.4, 169.5, 169.1, 167.8, 166.8, 157.2, 156.5, 155.1, 152.3, 151.3, 149.9, 148.2, 142.5, 139.8, 136.1, 135.7, 134.6, 131.9, 128.6, 127.3, 127.2, 126.2, 125.5, 124.3, 123.4, 121.6, 118.0, 116.2, 107.2, 105.7, 104.6, 102.3, 101.3, 96.7, 84.3, 78.1, 77.0, 76.7, 71.6, 71.3, 70.7, 70.1, 69.7, 63.1, 61.8, 61.2, 61.0, 58.4, 56.7, 54.9, 53.9, 53.7, 50.9, 41.0, 37.1, 33.2, 32.5, 27.8, 24.0, 23.8, 22.7, 22.4, 22.2, 17.7, 16.9.

HR-ESI-MS, positive mode (m/z): 1542.4782 $[M+H]^+$ (calc.: 1542.4793).

Synthesis of *N*-(3-aminopropyl)-4-benzoylbenzamide **6**.[191,194] 4-benzoylbenzoic acid (500 mg, 2.2 mmol, 1 eq) was dissolved with DMAP (5 mg, cat.) in 5 mL DMF and stirred at 22 °C for 10 min with DIC (379 µL, 2.4 mmol, 1.1 eq) for pre-activation. 1,3-Diaminopropane (184 µL, 2.2 mmol, 1 eq) was added and the reaction was stirred 2 h at 22 °C.

30 mL 0.1 % (v/v) TFA in H_2O were added and the aq. phase was extracted twice with 30 mL EtOAc. The combined organic phases were extracted with 50 mL 0.1 % (v/v) TFA in H_2O. The aq. phases were pooled and the solvent was removed *in vacuo*. 447 mg of a yellow foam were obtained (72 %) and used without further purification.

^{1}H NMR (360 MHz, d_6-DMSO, δ/ppm): 8.01 (d, J = 8.3 Hz, 2H, H_{arom}), 7.79 (d, J = 8.4 Hz, 2H, H_{arom}), 7.66 (dd, J = 6.3, 2.3 Hz, 2H, 2x H_{arom}), 7.44 (dd, J = 6.6, 3.6 Hz, 1H, 1x H_{arom}), 7.12 (dd, J = 6.3, 3.0 Hz, 2H, 2x H_{arom}), 3.44 – 3.01 (m, 2H, 2x C=ONHCH_2), 2.88 (t, J = 11.8 Hz, 2H, 2x CH_2NH_2), 1.88 – 1.73 (m, 2H, 2x CH_2CH_2CH_2).

^{13}C NMR (91 MHz, d_6-DMSO, δ/ppm): 196.7 (PhC=OPh), 162.3 (C=ONH), 142.9 (CqC=O), 129.7 (2x C_{arom}), 129.6 (C_{arom}), 128.6 (2x C_{arom}), 127.3 (C_{arom}), 122.5 (2x C_{arom}), 118.1 (2x C_{arom}), 111.2 (C_{arom}), 36.8 (NHCH_2), 35.8 (CH_2NH_2), 23.3 (CH_2CH_2CH_2).

HR-ESI-MS, positive mode (m/z): 283.1448 $[M+Na]^+$ (calc.: 283.1441).

N'-hex-5-ynamide C-(3-aminopropyl)-4-benzoylbenzamide vancomycin Probe **1**.[192] Vancomycin derivative **5** (20 mg, 13 µmol, 1 eq) was dissolved together with **6** (7.3 mg, 26 µmol, 2 eq) in 600 µL DMF. DIPEA (11.4 µL, 65 µmol, 5 eq), PyBOP (7.4 mg, 14 µmol, 1.1 eq) and HOBT (13 % H_2O, 2.1 mg, 14 µmol, 1.1 eq) were added in sequence and the reaction mixture was shaken for 16 h at 22 °C in the dark. The reaction was crashed into 6 mL ice cold Et_2O. The precipitate that formed was centrifuged at 10000 g and 4 °C for 15 min and the clear supernatant was removed. The pellet was air-dried for 30 min and the crude product was purified *via* HPLC yielding 1.7 mg of a color-less solid (7 %).

HPLC analysis, mobile phase (HPLC grade): A = water with 0.1% (v/v) TFA, B = acetonitril with 0.1% (v/v) TFA. Gradient: T_0: B = 0%; T_{70}: B = 70%. Retention time: 33.0 min.

^{1}H NMR (500 MHz, d_6-DMSO, δ/ppm): 9.33 (s, 1H), 9.05 (s, 1H), 8.79 (s, 1H), 8.67 (s, 1H), 8.52 (s, 1H), 8.01 (d, J = 8.4 Hz, 2H), 7.86 (s, 1H), 7.81 (d, J = 8.4 Hz, 2H), 7.76 (d, J = 7.1 Hz, 2H), 7.71 (s, 1H), 7.60 (s, 1H), 7.58 (s, 2H), 7.57 (s, 1H), 7.45 (s, 1H), 7.43 (s, 1H), 7.31 (d, J = 8.3 Hz, 1H), 7.22 (s, 1H), 7.17 (s, 1H), 6.98 (s, 2H), 6.76 (d, J = 8.4 Hz, 1H), 6.71 (s, 1H), 6.69 (s, 1H), 6.56 (s, 1H), 6.36 (d, J = 1.8 Hz, 1H), 6.27 (d, J = 2.0 Hz, 1H), 5.93 (s, 1H), 5.79 (s, 1H), 5.75 (s, 1H), 5.69 (s, 1H), 5.62 (s, 1H), 5.32 (s, 1H), 5.31 (s, 1H), 5.31 (s, 1H), 5.30 (s, 1H), 5.18 (s, 1H), 5.17 (s, 1H), 5.16 (s, 1H), 4.93 (s, 1H), 4.66 (d, J = 6.7 Hz, 1H), 4.46 (s, 1H), 4.45 (s, 1H), 4.37 (d, J = 5.4 Hz, 1H), 4.24 (d, J = 10.4 Hz, 1H), 4.05 (s, 1H), 3.68 (d, J = 10.1 Hz, 1H), 3.55 (d, J = 8.8 Hz, 1H), 3.52 (d, J = 10.9 Hz, 1H), 3.40 (covered by H2O, 3H), 3.30 – 3.23 (m, 3H), 3.20 (s, 1H), 3.03 – 2.99 (m, 2H), 2.75 (t, J = 2.6 Hz, 1H), 2.65 (s, 1H), 2.52 (s, 1H), 2.27 – 2.13 (m, 5H), 2.14 – 2.04 (m, 8H), 1.98 (d, J = 13.0 Hz, 1H), 1.79 (d, J = 9.8 Hz, 1H), 1.65 (s, 1H), 1.60 – 1.55 (m, 1H), 1.44 – 1.39 (m, 1H), 1.23 (s, 1H), 1.02 (d, J = 6.3 Hz, 3H), 0.91 (d, J = 6.1 Hz, 3H), 0.86 (d, J = 6.1 Hz, 3H).

^{13}C NMR (126 MHz, d_6-DMSO, δ/ppm): 195.43, 170.80, 170.35, 170.20, 169.30, 169.22, 169.14, 168.40, 167.70, 166.07, 165.84, 157.07, 156.32, 155.10, 152.53, 151.12, 150.23, 148.27, 142.29, 140.34, 139.18, 137.73, 136.67, 135.61, 133.04, 129.73, 129.68, 129.56, 128.69, 127.43, 127.37, 127.28, 127.22, 127.02, 126.44, 126.25, 125.39, 125.36, 124.35, 123.34, 121.84, 118.34, 118.17, 116.25, 115.96, 107.64, 106.28, 104.83, 102.09, 101.13, 97.55, 84.26, 77.76, 77.13, 76.74, 71.89, 71.39, 70.28, 70.04, 69.66, 63.25, 62.04, 61.30, 61.15, 58.85, 57.87, 54.92, 53.92, 53.71, 51.09, 40.10, 36.79, 36.33, 34.99, 34.52, 31.25, 29.29, 25.95, 24.34, 23.68, 23.07, 22.73, 22.36, 17.41, 17.34.

HR-ESI-MS, positive mode (m/z): 1806.6060 $[M+H]^+$ (calc.: 1806.6056).

N'- benzoylbenzamide vancomycin **7**.[192] To a solution of Vancomycin hydrochloride (100 mg, 68 µmol, 1.0 eq) in 600 µL DMF, DIPEA (33 µL, 201 µmol, 3.0 eq) was added. 4-benzoylbenzoic acid (16 mg, 71 µmol, 1.05 eq) was pre-activated with PyBOP (39 mg, 74 µmol, 1.1 eq), HOBT (13 % H_2O, 11 mg, 74 µmol, 1.1 eq) and DIPEA (11 µL, 68 µmol, 1 eq) in 200 µL DMF. After 10 min the two solutions were combined and shaken for 2 h at 22 °C. The reaction mixture was subsequently poured into 20 mL ice cold Et_2O. The resulting precipitate was treated as described before in the case of probe **1**. The residue was purified by HPLC yielding 62 mg of a colorless solid (56 %).

HPLC analysis, mobile phase (HPLC grade): A = water with 0.1% (v/v) TFA, B = acetonitrile with 0.1% (v/v) TFA. Gradient: T_0: B = 0%; T_{70}: B = 70%. Retention time: 21.6 min.

^{1}H NMR (500 MHz, d_6-DMSO, δ/ppm): 9.47 (s, 1H), 9.19 (s, 1H), 9.09 (s, 1H), 8.70 (s, 1H), 8.57 (s, 1H), 7.95 (d, J = 5.9 Hz, 2H), 7.86 (s, 1H), 7.82 (d, J = 8.5 Hz, 2H), 7.76 (d, J = 8.1 Hz, 2H), 7.67 (s, 1H), 7.59 (s, 1H), 7.58 (s, 2H), 7.56 (s, 1H), 7.46 (s, 1H), 7.45 (s, 1H), 7.35 (s, 1H), 7.29 (d, J = 4.1 Hz, 1H), 7.20 (s, 1H), 7.11 (s, 2H), 6.77 (s, 1H), 6.73 (s, 1H), 6.72 (s, 1H), 6.70 (s, 1H), 6.40 (d, J = 7.8 Hz, 1H), 6.25 (d, J = 4.5 Hz, 1H), 5.97 (br s, 1H), 5.77 (s, 1H), 5.76 (s, 1H), 5.62 (s, 1H), 5.52 (s, 1H), 5.34 (s, 1H), 5.32 (s, 1H), 5.31 (s, 1H), 5.24 (s, 1H), 5.23 (s, 1H), 5.20 (s, 1H), 5.11 (s, 1H), 4.94 (s, 1H), 4.79 – 4.74 (m, 1H), 4.67 (d, J = 5.3 Hz, 1H), 4.46 (s, 1H), 4.43 (d, J = 5.4 Hz, 1H), 4.20 (s, 1H), 3.95 (s, 1H), 3.70 (d, J = 10.3 Hz, 1H), 3.58 (s, 1H), 3.53 (s, 1H), 3.36 (s, 1H), 3.30 – 3.17 (m, 3H), 3.14 (s, 1H), 2.81 (s, 1H), 2.67 – 2.62 (m, 2H), 2.28 – 2.12 (m, 5H), 2.00 – 1.86 (m, 6H), 1.78 – 1.52 (m, 5H), 1.09 – 1.06 (m, 1H), 0.96 (d, J = 6.4 Hz, 3H), 0.91 (d, J = 5.9 Hz, 3H), 0.86 (d, J = 6.0 Hz, 3H).

^{13}C NMR (126 MHz, d_6-DMSO, δ/ppm): 195.50, 172.62, 170.46, 169.19, 169.16, 167.89, 167.80, 167.58, 166.18, 165.05, 158.26, 157.24, 156.59, 155.13, 152.62, 151.22, 148.31, 142.49, 139.28, 138.85, 137.98, 136.77, 135.70, 133.09, 129.90, 129.75, 129.48, 128.74, 127.49, 127.43, 127.41, 127.35, 127.30, 126.97, 126.50, 126.28, 125.63, 124.41, 123.45, 121.63, 118.11, 118.02, 116.24, 115.80, 113.44, 105.71, 104.85, 102.36, 101.29, 97.62, 78.30, 77.13, 76.77, 71.68, 71.44, 70.32, 70.12, 63.27, 63.17, 61.85, 61.27, 59.60, 58.92, 54.90, 53.99, 53.79, 51.12, 40.12, 35.51, 32.77, 31.28, 24.76, 23.74, 22.81, 22.35, 17.47.

ESI-MS, positive mode (m/z): 1658.4966 $[M+H]^+$ (calc.: 1658.4972).

N'-benzoylbenzamide *C* propargylamide vancomycin probe **2**.[192] To a solution of vancomycin derivative **7** (50 mg, 30 µmol, 1.05 eq) in 300 µL DMF 3-amino-1-propyne (1.9 µL, 29 µmol, 1.0 eq) was added. HOBT (13 % H_2O, 5 mg, 32 µmol, 1.1 eq), PyBOP (17 mg, 32 µmol, 1.1 eq) and DIPEA (15 µL, 90 µmol, 3.2 eq) were added and the reaction was stirred 2 h at 22 °C. The reaction mixture was subsequently poured into ice cold Et_2O and treated as described before for probe **1**.

The residue was purified by HPLC yielding 38 mg of a colorless solid (75 %).

HPLC analysis, mobile phase (HPLC grade): A = water with 0.1% (v/v) TFA, B = acetonitril with 0.1% (v/v) TFA. Gradient: T_0: B = 0%; T_{70}: B = 70%. Retention time: 22.2 min.

^{1}H NMR (500 MHz, d_6-DMSO, δ/ppm): 9.34 (s, 1H), 9.00 (s, 2H), 8.69 (s, 1H), 8.64 (s, 1H), 8.48 (s, 1H), 8.39 (s, 2H), 7.87 (d, J = 8.0 Hz, 2H), 7.82 (d, J = 7.8 Hz, 2H), 7.77 (d, J = 7.7 Hz, 2H), 7.74 (d, J = 7.4 Hz, 2H), 7.65 (s, 1H), 7.58 (s, 1H), 7.56 (s, 1H), 7.46 (s, 1H), 7.34 (s, 1H), 7.29 (s, 1H), 7.20 (s, 1H), 7.12 (d, J = 8.2 Hz, 1H), 7.08 (d, J = 8.0 Hz, 1H), 6.75 (s, 1H), 6.71 (s, 1H), 6.69 (s, 1H), 6.66 (s, 1H), 6.38 (d, J = 7.4 Hz, 1H), 6.22 (s, 1H), 5.96 (s, 1H), 5.84 (s, 1H), 5.76 (s, 1H), 5.63 (s, 1H), 5.52 (s, 1H), 5.34 (s, 1H), 5.32 (s, 1H), 5.30 (s, 1H), 5.25 (s, 1H), 5.24 (s, 1H), 5.19 (s, 1H), 4.94 (s, 1H), 4.77 (d, J = 6.2 Hz, 1H), 4.55 (s, 1H), 4.45 (s, 1H), 4.40 (s, 1H), 4.22 (s, 1H), 3.96 (s, 1H), 3.91 – 3.84 (m, 1H), 3.69 (s, 1H), 3.28 (s, 3H), 3.13 (s, 1H), 2.81 (s, 1H), 2.64 (s, 1H), 2.36 (s, 1H), 2.26 – 2.11 (m, 6H), 2.01 – 1.93 (m, 1H), 1.80 – 1.64 (m, 2H), 1.58 (s, 1H), 1.28 (s, 1H), 1.07 (s, 1H), 0.96 (d, J = 6.3 Hz, 3H), 0.91 (d, J = 5.7 Hz, 3H), 0.86 (d, J = 5.9 Hz, 3H).

^{13}C NMR (126 MHz, d_6-DMSO, δ/ppm): 195.46, 170.92, 170.10, 169.13, 169.10, 169.05, 168.19, 167.72, 166.13, 165.00, 158.15, 157.15, 155.11, 152.55, 151.18, 150.19, 148.23, 142.38, 139.24, 138.83, 137.47, 136.72, 136.34, 133.06, 129.87, 129.72, 129.45, 128.71, 127.47, 127.44, 127.27, 127.16, 126.93, 126.42, 126.18, 125.46, 125.41, 124.42, 123.43, 121.82, 118.09, 117.92, 116.33, 115.72, 109.58, 106.46, 104.79, 102.15, 101.26, 96.81, 81.25, 77.21, 77.13, 76.81, 73.00, 71.36, 70.85, 70.28, 69.97, 63.15, 62.02, 61.30, 61.24, 58.96, 57.48, 55.02, 53.87, 53.77, 51.12, 40.19, 35.47, 32.74, 31.23, 28.16, 24.79, 22.82, 22.35, 17.48, 16.81.

ESI-MS, positive mode (m/z): 1696.5234 $[M+H]^+$ (calc.: 1696.5225).

3-(4-benzoylphenyl)-2-(hex-5-ynamido)propanoic acid **8** - BP minimal probe.[197] 2-amino-3-(4-benzoylphenyl)propanoic acid (300 mg, 1.1 mmol, 1.0 eq) was dissolved in 4 mL CH_2Cl_2 with DIPEA (474 µL, 2.8 mmol, 2.5 eq). **1** (242 µL, 1.5 mmol, 1.3 eq) was added and the reaction was stirred 1.5 h at 22 °C. The solvent was removed *in vacuo* and the crude product purified *via* HPLC yielding 342 mg of a yellow foam (85 %).

HPLC analysis, mobile phase (HPLC grade): A = water with 0.1% (v/v) TFA, B = acetonitrile with 0.1% (v/v) TFA. Gradient: T_0: B = 0%; T_1: B = 60%; T_7: B = 80%. Retention time: 3.5 min.

^{1}H NMR (500 MHz, $CDCl_3$, δ/ppm): 10.00 (s, 1 H, CO_2H), 7.75 (d, J = 7.1 Hz, 2 H, H_{arom}), 7.71 (d, J = 8.2 Hz, 2 H, H_{arom}), 7.58 (t, J = 7.4 Hz, 1 H, H_{arom}), 7.46 (t, J = 7.7 Hz, 2 H, H_{arom}), 7.29 (d, J = 8.1 Hz, 2 H, H_{arom}), 6.61 (d, J = 7.6 Hz, 1 H, NH), 4.94 (ps. q, J = 6.1 Hz, 1 H, CH-CO_2H), 3.35 (dd, J = 14.1, 5.7, 1 H, C_{arom}–

CH_aH_b), 3.19 (dd, 1 H, J = 14.0, 6.4 Hz, C_{arom}–CH_aH_b), 2.36 (t, J = 7.3, 2 H, NHC=OCH_2), 2.25–2.15 (m, 2 H, HC≡CCH_2), 1.95 (t, J = 2.6 Hz, 1 H, HC≡C), 1.81 (ps. quint, J = 6.8 Hz, 2 H, HC≡C-CH_2CH_2).

^{13}C NMR (90 MHz, $CDCl_3$, δ/ppm): 196.6, 173.8, 172.9, 141.0, 137.4, 136.4, 132.6, 130.4, 130.1, 130.0, 129.8, 129.4, 128.5, 128.3, 128.3, 83.2, 69.5, 53.1, 37.4, 34.7, 24.0, 17.7.

ESI-MS, positive mode (m/z): 364.1544 $[M+H]^+$ (calc.: 364.1549).

N'-3-(4-benzoylphenyl)-2-(hex-5-ynamido)propanoic amide vancomycin Probe **3**.[192] To a solution of Vancomycin hydrochloride (100 mg, 68 µmol, 1.0 eq) in 700 µL DMF, DIPEA (33 µL, 201 µmol, 3.0 eq) was added. PyBOP (39 mg, 74 µmol, 1.1 eq) and HOBT (13 % H_2O, 11 mg, 74 µmol, 1.1 eq) were dissolved in DMF. DIPEA (11 µL, 68 µmol, 1 eq) and a solution of 3-(4-benzoylphenyl)-2-(hex-5-ynamido)propanoic acid **8** (210 mg/ml in DCM, 120 µL, 71 µmol, 1.05 eq) were added. After 10 min of pre-activating the carboxylic acid, the two solutions were combined and shaken for 2 h at 22 °C. Before HPLC purification, the reaction mixture was treated as described before for probe **1**. 76 mg of a colorless solid (63 %) were obtained.

^{1}H NMR (500 MHz, d_6-DMSO, δ/ppm): 9.48 (s, 1H), 9.20 (s, 1H), 9.00 (s, 1H), 8.68 (s, 1H), 8.53 (s, 1H), 8.15 (s, 2H), 7.85 (d, J = 10.0 Hz, 1H), 7.71 (d, J = 7.7 Hz, 2H), 7.66 (d, J = 7.0 Hz, 2H), 7.62 (d, J = 7.9 Hz, 1H), 7.57 (s, 1H), 7.56 (s, 2H), 7.54 (s, 1H), 7.45 (s, 1H), 7.38 (s, 1H), 7.33 (s, 1H), 7.25 (s, 1H), 7.17 (s, 1H), 7.08 – 6.99 (m, 2H), 6.77 (d, J = 8.3 Hz, 1H), 6.71 (d, J = 8.7 Hz, 1H), 6.61 (s, 1H), 6.49 (s, 1H), 6.40 (s, 1H), 6.25 (s, 1H), 5.98 (s, 1H), 5.76 (s, 1H), 5.74 (s, 1H), 5.60 (s, 1H), 5.52 (s, 1H), 5.32 (s, 1H), 5.31 (s, 1H), 5.26 (s, 1H), 5.24 (s, 1H), 5.22 (s, 1H), 5.17 (s, 1H), 5.11 (s, 1H), 4.94 (s, 1H), 4.94 (s, 1H), 4.68 (d, J = 7.2 Hz, 1H), 4.47 (s, 1H), 4.43 (s, 1H), 4.26 (s, 1H), 4.19 (s, 1H), 3.95 (s, 1H), 3.67 (s, 1H), 3.37 (s, 1H), 3.28 – 3.25 (m, 5H), 2.86 (s, 1H), 2.77 – 2.71 (m, 1H), 2.65 (s, 1H), 2.25 (s, 5H), 2.13 (s, 6H), 2.00 (s, 1H), 1.78 – 1.50 (m, 3H), 1.40 (s, 1H), 1.28 (s, 1H), 1.07 (s, 1H), 0.91 (d, J = 5.5 Hz, 3H), 0.86 (d, J = 5.7 Hz, 3H), 0.80 (d, J = 6.2 Hz, 3H).

^{13}C NMR (126 MHz, d_6-DMSO, δ/ppm): 195.74, 172.66, 171.64, 170.96, 170.24, 170.13, 169.94, 169.24, 167.94, 167.48, 166.20, 157.28, 156.62, 155.17, 152.65, 151.26, 150.27, 148.37, 142.49, 139.56, 139.27, 137.34, 136.16, 135.76, 132.64, 129.84, 129.59, 129.47, 128.62, 127.55, 127.45, 127.31, 127.06, 126.61, 126.49, 126.32, 125.64, 125.52, 124.47, 123.52, 121.65, 118.19, 118.06, 116.33, 115.82, 107.53, 105.75, 104.90, 102.41, 101.40, 97.65, 84.14, 77.67, 77.13, 76.75, 71.73, 71.53, 70.82, 70.41, 70.12, 63.18, 61.91, 61.31, 61.27, 59.67, 58.99, 56.74, 54.01, 53.78, 53.31, 51.11, 40.22, 35.89, 35.04, 34.00, 31.30, 30.02, 24.65, 24.40, 23.78, 22.90, 22.37, 17.37, 17.25.

ESI-MS, positive mode (m/z): 1795.5807 $[M+H]^+$ (calc.: 1795.5812).

Bacterial strains *Staphylococcus aureus* strains NCTC 8325 and Mu50 / ATCC 700699 (both from Institute Pasteur, France), and *Enterococcus faecalis* strains V583 / ATCC 700802 and OF1RF / ATCC 47077 (both form LGC Standards) were maintained in BHB (brain-heart broth) medium at 37 °C.

MIC measurements Over night cultures of the bacteria were diluted in fresh BHB medium to OD_{600} = 0.01 and 100 µL were incubated in Nunclon 96-well plates with round shaped bottom with 1 µL of the corresponding DMSO stocks of vancomycin and the probes at varying concentrations. The samples were incubated 12 h at 37 °C and the optical densities obtained for MIC calculation. All experiments were conducted at least in triplicates and DMSO served as control.

Preparation of proteomes for *in vitro* experiments The proteome of the bacterial strains were prepared from 1 L liquid cultures in BHB medium harvested 1 h after transition in the stationary phase by centrifugation at 4000 g. The bacterial cell pellet was washed with PBS, resuspended in PBS buffer and lysed by sonication with a Bandelin Sonopuls under ice cooling. Membrane and cytosol were separated by centrifugation at 18000 g for 45 min.

In vitro analytical and preparative labeling experiments Proteome samples were adjusted to a final concentration of 1 mg protein/mL by dilution in PBS prior to probe labeling. Analytical experiments were carried out in 43 µL total volume, such that once CC reagents were added, a total reaction volume of 50 µL was reached. In the case of competitive displacement experiments vancomycin hydrochloride was added in various excess (1 µL of DMSO stocks) and the proteoms were pre-incubated with the antibiotic for 15 min at 22 °C. Reactions were initiated by addition of 1 µM of probe and allowed to incubate (additional) 15 min at 22 °C. Then they were irradiated in aliquots of 20 µL in open polystyrene micro well plates for 120 min on ice with 366 nm UV light (Benda UV hand lamp NU-15 W). For heat controls the proteome was denatured with 2 % SDS (4 µL of 21.5% SDS) at 95 °C for 6 min and cooled to 22 °C before the probe was applied. Following incubation, reporter tagged-azide reagents (13 µM rhodamine-azide (1 µL) for analytical or 20 µM rhodamine-biotin-azide for preparative scale) were added followed by 1 mM TCEP (1 µL) and 100 µM ligand (3 µL). Samples were gently vortexed and the cycloaddition initiated by the addition of 1 mM $CuSO_4$ (1 µL). The reactions were incubated at 22 °C for 1 h. For analytical gel electrophoresis, 50 µL 2x SDS loading buffer were added and 50 µL applied on the gel. Fluorescence was recorded in a Fujifilm LAS-4000 Luminescent Image Analyzer with a Fujinon VRF43LMD3 Lens and a 575DF20 filter.

Preparative experiments were carried out in a final volume of 2 mL proteome sample. Reactions for enrichment were carried out together with a control lacking the probe to compare the results of the biotin-avidin enriched samples with the background of unspecific protein binding on avidin-agarose beads. After CC proteins were precipitated using a 5-fold volume of pre-chilled acetone. Samples were stored on ice for 60 min and centrifuged at 16000 g for 10 min. The supernatant was discarded and the pellet washed two times with 200 µL of pre-chilled methanol and resuspended by sonication. Subsequently, the pellet was dissolved in 1 mL PBS with 0.4 % SDS by sonication and incubated under gentle mixing with 50 µL of avidin-agarose beads (Sigma-Aldrich) for 1 h at room temperature. The beads were washed three times with 1 mL of PBS/0.4 % SDS, twice with 1 mL of 6 M urea and three times with 1 mL PBS. 50 µL of 2x SDS loading buffer were added and the proteins released for preparative SDS-PAGE by 6 min incubation at 95 °C. Gel bands were isolated, washed and tryptically digested as described previously.[209]

In situ experiments For analytical *in situ* studies, bacteria were grown in BHB medium and harvested 1 h after reaching stationary phase by centrifugation. After washing with PBS, the cells were resuspended in 200 µL PBS. Bacteria were incubated 15 min at 22 °C with 10 µM of probe followed by irradiation at 366 nm on ice for 2 h. Competitive *in situ* experiments with vancomycin were performed as described for the *in vitro* case. Subsequently, the cells were washed twice with PBS and lysed by sonication in 100 µL PBS. The proteomes were separated into cytosolic and membrane fractions, followed by CC as described above.

Mass spectrometry and bioinformatics Tryptic peptides were loaded onto a Dionex C_{18} Nano Trap Column (100 µm) and subsequently eluted and separated by a Dionex C_{18} PepMap 100 (3 µm) column for analysis by tandem MS followed by high resolution MS using a coupled Dionex Ultimate 3000 LC-Thermo LTQ Orbitrap XL system. The mass spectrometry data were searched using the SEQUEST algorithm against the corresponding databases *via* the software "bioworks". The search was limited to only tryptic peptides, two missed cleavage sites, monoisotopic precursor ions and a peptide tolerance of < 10 ppm. Filters were set to further refine the search results. The X_{corr} vs. charge state filter was set to X_{corr} values of 1.5, 2.0 and 2.5 for charge states +1, +2 and +3, respectively. The number of different peptides has to be ≤ 2 and the peptide probability filter was set to < 0.001. These filter values are similar to others previously reported for SEQUEST analysis. Minimum P-values and X_{corr} values of each run as well as the total number of obtained peptides are reported in Table S1.

Recombinant expression The major hits of MS analysis were recombinantly expressed in *E. coli* as an internal control of the MS results by using the Invitrogen Gateway Technology. Target genes were amplified from the corresponding genomes by PCR with an AccuPrime Pfx DNA Polymerase kit with 65 ng of genomic DNA as template, prepared by standard protocols. attB1 forward primer and attB2 reverse primer were designed to yield attB-PCR products needed for Gateway Technology. The sequences of these primers can be found in Supporting Table S3.

PCR products were separated and identified on 1 % agarose gels containing 0.2 µg/ml ethidium bromide and gel bands were isolated and extracted with an E.Z.N.A. MicroElute Gel Extraction Kit. Concentrations of DNA were measured with a TECAN Infinite 200 PRO and the corresponding NanoQuant Plate. 100 fmol of purified attB-PCR product and 50 fmol of attP-containing donor vector pDONR201 in TE buffer were used for *in vitro* BP recombination reaction with BP Clonase II enzyme mix to yield the appropriate attL-containing entry clone. After transformation in chemically competent One Shot TOP10 *E. coli* (Invitrogen), cells were plated on LB agar plates containing 25 µg/mL kanamycin. Clones of transformed cells were selected and grown in LB medium supplemented with kanamycin. Cells were harvested and plasmids were isolated using an E.Z.N.A. Plasmid Mini Kit. The corresponding attB-containing expression clone was generated by *in vitro* LR recombination reaction of approx. 50 fmol of the attL-containing entry clone and 50 fmol of an attR-containing destination vector pDEST007 or Invitrogen Champion pET300 NT-DEST using LR Clonase II enzyme mix in TE buffer.[210] The expression clone was transformed in chemically competent BL21 *E. coli* cells (Novagen) and selected on LB agar plates containing 100 µg/mL ampicillin. Validity of the clones was confirmed by plasmid sequence analysis. Recombinant clones were grown in ampicillin LB medium and target gene expression was induced with anhydrotetracyclin or IPTG depending on the expression vector used.

ATLam, that was overexpressed using the pET300 NT-DEST, was purified with Profinity IMAC Resin from BioRad corresponding to the manufacture's manual. The protein was desalted into the assay buffer using a GE Healthcare ÄKTApurifier system equipped with a HiTrap Desalting Column (5 mL). Purity was checked *via* SDS-PAGE and coomasie stain.

Peptidoglycan assay To evaluate the effect of vancomycin on the degradation of peptidoglycan *via* ATL the following assay was performed according to published procedures.[211,212] Peptidoglycan from *Staphylococcus aureus* (Sigma-Aldrich) was suspended in ddH_2O to yield 3.3 mg/mL. The molarities given were calculated with respect to the molecular weight of the murein monomers. The

measurement of OD_{600} was carried out with a Tecan Infinite 200 PRO plate reader in 96-well plates with lid and flat well shape at 30 °C.

For inhibitory studies the enzyme was preincubated with vancomycin for 5 min and finally diluted to a concentration of 0,5 µg/ml (7.7 nM) with the substrate suspension of $OD_{600} \approx 0.3$. OD_{600} was measured over 30 min and the 96-well was shaken constantly. The decrease of OD_{600} within this time was set to 100 % for the uninhibited reaction. The other reactions are given in relation to this value (Figure 4). The IC_{50} was determined from the fitted curve shown in Figure 4 as the inhibitor concentration where the protein shows half-maximal activity.

For Michaelis-Menten kinetics, substrate concentrations were varied form 1 mM to 0.125 mM and the corresponding enzyme turnover monitored as described above. The enzyme concentration was kept constant at 7.7 nM. K_M was determined *via* a Lineweaver-Burk plot with the x-intercept of the graph representing $-1/K_M$ (Figure 4). K_I was directly calculated from these values.[213]

Expression analysis *E. faecalis* V583 was grown over night with half maximal MIC of vancomycin and without antibiotic selection. Total bacterial RNA was isolated with the Bio-Rad Aurum Total RNA mini kit and transcribed to cDNA immediately by reverse transcriptase and a random hexamer primer set using an iScript Select cDNA synthesis kit (Bio-Rad). For RT PCR, specific primers were designed for pABC to amplify a sequence specific for this gene of interest with Primer-BLAST. RT PCR was conducted in a two-step thermal protocol using a SsoFast EvaGreen Supermix kit (Bio-Rad) with white Low-Profile 96-Well Unskirted PCR Plates in a Bio-Rad CFX96 Real-Time PCR Detection System. The polymerase was activated in an initial denaturation step for 30 s at 95.0 °C. Forty cycles were then run, consisting each of 5 s at 95.0 °C, followed by 10 s annealing and elongation at 61 °C. A melting curve was measured to ensure specific replication of the target sequences only. GAP and LAS genes were used as internal standards for ΔΔCq analysis. Primer sequences can be found in Table S3. Cq and Cq mean values are shown in Table S2.

Supporting Information: Additional figures containing fluorescent gel scans, primer sequences, mass spectrometry and real time PCR data. This material is available in the appendix.

Author contribution: JE made substantial contributions to conception and design of the experiments and acquisition, analysis and interpretation of MS data, RO did preliminary studies in the synthesis of the probes and for the labeling, SAS drafted the project and the article.

Chapter 2: Pretubulysin derived probes as novel tools for monitoring the microtubule network *via* Activity-Based Protein Profiling and Fluorescence Microscopy

Jürgen Eirich, Jens L. Burkhart, Angelika Ullrich, Georg C. Rudolf, Angelika Vollmar, Stefan Zahler, Uli Kazmaier and Stephan A. Sieber

Published in

Mol. BioSyst., 2012,8, 2067-2075

DOI: 10.1039/C2MB25144B

Received 13 Apr 2012, Accepted 18 May 2012

Abstract Microtubules (mt) are highly dynamic polymers composed of alpha- and beta-tubulin monomers that are present in all dividing and non-dividing cells. A broad variety of natural products exists that are known to interfere with the microtubule network, by either stabilizing or de-stabilizing these rope-like polymers. Among those tubulysins represent a new and potent class of cytostatic tetrapeptides originating from myxobacteria. Early studies suggested that tubulysins interact with the eukaryotic cytoskeleton by inhibition of tubulin polymerization with EC_{50} values in the picomolar range. Recently, pretubulysins have been described to retain the high tubulin-degradation activity of their more complex tubulysin relatives and represent an easier synthetic target with an efficient synthesis already in place. Although tubulin has been suggested as the dedicated target of tubulysin a comprehensive molecular target analysis of pretubulysin in the context of the whole proteome has not been carried out so far. Here we utilize synthetic chemistry to develop two pretubulysin photoaffinity probes which were applied in cellular activity-based protein profiling and imaging studies in order to unravel and visualize dedicated targets. Our results clearly show a remarkable selectivity of pretubulysin for beta-tubulin which we independently confirmed by a mass-spectrometric based proteomic profiling platform as well as by tubulin antibody based co-staining on intact cells.

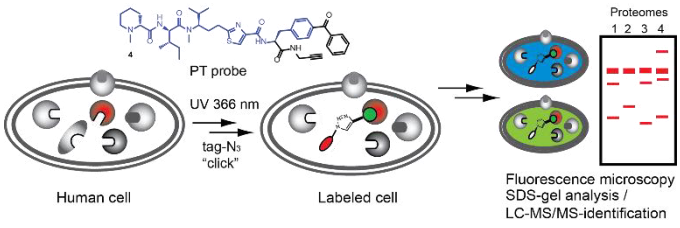

Introduction Microtubules are highly dynamic polymers composed of α- and β-tubulin monomers that are present in all dividing and non-dividing cells.[214,215] These components of the cytoskeleton play a major role in forming the spindle apparatus during mitosis, which was recognized early on as an interesting drug target for selective inhibition of the growth of fast dividing cells, e.g. in cancer.[216-220] A broad variety of natural products originating from different organisms exists which are known to interfere with the microtubule network, by either stabilizing or de-stabilizing these rope-like polymers already since the 1970s.[217,218,221,222] Some of them are marketed drugs, in clinical trials or subject to academic research. In 2000 *Sasse et al.* discovered a new class of cytostatic tetrapeptides originating from myxobacteria termed tubulysins **1** (Figure 1).[223] These molecules are assembled by hybrid polyketide synthases/non-ribosomal peptide synthetases and consist of one proteinogenic, isoleucine (Ile), and three non-proteinogenic amino acids including *N*-methylpipecolic acid (Mep), tubuvaline (Tuv) and a chain extended analogue of either phenylalanine or tyrosine called tubuphenylalanine (Tup) or tubutyrosine (Tut), respectively. Early studies suggested that tubulysins interact with the eukaryotic cytoskeleton by inhibition of tubulin polymerization with EC_{50} values in the picomolar range.[223-225] This potency even exceeds that of other tubulin modifiers such as taxol, vinblastin and epothilone by 20- to 100- fold[226] and consequently ranks tubulysins as the most promising lead structures for pharmaceutical application. However, several prerequisites have to be considered in

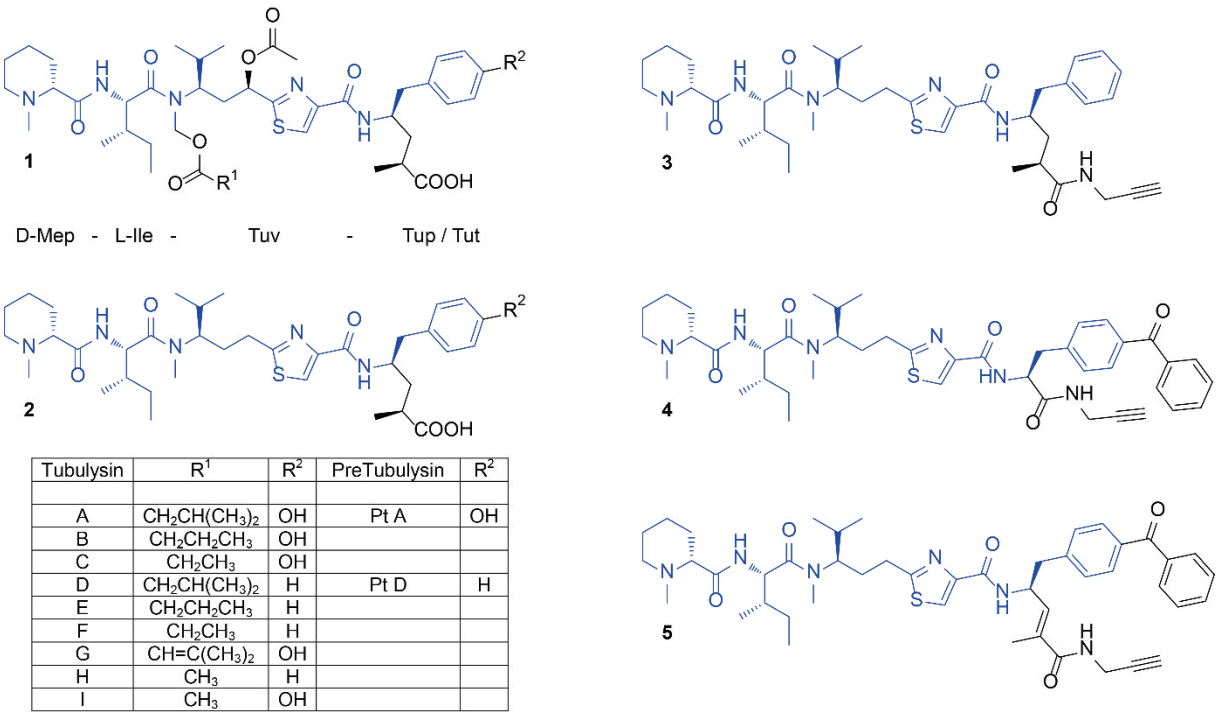

Tubulysin	R^1	R^2	PreTubulysin	R^2
A	$CH_2CH(CH_3)_2$	OH	Pt A	OH
B	$CH_2CH_2CH_3$	OH		
C	CH_2CH_3	OH		
D	$CH_2CH(CH_3)_2$	H	Pt D	H
E	$CH_2CH_2CH_3$	H		
F	CH_2CH_3	H		
G	$CH=C(CH_3)_2$	OH		
H	CH_3	H		
I	CH_3	OH		

*Figure 1: Probe design – Structures of the naturally occurring tubulysins **1** and pretubulysin (Pt) **2** (left) as well as derived probes (Pt propargyl amid **3**, benzophenone probes **4** and **5**) (right) with common core motive indicated in blue.*

order to initiate a drug development program. First, easy synthetic access for natural product derivatization has to be established in order to investigate structure activity relationships (SAR) and provide sufficient compound quantities for pharmacological testing. Moreover, although tubulin has been established as the dedicated target, no information about undesired off-targets in eukaryotic cells is available. Previous SAR studies already revealed several positions with increased tolerance for derivatization.[226-230] One important finding included the replacement of a chemically labile *N,O*-acetal of tubulysin **1** by alkyl groups and the removal of the acetoxy group at the central amino acid tubuvaline (Tuv). The resulting chemically less complex compounds are called pretubulysins (Pt) **2** and have been also found in nature as biosynthetic precursors of the tubulysins (Figure 1).[231,232] Interestingly, pretubulysins retain the high tubulin-degradation activity of their more complex tubulysin relatives and represent an easier synthetic target with an efficient synthesis already in place.[226,233] Here we utilize this well established route to develop two pretubulysin photoaffinity probes **4** and **5** which are applied in cellular activity based protein profiling and imaging studies in order to unravel and visualize dedicated targets (Figure 2).[16,48,187,188,234] Our results clearly show a remarkable selectivity of pretubulysin for tubulin which we independently confirmed by a mass-spectrometric based proteomic profiling platform as well as by tubulin antibody based co-staining on intact cells.

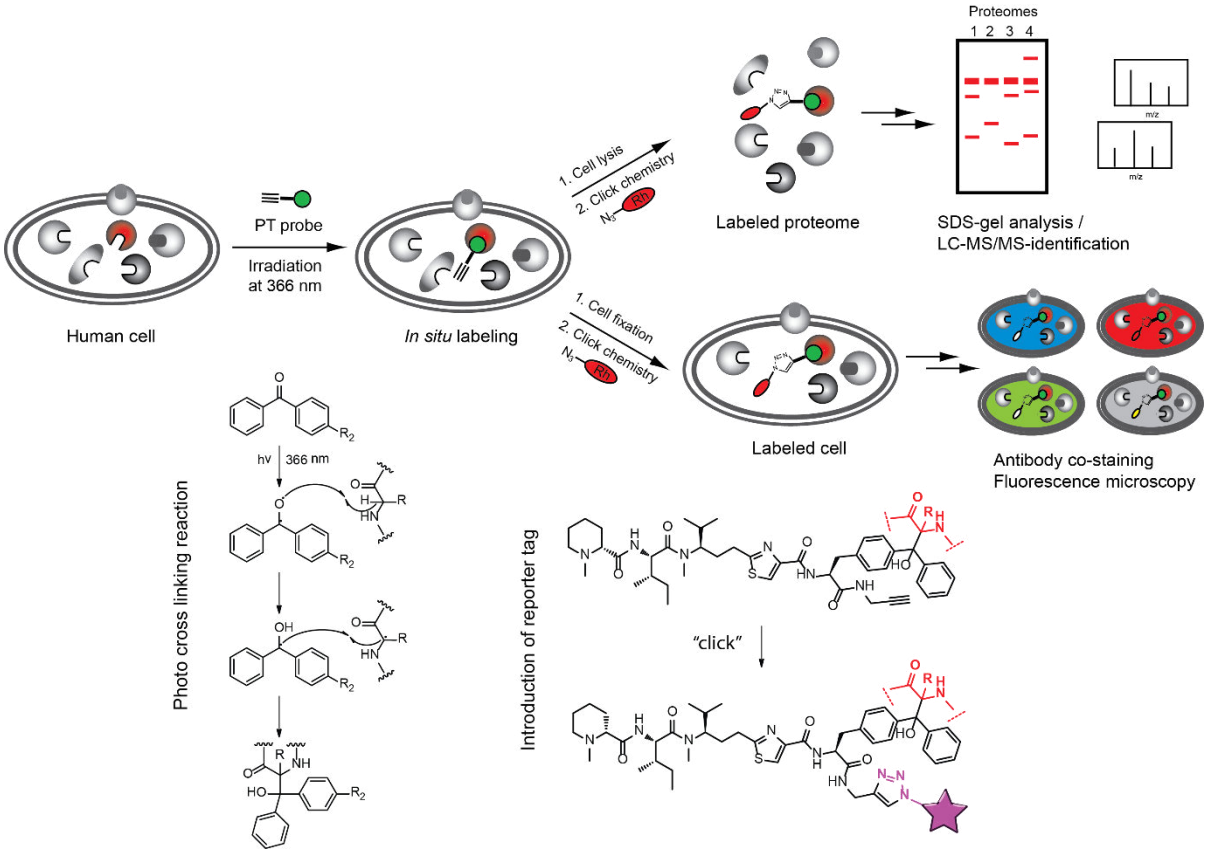

Figure 2: Experimental Design – General labeling procedure with UV-induced cross-link between target protein and probe in living cells (left) enables a broad variety of down-stream applications such as MS based proteomics as well as fluorescence imaging depending on the reporter tag introduced via bio-orthogonal click-chemistry (right).

Methods and Materials

Synthesis For synthetic details please refer to the Supporting Information.

Cell culture The cell lines Hela, H460 and Jurkat were grown in RPMI-1640, A549 in DMEM (high glucose) with 10 % FBS in 5 % CO_2 at 37 °C. The adherently growing cell lines were detached with trypsin-EDTA.

MTT Assay Cells were grown in 96-well-plates at a concentration of 5000 cells per cavity. After removing the growth medium by suction compounds **2**, **3**, **4** and **5** in 100 µL medium (without FBS) with a final DMSO concentration of 1 % were added and the cells incubated for 24 h at 37 °C and 5 % CO_2. After 24 h of exposure, 20 µL (5 mg / mL) filtered MTT stock solution in PBS were added and the medium mixed by gentle pipetting. The cells were incubated at 37 °C and 5 % CO_2 for 1.5 h to allow the MTT to be metabolized and the reaction was controlled under the microscope. Subsequently, the medium was removed and the produced formazan resuspended in 200 µL DMSO by placing the well-plate on a shaking table for 2 min and 650 rpm. The optical density was read out at λ = 570 nm and λ = 630 nm with a Tecan Infinite 200 PRO NanoQuant microplate reader and the background was subtracted at λ = 630 nm. Cells incubated with 1 % DMSO served as control. Three independent replicates were conducted. The EC_{50} values were determined using the non-linear fit for dose response of OriginPRO 8.5.1.

In vitro Analytical Labeling Experiments Cells were detached by scraping from the culture dishes. The pellet was homogenized in PBS by sonication with a Bandelin Sonopuls instrument with 5 x 15 sec pulsed at 70 % max. power under ice cooling. Proteome samples were adjusted to a final concentration of 2 mg protein/mL by dilution in PBS prior to probe labeling. The experiments were carried out in 43 µL total volume, such that once click chemistry (CC) reagents were added, a total reaction volume of 50 µL was reached. In the case of competitive displacement experiments Pt was added and the proteomes were preincubated with the compound for 15 min at 22 °C. Reactions were initiated by addition of varying concentrations of probe and allowed to incubate (additional) 15 min at 22 °C. Then they were irradiated in open polystyrene microwell plates for 60 min on ice with 366 nm UV light (Benda UV hand lamp NU-15 W). For heat controls the proteome was denatured with 2 % SDS (4 µL of

21.5 % SDS) at 95 °C for 6 min and cooled to 22 °C before the probe was applied. Following incubation, 13 µM rhodamine-azide (Rh-N_3) (1 µL) followed by 1 mM TCEP (1 µL) and 100 µM TBTA ligand (3 µL) were added. Samples were gently vortexed and the cycloaddition was initiated by the addition of 1 mM $CuSO_4$ (1 µL).

The reactions were incubated at 22 °C for 1 h. For gel electrophoresis, 50 µL of 2 x SDS loading buffer was added, and 50 µL applied on the gel. Fluorescence was recorded in a Fujifilm LAS4000 luminescent image analyzer with a Fujinon VRF43LMD3 lens and a 575DF20 filter.

In situ Analytical and Preparative Experiments For preparative *in situ* studies cells were grown to 80 – 90 % confluence in cell culture petri dishes. After suction and washing with PBS, compound **5** was added in 15 mL medium without FCS and a final DMSO concentration of 0.1 %. The cells were incubated with the probe for different periods of time at 37 °C and 5 % CO_2. The medium was removed and the cells were covered with PBS prior to UV irradiation (0 °C, 1h, 366 nm). The cells were detached with a cell scraper, washed with PBS and the pellet homogenized by sonication. The proteomes were separated into cytosolic and membrane fractions, followed by CC either in 43 µL for analytical ABPP experiments or in a final volume of 1 mL of proteome sample with 20 µM trifunctional linker (2 µL), 1 µM TCEP (10 µL) and 100 µM TBTA ligand (30 µL) for preparative ABPP. Samples were gently vortexed, and the cycloaddition was initiated by the addition of 1 mM $CuSO_4$ (10 µL).

Reactions for enrichment were carried out together with a control lacking the probe to compare the results of the biotin-avidin-enriched samples with the background of unspecific protein binding on avidin-agarose beads. After CC proteins were precipitated using a 5-fold volume of prechilled acetone, samples were stored at – 20 °C for 60 min and centrifuged at 16000 g for 10 min. The supernatant was discarded and the pellet washed two times with 200 µL of prechilled methanol and resuspended by sonication. Subsequently, the pellet was dissolved in 1 mL of PBS with 0.2 % SDS by sonication and incubated under gentle mixing with 50 µL of avidin-agarose beads (Sigma-Aldrich) for 1 h at room temperature. The beads were washed three times with 1 mL of PBS/0.2 % SDS, twice with 1 mL of 6 M urea, and three times with 1 mL of PBS. 50 µL of 2 x SDS loading buffer were added and the proteins were released for preparative SDS-PAGE by 6 min incubation at 95 °C. Gel bands were isolated, washed, and tryptically digested as described previously.[235]

Mass Spectrometry and Bioinformatics Tryptic peptides were loaded onto a Dionex C_{18} Nano Trap Column (100 µm) and subsequently eluted and separated by a Dionex C_{18} PepMap 100 mm (3 µm)

column for analysis by tandem MS followed by high-resolution MS using a coupled Dionex Ultimate 3000 LC-Thermo LTQ Orbitrap XL system. The mass spectrometry data were searched using the SEQUEST algorithm against the corresponding databases *via* the software "Proteome Discoverer 1.3". The search was limited to only tryptic peptides, two missed cleavage sites, monoisotopic precursor ions, and a peptide tolerance of < 5 ppm.[196,235]

Fluorescence imaging HeLa cells were seeded in carriers compatible with high resolution microscopy (µ-slides, Ibidi). After two days, cells were incubated with the respective pretubulysin derivatives for 1 to 30 min. Subsequently the cells were irradiated (366 nm) at 37 °C (in order to keep the microtubules intact) for 10 min, and then rapidly fixed in methanol (- 20 °C). After 3 washing steps in PBS, cells were incubated for 20 min with a freshly prepared solution containing 775 µl PBS, 20 µl $CuSO_4$ (50 mM), 5 µl dye-azid (5 mM), and 200 µl ascorbic acid (500 mM). After three times washing with PBS, the cells were incubated with primary tubulin antibody (1:400, abcam rabbit anti β tubulin) for 60 min, washed again three times, and the incubated with secondary antibody (goat anti rabbit AlexaFluor 488, Invitrogen, 1:400) and 1 µg/ml HOECHST for nuclear staining for 45 min. After three final washing steps, the samples were mounted with Permafluor (Thermo Scientific) and glass cover slides. The samples were observed on a confocal laser scanning microscope (LSM510 meta, Zeiss) with a 63x lens, using a pinhole diameter, which generates optical slices of 1 µm thickness.

Results and discussion

Chemical probe desgn and synthesis One major challenge in the design of photoaffinity probes for target discovery is the introduction of the photolinker as well as the tag which is required as a reporter for protein identification. While the tag is usually a small alkyne moiety that can be modified by post-labeling *via* the Huisgen-Sharpless-Meldal cycloaddition[136,140,141,236] the photolinker is bulky and may cause a steric clash in the active site pocket / binding site of the target protein (Figure 2).[237,238] Therefore, a careful chemical design is required in order to incorporate the photolinker in a way that it is at least partially embedded into the compound scaffold. As pretubulysin **2** exhibits a *C*-terminal tubuphenylalanine (Tup) moiety which can be modified with only little loss of activity according to SAR[227-230] studies we decided to expand its aromatic system by carbonylative cross coupling to a photoactive benzophenone moiety.

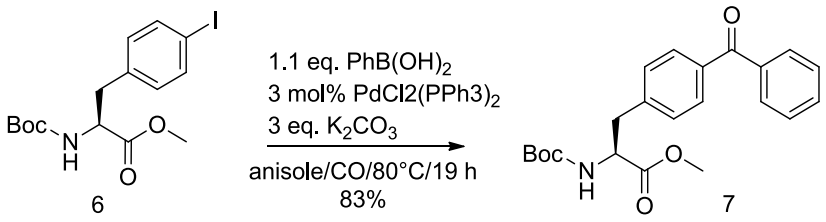

*Scheme 1: Carbonylative Cross-coupling leading to pB-Phe **7**.*

In order to assemble the pretubulysin photo probe we first established a reliable synthetic procedure for the p-benzoyl-phenylalanine (pB-Phe) building block (Scheme 1) before the more complex p-benzoyl-tubuphenylalanine (pB-Tup) moiety was approached. Carbonylative Suzuki coupling of Boc-p-iodophenylalanine methylester (**6**), prepared in three steps according to literature procedure,[239] with phenylboronic acid gave the desired product **7** in very good yield (83 %). For the synthesis of pB-Tup, **6** was first reduced to the corresponding aldehyde with DibalH and subsequently coupled with Wittig reagent **8** in a one-pot reaction to yield the p-iodo-tubuphenylalanine derivative (**9**). This compound was further modified with the above mentioned carbonylative Suzuki coupling to yield derivative **10** which closely resembles the desired building block with the exception of the double bond that is saturated in the natural product (Scheme 2). All attempts to selectively hydrogenate this bond failed

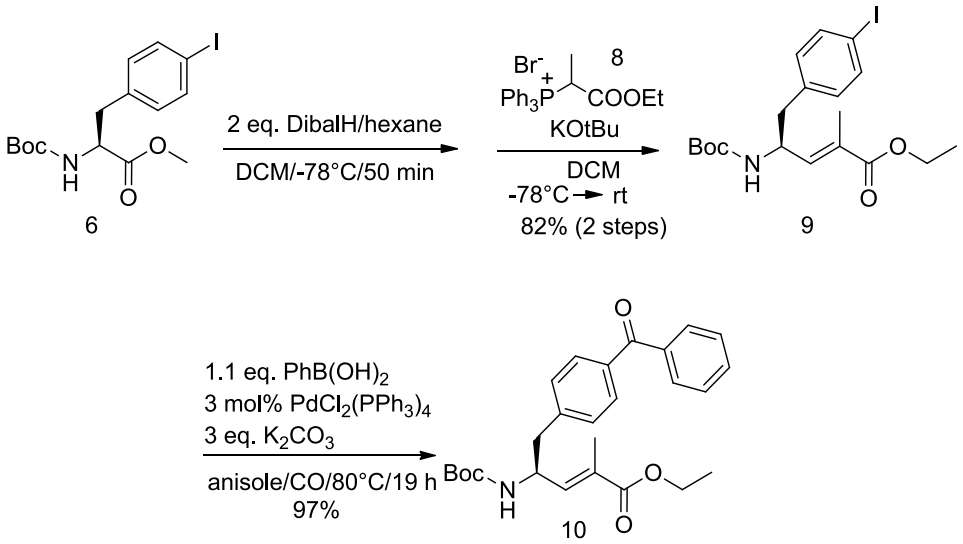

*Scheme 2: Synthtic route leading to pB-Tup precursor **10**.*

due to the loss of the carbonyl function within the benzophenone moiety. We therefore used the unsaturated precursor building block (**10** – Scheme 2) together with the shorter pB-Phe in order to assemble two structurally different pretubulysin probes **4** and **5**.

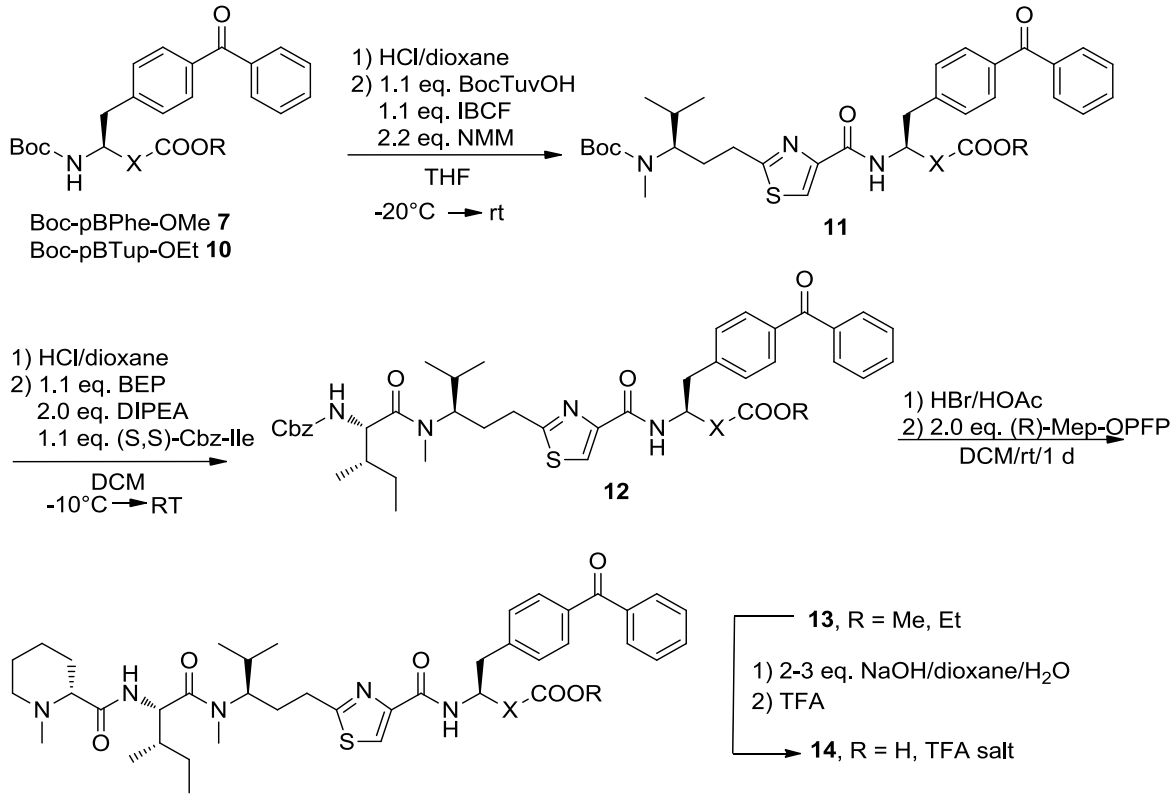

Compound	**pBTup/pBPhe**	X-COOR	**11**	Yield	**12**	Yield
	7	—COOMe	**11a**	85%	**12a**	86%
	10	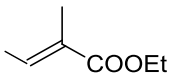	**11b**	92%	**12b**	90%
Compound	**12**	X-COOR	**13**	Yield	**14**	Yield[a]
	12a	—COOMe	**13a**	84%	**14a**	97%
	12b	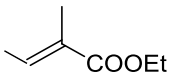	**13b**	66%	**14b**	92%

[a]isolated as TFA salt

*Scheme 3: Reactions leading to cross-linkable Pt derivatives **14** with deprotected C-terminus.*

The synthesis of both probes is outlined in Scheme 3 and 4. In brief, the two benzophenone precursors **7** and **10** were deprotected with HCl in dioxane and subsequently coupled with *N*-Boc-tubu-valine which was activated as a mixed anhydride. The *N*-terminal tripeptide was prepared according to literature procedures.[231,232] Subsequent deprotection and coupling with Cbz-(S,S)-isoleucine as well as (R)-*N*-methyl-pipecolic acid-pentafluorophenyl ester ((R)-Mep-OPFP), after Cbz-deprotection, gave the two *N*-methylated tetrapeptides (**13 a**/**b**) in good yields (Scheme 3). In the next step, the methyl

respectively ethyl ester was saponified with NaOH and the free tetrapeptides were converted to the TFA-salts to get the benzophenone derivatives **14** in excellent yield. Finally, propargylamine was coupled to the *C*-terminus yielding the desired probes **4** and **5** (Scheme 4).

In order to gain insights into the structure activity relationship (SAR) of the probe scaffolds we also prepared pretubulysin D (**2**) as well as its *C*-terminal alkynylated derivative (**3**) as reference compounds according to previous procedures.[102,103]

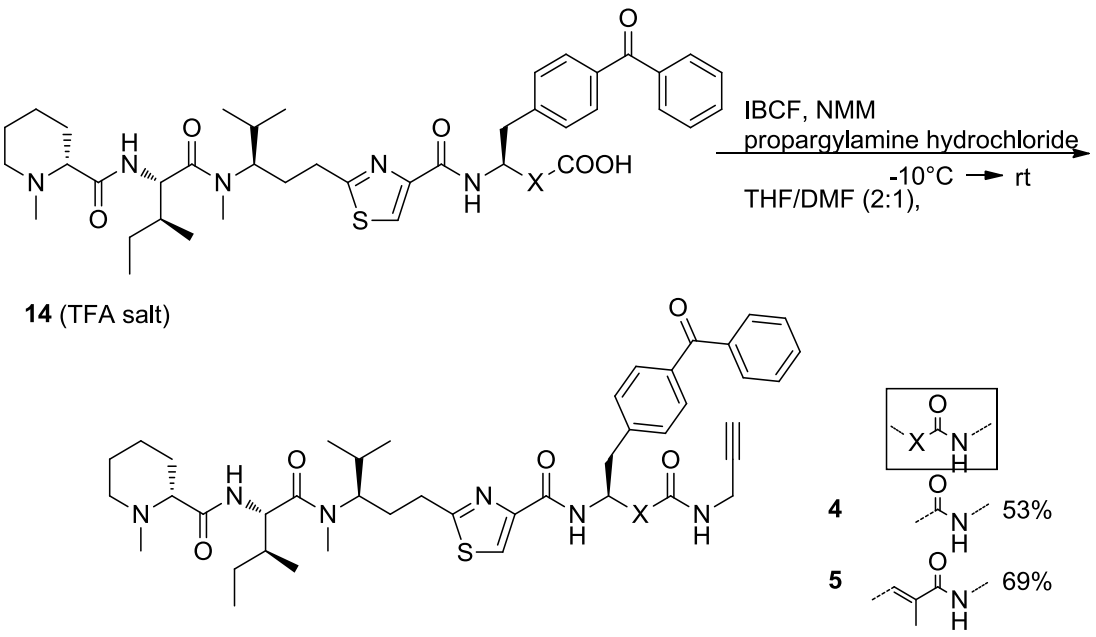

*Scheme 4: Final amide coupling reaction to introduce alkyne tag yielding desired probes **4** and **5**.*

Bioactivity

*Table 1: EC_{50} values for compounds **2**, **3**, **4** and **5** determined via MTT (24 h incubation time) in four different cell lines.*

	compound [µM]			
cell line	**2** (Pt)	**3**	**4**	**5**
Hela	0.02	1.2	7.9	13.4
H460	0.02	1.0	8.1	9.6
Jurkat	< 0.01	0.5	8.5	9.2
A549	3.9	40	27	43

Pretubulysin **2** exhibits very potent cytotoxycity against various cell-lines with EC_{50} values in the low nM range (Table 1).[102,103,226,233] In order to investigate the effect of structural remodeling on probe

potency we tested all three derivatives against various cell lines and obtained a significant drop in potency for probes **4** and **5**. The bioactivity of alkynylated derivative **3** was significantly better compared to the photo-probes emphasizing a higher tolerance for small modifications at the *C*-terminus. Although the introduction of the additional benzoyl moiety at the phenyl ring of tubuphenylalanine represented the least structural perturbation in order to gain access to benzophenone possible, the drop in potency indicated that this position is quite sensitive for alterations. Nevertheless, the obtained EC_{50}s of 8-13 µM for both probes still reflect elevated cytotoxicities with an unresolved mechanism of action. Since all results of cellular profiling will be validated with the unmodified natural product, e.g. in competitive profiling experiments (see below), the probes represent suitable tools and a promising starting point for target discovery.

Pretubulysin target analysis With the tool compounds in hand we next analyzed the cellular target(s) that are responsible for the observed cytotoxicity. Both probes were incubated for 1 h with intact Hela cells under *in situ* conditions (Experimental Section) and irradiated for 1 h at 360 nm in order to establish a covalent link between the probe molecule and all bound proteins.[235] Cells were lyzed by sonication and cytosolic as well as membrane fractions separated by centrifugation. Subsequent CC with a fluorescent rhodamine- azide tag followed by SDS polyacrylamide gel separation and fluorescent scanning revealed distinct bands that varied in intensity depending on the applied probe concentration (Figure 3, Supporting Figure 1).[184,185,240] While 500 µM, the highest concentration applied, led to the labeling of several proteins, a gradual reduction of probe concentration down to 1-10 µM significantly reduced the number of protein bands. One intense band with a molecular weight of about 60 kDa was labeled under all probe concentrations applied emphasizing a significant specificity and affinity of the probes for this protein target. Contrary, labeling of this band disappeared when Hela cell lysate was first denatured by heat treatment and subsequently labeled by the probe emphasizing a specific interaction between the folded protein and the probe (Supporting Figure 2) . A comparison of both concentration dependent labeling experiments suggests that probe **4** with the shorter C-terminal end exhibits a more pronounced selectivity for the above mentioned protein target compared to probe **5** (Supporting Figure 3). Based on the better labeling profile as well as the slightly higher cytotoxicity we conducted all subsequent labeling experiments with probe **4**. In order to evaluate the optimal pre-incubation time probe **4** was incubated with intact Hela cells for several durations ranging from **5** to 120 min. Subsequent irradiation for 1 h and in gel fluorescent scanning revealed that 60 min were already sufficient for effective labeling (Supporting Figure 4).

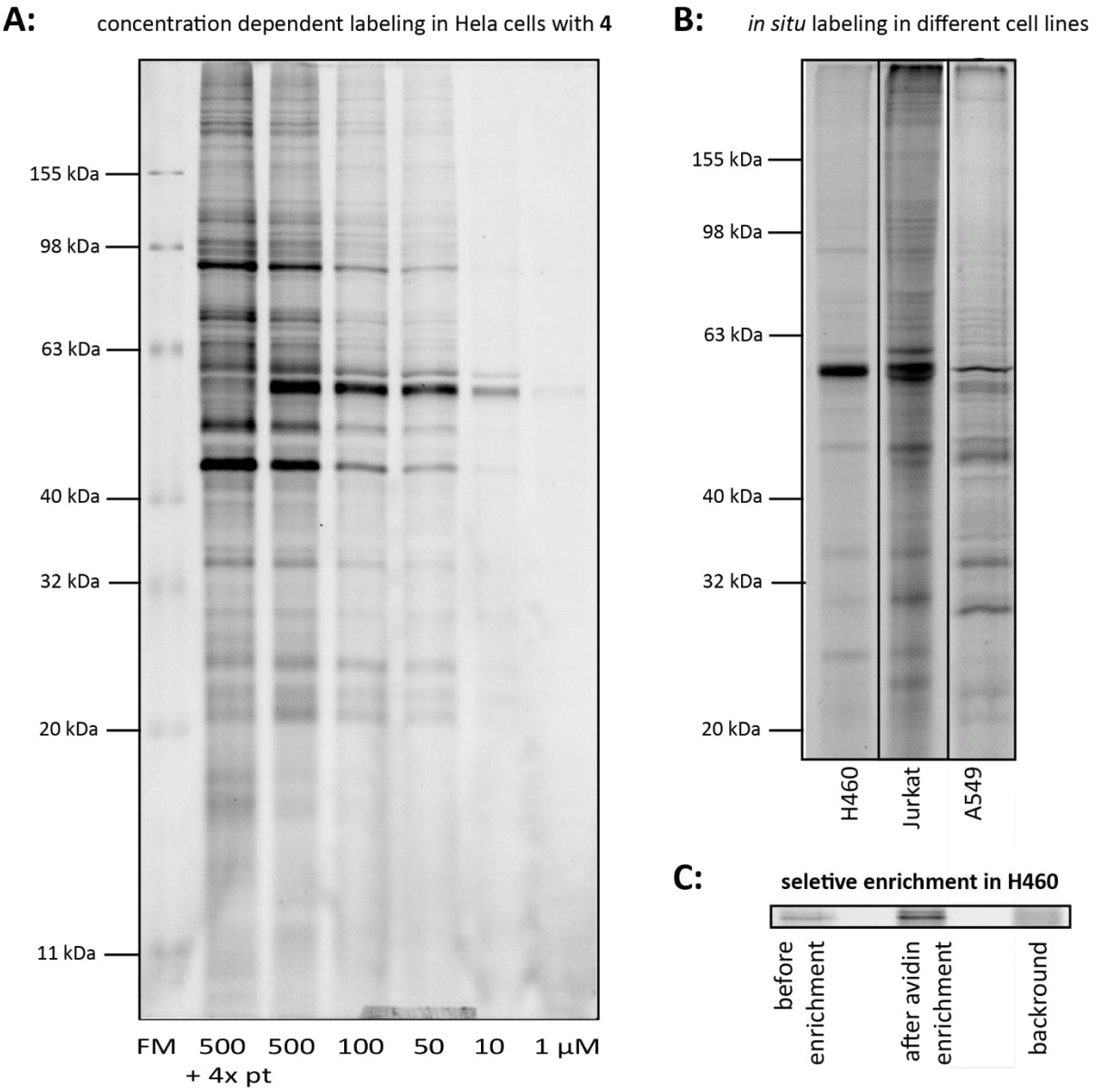

*Figure 3: Fluorescence scans of the in situ labeling in Hela cells with probe **4** (1 – 500 µM) in competition with Pt **2** (2 mM) (A) and in comparison with other cell lines (10 µM **4**) (B), selective enrichment of tubulin in H460 (5 µM **4**) (C).*

In order to evaluate which of the labeled protein bands in Hela cells corresponds to pretubulysin binding, we added the unmodified natural product in varying excess to intact cells followed by the probe and applied the standard irradiation labeling procedure. Interestingly, a 4-fold excess of pretubulysin was already sufficient to totally block the labeling of the prominent 60 kDa band which emphasizes a high affinity of the unmodified natural product for the protein binding site. Profiling of several other cell lines including H460, Jurkat and A549 with probe **4** at a concentration close to the EC_{50} (10 µM) revealed an intense protein band at the same molecular weight as the one observed in Hela emphasizing that the target is highly conserved throughout the different cell lines.

To reveal the identity of this protein band we utilized a proteomic enrichment strategy and incubated Hela cells with probe **4** followed by irradiation, lysis and CC in order to attach a trifunctional rhodamine-biotin-azide tag (Supporting Information).[235] The labeled protein was selectively enriched by binding to avidin beads and separated on a SDS gel after heat cleavage (Figure 3c). The enriched band was isolated, washed, tryptically digested and subject to mass spectrometric analysis. Peptide fragments were analyzed *via* the proteome discoverer software with the SEQUEST search algorithm. All experiments were carried out with a control in which no probe was added in order to subtract proteins that bind unspecifically to avidin. All experiments conclusively revealed tubulin as the primary target of the probes (Supporting Table 1). While inhibition of tubulin polymerization by tubulysin has been shown in *in vitro* assays previously,[223-225,241] it is an important result that the structurally less complex precursor pretubulysin also interacts specifically with tubulin explaining its potent bioactivity. Although our probes are significantly less potent compared to the unmodified natural product, competitive labeling demonstrates that pretubulysin specifically binds to tubulin with high affinity. However, based on our ABPP experiments we cannot exclude that other pretubulysin targets may exist which are not detectable by our probes. Due to the restrictions of ABPP, e.g. photocrosslinker, this problem cannot be easily resolved. Since tubulin represents at least a major target of pretubulysin which was detected for the first time *via* full proteome analysis we will focus on this protein and study the cellular effect of tubulin binding in more detail.

Fluorescence imaging Besides target identification another advantage of the probe molecules is their utility in imaging studies which is suitable to independently confirm the target and reveal insights into the function and possible effects of binding. We therefore incubated living Hela cells with various concentrations of probe **4**, irradiated the cells to covalently attach the molecule to the target protein and subsequently fixed the cells with methanol after different time points ranging from 1 to 30 min. Fixed cells were reacted with CC reagents (rhodamine-azide, ascorbic acid, ligand and $CuSO_4$), Hoechst DNA stain as well as tubulin antibodies for the visualization of the probe, the nucleus as well as microtubuli, respectively. A control experiment without the probe but in the presence of CC reagents revealed low background binding of the rhodamine dye which is mandatory for the visualization of specific binding partners (Figure 4a). While these pretubulysin untreated cells reveal a tight mesh of microtubuli, a 1 min incubation of 3 µM probe **3** already initiates significant damage of the filament assembly (Figure 4b). Interestingly, the same phenotype has been reported for pretubulysin previously[242-244] but so far the direct binding to tubulin could not be directly confirmed. Here we demonstrate by co-staining with the tubulin directed antibody as well as the fluorescent probe that pretubulysin derivative **4** binds to monomeric tubulin which appear as little spots in the image (Figure 4c and d). The sequestration of tubulin monomers prevents the filament assembly and explains its time dependent dissolution. The results of all imaging experiments are in line with our MS based

target analysis and demonstrate that monomeric tubulin is the point of pretubulysin attachment leading to inhibition of filament assembly and subsequent cell death.

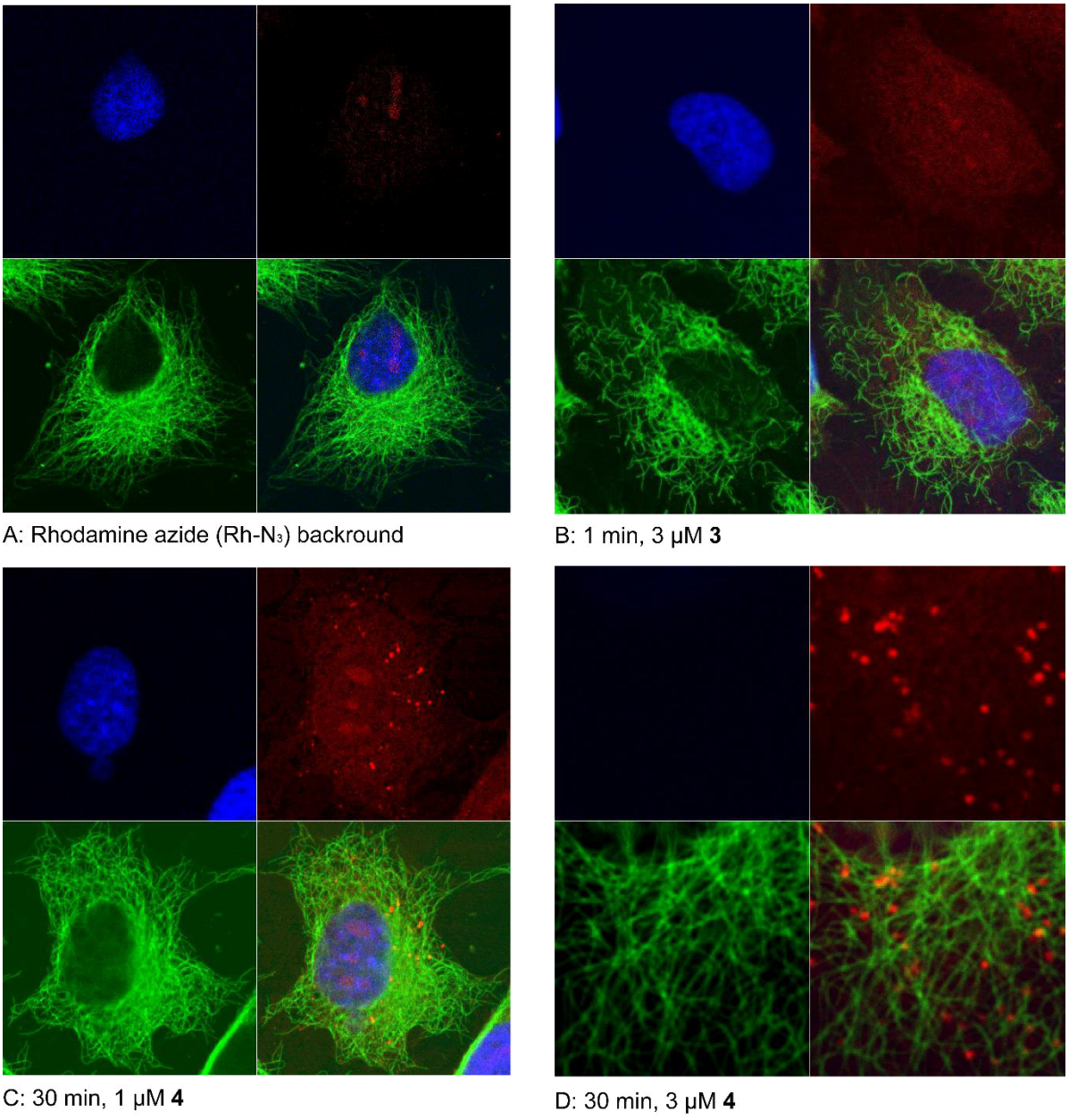

Figure 4: Fluorescent microscopy: A – D: top left - blue Hoechst, top right - red Rh-N_3, bottom left - green Antibody-Alexa488-conjugate, bottom right - overlay. Probe treatment of cells indicated individually.

From a chemical biology perspective photocrosslinking probe **4** revealed superior imaging properties over compound **3** that lacks the photoreactive moiety. Although compound **3** exhibited a stronger effect on microtubule assembly, the reversible binding was not stable enough to survive the washing procedures. Since photo-linkage is mandatory for the visualization of pretubulysin binding, a next

generation of photocrosslinking probes should focus on the introduction of smaller linker moieties such as diazirines in order to maintain the original potency.

In conclusion we designed and synthesized customized pretubulysin probes that revealed tubulin as the main target in living human cells. Although the introduction of the photocrosslinking moiety reduced the biological potency, competitive labeling studies revealed that beta tubulin is the dedicated binding partner of the unmodified natural product. Moreover, the application of both probes at concentrations close to their EC_{50} value (10 µM) revealed only beta tubulin as the predominant target emphasizing that this interaction is solely responsible for cell toxicity of these molecules. However, we cannot exclude that additional targets of pretubulysin may exist that could not be identified here due to the steric bulk of the photolinker. The results obtained in this study demonstrate the utility of our approach to identify tubulin as the main target within living cells of different origin as well as to monitor tubulin binding in cells and its associated inhibition of microtubuli assembly.

Supporting Information: Additional Fluorescent Gel Scans, MS Data, Compound Structures and synthesis of Trifunctional linker, Synthetic Procedures for Pretubulysin probes can be found in the appendix.

Author contribution: JE conceived and carried out the cell based experiments as well as the MS data acquisition and analysis, JLB and AU conducted the synthesis of the pretubulysin derivatives, GCR planed and conducted the synthesis of the new trifuntional linker, AV drafted the project and the article, SZ conducted the fluorescent microscopy experiments, UK drafted the synthesis of the pretubulysin derivatives, SAS drafted the project and the article.

Chapter 3: *N*-(1-(2-oxo-2-(phenylamino)ethyl)piperidin-4-yl)benzamides as reversible inhibitors of the protein disulfide isomerase

Abstract A major problem in cancer therapy is chemoresistance. Understanding the underlying mechanisms and finding the involved targets to fight this process is a key challenge in cancer research. Tumor cells are often characterized by mechanisms to sustain the stress induced by drug treatment. This results in the upregulation of Endoplasmic Reticulum (ER)-chaperones which then support cell survival and proliferation. The Protein Disulfide Isomerase (PDI) is one of those stress responders. It was shown to have a broad variety of substrates *in vitro* and can catalyze thiol exchange reactions of both intra- and intermolecular disulfide bonds.

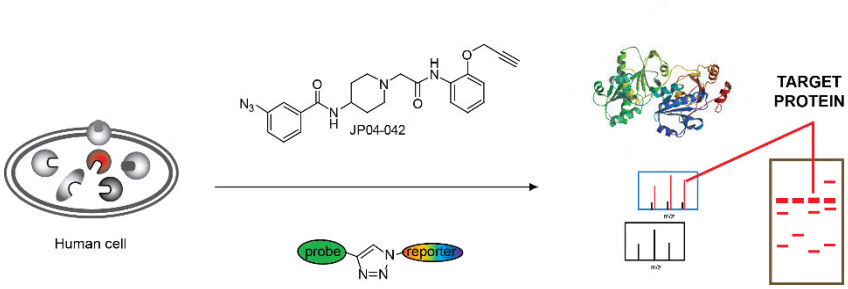

The role of PDI in diseases reaches far beyond cancer as it mediates the entry of toxins and viruses and plays a role in neurological disorders and infertility. Only a limited number of specific inhibitors was however published in the recent years.

A class of 21 small molecules, termed T8-xx, which strongly increased the sensitivity of various tumor cell lines to different chemotherapeutics without being cytotoxic themselves was found and characterized by Lilianna Schyschka. As the molecular target of these compounds is still unknown a probe was designed and synthesized. This molecule was used for a chemical proteomics approach to reveal its protein target(s).

The identification of PDI as an almost exclusive target of this compound was followed by *in vitro* characterization and validation. These experiments can promote chemical optimizing procedures and structure activity relationship studies.

This might represent a starting point to further investigate the interaction of the T8 family and the PDI *in vivo*, study their effect on cellular stress or their potential use as a chemo sensitizing agent.

Introduction

A major problem in cancer therapy is chemoresistance which heavily impairs the treatment of patients.[245-251] Both understanding the underlying mechanisms and finding new protein targets and agents to fight resistance against chemotherapeutic drugs remain key challenges in cancer research. Tumor cells are often characterized by general mechanisms to sustain high levels of cellular stress such as those induced by chemotherapeutic drugs.[252] Resistance results from numerous genetic and epigenetic changes occurring in cancer cells. They lead to dysregulation of intracellular signaling pathways. One of those alterations is the inability of cancer cells to undergo apoptosis or other types of programmed cell death.[253-255]

Tumor cells have developed a vast number of strategies to circumvent programmed cell death. The overexpression of anti apoptotic proteins like Bcl2 (B-cell lymphoma 2) or XIAP (X-linked Inhibitor of Apoptosis Protein) are just two examples for this strategy.[256] The knowledge of these mechanisms has led to the design of IAP (Inhibitor of Apoptosis Protein) inhibitors[257] or BH3 (Bcl-2 Homology domain 3) mimetics[258-260]. Endoplasmic Reticulum (ER)-chaperones are additional important players contributing to cancer cell survival and resistance to anticancer therapies. Since those cells proliferate rapidly they show increased levels of protein synthesis and need enhanced ER capacity and function.[261-263] Cells under ER-stress cope with this situation by the activation of the Unfolded Protein Response (UPR).[264] This also happens in cancer cells upon treatment with chemotherapeutics.[265-270] ER-chaperones such as Glucose Regulated Protein (GRP) 78 (Binding Protein - BiP)[271-280] or Protein Disulfide Isomerase (PDI) are upregulated and play an important role in the maintenance of ER homeostasis. As ER stress plays a critical role in tumor development and other diseases targeting ER-chaperones represent a suitable target to fight chemoresistance and others.[281-287]

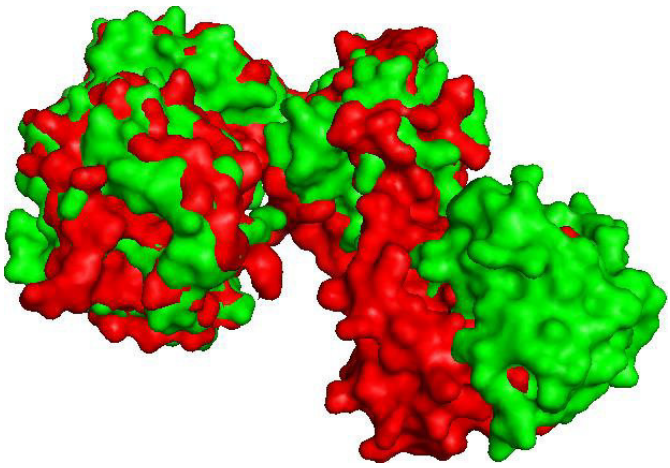

Scheme 1: Overlay of the surface representation of PDI derived from the crystal structure of its reduced (red, PDB-ID 4EKZ) and oxidized (green, PDB-ID 4EL1) form.[14]

The first identification of PDI-like activity in extracts from pancreas or liver was independently reported by *Venetianer*[288,289] and *Goldberger*[290] in 1963. The mature form of human PDI has 491 amino acids. Recently the crystal structures of the human full length PDI both in its reduced and its oxidized state have been published.[14] They are shown in Scheme 1. The protein is organized in four distinct domains, termed *a*, *b*, *b0*, and *a0*, plus a highly acidic C-terminal extension *c* and a 19-amino-acid interdomain linker between the *b0* and *a0* domains named *x*. This domain structure was revealed earlier by a combination of intron-exon analysis, partial proteolysis studies and the expression and characterization of isolated domains and their combinations.[291-294] The *a* and *a0* domains share significant homology with each other as well as with thioredoxin. Their geometry is varying in the different redox states (Scheme 1, lower right).

The PDI was shown to have a broad variety of substrates *in vitro*, including soybean and bovine pancreatic trypsin inhibitor[295,296], insulin[297,298], immunoglobulins[299-301], cholera toxin[302], ricin[303], and procollagen[304].

The enzyme can catalyze thiol disulfide exchange reactions (oxidation, reduction, isomerization) of both intra- and intermolecular disulfides. In addition PDI has also been suggested to have molecular chaperone activity.[305] It assists in the folding of proteins that contain disulfide bonds[306-308] as well as in the refolding of proteins bearing none[309,310]. The role of PDI in diseases reaches far beyond cancer and was recently reviewed by *Benham*[311]: The isomerase mediates the entry of toxins and viruses and plays a role in neurological disorders and infertility.

Although the PDI is well characterized and seems to have many cellular functions only a limited number of specific inhibitors was published in the recent years:

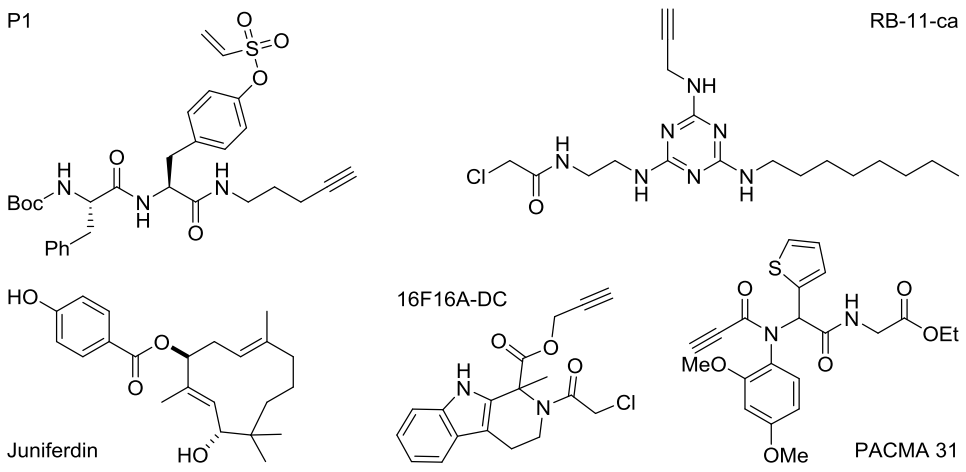

Scheme 2: Structures of known PDI inhibitors or derived probes.

P1[312], Juniferdin[313], 16F16[314], RB-11-ca[78], PACMA 31[315], Estradiol[316], 3,3',5-triiodo-L-thyronine (T3)[317]. Among those only P1, 16F16, RB-11-ca and PACMA 31 (all shown in Scheme 2) have been applied as specific PDI inhibitors but modify the enzyme in a covalent manner. However, their irreversible mode of action is undesired for pharmaceutical applications.[318-322] Covalent agents can cause heavy toxicity by indiscriminately binding off-target proteins or other cellular macromolecules.[323,324] The target protein can regain its activity when the inhibitor possesses an off-rate that is slower compared to the rate of re-synthesis of the target *in vivo*.[322]

Lilianna Schyschka tested a commercially available compound library containing a class of 21 small molecules (T8 – T8-20, two examples shown in Scheme 5). These compounds strongly increased the sensitivity of various tumor cell lines to different chemotherapeutics. They showed no effect and were not cytotoxic in non-tumor cells up to 25 µM.[325] Different biological effects caused by those compounds were characterized. In combination with known chemotherapeutic drugs, the T8 family leads to pronounced caspase-dependent apoptosis rates, inhibits clonogenic survival in a synergistic manner and displays chemosensitizing effects *in vivo.*

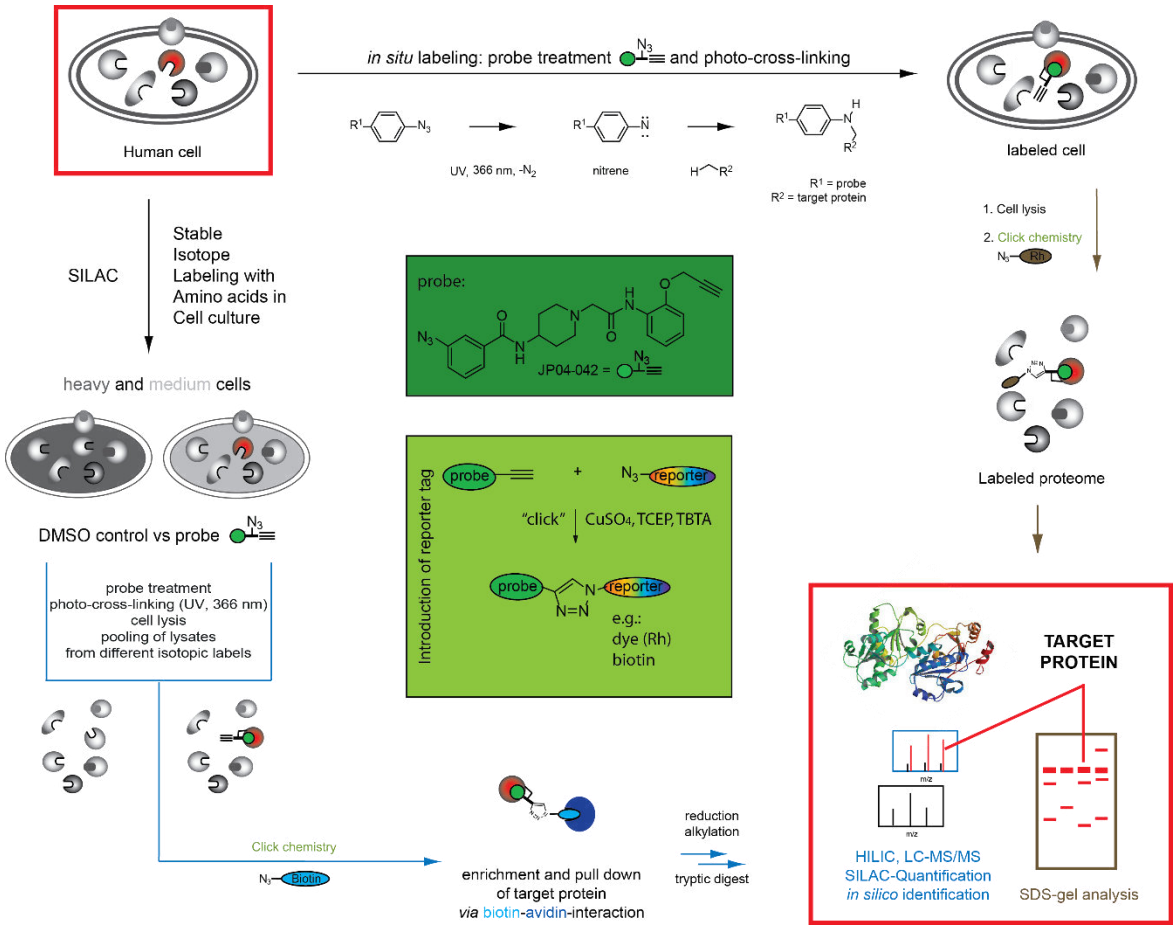

Scheme 3: Experimental design. The combination of an analytical, gel-based and a gel-free, preparative in situ labeling strategy leads to a synergistic identification and validation of the target protein. Crystal structure of PDI (4EL1) [14].

Identification and characterization of the protein targets of the T8 series

A probe was designed and synthesized by Judith Peters from the *Kazmaier* group (Universität des Saarlandes - JP04-042 is shown in Scheme 3 and 5) to gain deeper insight into the molecular bases of this effect. The aim was to use this molecule for a chemical proteomics approach[16-19] as a photo probe[326] and to reveal its and its parental compound's protein target(s) using SILAC[80,327,328] for a quantitative mass spectrometry (MS) analysis. The identification of PDI as an almost exclusive target of JP04-042 was followed by chemical optimizing procedures, structure activity relationship studies and *in vitro* characterization and validation of PDI as a promising novel target for chemo sensitization.

Results and discussion

The data so far suggests that the molecular target of JP04-042 is PDI. The photo probe, as well as the newly synthesized T8-derived structures (PSxz, Scheme 5) are promising PDI inhibitors *in vitro*. In order to identify the cellular targets of the T8 compound class A*ff*inity-Based Protein Profiling (AfBPP)[16-19,326] was performed. For this technology, the molecular scaffold needs to be equipped with an alkyne handle as well as a photo reactive group. A photo-cross-linker forms a reactive intermediate upon UV irradiation. This is trapped *via* the formation of a stable covalent bond between probe and target. This linkage persists all subsequent denaturing procedures down to the actual protein identification. In order to keep the compound small and cell permeable the attachment of a bulky rhodamine or biotin tag for the visualization and identification by MS was performed after protein binding and irradiation. The introduction of the reporter is mediated by click chemistry (CC). The reaction involves an alkyne incorporated in the probe and an azide incorporated in the tag. Based on the molecular structure of T8 the *Kazmaier* group rationalized that simple chemical manipulations would allow the introduction of the alkyne at various positions. As the original compound class carries a halogenated aromatic ring system the replacement of this moiety by an azide as a pseudohalogen yielding a phenlyazide was a straight forward way to introduce a powerful photolinker.[123,126] These conservative structural modifications would closely mimic the original structure and keep the affinity to the desired molecular targets.

T8 target identification

To identify the cellular targets of T8, human cancer cell lines (MDA-MB 231 and HeLa) were incubated with the photo probe JP04-042 in varying concentrations (Figure 1A). The probe was cross-linked to its cellular targets *in situ* in living cells *via* UV irradiation.

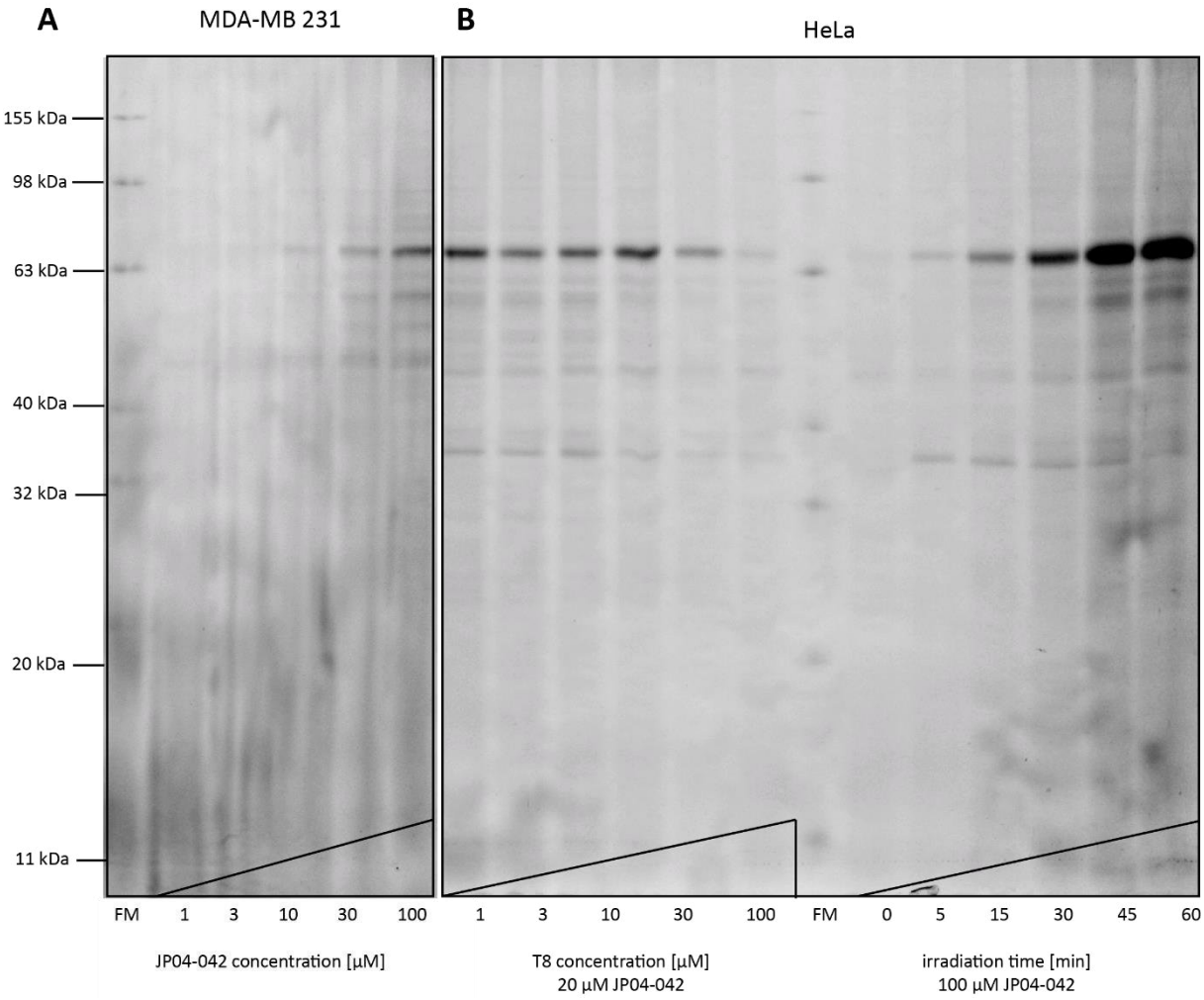

Figure 1: Analytical in situ *labeling. Fluorescent scans of gels after SDS-PAGE. Panel A: Concentration dependent labeling of living MDA-MB 231 breast cancer cells with JP04-042. Panel B: left: Competitive labeling of living HeLa cells with stable concentrations of JP04-042 and T8. right: time dependent labeling with varying irradiation times.*

After cell lysis a rhodamine azide, representing a reporter dye, was introduced *via* CC[136,139-141], to visualize potential targets on SDS-PAGE by fluorescent scanning. Different irradiations times (Figure 1B, right panel) and labeling conditions (e.g. probe dilution in DMEM or PBS, data not shown) were screened. Interestingly, one dominant protein band appeared at about 60 kDa emphasizing that the probe molecule selectively addresses a limited number of cellular targets. To conform the ability of the photo probe to still bind the molecular target of its mother compound, a competitive labeling in HeLa cells with a constant concentration of JP04-042 compared to varying concentrations of competitor T8 (Figure 1B, left) was conducted. An 1.5 fold excess of T8 (30 µM) over JP04-042 (20 µM) already shows a decrease in labeling intensity indicating that there is a competition of the photo probe and the initial screening hit for the same protein target in the living cell.

After finding optimal labeling conditions in the analytical experiments, target identification was performed with heavy and medium isotope labeled MDA-MB 231 breast cancer cells (For more details on the non-natural isotope patterns of the amino acids used for labeling see “Material and Methods”).

Heavy cells were treated with the probe and medium cells with DMSO as shuttle control. The populations should behave identically in the whole workflow (Scheme 3) except in the final MS measurement. The mass shift yielding from the two different isotopic patterns is used to calculate enrichment factors *in silico*. They are used to compare proteins binding selectively to the probe with unspecific (DMSO) background proteins. After UV cross-linking and cell lysis either a biotin-PEG-azid or a trifunctional linker (TFL)[329] was attached to the probe *via* CC. Proteins are then labeled with the analytical handle and enriched in a biotin avidin pull down. Proteins were either analyzed *via* SDS-PAGE or prepared for MS in a tryptic on-bead digest directly. All independent experiments revealed that PDI and some of its isoforms could be enriched up to 66-fold with the probe over the DMSO control out of a full proteome (see Table 1 for selected proteins or Supporting Tables 1 - 4 for full lists of each individual experiment). The enrichment factors listed represent the mean over three technical replicates in case of the gel-based work flow and the mean over five technical replicates for the gel-free preparations. When no corresponding isotopically labeled peptide was found a ration against the background was calculated.

The PDI shows by far the highest enrichment factors compared to other proteins identified by MS. Other proteins were only present in single replicates and/or showed low enrichment factors. Proteins with enrichment factors below two can be defined as background.[330] The molecular weight of PDI is in good correspondence with that of the protein marker band. The masses of other proteins identified as potential targets by MS do not meet these criteria. The isomerase was detected in all biological replicates and with different pre-fractionation techniques applied, either gel-based or gel-free. In addition the sum of Peptide Spectrum Matches (PSM) is the highest in the independent experiments.

Table 1: Selected protein hits with high enrichment factors in different replicates.

Accession Uniprot ID	Description	Fold enrichemnt probe/DMSO				MW [kDa]
		Gel-based	Gel-free, replicate			
			1	2	3	
P07237	Protein disulfide-isomerase	26	66	38	43	57.1
B3KQT9	cDNA PSEC0175 fis, clone OVARC1000169, highly similar to Protein disulfide-isomerase A3	18		10	18	54.1
Q96JJ7	Protein disulfide-isomerase TMX3				6	47.9
P13667	Protein disulfide-isomerase A4		40		5	72.9
Q96JJ7	Isoform 1 of Protein disulfide-isomerase TMX3			5		51.8
Q15084	Isoform 1 of Protein disulfide-isomerase A6		18			48.1
Detailed list of identified proteins in Supporting Table		1	2	3	4	

In vitro validation To verify the target, overexpressed PDI was labeled with JP04-042 *in vitro* successfully. The interaction of the photo probe and the T8/PS-derivatives with the target enzyme was

investigated in more detail in a turbidimetric assay. In this experiment the PDI-catalyzed insulin disulfide reduction can be followed. All tested compounds showed a concentration dependent inhibition with IC_{50} values down to the low µM range (Scheme 5). T8-18 as the most potent compound in Lilianna Schyschka's cell-based studies, showed only weak inhibition of PDI *in vitro*.[325] JP04-042 and the newly synthesized compounds seemed to be stronger inhibitors of the PDI in the insulin reduction assay. A possible explanation might be the azide moiety in the **X** substituent, which the most potent compounds have in common. This functionality is not present in the compounds of the T8 family.

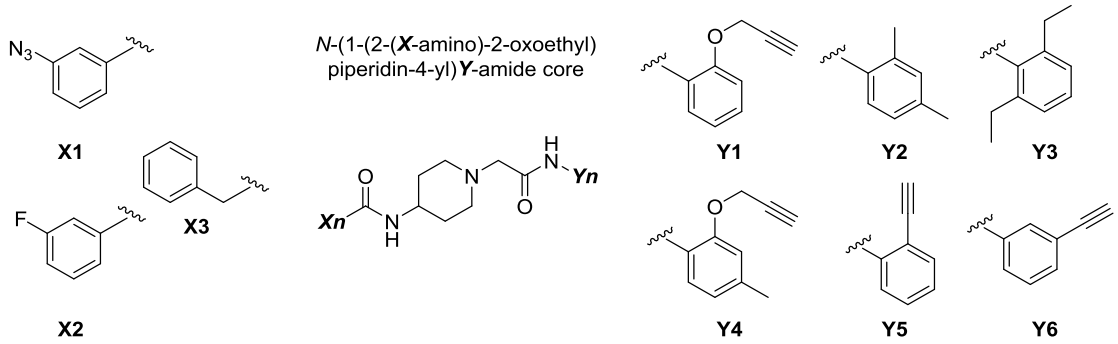

Compound	JP04-042	PS88	PS89	PS111	PS112	PS113
Substituent X	1	1	1	1	1	1
Substituent Y	1	2	3	4	5	6
IC_{50} [µM]	15 ± 1	182 ± 48	78 ± 17	121 ± 7	92 ± 6	173 ± 10
Compound	PS85	PS83	T8	PS84	T8-18	PS86
Substituent X	2	2	2	3	3	3
Substituent Y	1	2	3	1	2	3
IC_{50} [µM]	164 ± 22	240 ± 20	> 300	215 ± 17	> 300	203 ± 42

Scheme 5: Molecular core structure shared by all tested compounds (middle) and possible substituents (left and right). Photo probe JP04-042, examples from initial screen - selected hits T8 and T8-18, and the derived inhibitor library PSxyz. IC_{50} values of these compounds in the insulin reduction assay.

One *ortho* substitution on the **Y** ring seems to foster the inhibition of PDI. A 2,6 or a 2,4 substitution pattern has a negative effect. A substituent in *para* position of the **Y** ring also seems to lower the inhibitory effect of the compound.

The azide moiety can be transformed to an anime. This might happen under the reductive conditions that are present in the assay as well as in human cells.

Outlook The probe library can be further refined. The azide moiety should be replaced with an amide to resemble the possibility of an *in situ* reduction. This could be guided by the docking of known structures and potential synthesis targets into the PDI crystal structure.

The probe can be used in fluorescent microscopy studies. A colocalization of the probe and a PDI specific antibody would be an additional technique to validate the target identified by MS and further investigate the probe target interaction in the native context.

In vivo studies with the new JP- and PS-compounds should be conducted in living cells. This experiments can proof that the stronger inhibition of PDI *in vitro* also translates to stronger effects in cells when these compounds are applied in combination with known chemotherapeutics that cause ER stress. This could be further supplemented with the *in situ* overexpression or knock-downs of PDI. Those genetic measures could then compensate or mimic the phenotypes that arise from the inhibition of the enzyme by the PS compounds. As a long-term perspective the JP04-042 inspired compounds could be used in an animal cancer model.

Material and Methods

Synthesis of photo probe and compounds for SAR studies and optimization as PDI inhibitors was conducted by Judith Peters, Phil Servatius and Uli Kazmaier.

Cell culture Media and supplements were obtained from PAA. Additional amino acids for SILAC experiments were obtained from Cambridge Isotope Laboratories (CIL).

MDA-MB 231 and HeLa cells were maintained in DMEM (high glucose) supplemented with 10 % fetal bovine serum and 2 mM L-glutamine in a 5 % CO_2 incubator at 37 °C and detached with trypsin-EDTA.

Analytical *in situ* labeling and competition For analytical labeling, cells were seeded in 6-well plates and grown to 90 % confluency. After suction of the medium and washing with PBS, compound stocks were added in 1 mL PBS and a final DMSO concentration of 0.1 %. The cells were incubated with the probe for different periods of time at 37 °C and 5 % CO_2. In case of competitive labeling cells were incubated with the non-probe compound and after an additional washing step with the photo probe again. Cells were irradiated (0 °C, up to 1 h, 366 nm, Philips TL-D 18 W BLB), detached with a cell scraper, washed with PBS and the pellets lysed in 100 µL PBS with 1 % (v/v) NP40 and 1 % (w/v) DOC (15 min, 0 °C). Following centrifugation (20k g, 15 min, 4 °C) the supernatant was supplemented with 10 mM rhodamine-azide (Rh-N_3) (2 µL), 1 mM TCEP (2 µL) and 100 mM TBTA ligand (6 µL). Samples

were gently vortexed and the cycloaddition was initiated by the addition of 1 mM $CuSO_4$ (2 µL). The reaction mixtures were incubated at 22 °C for 1 h. For gel electrophoresis, 100 µL 2x SDS loading buffer was added and 50 µL applied per lane on a gel. Fluorescence was recorded using a Fujifilm LAS 4000 luminescent image analyzer with a Fujinon VRF43LMD3 lens and a 575DF20 filter.

Preparative *in situ* labeling in MDA-MB 231 and quantification *via* SILAC[331] MDA-MB 231 cells were passaged six times in SILAC-DMEM (PAA) supplemented with 10 % dialyzed FBS and 2 mM L-glutamine (PAA) as well as 50 mg [$^{13}C_6$,$^{15}N_4$] L- Arginine x HCl and 50 mg [$^{13}C_6$,$^{15}N_2$] L-Lysine x 2 HCl (CIL) resulting in "heavy" cells or [$^{13}C_6$] L-Arginine x HCl and [4,4,5,5-D_4]L-Lysine x 2 HCl (CIL) in corresponding molarities resulting in "medium" cells. Heavy and medium MDA-MB 231 cells were plated out on 15 cm dishes and grown to 90 % confluency. The cells were washed with PBS, and either heavy or medium cells were treated with 10 µM compound and the other isotopic label with the corresponding amount of DMSO in 10 mL PBS for 1 h at 37 °C and 5 % CO_2. Cells were irradiated (0 °C, 1 h, 366 nm, Philips TL-D 18 W BLB), detached with a cell scraper, washed with PBS and the pellets lysed in 1 mL PBS with 1 % (v/v) NP40 and 1 % (w/v) DOC (15 min, 0 °C). Following centrifugation (20k g, 15 min, 4 °C) the protein concentrations of the supernatants were measured using a BCA assay (Roth) and equal protein amounts resulting from heavy or medium cells incubated with the probe and the corresponding DMSO control of the opposite label were pooled. The lysates were supplemented with 10 mM trifunctional linker (TFL, 6 µL) for gel-based approaches, 1 mM TCEP (20 µL) and 100 mM TBTA ligand (60 µL). Samples were gently vortexed and the cycloaddition was initiated by the addition of 1 mM $CuSO_4$ (20 µL). For gel-free workflows Azide-PEG_3-biotin conjugate (Jena Bioscience, 6 µL) was used instead of the TFL. The reaction mixtures were incubated at 22 °C for 1 h. Proteins were precipitated by the addition of a 5-fold volume excess of acetone and incubated over night at − 20 °C. The samples were centrifuged at 16k g for 10 min. The supernatant was discarded and the pellet washed two times with 400 µL of prechilled methanol. Subsequently, the pellet was dissolved in 1 mL of PBS with 0.2 % SDS by sonication and incubated under gentle mixing with 100 µL of avidin-agarose beads (Sigma-Aldrich) for 1 h at room temperature. The beads were washed three times with 1 mL of PBS/0.2 % SDS, twice with 1 mL of 6 M urea, and three times with 1 mL of PBS. For gel analysis 50 µL 2x SDS loading buffer were added and the proteins were released for preparative SDS-PAGE by 6 min incubation at 95 °C. Gel bands were isolated and washed. The proteins were reduced, alkylated and tryptically digested as described previously[332]: In short gel pieces were treated with 100 µL 10 mM DTT for 45 min on 56 °C followed by 100 µl 55 mM IAA, 30 min, in the dark at 22 °C. After washing 100 µl digest solution (1 µl of trypsin (0.5 mg/mL) in 100 µl 25 mM ABC) were added and the reaction was incubated at 37 °C over night. The resulting peptides were extracted from the gel, dried and reconstituted in 0.5 % FA to be measured directly *via* LC-MS/MS. For gel-free analysis the proteins were reduced, alkylated and tryptically digested on the beads as described previously[333]: In short the beads were suspended in

500 µL 6 M urea in PBS, 25 µl TCEP in water (57 mg/ml) was added and the reaction was incubated for 65 °C for 15 min. For alkylation 25 µl iodoacetamide in water (74 mg/ml) were added and incubated for 30 min on 35 °C. For the digest, 950 µl of PBS and 4 µl of trypsin (0.5 mg/ml) were added. The reaction was incubated over night on 37 °C and stopped by the addition of TFA (0.1 % final concentration). The resulting peptides were desalted and concentrated using Sep-Pak C_{18} cartridges (Waters). The C_{18} material was treated with 2 mL MeCN, 0.5 % FA, 1 mL 50 % MeCN, 0.5 % FA and 2 mL ddH_2O 0.1 % TFA prior to sample loading. The agarose beads were pelleted, washed twice with 200 µL 0.1 % TFA and the peptide solution loaded to the cartridges. Peptides bound to the cartridges were washed with 2 mL ddH_2O, 0.1 % TFA and eluted with two times 30 µL 60 % MeCN, 0.5 % FA. The peptides were dried and reconstituted in 0.5 % FA to be measured directly *via* LC-MS/MS or subjected to HILIC pre-fractionation.

Pre-fractionation of peptides *via* HILIC[334] Tryptic peptides were pre-fractionated off-line using a Dionex Ultimate 3000 HPLC system equipped with a Waters XBridge HILIC 150 x 2.1 mm, 3.5 µM column. Analytes were loaded in 20 µL buffer A (95 % MeCN, 10 mM H_4NHCO_2, pH 3) and separated over a gradient from 5 % B (5 % MeCN, 10 mM H_4NHCO_2, pH 3) to 30 % B vs. A over 50 min with a flow of 200 µL/min. The resulting fractions were pooled according to their absorbance at 215 nm.

Mass spectrometry and bioinformatics Tryptic peptides either yielding from gel extraction, on bead digest or HILIC pre-fractionation were loaded onto a Dionex C_{18} Nano Trap Column (100 mm) and subsequently eluted and separated by a Dionex C_{18} PepMap 100 mm (3 µm) column for analysis by tandem MS followed by high-resolution MS using a coupled Dionex Ultimate 3000 nano LC-Thermo LTQ Orbitrap XL system. The mass spectrometry data were searched using the SEQUEST algorithm and a local Mascot-Server (2.3.0) against the human IPI database (V3.87) *via* the software ‘‘Proteome Discoverer 1.4’’. In addition to methionine oxidation and *N*-Acetylation, SILAC aa were included as dynamic modifications, as well as a static acetamide modification of Cys. The search was limited to only tryptic peptides, two missed cleavage sites, monoisotopic precursor ions, and a peptide tolerance of 0.8 ppm.

In vitro insulin assay[335,336] For the turbidometric assay 20 nM PDI (Novus Biologicals) was incubated for 1 h at 22 °C in 100 µL assay buffer (100 mM potassium phosphate, 0.2 mM EDTA, 60 µM DTT, pH 7.0), with varying concentrations of probes or DMSO as control. After addition of 1 mg/mL bovine insulin (Sigma-Aldrich) as a substrate, OD_{650} was observed with a Tecan infinite 200 plate reader at 37 °C for 3 h. The initial slope of the optical density was determined and that of the control set to

100 %. IC_{50} values were determined as the concentration of probe where the enzyme showed half-maximal activity.

Supporting Information: Additional MS Data can be found in the appendix.

Concluding remarks

Small molecule photo affinity probes derived from different sources were used to identify their targets in complex proteomes. The probes were obtained by semisynthesis *via* the modification of a comercially available natural product or the molecules were provided by cooperation partners. The probes contained a photo reactive cross-linker and an alkyne reporter. The protein targets of the probes could be labeled in intact human or bacterial cells and be identified by mass spectrometry. These hits could be verified by the labeling of the isolated proteins and the interactions were further characterized by the inhibition of the targets in specific *in vitro* functional assays.

References

(1) Dreger, M. *European Journal of Biochemistry* **2003**, *270*, 569.

(2) Mann, M.; Ong, S. E.; Gronborg, M.; Steen, H.; Jensen, O. N.; Pandey, A. *Trends in Biotechnology* **2002**, *20*, 261.

(3) Dreger, M. *Mass Spectrometry Reviews* **2003**, *22*, 27.

(4) Bauer, A.; Kuster, B. *European Journal of Biochemistry* **2003**, *270*, 570.

(5) Kruse, U.; Bantscheff, M.; Drewes, G.; Hopf, C. *Molecular & Cellular Proteomics* **2008**, *7*, 1887.

(6) Schenone, M.; Dancik, V.; Wagner, B. K.; Clemons, P. A. *Nat Chem Biol* **2013**, *9*, 232.

(7) Lenz, T.; Fischer, J. J.; Dreger, M. *Journal of Proteomics* **2011**, *75*, 100.

(8) Bruce, C.; Stone, K.; Gulcicek, E.; Williams, K. *Current protocols in bioinformatics / editoral board, Andreas D. Baxevanis ... [et al.]* **2013**, *Chapter 13*, Unit 13.21.

(9) Cravatt, B. F.; Simon, G. M.; Yates, J. R., III *Nature* **2007**, *450*, 991.

(10) Bantscheff, M.; Eberhard, D.; Abraham, Y.; Bastuck, S.; Boesche, M.; Hobson, S.; Mathieson, T.; Perrin, J.; Raida, M.; Rau, C.; Reader, V.; Sweetman, G.; Bauer, A.; Bouwmeester, T.; Hopf, C.; Kruse, U.; Neubauer, G.; Ramsden, N.; Rick, J.; Kuster, B.; Drewes, G. *Nature Biotechnology* **2007**, *25*, 1035.

(11) Lenz, T.; Poot, P.; Weinhold, E.; Dreger, M. *Methods in molecular biology (Clifton, N.J.)* **2012**, *803*, 97.

(12) Liu, Y. S.; Patricelli, M. P.; Cravatt, B. F. *P Natl Acad Sci USA* **1999**, *96*, 14694.

(13) Rix, U.; Hantschel, O.; Duernberger, G.; Rix, L. L. R.; Planyavsky, M.; Fernbach, N. V.; Kaupe, I.; Bennett, K. L.; Valent, P.; Colinge, J.; Kocher, T.; Superti-Furga, G. *Blood* **2007**, *110*, 4055.

(14) Wang, C.; Li, W.; Ren, J.; Fang, J.; Ke, H.; Gong, W.; Feng, W.; Wang, C.-C. *Antioxid Redox Signal* **2012**.

(15) Jeffery, D. A.; Bogyo, M. *Current Opinion in Biotechnology* **2003**, *14*, 87.

(16) Evans, M. J.; Saghatelian, A.; Sorensen, E. J.; Cravatt, B. F. *Nat Biotechnol* **2005**, *23*, 1303.

(17) Evans, M. J.; Cravatt, B. F. *Chem Rev* **2006**, *106*, 3279.

(18) Cravatt, B. F.; Sorensen, E. J. *Curr. Opin. Chem. Biol.* **2000**, *4*, 663.

(19) Fonovic, M.; Bogyo, M. *Expert Rev Proteomics* **2008**, *5*, 721.

(20) Kalesh, K. A.; Sim, D. S. B.; Wang, J.; Liu, K.; Lin, Q.; Yao, S. Q. *Chemical Communications* **2010**, *46*, 1118.

(21) Keppler, O. T.; Horstkorte, R.; Pawlita, M.; Schmidts, C.; Reutter, W. *Glycobiology* **2001**, *11*, 11R.

(22) Prescher, J. A.; Bertozzi, C. R. *Nature Chemical Biology* **2005**, *1*, 13.

(23) Sletten, E. M.; Bertozzi, C. R. *Angew Chem Int Edit* **2009**, *48*, 6974.

(24) Tate, E. W. *Journal of chemical biology* **2008**, *1*, 17.

(25) Kalesh, K. A.; Shi, H.; Ge, J.; Yao, S. Q. *Organic & Biomolecular Chemistry* **2010**, *8*, 1749.

(26) Dalhoff, C.; Lukinavicius, G.; Klimasauskas, S.; Weinhold, E. *Nature Chemical Biology* **2006**, *2*, 31.

(27) Binda, O.; Boyce, M.; Rush, J. S.; Palaniappan, K. K.; Bertozzi, C. R.; Gozani, O. *Chembiochem : a European journal of chemical biology* **2011**, *12*, 330.

(28) Martin, B. R.; Cravatt, B. F. *Nature Methods* **2009**, *6*, 135.

(29) Yang, Y.-Y.; Ascano, J. M.; Hang, H. C. *Journal of the American Chemical Society* **2010**, *132*, 3640.

(30) Prescher, J. A.; Dube, D. H.; Bertozzi, C. R. *Nature* **2004**, *430*, 873.

(31) Chi, Y.; Welcker, M.; Hizli, A. A.; Posakony, J. J.; Aebersold, R.; Clurman, B. E. *Genome Biology* **2008**, *9*.

(32) Elphick, L. M.; Lee, S. E.; Gouverneur, V.; Mann, D. J. *ACS chemical biology* **2007**, *2*, 299.

(33) Chan, L. N.; Hart, C.; Guo, L.; Nyberg, T.; Davies, B. S. J.; Fong, L. G.; Young, S. G.; Agnew, B. J.; Tamanoi, F. *Electrophoresis* **2009**, *30*, 3598.

(34) DeGraw, A. J.; Palsuledesai, C.; Ochocki, J. D.; Dozier, J. K.; Lenevich, S.; Rashidian, M.; Distefano, M. D. *Chemical Biology & Drug Design* **2010**, *76*, 460.

(35) Sieber, S. A.; Niessen, S.; Hoover, H. S.; Cravatt, B. F. *Nat. Chem. Biol.* **2006**, *2*, 274.

(36) Balakrishnan, A.; Patel, B.; Sieber, S. A.; Chen, D.; Pachikara, N.; Zhong, G.; Cravatt, B. F.; Fan, H. *J. Biol. Chem.* **2006**, *281*, 16691.

(37) Nakai, R.; Salisbury, C. M.; Rosen, H.; Cravatt, B. F. *Bioorg. Med. Chem.* **2009**, *17*, 1101.

(38) Nakai, R.; Salisbury, C. M.; Rosen, H.; Cravatt, B. F. *Bioorganic & Medicinal Chemistry* **2009**, *17*, 1101.

(39) Ballell, L.; Alink, K. J.; Slijper, M.; Versluis, C.; Liskamp, R. M. J.; Pieters, R. J. *Chembiochem : a European journal of chemical biology* **2005**, *6*, 291.

(40) Ballell, L.; van, S. M.; Buchalova, K.; Liskamp, R. M. J.; Pieters, R. J. *Org. Biomol. Chem.* **2006**, *4*, 4387.

(41) Pieters, R. J. *Chembiochem : a European journal of chemical biology* **2006**, *7*, 721.

(42) Salisbury, C. M.; Cravatt, B. F. *Qsar & Combinatorial Science* **2007**, *26*, 1229.

(43) Salisbury, C. M.; Cravatt, B. F. *J. Am. Chem. Soc.* **2008**, *130*, 2184.

(44) Qiu, W.-W.; Xu, J.; Li, J.-Y.; Li, J.; Nan, F.-J. *Chembiochem : a European journal of chemical biology* **2007**, *8*, 1351.

(45) Jessani, N.; Humphrey, M.; McDonald, W. H.; Niessen, S.; Masuda, K.; Gangadharan, B.; Yates, J. R.; Mueller, B. M.; Cravatt, B. F. *P Natl Acad Sci USA* **2004**, *101*, 13756.

(46) Morak, M.; Schmidinger, H.; Krempl, P.; Rechberger, G.; Kollroser, M.; Birner-Gruenberger, R.; Hermetter, A. *Journal of Lipid Research* **2009**, *50*, 1281.

(47) Patricelli, M. P.; Cravatt, B. F. *Biochemistry* **1999**, *38*, 14125.

(48) Cravatt, B. F.; Sorensen, E. J. *Current Opinion in Chemical Biology* **2000**, *4*, 663.

(49) Koester, H.; Little, D. P.; Luan, P.; Muller, R.; Siddiqi, S. M.; Marappan, S.; Yip, P. *Assay and Drug Development Technologies* **2007**, *5*, 381.

(50) Lapinsky, D. J. *Bioorganic & Medicinal Chemistry* **2012**, *20*, 6237.

(51) Hatanaka, Y.; Sadakane, Y. *Current Topics in Medicinal Chemistry* **2002**, *2*, 271.

(52) Dorman, G.; Prestwich, G. D. *Trends in Biotechnology* **2000**, *18*, 64.

(53) Coin, I.; Perrin, M. H.; Vale, W. W.; Wang, L. *Angew Chem Int Ed Engl* **2011**, *50*, 8077.

(54) Karaman, M. W.; Herrgard, S.; Treiber, D. K.; Gallant, P.; Atteridge, C. E.; Campbell, B. T.; Chan, K. W.; Ciceri, P.; Davis, M. I.; Edeen, P. T.; Faraoni, R.; Floyd, M.; Hunt, J. P.; Lockhart, D. J.; Milanov, Z. V.; Morrison, M. J.; Pallares, G.; Patel, H. K.; Pritchard, S.; Wodicka, L. M.; Zarrinkar, P. P. *Nature Biotechnology* **2008**, *26*, 127.

(55) Luo, Y.; Blex, C.; Baessler, O.; Glinski, M.; Dreger, M.; Sefkow, M.; Koster, H. *Mol Cell Proteomics* **2009**, *8*, 2843.

(56) Rotili, D.; Altun, M.; Kawamura, A.; Wolf, A.; Fischer, R.; Leung, I. K. H.; Mackeen, M. M.; Tian, Y.-m.; Ratcliffe, P. J.; Mai, A.; Kessler, B. M.; Schofield, C. J. *Chemistry & Biology* **2011**, *18*, 642.

(57) Best, M. D. *Biochemistry* **2009**, *48*, 6571.

(58) Sumranjit, J.; Chung, S. J. *Molecules (Basel, Switzerland)* **2013**, *18*, 10425.

(59) Kolb, H. C.; Finn, M. G.; Sharpless, K. B. *Angew Chem Int Edit* **2001**, *40*, 2004.

(60) Kolb, H. C.; Sharpless, K. B. *Drug Discovery Today* **2003**, *8*, 1128.

(61) Manetsch, R.; Krasinski, A.; Radic, Z.; Raushel, J.; Taylor, P.; Sharpless, K. B.; Kolb, H. C. *J Am Chem Soc* **2004**, *126*, 12809.

(62) Mocharla, V. P.; Colasson, B.; Lee, L. V.; Roper, S.; Sharpless, K. B.; Wong, C. H.; Kolb, H. C. *Angew Chem Int Ed Engl* **2004**, *44*, 116.

(63) Munder, M.; Schneider, H.; Luckner, C.; Giese, T.; Langhans, C. D.; Fuentes, J. M.; Kropf, P.; Mueller, I.; Kolb, A.; Modolell, M.; Ho, A. D. *Blood* **2006**, *108*, 1627.

(64) Whiting, M.; Muldoon, J.; Lin, Y. C.; Silverman, S. M.; Lindstrom, W.; Olson, A. J.; Kolb, H. C.; Finn, M. G.; Sharpless, K. B.; Elder, J. H.; Fokin, V. V. *Angew Chem Int Ed Engl* **2006**, *45*, 1435.

(65) Geurink, P. P.; Prely, L. M.; van der Marel, G. A.; Bischoff, R.; Overkleeft, H. S. *Topics in current chemistry* **2012**, *324*, 85.

(66) Dubinsky, L.; Krom, B. P.; Meijler, M. M. *Bioorg. Med. Chem.* **2012**, *20*, 554.

(67) Xu, C.; Soragni, E.; Chou, C. J.; Herman, D.; Plasterer, H. L.; Rusche, J. R.; Gottesfeld, J. M. *Chemistry & Biology* **2009**, *16*, 980.

(68) Dubinsky, L.; Jarosz, L. M.; Amara, N.; Krief, P.; Kravchenko, V. V.; Krom, B. P.; Meijler, M. M. *Chem Commun (Camb)* **2009**, 7378.

(69) Daub, H. *Biochim Biophys Acta* **2005**, *1754*, 183.

(70) Sharma, K.; Weber, C.; Bairlein, M.; Greff, Z.; Keri, G.; Cox, J.; Olsen, J. V.; Daub, H. *Nat Methods* **2009**, *6*, 741.

(71) Tao, W. A.; Aebersold, R. *Curr Opin Biotechnol* **2003**, *14*, 110.

(72) Matthiesen, R.; Carvalho, A. S. *Methods in molecular biology* **2010**, *593*, 187.

(73) Aebersold, R.; Mann, M. *Nature* **2003**, *422*, 198.

(74) Blagoev, B.; Kratchmarova, I.; Ong, S. E.; Nielsen, M.; Foster, L. J.; Mann, M. *Nature Biotechnology* **2003**, *21*, 315.

(75) Ong, S. E.; Mann, M. *Nat Chem Biol* **2005**, *1*, 252.

(76) Ranish, J. A.; Yi, E. C.; Leslie, D. M.; Purvine, S. O.; Goodlett, D. R.; Eng, J.; Aebersold, R. *Nat Genet* **2003**, *33*, 349.

(77) Rix, U.; Superti-Furga, G. *Nature Chemical Biology* **2009**, *5*, 616.

(78) Banerjee, R.; Pace, N. J.; Brown, D. R.; Weerapana, E. *J Am Chem Soc* **2013**, *135*, 2497.

(79) Cisar, J. S.; Cravatt, B. F. *Journal of the American Chemical Society* **2012**, *134*, 10385.

(80) Ong, S.-E.; Blagoev, B.; Kratchmarova, I.; Kristensen, D. B.; Steen, H.; Pandey, A.; Mann, M. *Mol Cell Proteomics* **2002**, *1*, 376.

(81) Ong, S.-E.; Schenone, M.; Margolin, A. A.; Li, X.; Do, K.; Doud, M. K.; Mani, D. R.; Kuai, L.; Wang, X.; Wood, J. L.; Tolliday, N. J.; Koehler, A. N.; Marcaurelle, L. A.; Golub, T. R.; Gould, R. J.; Schreiber, S. L.; Carr, S. A. *P Natl Acad Sci USA* **2009**, *106*, 4617.

(82) Boersema, P. J.; Raijmakers, R.; Lemeer, S.; Mohammed, S.; Heck, A. J. R. *Nat. Protocols* **2009**, *4*, 484.

(83) Kovanich, D.; Cappadona, S.; Raijmakers, R.; Mohammed, S.; Scholten, A.; Heck, A. J. *Anal Bioanal Chem* **2012**, *404*, 991.

(84) Boersema, P. J.; Aye, T. T.; van Veen, T. A.; Heck, A. J.; Mohammed, S. *Proteomics* **2008**, *8*, 4624.

(85) Hsu, J. L.; Huang, S. Y.; Chow, N. H.; Chen, S. H. *Anal Chem* **2003**, *75*, 6843.

(86) Raijmakers, R.; Berkers, C. R.; de Jong, A.; Ovaa, H.; Heck, A. J.; Mohammed, S. *Mol Cell Proteomics* **2008**, *7*, 1755.

(87) Ong, S.-E.; Mann, M. *Nat Chem Biol* **2005**, *1*, 252.

(88) Altelaar, A. F. M.; Frese, C. K.; Preisinger, C.; Hennrich, M. L.; Schram, A. W.; Timmers, H. T. M.; Heck, A. J. R.; Mohammed, S. *Journal of Proteomics* **2013**, *88*, 14.

(89) Schenone, M.; Dancik, V.; Wagner, B. K.; Clemons, P. A. *Nature Chemical Biology* **2013**, *9*, 232.

(90) Messana, I.; Cabras, T.; Iavarone, F.; Vincenzoni, F.; Urbani, A.; Castagnola, M. *Journal of Separation Science* **2013**, *36*, 128.

(91) Liang, S.; Xu, Z.; Xu, X.; Zhao, X.; Huang, C.; Wei, Y. *Comb Chem High Throughput Screen* **2012**, *15*, 221.

(92) Martyniuk, C. J.; Alvarez, S.; McClung, S.; Villeneuve, D. L.; Ankley, G. T.; Denslow, N. D. *J Proteome Res* **2009**, *8*, 2186.

(93) Martyniuk, C. J.; Denslow, N. D. *General and comparative endocrinology* **2009**, *164*, 135.

(94) Shaw, P. G.; Chaerkady, R.; Wang, T.; Vasilatos, S.; Huang, Y.; Van Houten, B.; Pandey, A.; Davidson, N. E. *PLoS One* **2013**, *8*, e76220.

(95) Yan, G. R.; Tan, Z.; Wang, Y.; Xu, M. L.; Yu, G.; Li, Y.; He, Q. Y. *Proteomics* **2013**.

(96) Daub, H.; Olsen, J. V.; Bairlein, M.; Gnad, F.; Oppermann, F. S.; Koerner, R.; Greff, Z.; Keri, G.; Stemmann, O.; Mann, M. *Molecular Cell* **2008**, *31*, 438.

(97) Dephoure, N.; Zhou, C.; Villen, J.; Beausoleil, S. A.; Bakalarski, C. E.; Elledge, S. J.; Gygi, S. P. *P Natl Acad Sci USA* **2008**, *105*, 10762.

(98) Olsen, J. V.; Vermeulen, M.; Santamaria, A.; Kumar, C.; Miller, M. L.; Jensen, L. J.; Gnad, F.; Cox, J.; Jensen, T. S.; Nigg, E. A.; Brunak, S.; Mann, M. *Science Signaling* **2010**, *3*.

(99) Vermeulen, M.; Eberl, H. C.; Matarese, F.; Marks, H.; Denissov, S.; Butter, F.; Lee, K. K.; Olsen, J. V.; Hyman, A. A.; Stunnenberg, H. G.; Mann, M. *Cell* **2010**, *142*, 967.

(100) Krijgsveld, J.; Ketting, R. F.; Mahmoudi, T.; Johansen, J.; Artal-Sanz, M.; Verrijzer, C. P.; Plasterk, R. H. A.; Heck, A. J. R. *Nature Biotechnology* **2003**, *21*, 927.

(101) Krueger, M.; Moser, M.; Ussar, S.; Thievessen, I.; Luber, C. A.; Forner, F.; Schmidt, S.; Zanivan, S.; Faessler, R.; Mann, M. *Cell* **2008**, *134*, 353.

(102) Wu, C. C.; MacCoss, M. J.; Howell, K. E.; Matthews, D. E.; Yates, J. R. *Analytical Chemistry* **2004**, *76*, 4951.

(103) Geiger, T.; Cox, J.; Ostasiewicz, P.; Wisniewski, J. R.; Mann, M. *Nature Methods* **2010**, *7*, 383.

(104) Monetti, M.; Nagaraj, N.; Sharma, K.; Mann, M. *Nature Methods* **2011**, *8*, 655.

(105) Bendall, S. C.; Hughes, C.; Stewart, M. H.; Doble, B.; Bhatia, M.; Lajoie, G. A. *Molecular & Cellular Proteomics* **2008**, *7*, 1587.

(106) Frohlich, F.; Christiano, R.; Walther, T. C. *Mol Cell Proteomics* **2013**, *12*, 1995.

(107) Hsu, J. L.; Huang, S. Y.; Chow, N. H.; Chen, S. H. *Analytical Chemistry* **2003**, *75*, 6843.

(108) Munoz, J.; Stange, D. E.; Schepers, A. G.; van de Wetering, M.; Koo, B.-K.; Itzkovitz, S.; Volckmann, R.; Kung, K. S.; Koster, J.; Radulescu, S.; Myant, K.; Versteeg, R.; Sansom, O. J.; van Es, J. H.; Barker, N.; van Oudenaarden, A.; Mohammed, S.; Heck, A. J. R.; Clevers, H. *Embo Journal* **2012**, *31*, 3079.

(109) Ross, P. L.; Huang, Y. L. N.; Marchese, J. N.; Williamson, B.; Parker, K.; Hattan, S.; Khainovski, N.; Pillai, S.; Dey, S.; Daniels, S.; Purkayastha, S.; Juhasz, P.; Martin, S.; Bartlet-Jones, M.; He, F.; Jacobson, A.; Pappin, D. J. *Molecular & Cellular Proteomics* **2004**, *3*, 1154.

(110) Thompson, A.; Schafer, J.; Kuhn, K.; Kienle, S.; Schwarz, J.; Schmidt, G.; Neumann, T.; Hamon, C. *Analytical Chemistry* **2003**, *75*, 1895.

(111) Yao, X. D.; Freas, A.; Ramirez, J.; Demirev, P. A.; Fenselau, C. *Analytical Chemistry* **2001**, *73*, 2836.

(112) Gygi, S. P.; Rist, B.; Gerber, S. A.; Turecek, F.; Gelb, M. H.; Aebersold, R. *Nature Biotechnology* **1999**, *17*, 994.

(113) Oda, Y.; Owa, T.; Sato, T.; Boucher, B.; Daniels, S.; Yamanaka, H.; Shinohara, Y.; Yokoi, A.; Kuromitsu, J.; Nagasu, T. *Analytical Chemistry* **2003**, *75*, 2159.

(114) Ross, P. L.; Huang, Y. N.; Marchese, J. N.; Williamson, B.; Parker, K.; Hattan, S.; Khainovski, N.; Pillai, S.; Dey, S.; Daniels, S.; Purkayastha, S.; Juhasz, P.; Martin, S.; Bartlet-Jones, M.; He, F.; Jacobson, A.; Pappin, D. J. *Mol. Cell. Proteomics* **2004**, *3*, 1154.

(115) Thompson, A.; Schaefer, J.; Kuhn, K.; Kienle, S.; Schwarz, J.; Schmidt, G.; Neumann, T.; Johnstone, R. A. W.; Mohammed, A. K. A.; Hamon, C. *Analytical Chemistry* **2006**, *78*, 4235.

(116) Mertins, P.; Udeshi, N. D.; Clauser, K. R.; Mani, D. R.; Patel, J.; Ong, S. E.; Jaffe, J. D.; Carr, S. A. *Mol Cell Proteomics* **2012**, *11*, M111.014423.

(117) Das, J. *Chemical Reviews* **2011**, *111*, 4405.

(118) Dubinsky, L.; Krom, B. P.; Meijler, M. M. *Bioorganic & Medicinal Chemistry* **2012**, *20*, 554.

(119) Hashimoto, M.; Hatanaka, Y. *Eur. J. Org. Chem.* **2008**, 2513.

(120) Sadakane, Y.; Hatanaka, Y. *Analytical Sciences* **2006**, *22*, 209.

(121) Sadakane, Y.; Hatanaka, Y. *Anal. Sci.* **2006**, *22*, 209.

(122) Dorman, G.; Prestwich, G. D. *Biochemistry* **1994**, *33*, 5661.

(123) Staros, J. V.; Bayley, H.; Standring, D. N.; Knowles, J. R. *Biochemical and Biophysical Research Communications* **1978**, *80*, 568.

(124) Bush, J. T.; Walport, L. J.; McGouran, J. F.; Leung, I. K. H.; Berridge, G.; van Berkel, S. S.; Basak, A.; Kessler, B. M.; Schofield, C. J. *Chemical Science* **2013**.

(125) Mackinnon, A. L.; Taunton, J. *Current protocols in chemical biology* **2009**, *1*, 55.

(126) Bergeron, R. J.; Dionis, J. B.; Ingeno, M. J. *The Journal of Organic Chemistry* **1987**, *52*, 144.

(127) Brunner, J. *Annu Rev Biochem* **1993**, *62*, 483.

(128) MacKinnon, A. L.; Garrison, J. L.; Hegde, R. S.; Taunton, J. *J Am Chem Soc* **2007**, *129*, 14560.

(129) Platz, M.; Admasu, A. S.; Kwiatkowski, S.; Crocker, P. J.; Imai, N.; Watt, D. S. *Bioconjug Chem* **1991**, *2*, 337.

(130) Ford, F.; Yuzawa, T.; Platz, M. S.; Matzinger, S.; Fülscher, M. *Journal of the American Chemical Society* **1998**, *120*, 4430.

(131) Dorman, G.; Prestwich, G. D. *Biochemistry* **1994**, *33*, 5661.

(132) Wittelsberger, A.; Thomas, B. E.; Mierke, D. F.; Rosenblatt, M. *FEBS Lett* **2006**, *580*, 1872.

(133) Sadaghiani, A. M.; Verhelst, S. H. L.; Bogyo, M. *Current Opinion in Chemical Biology* **2007**, *11*, 20.

(134) Saxon, E.; Bertozzi, C. R. *Science (Washington, D. C.)* **2000**, *287*, 2007.

(135) Rostovtsev, V. V.; Green, L. G.; Fokin, V. V.; Sharpless, K. B. *Angew. Chem., Int. Ed.* **2002**, *41*, 2596.

(136) Huisgen, R. *1,3 Dipolar Cylcoaddition Chemistry*; Wiley: New York, 1984.

(137) Speers, A. E.; Cravatt, B. F. *Chem. Biol.* **2004**, *11*, 535.

(138) Salisbury, C. M.; Cravatt, B. F. *QSAR Comb. Sci.* **2007**, *26*, 1229.

(139) Rostovtsev, V. V.; Green, J. G.; Fokin, V. V.; Sharpless, K. B. *Angew. Chem. Int. Ed. Engl.* **2002**, *41*, 2596.

(140) Wang, Q.; Chan, T. R.; Hilgraf, R.; Fokin, V. V.; Sharpless, K. B.; Finn, M. G. *J. Amer. Chem. Soc.* **2003**, *125*, 3192.

(141) Tornøe, C. W.; Christensen, C.; Meldal, M. *J Org Chem* **2002**, *67*, 3057.

(142) Staudinger, H.; Meyer, J. *Helv. Chim. Acta* **1919**, *2*, 635.

(143) Hackenberger, C. P. R.; Schwarzer, D. *Angew Chem Int Edit* **2008**, *47*, 10030.

(144) van Berkel, S. S.; van Eldijk, M. B.; van Hest, J. C. M. *Angew Chem Int Edit* **2011**, *50*, 8806.

(145) Schilling, C. I.; Jung, N.; Biskup, M.; Schepers, U.; Brase, S. *Chem Soc Rev* **2011**, *40*, 4840.

(146) Rudolf, G. C.; Heydenreuter, W.; Sieber, S. A. *Current Opinion in Chemical Biology* **2013**, *17*, 110.

(147) Debets, M. F.; van, B. S. S.; Dommerholt, J.; Dirks, A. J.; Rutjes, F. P. J. T.; van, D. F. L. *Acc. Chem. Res.* **2011**, *44*, 805.

(148) Kennedy, D. C.; McKay, C. S.; Legault, M. C. B.; Danielson, D. C.; Blake, J. A.; Pegoraro, A. F.; Stolow, A.; Mester, Z.; Pezacki, J. P. *Journal of the American Chemical Society* **2011**, *133*, 17993.

(149) Rudolf, G. C.; Sieber, S. A. *Chembiochem : a European journal of chemical biology* **2013**, n/a.

(150) Besanceney-Webler, C.; Jiang, H.; Zheng, T.; Feng, L.; del Amo, D. S.; Wang, W.; Klivansky, L. M.; Marlow, F. L.; Liu, Y.; Wu, P. *Angew Chem Int Edit* **2011**, *50*, 8051.

(151) del Amo, D. S.; Wang, W.; Jiang, H.; Besanceney, C.; Yan, A. C.; Levy, M.; Liu, Y.; Marlow, F. L.; Wu, P. *Journal of the American Chemical Society* **2010**, *132*, 16893.

(152) Chan, T. R.; Hilgraf, R.; Sharpless, K. B.; Fokin, V. V. *Organic Letters* **2004**, *6*, 2853.

(153) Hong, V.; Presolski, S. I.; Ma, C.; Finn, M. G. *Angew Chem Int Edit* **2009**, *48*, 9879.

(154) Presolski, S. I.; Hong, V.; Cho, S.-H.; Finn, M. G. *Journal of the American Chemical Society* **2010**, *132*, 14570.

(155) Besanceney-Webler, C.; Jiang, H.; Wang, W.; Baughn, A. D.; Wu, P. *Bioorg. Med. Chem. Lett.* **2011**, *21*, 4989.

(156) Uttamapinant, C.; Tangpeerachaikul, A.; Grecian, S.; Clarke, S.; Singh, U.; Slade, P.; Gee, K. R.; Ting, A. Y. *Angew Chem Int Edit* **2012**, *51*, 5852.

(157) Agard, N. J.; Prescher, J. A.; Bertozzi, C. R. *Journal of the American Chemical Society* **2004**, *126*, 15046.

(158) Baskin, J. M.; Prescher, J. A.; Laughlin, S. T.; Agard, N. J.; Chang, P. V.; Miller, I. A.; Lo, A.; Codelli, J. A.; Bertozzi, C. R. *Proc. Natl. Acad. Sci. U. S. A.* **2007**, *104*, 16793.

(159) Baskin, J. M.; Prescher, J. A.; Laughlin, S. T.; Agard, N. J.; Chang, P. V.; Miller, I. A.; Lo, A.; Codelli, J. A.; Bertozzi, C. R. *P Natl Acad Sci USA* **2007**, *104*, 16793.

(160) Ning, X.; Guo, J.; Wolfert, M. A.; Boons, G.-J. *Angew Chem Int Edit* **2008**, *47*, 2253.

(161) Nessen, M. A.; Kramer, G.; Back, J.; Baskin, J. M.; Smeenk, L. E. J.; de, K. L. J.; van, M. J. H.; de, J. L.; Bertozzi, C. R.; Hiemstra, H.; de, K. C. G. *J. Proteome Res.* **2009**, *8*, 3702.

(162) Dommerholt, J.; Schmidt, S.; Temming, R.; Hendriks, L. J. A.; Rutjes, F. P. J. T.; van Hest, J. C. M.; Lefeber, D. J.; Friedl, P.; van Delft, F. L. *Angew Chem Int Edit* **2010**, *49*, 9422.

(163) Jewett, J. C.; Sletten, E. M.; Bertozzi, C. R. *Journal of the American Chemical Society* **2010**, *132*, 3688.

(164) Dehnert, K. W.; Baskin, J. M.; Laughlin, S. T.; Beahm, B. J.; Naidu, N. N.; Amacher, S. L.; Bertozzi, C. R. *Chembiochem : a European journal of chemical biology* **2012**, *13*, 353.

(165) Blackman, M. L.; Royzen, M.; Fox, J. M. *Journal of the American Chemical Society* **2008**, *130*, 13518.

(166) Chen, W.; Wang, D.; Dai, C.; Hamelberg, D.; Wang, B. *Chemical Communications* **2012**, *48*, 1736.

(167) Devaraj, N. K.; Weissleder, R.; Hilderbrand, S. A. *Bioconjugate Chemistry* **2008**, *19*, 2297.

(168) Liu, D. S.; Tangpeerachaikul, A.; Selvaraj, R.; Taylor, M. T.; Fox, J. M.; Ting, A. Y. *Journal of the American Chemical Society* **2012**, *134*, 792.

(169) Rossin, R.; Verkerk, P. R.; van den Bosch, S. M.; Vulders, R. C. M.; Verel, I.; Lub, J.; Robillard, M. S. *Angew Chem Int Edit* **2010**, *49*, 3375.

(170) Taylor, M. T.; Blackman, M. L.; Dmitrenko, O.; Fox, J. M. *Journal of the American Chemical Society* **2011**, *133*, 9646.

(171) Kahne, D.; Leimkuhler, C.; Lu, W.; Walsh, C. *Chem Rev* **2005**, *105*, 425.

(172) Anderson, J. S.; Matsuhashi, M.; Haskin, M. A.; Strominger, J. L. *Proc Natl Acad Sci U S A* **1965**, *53*, 881.

(173) Perkins, H. R. *Biochem J* **1969**, *111*, 195.

(174) Hanaki, H.; Kuwahara-Arai, K.; Boyle-Vavra, S.; Daum, R. S.; Labischinski, H.; Hiramatsu, K. *J Antimicrob Chemother* **1998**, *42*, 199.

(175) Sieradzki, K.; Tomasz, A. *J Bacteriol* **1997**, *179*, 2557.

(176) Utaida, S.; Pfeltz, R. F.; Jayaswal, R. K.; Wilkinson, B. J. *Antimicrob Agents Chemother* **2006**, *50*, 1541.

(177) Sieradzki, K.; Tomasz, A. *J Bacteriol* **2003**, *185*, 7103.

(178) Nannini, E.; Murray, B. E.; Arias, C. A. *Curr Opin Pharmacol* **2010**, *10*, 516.

(179) Boyle-Vavra, S.; Challapalli, M.; Daum, R. S. *Antimicrob Agents Chemother* **2003**, *47*, 2036.

(180) Sieradzki, K.; Tomasz, A. *Antimicrob Agents Chemother* **2006**, *50*, 527.

(181) Chen, L.; Walker, D.; Sun, B.; Hu, Y.; Walker, S.; Kahne, D. *Proc Natl Acad Sci U S A* **2003**, *100*, 5658.

(182) Sinha Roy, R.; Yang, P.; Kodali, S.; Xiong, Y.; Kim, R. M.; Griffin, P. R.; Onishi, H. R.; Kohler, J.; Silver, L. L.; Chapman, K. *Chem Biol* **2001**, *8*, 1095.

(183) Koteva, K.; Hong, H. J.; Wang, X. D.; Nazi, I.; Hughes, D.; Naldrett, M. J.; Buttner, M. J.; Wright, G. D. *Nat Chem Biol* **2010**, *6*, 327.

(184) Speers, A. E.; Adam, G. C.; Cravatt, B. F. *Journal of the American Chemical Society* **2003**, *125*, 4686.

(185) Speers, A. E.; Cravatt, B. F. *Chembiochem : a European journal of chemical biology* **2004**, *5*, 41.

(186) Blum, G.; von Degenfeld, G.; Merchant, M. J.; Blau, H. M.; Bogyo, M. *Nat Chem Biol* **2007**, *3*, 668.

(187) Evans, M. J.; Cravatt, B. F. *Chemical Reviews* **2006**, *106*, 3279.

(188) Böttcher, T.; Pitscheider, M.; Sieber, S. A. *Angew Chem Int Ed Engl* **2010**, *49*, 2680.

(189) Greenbaum, D.; Baruch, A.; Hayrapetian, L.; Darula, Z.; Burlingame, A.; Medzihradszky, K. F.; Bogyo, M. *Mol. Cell. Proteomics* **2002**, *1*, 60.

(190) Anderson, G. W., Zimmermann, J.E., Callahan, F.M. *J Am Chem Soc* **1964**, *86*, 1655.

(191) Ito, Y., Kano, G., Nakamura, N. *J Org Chem* **1998**, *63*, 5643.

(192) Griffin, J. H.; Linsell, M. S.; Nodwell, M. B.; Chen, Q.; Pace, J. L.; Quast, K. L.; Krause, K. M.; Farrington, L.; Wu, T. X.; Higgins, D. L.; Jenkins, T. E.; Christensen, B. G.; Judice, J. K. *J Am Chem Soc* **2003**, *125*, 6517.

(193) Kim, S. J.; Matsuoka, S.; Patti, G. J.; Schaefer, J. *Biochemistry* **2008**, *47*, 3822.

(194) Smith, M. D.; Gong, D.; Sudhahar, C. G.; Reno, J. C.; Stahelin, R. V.; Best, M. D. *Bioconjug Chem* **2008**, *19*, 1855.

(195) Orth, R.; Sieber, S. A. *J. Org. Chem.* **2009**, *74*, 8476.

(196) Böttcher, T.; Sieber, S. A. *Angew Chem Int Ed Engl* **2008**, *47*, 4600.

(197) Kunzmann, M. H.; Staub, I.; Boettcher, T.; Sieber, S. A. *Biochemistry* **2011**, *50*, 910.

(198) Biswas, R.; Voggu, L.; Simon, U. K.; Hentschel, P.; Thumm, G.; Gotz, F. *FEMS Microbiol Lett* **2006**, *259*, 260.

(199) Oshida, T.; Sugai, M.; Komatsuzawa, H.; Hong, Y. M.; Suginaka, H.; Tomasz, A. *Proc Natl Acad Sci U S A* **1995**, *92*, 285.

(200) Sugai, M. *J Infect Chemother* **1997**, *3*, 113.

(201) Zoll, S.; Patzold, B.; Schlag, M.; Gotz, F.; Kalbacher, H.; Stehle, T. *PLoS Pathog* **2011**, *6*, e1000807.

(202) Antignac, A.; Sieradzki, K.; Tomasz, A. *J Bacteriol* **2007**, *189*, 7573.

(203) Kajimura, J.; Fujiwara, T.; Yamada, S.; Suzawa, Y.; Nishida, T.; Oyamada, Y.; Hayashi, I.; Yamagishi, J.; Komatsuzawa, H.; Sugai, M. *Mol Microbiol* **2005**, *58*, 1087.

(204) Garmory, H. S.; Titball, R. W. *Infect Immun* **2004**, *72*, 6757.

(205) Davidson, A. L.; Dassa, E.; Orelle, C.; Chen, J. *Microbiol Mol Biol Rev* **2008**, *72*, 317.

(206) van Veen, H. W.; Higgins, C. F.; Konings, W. N. *Res Microbiol* **2001**, *152*, 365.

(207) Paulsen, I. T.; Banerjei, L.; Myers, G. S.; Nelson, K. E.; Seshadri, R.; Read, T. D.; Fouts, D. E.; Eisen, J. A.; Gill, S. R.; Heidelberg, J. F.; Tettelin, H.; Dodson, R. J.; Umayam, L.; Brinkac, L.; Beanan, M.; Daugherty, S.; DeBoy, R. T.; Durkin, S.; Kolonay, J.; Madupu, R.; Nelson, W.; Vamathevan, J.; Tran, B.; Upton, J.; Hansen, T.; Shetty, J.; Khouri, H.; Utterback, T.; Radune, D.; Ketchum, K. A.; Dougherty, B. A.; Fraser, C. M. *Science* **2003**, *299*, 2071.

(208) Burnie, J.; Carter, T.; Rigg, G.; Hodgetts, S.; Donohoe, M.; Matthews, R. *FEMS Immunol Med Microbiol* **2002**, *33*, 179.

(209) Sieber, S. A.; Niessen, S.; Hoover, H. S.; Cravatt, B. F. *Nature Chemical Biology* **2006**, *2*, 274.

(210) Ober, M.; Muller, H.; Pieck, C.; Gierlich, J.; Carell, T. *J Am Chem Soc* **2005**, *127*, 18143.

(211) Kuroda, A., Sekiguchi, J. *J Gen Microbiol* **1990**, *136*, 2209.

(212) Ayusawa, D., Yoneda, Y., Yamane, K., Maruo, B. *J Bacteriol* **1975**, *124*, 459.

(213) Cer, R. Z.; Mudunuri, U.; Stephens, R.; Lebeda, F. J. *Nucleic Acids Res* **2009**, *37*, W441.

(214) Olmsted, J. B.; Borisy, G. G. *Biochemistry* **1973**, *12*, 4282.

(215) Olmsted, J. B.; Borisy, G. G. *Annu Rev Biochem* **1973**, *42*, 507.

(216) Giannakakou, P.; Sackett, D.; Fojo, T. *J Natl Cancer I* **2000**, *92*, 182.

(217) Jordan, A.; Hadfield, J. A.; Lawrence, N. J.; McGown, A. T. *Med Res Rev* **1998**, *18*, 259.
(218) Stanton, R. A.; Gernert, K. M.; Nettles, J. H.; Aneja, R. *Med Res Rev* **2011**, *31*, 443.
(219) Wilson, L.; Jordan, M. A. *J Chemother* **2004**, *16 Suppl 4*, 83.
(220) Dumontet, C.; Jordan, M. A. *Nature reviews. Drug discovery* **2010**, *9*, 790.
(221) Wani, M. C.; Taylor, H. L.; Wall, M. E.; Coggon, P.; McPhail, A. T. *J Am Chem Soc* **1971**, *93*, 2325.
(222) Schiff, P. B.; Fant, J.; Horwitz, S. B. *Nature* **1979**, *277*, 665.
(223) Sasse, F.; Steinmetz, H.; Heil, J.; Hofle, G.; Reichenbach, H. *The Journal of antibiotics* **2000**, *53*, 879.
(224) Steinmetz, H.; Glaser, N.; Herdtweck, E.; Sasse, F.; Reichenbach, H.; Hofle, G. *Angew Chem Int Ed Engl* **2004**, *43*, 4888.
(225) Khalil, M. W.; Sasse, F.; Lunsdorf, H.; Elnakady, Y. A.; Reichenbach, H. *Chembiochem : a European journal of chemical biology* **2006**, *7*, 678.
(226) Ullrich, A.; Chai, Y.; Pistorius, D.; Elnakady, Y. A.; Herrmann, J. E.; Weissman, K. J.; Kazmaier, U.; Müller, R. *Angewandte Chemie International Edition* **2009**, *48*, 4422.
(227) Wipf, P.; Wang, Z. Y. *Organic Letters* **2007**, *9*, 1605.
(228) Patterson, A. W.; Peltier, H. M.; Ellman, J. A. *Journal of Organic Chemistry* **2008**, *73*, 4362.
(229) Raghavan, B.; Balasubramanian, R.; Steele, J. C.; Sackett, D. L.; Fecik, R. A. *J. Med. Chem.* **2008**, *51*, 1530.
(230) Balasubramanian, R.; Raghavan, B.; Steele, J. C.; Sackett, D. L.; Fecik, R. A. *Bioorg. Med. Chem. Lett.* **2008**, *18*, 2996.
(231) Ullrich, A.; Herrmann, J.; Muller, R.; Kazmaier, U. *European Journal of Organic Chemistry* **2009**, 6367.
(232) Herrmann, J.; Elnakady, Y. A.; Wiedmann, R. M.; Ullrich, A.; Rohde, M.; Kazmaier, U.; Vollmar, A. M.; Muller, R. *PLoS One* **2012**, *7*, e37416.
(233) Burkhart, J. L.; Muller, R.; Kazmaier, U. *European Journal of Organic Chemistry* **2011**, 3050.
(234) Fonovic, M.; Bogyo, M. *Expert Review of Proteomics* **2008**, *5*, 721.
(235) Eirich, J.; Orth, R.; Sieber, S. A. *Journal of the American Chemical Society* **2011**, *133*, 12144.
(236) Rostovtsev, V. V.; Green, L. G.; Fokin, V. V.; Sharpless, K. B. *Angew Chem Int Edit* **2002**, *41*, 2596.
(237) Tanaka, Y.; Bond, M. R.; Kohler, J. J. *Molecular bioSystems* **2008**, *4*, 473.
(238) Nodwell, M. B.; Sieber, S. A. *Top. Curr. Chem.* **2012**, *324*, 1.
(239) Lei, H. Y.; Stoakes, M. S.; Herath, K. P. B.; Lee, J. H.; Schwabacher, A. W. *Journal of Organic Chemistry* **1994**, *59*, 4206.
(240) Speers, A. E.; Cravatt, B. F. *Chemistry & Biology* **2004**, *11*, 535.
(241) Elnakady, Y. A.; Sasse, F.; Lunsdorf, H.; Reichenbach, H. *Biochemical pharmacology* **2004**, *67*, 927.
(242) Rath, S.; Furst, R.; Ullrich, A.; Burkhart, J. L.; Herrmann, J. E.; Liebl, J.; Guenther, M.; Vollmar, A. M.; Kazmaier, U.; Zahler, S. *J Vasc Res* **2011**, *48*, 231.
(243) Rath, S.; Furst, R.; Ullrich, A.; Burkhart, J.; Vollmar, A. M.; Kazmaier, U.; Zahler, S. *N-S Arch Pharmacol* **2011**, *383*, 28.
(244) Kretzschmann, V.; Ullrich, A.; Zahler, S.; Vollmar, A. M.; Kazmaier, U.; Furst, R. *J Vasc Res* **2011**, *48*, 113.
(245) Wong, R. S. Y.; Cheong, S.-K. *Malays J Pathol* **2012**, *34*, 77.
(246) Raetz, E. A.; Bhatla, T. *Hematology Am Soc Hematol Educ Program* **2012**, *2012*, 129.
(247) Warsame, R.; Grothey, A. *Expert Rev Anticancer Ther* **2012**, *12*, 1327.
(248) Mackenzie, R. P.; McCollum, A. D. *Expert Rev Anticancer Ther* **2009**, *9*, 1473.
(249) Squadroni, M.; Fazio, N. *Eur Rev Med Pharmacol Sci* **2010**, *14*, 386.

(250) Ali, A. Y.; Farrand, L.; Kim, J. Y.; Byun, S.; Suh, J.-Y.; Lee, H. J.; Tsang, B. K. *Annals of the New York Academy of Sciences* **2012**, *1271*, 58.

(251) Crown, J.; O'Shaughnessy, J.; Gullo, G. *Ann Oncol* **2012**, *23 Suppl 6*, vi56.

(252) Lovat, P. E.; Corazzari, M.; Armstrong, J. L.; Martin, S.; Pagliarini, V.; Hill, D.; Brown, A. M.; Piacentini, M.; Birch-Machin, M. A.; Redfern, C. P. F. *Cancer research* **2008**, *68*, 5363.

(253) Souza, A. C. S.; de Fatima, A.; da Silveira, R. B.; Justo, G. Z. *Curr Drug Targets* **2012**, *13*, 1072.

(254) La Porta, C. A. M. *Curr Cancer Drug Targets* **2009**, *9*, 391.

(255) La Porta, C. A. M. *Curr Med Chem* **2007**, *14*, 387.

(256) Hartman, M. L.; Czyz, M. *Cancer letters* **2013**, *331*, 24.

(257) Wang, S.; Bai, L.; Lu, J.; Liu, L.; Yang, C.-Y.; Sun, H. *Journal of mammary gland biology and neoplasia* **2012**, *17*, 217.

(258) Bodur, C.; Basaga, H. *Curr Med Chem* **2012**, *19*, 1804.

(259) Thomas, S.; Quinn, B. A.; Das, S. K.; Dash, R.; Emdad, L.; Dasgupta, S.; Wang, X.-Y.; Dent, P.; Reed, J. C.; Pellecchia, M.; Sarkar, D.; Fisher, P. B. *Expert Opin Ther Targets* **2013**, *17*, 61.

(260) Billard, C. *Leukemia* **2012**, *26*, 2032.

(261) Castelli, C.; Rivoltini, L.; Rini, F.; Belli, F.; Testori, A.; Maio, M.; Mazzaferro, V.; Coppa, J.; Srivastava, P. K.; Parmiani, G. *Cancer immunology, immunotherapy : CII* **2004**, *53*, 227.

(262) Wang, X. Y.; Facciponte, J. G.; Subjeck, J. R. *Handbook of experimental pharmacology* **2006**, 305.

(263) Zhao, Y.; Butler, E. B.; Tan, M. *Cell death & disease* **2013**, *4*, e532.

(264) Wang, S.; Kaufman, R. J. *The Journal of cell biology* **2012**, *197*, 857.

(265) Benbrook, D. M.; Long, A. *Experimental oncology* **2012**, *34*, 286.

(266) Bravo, R.; Parra, V.; Gatica, D.; Rodriguez, A. E.; Torrealba, N.; Paredes, F.; Wang, Z. V.; Zorzano, A.; Hill, J. A.; Jaimovich, E.; Quest, A. F.; Lavandero, S. *International review of cell and molecular biology* **2013**, *301*, 215.

(267) Clarke, R.; Cook, K. L.; Hu, R.; Facey, C. O.; Tavassoly, I.; Schwartz, J. L.; Baumann, W. T.; Tyson, J. J.; Xuan, J.; Wang, Y.; Warri, A.; Shajahan, A. N. *Cancer research* **2012**, *72*, 1321.

(268) Siegelin, M. D. *Expert Opin Ther Targets* **2012**, *16*, 801.

(269) Suh, D. H.; Kim, M. K.; Kim, H. S.; Chung, H. H.; Song, Y. S. *Annals of the New York Academy of Sciences* **2012**, *1271*, 20.

(270) Zanetti, M. *Annals of the New York Academy of Sciences* **2013**, *1284*, 6.

(271) Lee, A. S. *Methods (San Diego, Calif.)* **2005**, *35*, 373.

(272) Li, J.; Lee, A. S. *Current molecular medicine* **2006**, *6*, 45.

(273) Lee, A. S. *Cancer research* **2007**, *67*, 3496.

(274) Ni, M.; Lee, A. S. *FEBS Lett* **2007**, *581*, 3641.

(275) Matus, S.; Lisbona, F.; Torres, M.; Leon, C.; Thielen, P.; Hetz, C. *Current molecular medicine* **2008**, *8*, 157.

(276) Dudek, J.; Benedix, J.; Cappel, S.; Greiner, M.; Jalal, C.; Muller, L.; Zimmermann, R. *Cellular and molecular life sciences : CMLS* **2009**, *66*, 1556.

(277) Yoo, S. A.; You, S.; Yoon, H. J.; Kim, D. H.; Kim, H. S.; Lee, K.; Ahn, J. H.; Hwang, D.; Lee, A. S.; Kim, K. J.; Park, Y. J.; Cho, C. S.; Kim, W. U. *The Journal of experimental medicine* **2012**, *209*, 871.

(278) Gorbatyuk, M. S.; Gorbatyuk, O. S. *Journal of genetic syndrome & gene therapy* **2013**, *4*.

(279) Komita, M.; Jin, H.; Aoe, T. *Anesthesia and analgesia* **2013**.

(280) Schonthal, A. H. *Biochemical pharmacology* **2013**, *85*, 653.

(281) Nahleh, Z.; Tfayli, A.; Najm, A.; El Sayed, A.; Nahle, Z. *Future Med Chem* **2012**, *4*, 927.

(282) Rappa, F.; Farina, F.; Zummo, G.; David, S.; Campanella, C.; Carini, F.; Tomasello, G.; Damiani, P.; Cappello, F.; EC, D. E. M.; Macario, A. J. *Anticancer Res* **2012**, *32*, 5139.

(283) Garcia-Carbonero, R.; Carnero, A.; Paz-Ares, L. *The lancet oncology* **2013**, *14*, e358.

(284) Ischia, J.; Saad, F.; Gleave, M. *Current opinion in urology* **2013**, *23*, 194.

(285) MacVicar, G. R.; Hussain, M. H. *Current opinion in oncology* **2013**, *25*, 252.

(286) Murphy, M. E. *Carcinogenesis* **2013**, *34*, 1181.
(287) Siegelin, M. D. *Cancer letters* **2013**, *333*, 133.
(288) Venetianer, P.; Straub, F. B. *Acta Physiologica Academiae Scientiarum Hungaricae* **1963**, *24*, 41.
(289) Venetianer, P.; Straub, F. B. *Biochimica Et Biophysica Acta* **1963**, *67*, 166.
(290) Goldberger, R. F.; Epstein, C. J.; Anfinsen, C. B. *Journal of Biological Chemistry* **1963**, *238*, 628.
(291) Alanen, H. I.; Salo, K. E. H.; Pekkala, M.; Siekkinen, H. M.; Pirneskoski, A.; Ruddock, L. W. *Antioxidants & Redox Signaling* **2003**, *5*, 367.
(292) Darby, N. J.; Kemmink, J.; Creighton, T. E. *Biochemistry* **1996**, *35*, 10517.
(293) Edman, J. C.; Ellis, L.; Blacher, R. W.; Roth, R. A.; Rutter, W. J. *Nature* **1985**, *317*, 267.
(294) Freedman, R. B.; Gane, P. J.; Hawkins, H. C.; Hlodan, R.; McLaughlin, S. H.; Parry, J. W. L. *Biological Chemistry* **1998**, *379*, 321.
(295) Steiner, R. F.; Delorenz.F; Anfinsen, C. B. *Journal of Biological Chemistry* **1965**, *240*, 4648.
(296) Creighton, T. E. *Bioessays* **1992**, *14*, 195.
(297) Varandani, P. T.; Nafz, M. A. *Archives of Biochemistry and Biophysics* **1970**, *141*, 533.
(298) Varandani, P. T.; Nafz, M. A.; Chandler, M. L. *Biochemistry* **1975**, *14*, 2115.
(299) Dellacor.E; Parkhous.Rm *Biochemical Journal* **1973**, *136*, 597.
(300) Murkofsky, N. A.; Lamm, M. E. *Journal of Biological Chemistry* **1979**, *254*, 2181.
(301) Roth, R. A.; Pierce, S. B. *Biochemistry* **1987**, *26*, 4179.
(302) Moss, J.; Stanley, S. J.; Morin, J. E.; Dixon, J. E. *Journal of Biological Chemistry* **1980**, *255*, 1085.
(303) Barak, N. N.; Neumann, P.; Sevvana, M.; Schutkowski, M.; Naumann, K.; Malesevic, M.; Reichardt, H.; Fischer, G.; Stubbs, M. T.; Ferrari, D. M. *Journal of Molecular Biology* **2009**, *385*, 1630.
(304) Forster, S. J.; Freedman, R. B. *Bioscience Reports* **1984**, *4*, 223.
(305) Wang, C. C.; Tsou, C. L. *Faseb Journal* **1993**, *7*, 1515.
(306) Puig, A.; Gilbert, H. F. *Journal of Biological Chemistry* **1994**, *269*, 7764.
(307) Winter, J.; Klappa, P.; Freedman, R. B.; Lilie, H.; Rudolph, R. *Journal of Biological Chemistry* **2002**, *277*, 310.
(308) Yao, Y.; Zhou, Y. C.; Wang, C. C. *Embo Journal* **1997**, *16*, 651.
(309) Song, J. L.; Wang, C. C. *European Journal of Biochemistry* **1995**, *231*, 312.
(310) Cai, H.; Wang, C. C.; Tsou, C. L. *Journal of Biological Chemistry* **1994**, *269*, 24550.
(311) Benham, A. M. *Antioxidants & Redox Signaling* **2012**, *16*, 781.
(312) Ge, J.; Zhang, C.-J.; Li, L.; Chong, L. M.; Wu, X.; Hao, P.; Sze, S. K.; Yao, S. Q. *ACS chemical biology* **2013**.
(313) Khan, M. M.; Simizu, S.; Lai, N. S.; Kawatani, M.; Shimizu, T.; Osada, H. *ACS chemical biology* **2011**, *6*, 245.
(314) Hoffstrom, B. G.; Kaplan, A.; Letso, R.; Schmid, R. S.; Turmel, G. J.; Lo, D. C.; Stockwell, B. R. *Nat Chem Biol* **2010**, *6*, 900.
(315) Xu, S.; Butkevich, A. N.; Yamada, R.; Zhou, Y.; Debnath, B.; Duncan, R.; Zandi, E.; Petasis, N. A.; Neamati, N. *Proc Natl Acad Sci U S A* **2012**, *109*, 16348.
(316) Tsibris, J. C.; Hunt, L. T.; Ballejo, G.; Barker, W. C.; Toney, L. J.; Spellacy, W. N. *J Biol Chem* **1989**, *264*, 13967.
(317) Guthapfel, R.; Gueguen, P.; Quemeneur, E. *Eur J Biochem* **1996**, *242*, 315.
(318) Gerona-Navarro, G.; Perez de Vega, M. J.; Garcia-Lopez, M. T.; Andrei, G.; Snoeck, R.; De Clercq, E.; Balzarini, J.; Gonzalez-Muniz, R. *J Med Chem* **2005**, *48*, 2612.
(319) Beck, P.; Dubiella, C.; Groll, M. *Biol Chem* **2012**, *393*, 1101.
(320) Smith, A. J.; Zhang, X.; Leach, A. G.; Houk, K. N. *J Med Chem* **2009**, *52*, 225.
(321) Serafimova, I. M.; Pufall, M. A.; Krishnan, S.; Duda, K.; Cohen, M. S.; Maglathlin, R. L.; McFarland, J. M.; Miller, R. M.; Frodin, M.; Taunton, J. *Nat Chem Biol* **2012**, *8*, 471.

(322) Singh, J.; Petter, R. C.; Baillie, T. A.; Whitty, A. *Nature reviews. Drug discovery* **2011**, *10*, 307.

(323) Brodie, B. B.; Reid, W. D.; Cho, A. K.; Sipes, G.; Krishna, G.; Gillette, J. R. *P Natl Acad Sci USA* **1971**, *68*, 160.

(324) Jollow, D. J.; Mitchell, J. R.; Potter, W. Z.; Davis, D. C.; Gillette, J. R.; Brodie, B. B. *Journal of Pharmacology and Experimental Therapeutics* **1973**, *187*, 195.

(325) Schyschka, L. Dissertation, LMU München, 2009.

(326) Geurink, P. P.; Prely, L. M.; van der Marel, G. A.; Bischoff, R.; Overkleeft, H. S. *Topics in current chemistry* **2012**, *324*, 85.

(327) Jiang, H.; English, A. M. *J Proteome Res* **2002**, *1*, 345.

(328) Zhu, H.; Pan, S.; Gu, S.; Bradbury, E. M.; Chen, X. *Rapid Commun Mass Spectrom* **2002**, *16*, 2115.

(329) Eirich, J.; Burkhart, J. L.; Ullrich, A.; Rudolf, G. C.; Vollmar, A.; Zahler, S.; Kazmaier, U.; Sieber, S. A. *Molecular bioSystems* **2012**, *8*, 2067.

(330) Ong, S. E.; Kratchmarova, I.; Mann, M. *Journal of Proteome Research* **2003**, *2*, 173.

(331) Cisar, J. S.; Cravatt, B. F. *J Am Chem Soc* **2012**, *134*, 10385.

(332) Sieber, S. A.; Niessen, S.; Hoover, H. S.; Cravatt, B. F. *Nat Chem Biol* **2006**, *2*, 274.

(333) Weerapana, E.; Speers, A. E.; Cravatt, B. F. *Nat Protoc* **2007**, *2*, 1414.

(334) Di Palma, S.; Mohammed, S.; Heck, A. J. R. *Nat Protoc* **2012**, *7*, 2041.

(335) Smith, A. M.; Chan, J.; Oksenberg, D.; Urfer, R.; Wexler, D. S.; Ow, A.; Gao, L.; McAlorum, A.; Huang, S. G. *Journal of biomolecular screening* **2004**, *9*, 614.

(336) Holmgren, A. *J Biol Chem* **1979**, *254*, 9627.

Appendix

Supporting Information for "Unraveling the Protein Targets of Vancomycin in Living *S. aureus* and *E. faecalis* Cells"

Supporting Information

Unraveling the protein targets of vancomycin in living *S. aureus* and *E. faecalis* cells

Jürgen Eirich, Ronald Orth and Stephan A. Sieber

Table S1. Proteins identified by mass spectrometry.

Sample	Protein	P (pro) / P (pep)	Score / XC	Coverage / DeltaCn	MW / Sp	Peptide (Hits) / Ions
VSE-M	Q837D2_ENTFA Peptide ABC transporter, ATP-binding protein OS=Enterococcus faecalis GN=EF_0911	1.39E-09	20	8.80	38829.4	2 (2 0 0 0 0)
Mu50-M	ATL_STAAM Bifunctional autolysin precursor [Includes: N-acetylmuramoyl-L-alanine amidase - Staphylococcus aureus (strain Mu50 / ATCC 700699)	2.17E-09	40.20	4.2	136666.6	4 (4 0 0 0 0)

Complete Ref. 40:
Paulsen, I. T.; Banerjei, L.; Myers, G. S.; Nelson, K. E.; Seshadri, R.; Read, T. D.; Fouts, D. E.; Eisen, J. A.; Gill, S. R.; Heidelberg, J. F.; Tettelin, H.; Dodson, R. J.; Umayam, L.; Brinkac, L.; Beanan, M.; Daugherty, S.; DeBoy, R. T.; Durkin, S.; Kolonay, J.; Madupu, R.; Nelson, W.; Vamathevan, J.; Tran, B.; Upton, J.; Hansen, T.; Shetty, J.; Khouri, H.; Utterback, T.; Radune, D.; Ketchum, K. A.; Dougherty, B. A.; Fraser, C. M. *Science* **2003**, *299*, 2071-4.

Table S2. Real time PCR data for the pABC gene of interest and two genes for standardization to compare bacteria with (half MIC, 4 µg/mL) and without (0 µg) vancomycin selection.

Fluor	Target	Content	Sample	Cq	Cq Mean	Cq Std. Dev
SYBR	pABC	Unkn-1	VRE-0µg	17,47	17,50	0,047
SYBR	pABC	Unkn-1	VRE-0µg	17,53	17,50	0,047
SYBR	pABC	NTC		39,27	39,27	0,000
SYBR	lsa	Unkn-2	VRE-0µg	17,17	17,19	0,050
SYBR	lsa	Unkn-2	VRE-0µg	17,25	17,19	0,050
SYBR	lsa	Unkn-2	VRE-0µg	17,15	17,19	0,050
SYBR	lsa	NTC		37,82	37,82	0,000
SYBR	GAP	Unkn-4	VRE-0µg	18,49	18,29	0,178
SYBR	GAP	Unkn-4	VRE-0µg	18,22	18,29	0,178
SYBR	GAP	Unkn-4	VRE-0µg	18,15	18,29	0,178
SYBR	GAP	NTC		36,30	36,30	0,000
SYBR	pABC	Unkn-5	VRE-4µg	18,58	18,57	0,050
SYBR	pABC	Unkn-5	VRE-4µg	18,61	18,57	0,050
SYBR	pABC	Unkn-5	VRE-4µg	18,52	18,57	0,050
SYBR	lsa	Unkn-6	VRE-4µg	18,47	18,49	0,016
SYBR	lsa	Unkn-6	VRE-4µg	18,49	18,49	0,016
SYBR	lsa	Unkn-6	VRE-4µg	18,50	18,49	0,016
SYBR	GAP	Unkn-8	VRE-4µg	19,23	19,13	0,094
SYBR	GAP	Unkn-8	VRE-4µg	19,06	19,13	0,094
SYBR	GAP	Unkn-8	VRE-4µg	19,09	19,13	0,094

Table S3. Primer sequences used for GATEWAY cloning and qPCR.

Cloning primers	
pABC fwd	GGGGACAAGTTTGTACAAAAAAGCAGGCTTTACTATGGAAAAAGTATTAGAAG
pABC rev	GGGGACCACTTTGTACAAGAAAGCTGGGTGTTAATTACTACCTCCTGGAT
ATLam fwd	GGGGACAAGTTTGTACAAAAAAGCAGGCTTTGCTTCAGCACAACCAAGATC
ATLam rev	GGGGACCACTTTGTACAAGAAAGCTGGGTGTTTTACAGCTGTTTTTGGTTGTGC
ATLam STOP rev	GGGGACCACTTTGTACAAGAAAGCTGGGTGCTATTTTACAGCTGTTTTTGGTTGTGC
ATLfl fwd	GGGGACAAGTTTGTACAAAAAAGCAGGCTTTGCTGAGACGACACAAGATC
ATLfl rev	GGGGACCACTTTGTACAAGAAAGCTGGGTGTTATTTATATTGTGGGATGTCGAAG
qPCR primers	
GAD fwd	ATCCACGCTTACACAGGTGACCA
GAD rev	AGGAACACGTTGAGCAGCGC
pABC fwd	TGGTGGGCAACGTCAACGGA
pABC rev	CAGCCACGTTTGCTACTACCCCT
LSA fwd	GCGCGTAATGAAGCGCTCGA
LSA rev	TCCGACAATTTCTCCCGCGT

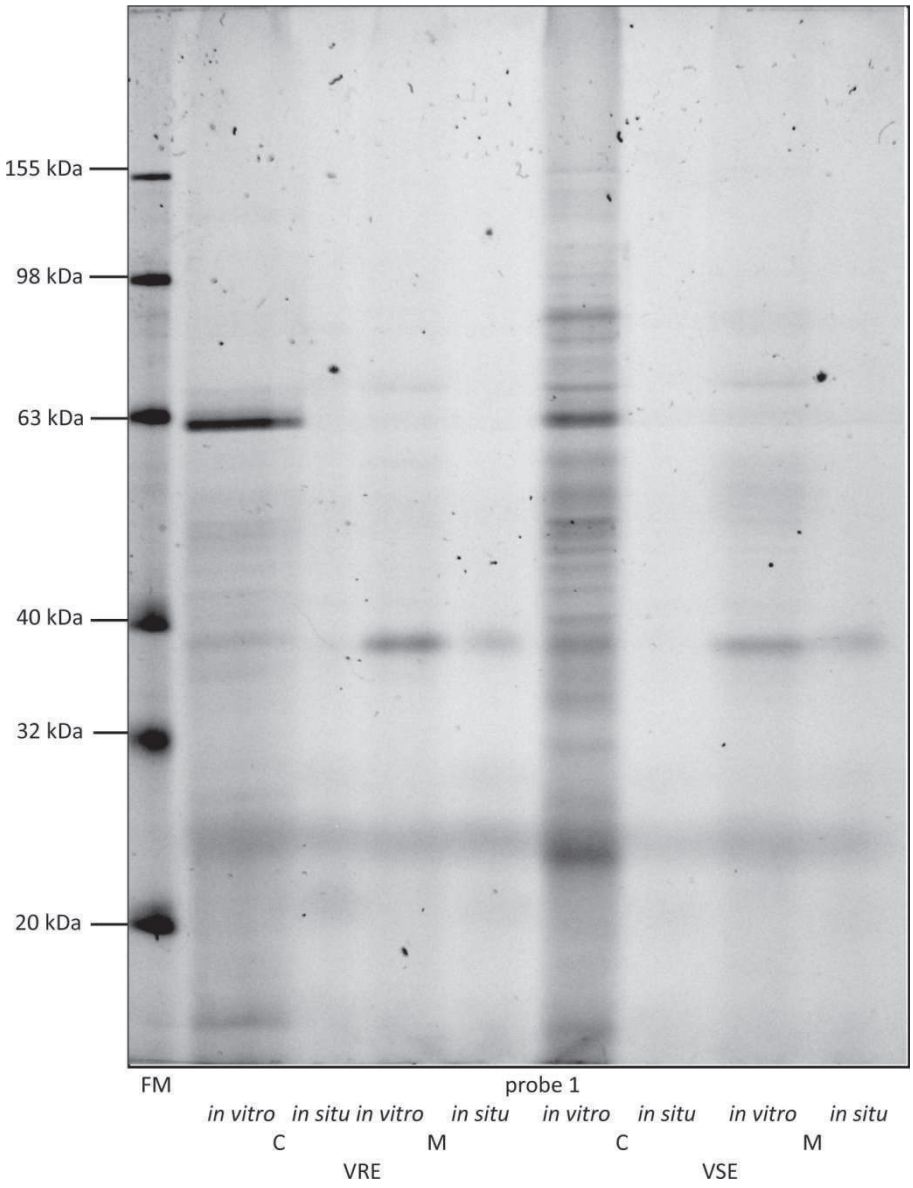

Figure S1 Comparison of *in situ* and *in vitro* labeling of *E. faecalis* with probe **1** and 1 h irradiation time. FM: Invitrogen BenchMark Fluorescent Protein Standard. C = cytosol, M = membrane.

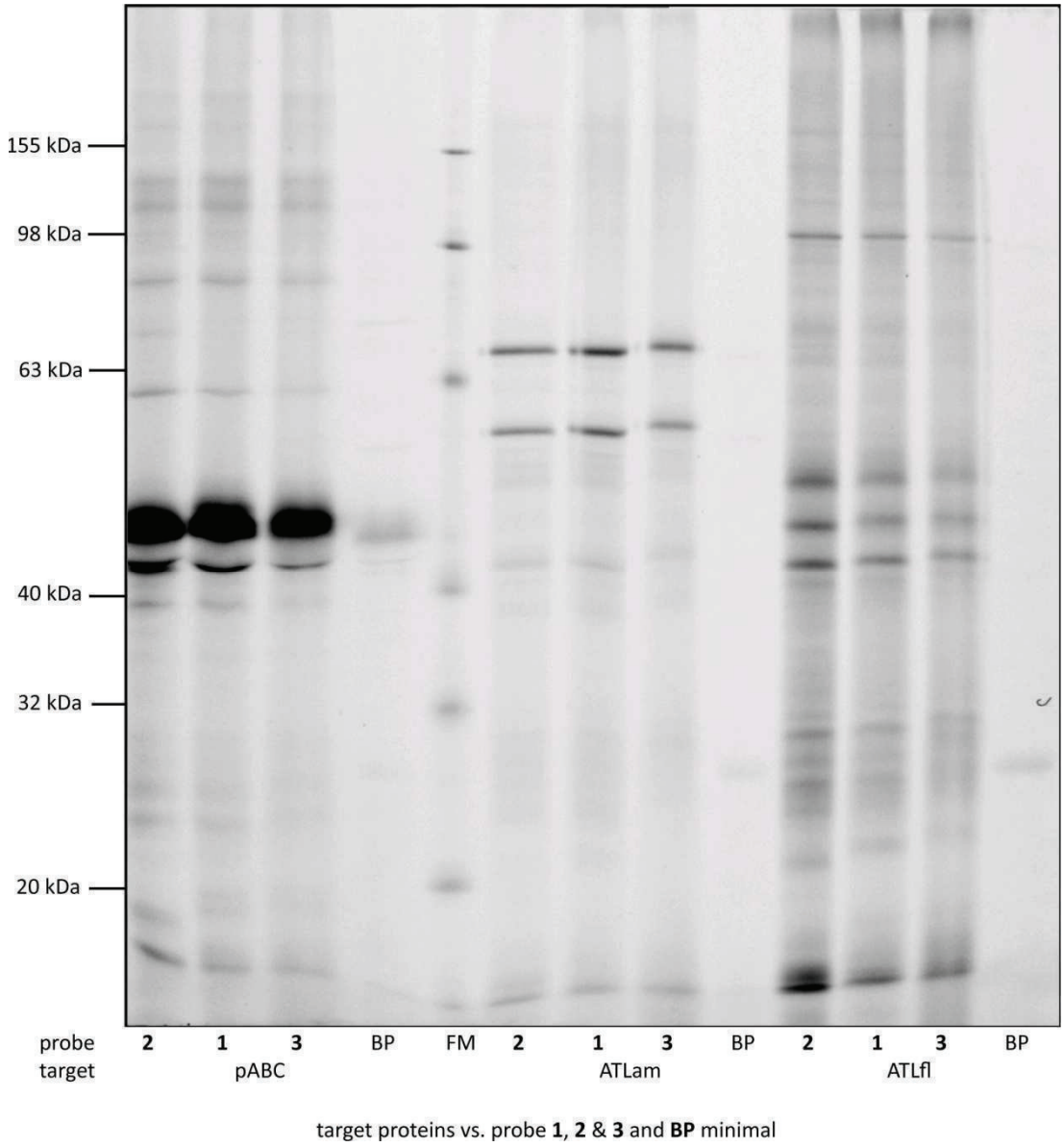

Figure S2 Comparison of labeling of overexpressed target enzymes with probes **1**, **2**, **3** and the **BP** minimal probe on a fluorescence scan of a PA gel. FM: Invitrogen BenchMark Fluorescent Protein Standard.

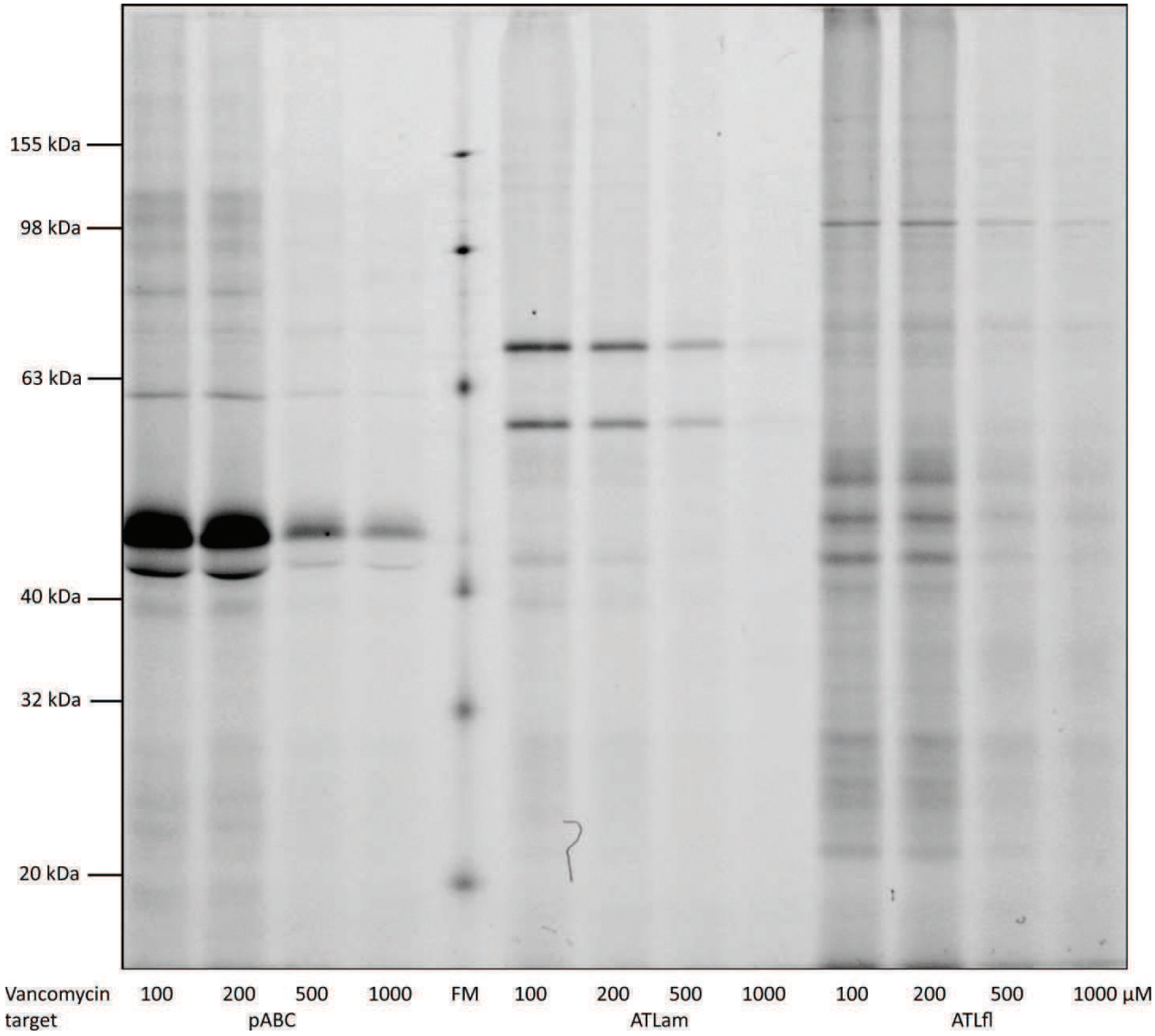

Figure S3 Competition of probe **1** with vancomycin in binding the overexpressed target enzymes on a fluorescence gel. Probe **1** 10 µM. Vancomycin 10, 20, 50, 100 fold excess.

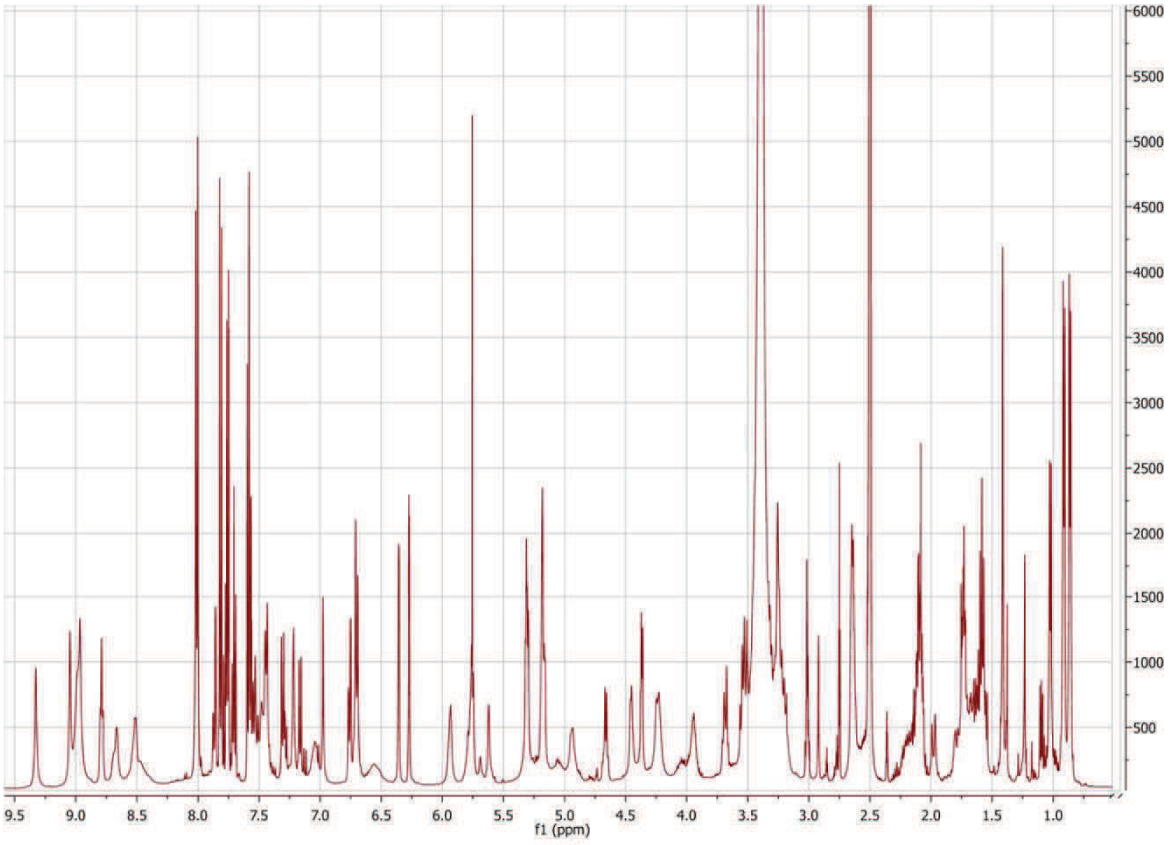
6000
5500
5000
4500
4000
3500
3000
2500
2000
1500
1000
500
9.5 9.0 8.5 8.0 7.5 7.0 6.5 6.0 5.5 5.0 4.5 4.0 3.5 3.0 2.5 2.0 1.5 1.0
f1 (ppm)

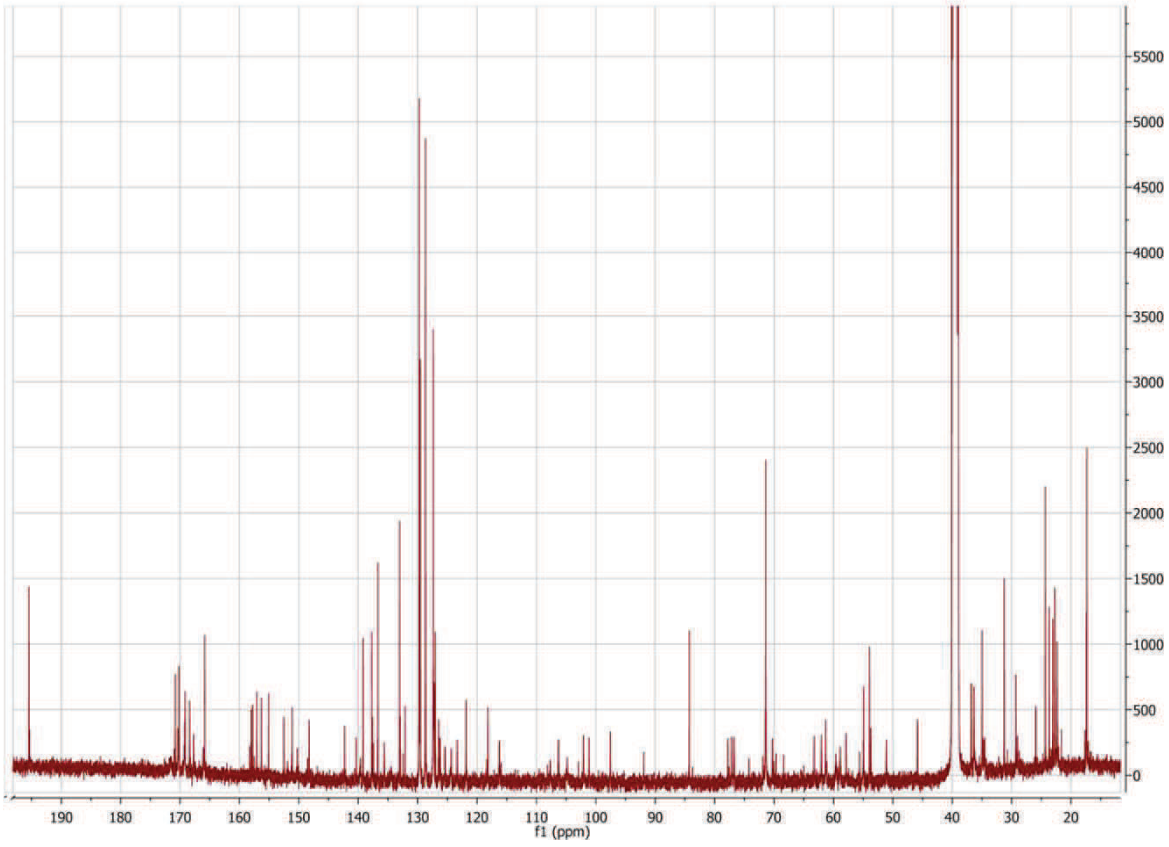
5500
5000
4500
4000
3500
3000
2500
2000
1500
1000
500
0
190 180 170 160 150 140 130 120 110 100 90 80 70 60 50 40 30 20
f1 (ppm)

Scheme S1: ^{1}H and ^{13}C NMR spectra of probe **1** in d_6DMSO.

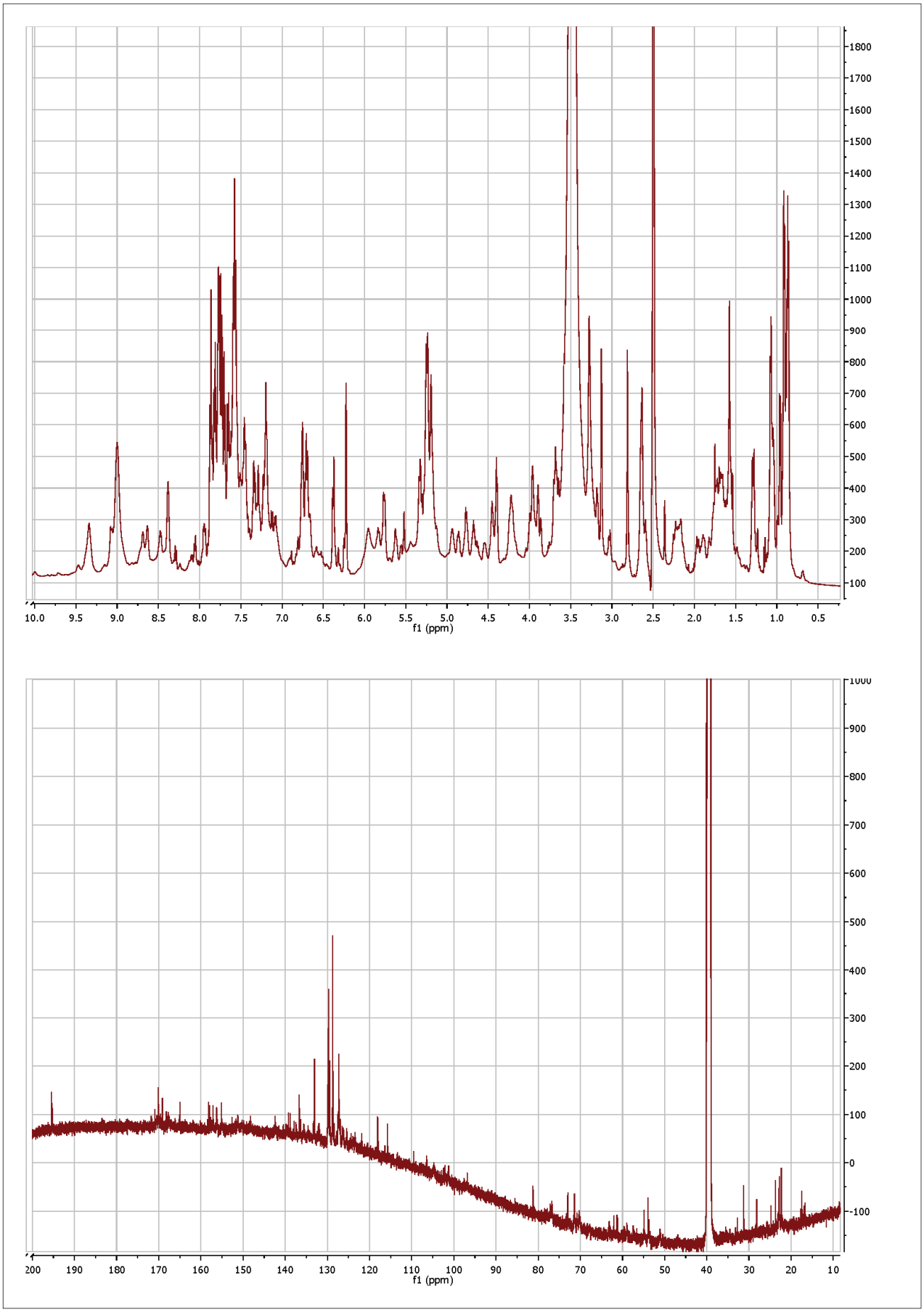

Scheme S2: ^{1}H and ^{13}C NMR spectra of probe **2** in d_6DMSO.

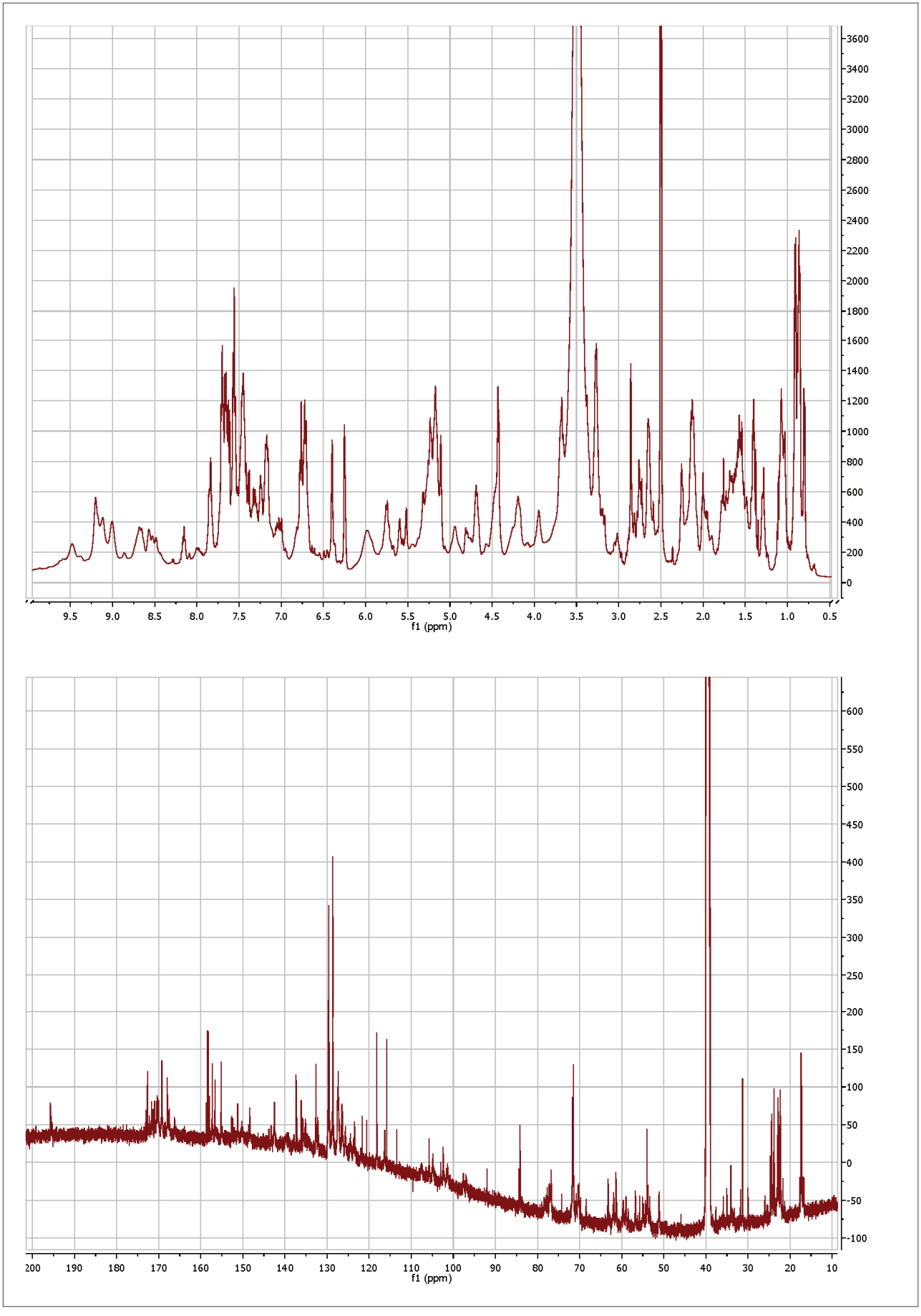

Sch

eme S3: ^{1}H and ^{13}C NMR spectra of probe **3** in d_6DMSO.

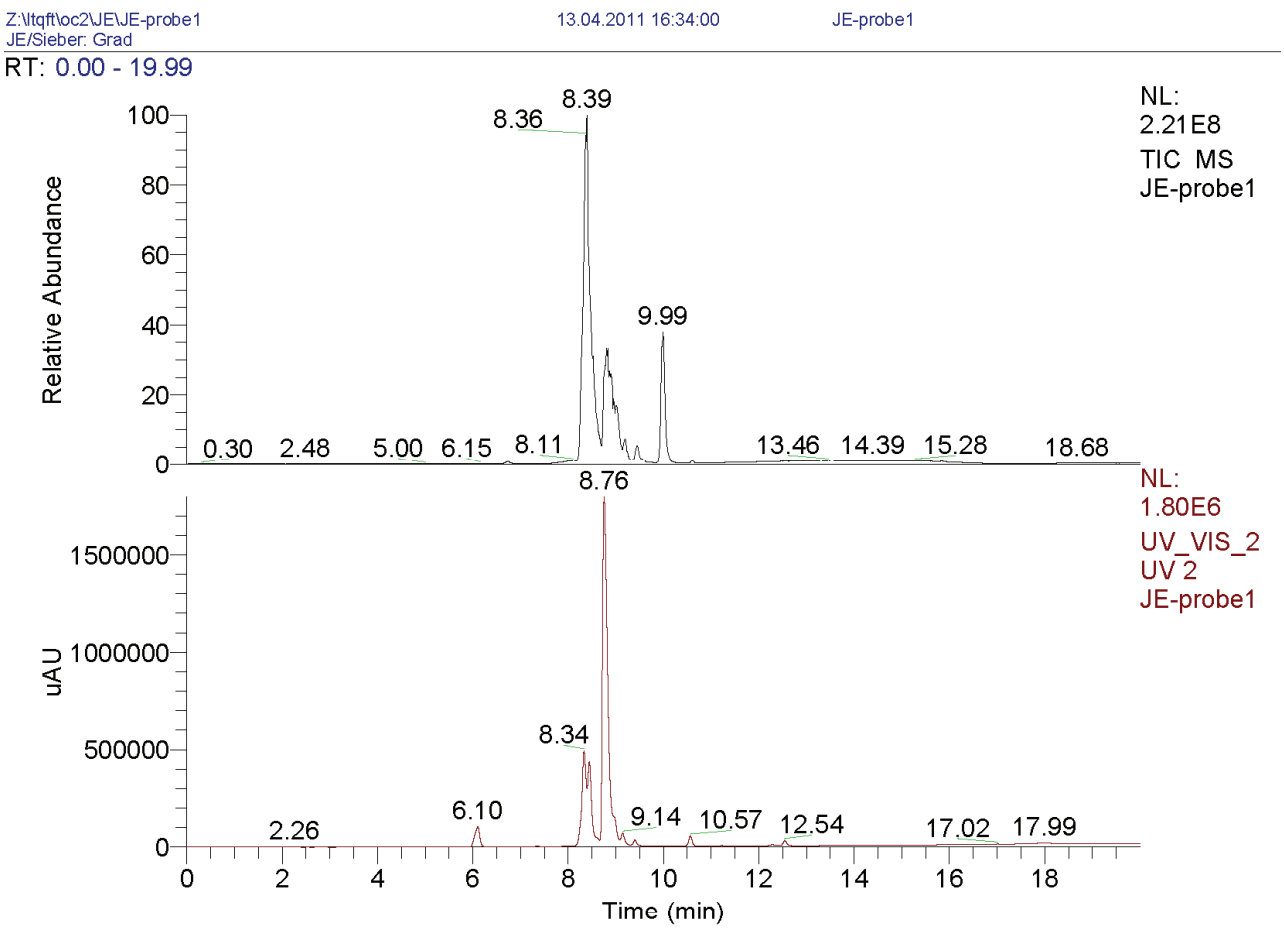
Z:\ltqft\oc2\JE\JE-probe1
13.04.2011 16:34:00
JE-probe1
JE/Sieber: Grad
RT: 0.00 - 19.99
Relative Abundance
8.39
8.36
9.99
0.30
2.48
5.00
6.15
8.11
13.46
14.39
15.28
18.68
NL:
2.21E8
TIC MS
JE-probe1
8.76
uAU
8.34
2.26
6.10
9.14
10.57
12.54
17.02
17.99
NL:
1.80E6
UV_VIS_2
UV 2
JE-probe1
Time (min)

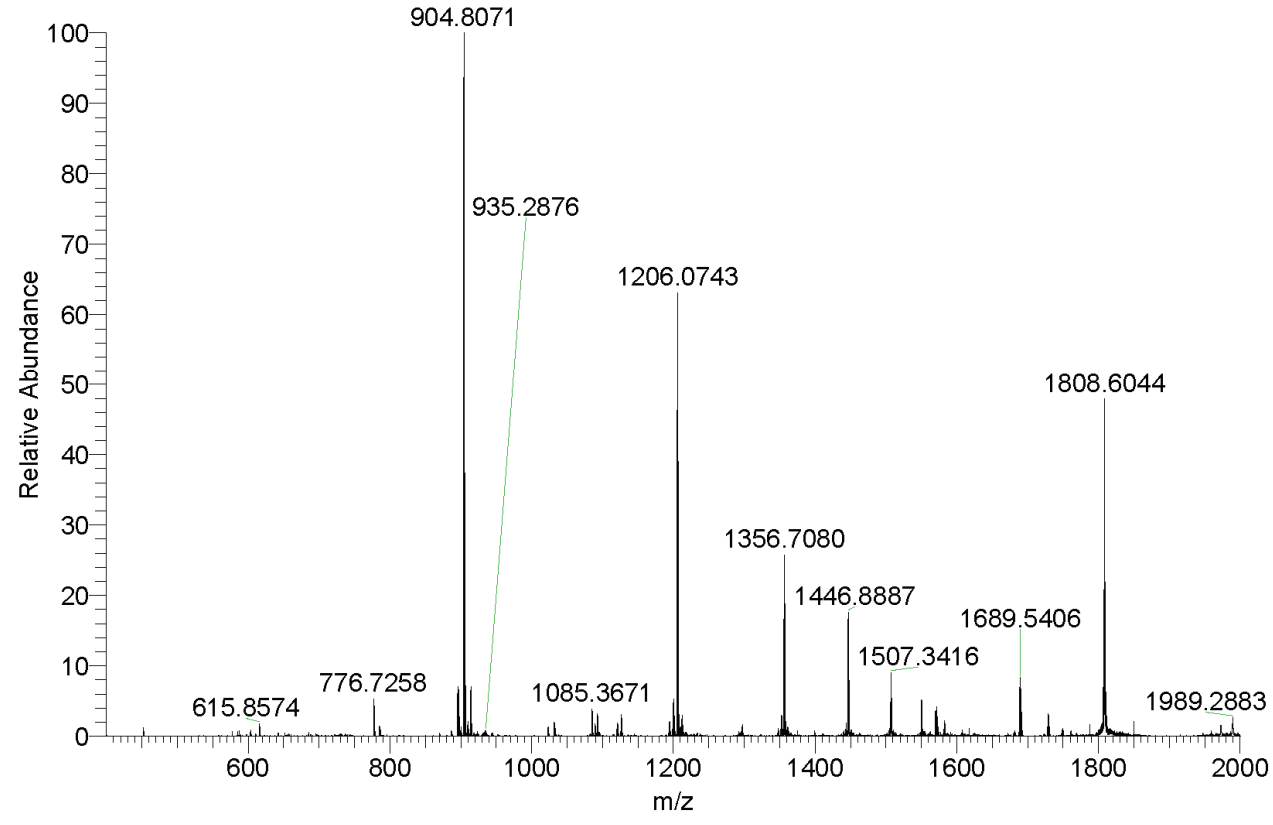
JE-probe1 #299-325 RT: 8.62-9.02 AV: 27 NL: 1.14E6
T: FTMS + p ESI Full ms [400.00-2000.00]
Relative Abundance
904.8071
935.2876
1206.0743
1808.6044
1356.7080
1446.8887
1689.5406
1507.3416
776.7258
615.8574
1085.3671
1989.2883
m/z

Sch

eme S4: HPLC- & HR-ESI-MS spectra of probe **1**.

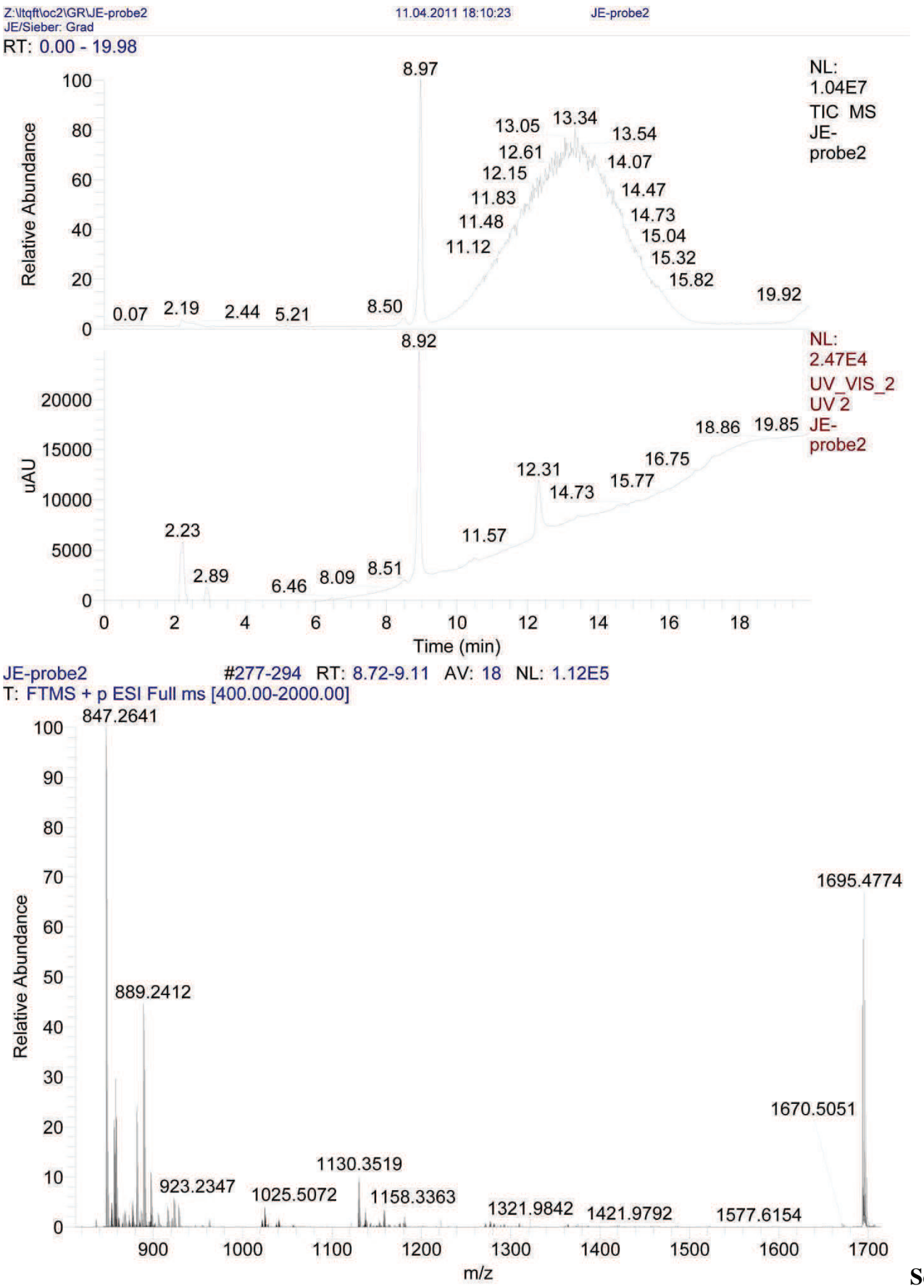

Scheme S5: HPLC- & HR-ESI-MS spectra of probe **2**.

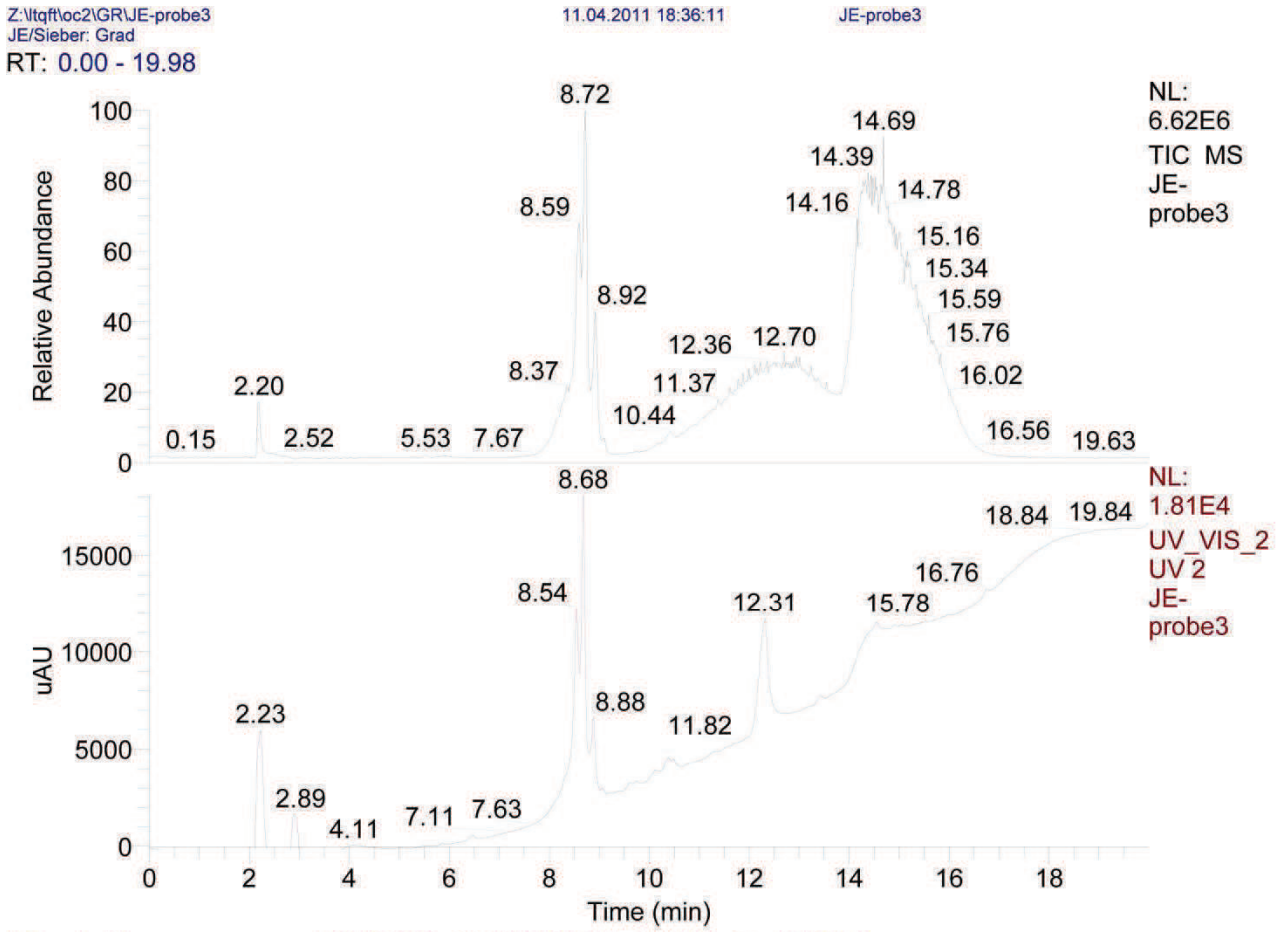
Z:\ltqft\oc2\GR\JE-probe3
JE/Sieber: Grad
11.04.2011 18:36:11
JE-probe3
RT: 0.00 - 19.98
NL:
6.62E6
TIC MS
JE-
probe3
Relative Abundance
8.72
14.69
14.39
8.59
14.16
14.78
15.16
15.34
8.92
15.59
15.76
12.36
12.70
8.37
16.02
11.37
2.20
10.44
16.56
19.63
0.15
2.52
5.53
7.67
NL:
1.81E4
UV_VIS_2
UV 2
JE-
probe3
uAU
8.68
18.84
19.84
16.76
8.54
12.31
15.78
8.88
2.23
11.82
2.89
4.11
7.11
7.63
Time (min)

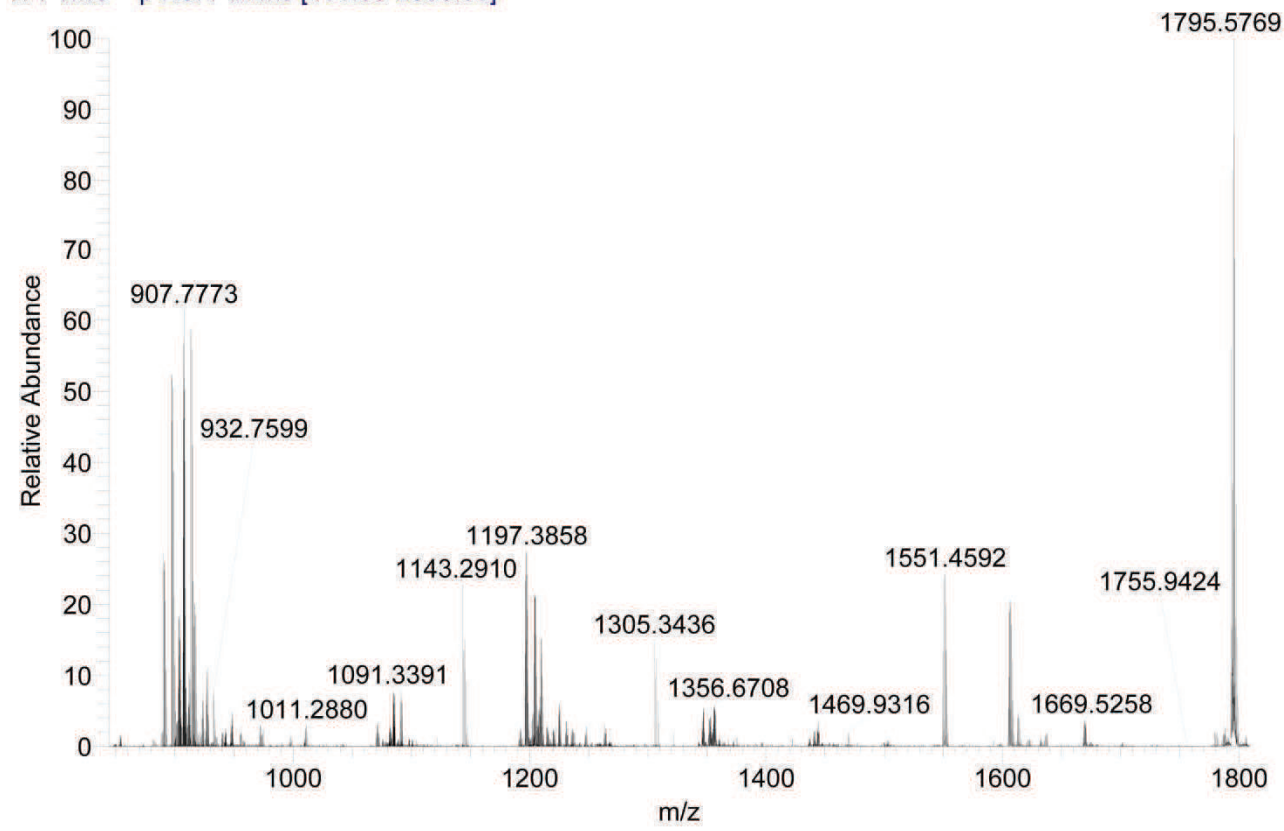
JE-probe3
#270-289 RT: 8.42-8.79 AV: 20 NL: 5.39E4
T: FTMS + p ESI Full ms [400.00-2000.00]
1795.5769
Relative Abundance
907.7773
932.7599
1197.3858
1143.2910
1551.4592
1755.9424
1305.3436
1091.3391
1356.6708
1011.2880
1469.9316
1669.5258
m/z

Sch

eme S6: HPLC- & HR-ESI-MS spectra of probe **3**.

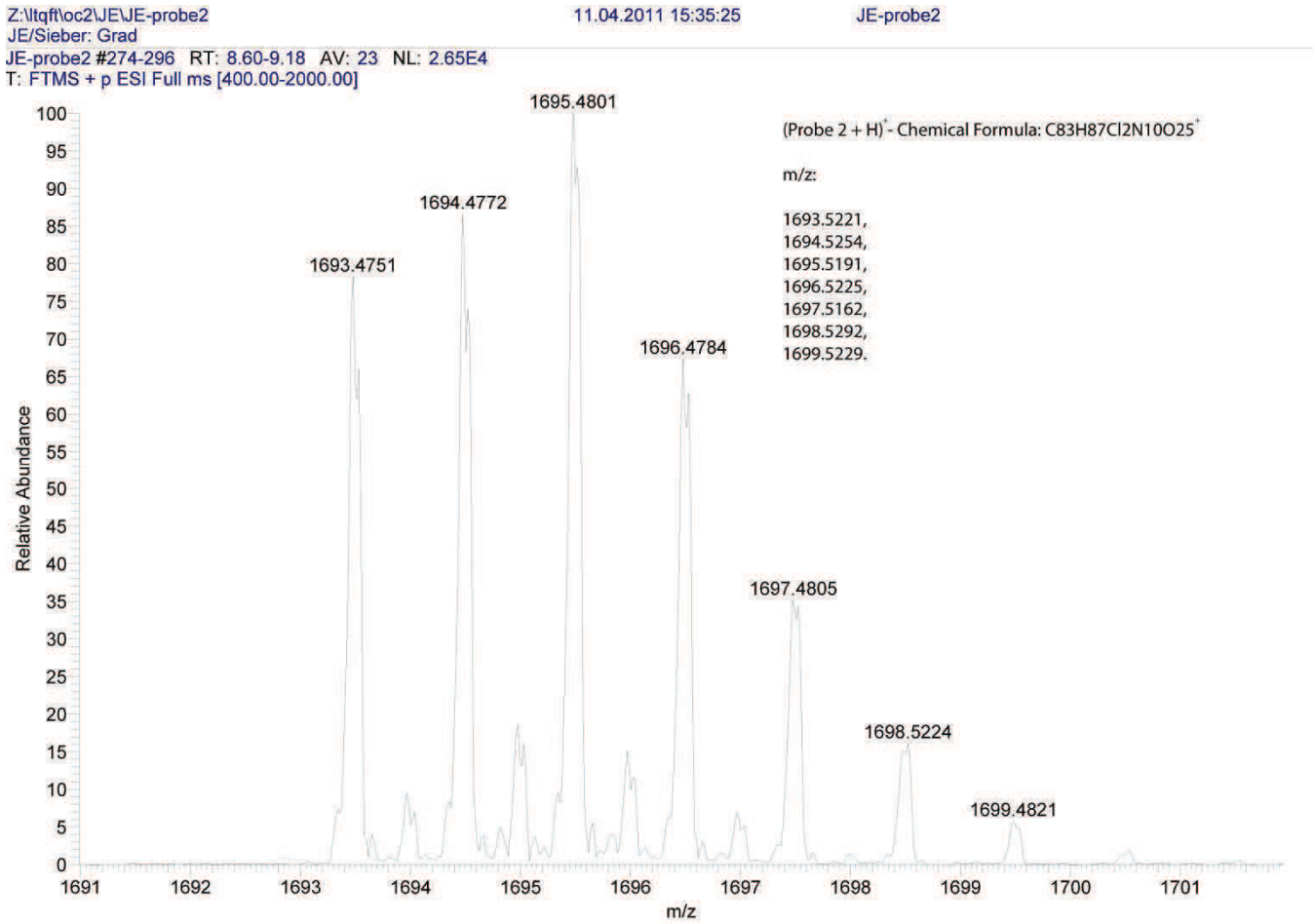

Scheme S7: HR-ESI-MS spectrum of probe **2** zoomed to its specific isotopic pattern.

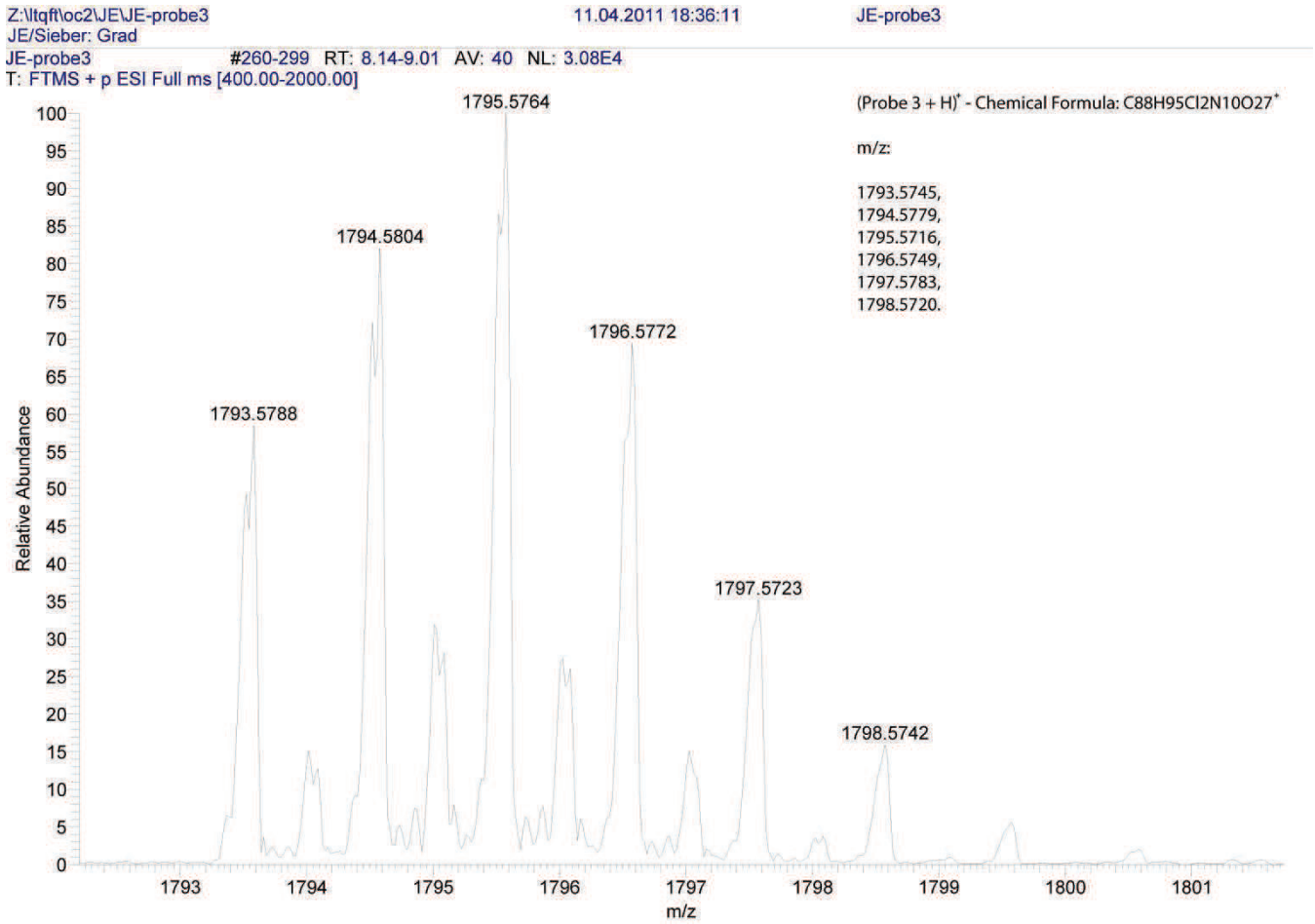

Scheme S8: HR-ESI-MS spectrum of probe **3** zoomed to its specific isotopic pattern.

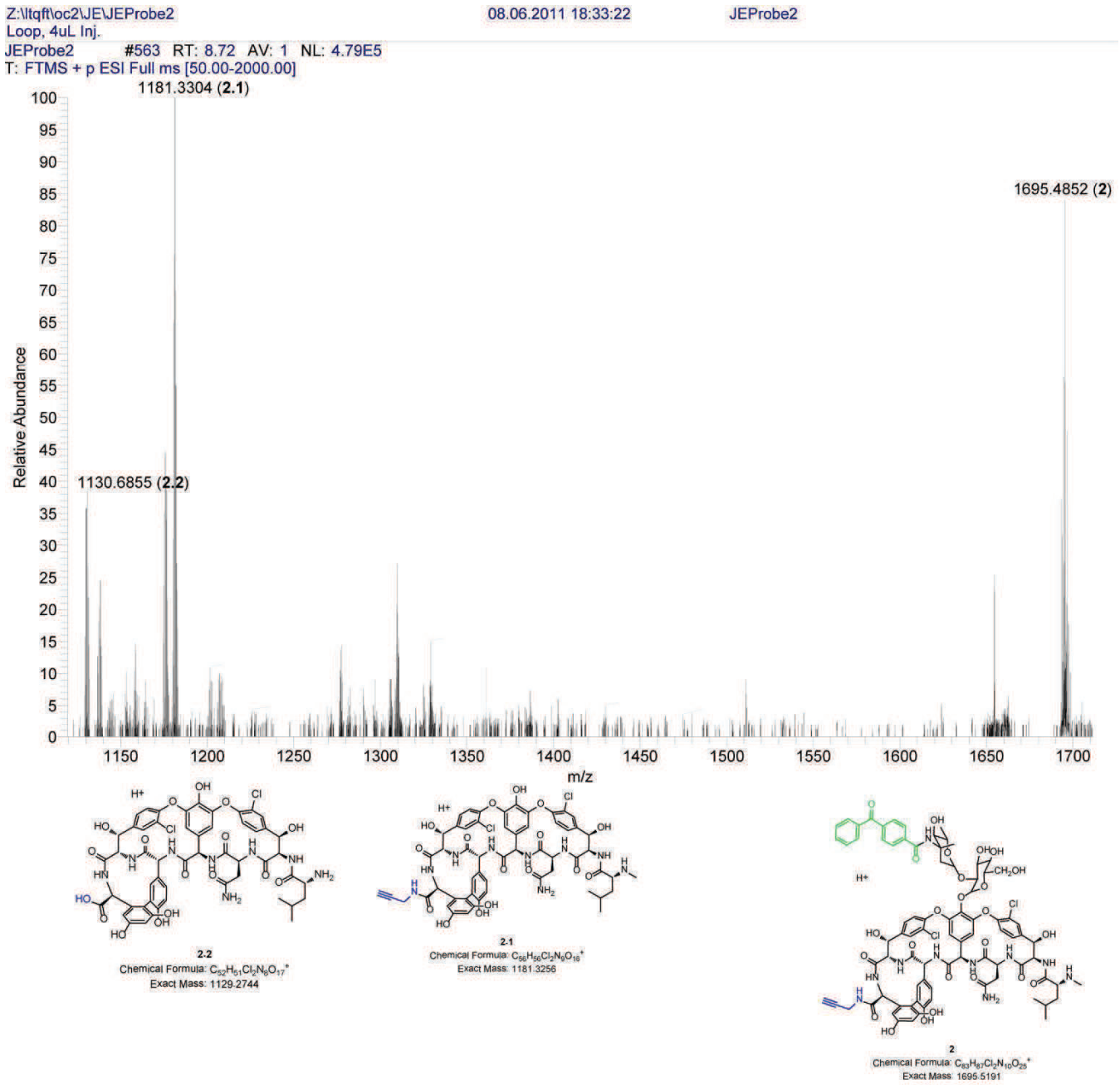

Scheme S9: HR-ESI-MS spectrum of probe **2** with specific fragmentation pattern.

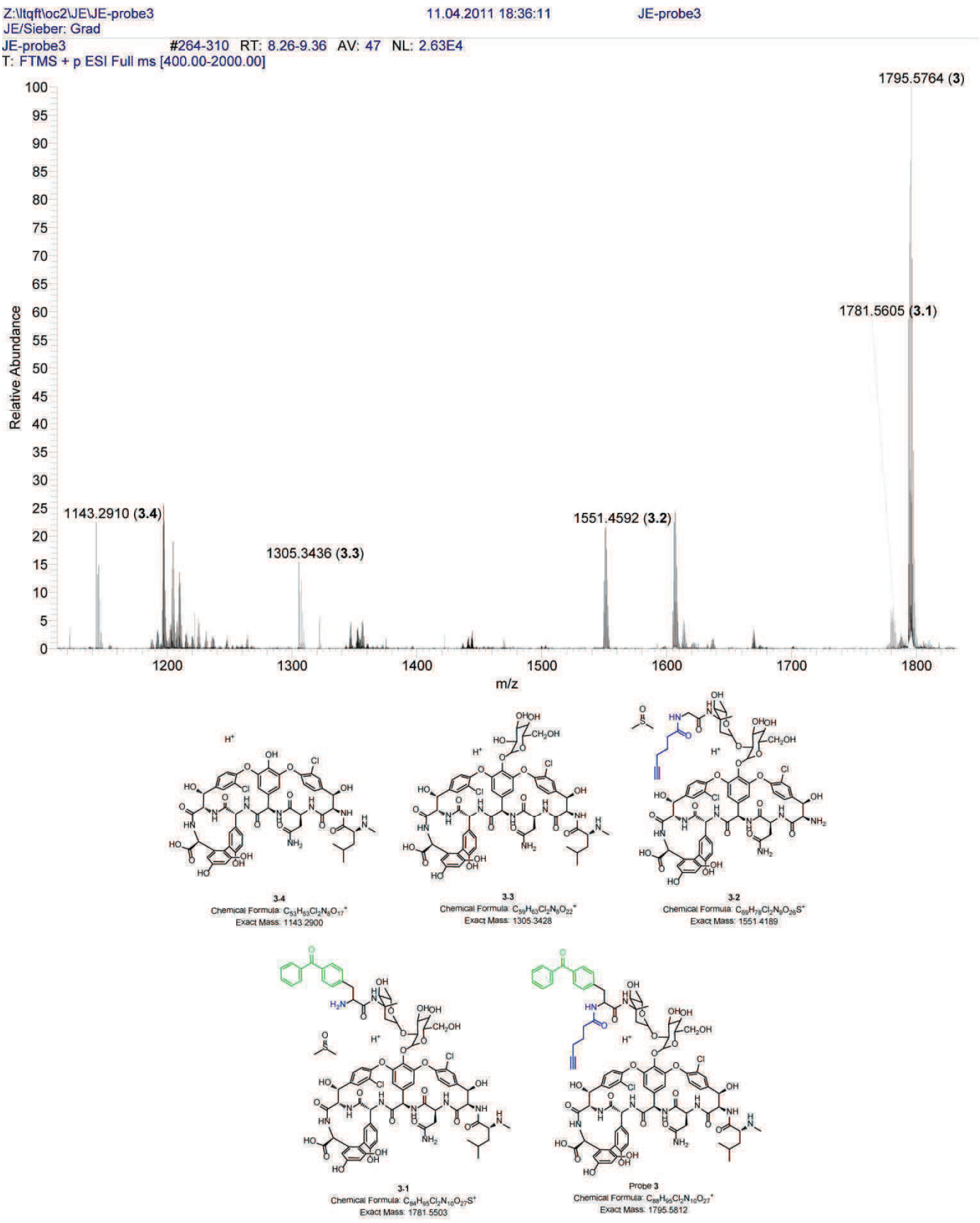

Scheme S10: HR-ESI-MS spectrum of probe **3** with specific fragmentation pattern.

Supplementary information for “Pretubulysin derived probes as novel tools for monitoring the microtubule network *via* activity-based protein profiling and fluorescence microscopy”

Electronic Supplementary Material (ESI) for Molecular BioSystems

Supporting Information

Pretubulysin derived probes as novel tools for monitoring the microtubule network via Activity-Based Protein Profiling and Fluorescence Microscopy

Jürgen Eirich, Jens L. Burkhart, Angelika Ullrich, Georg C. Rudolf, Angelika Vollmar, Stefan Zahler, Uli Kazmaier and Stephan A. Sieber

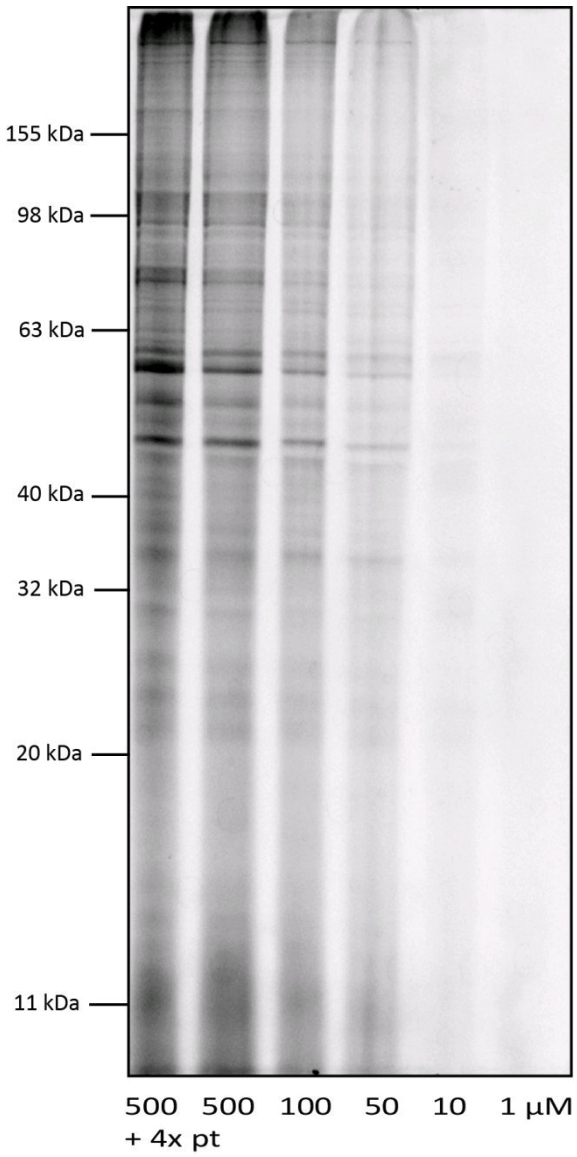

Supporting Figure 1: Concentration dependent *in situ* labeling (1 h incubation, 1 h UV irradiation) of membrane proteins in living Hela cells with compound **4**.

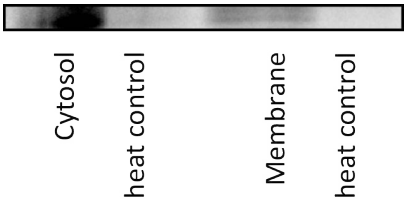

Supporting Figure 2: Heat controls of *in vitro* labeling of cytosolic and membrane proteins at about 60 kDa in Hela cell lysate with compound **4** (10 μM).

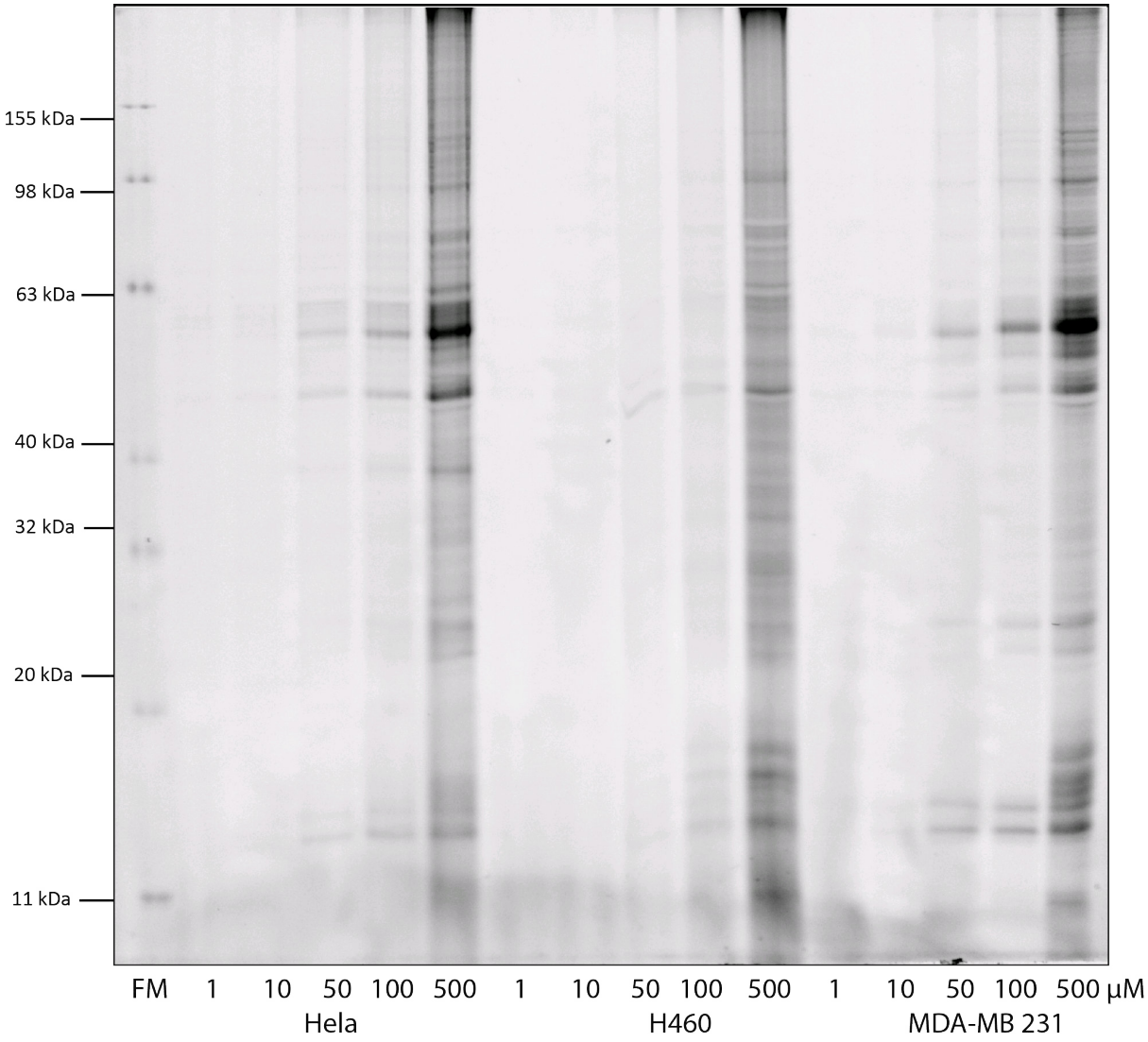

Supporting Figure 3: Concentration dependent *in situ* labeling of cytosolic proteins in different cell lines with probe **5** (10 µM).

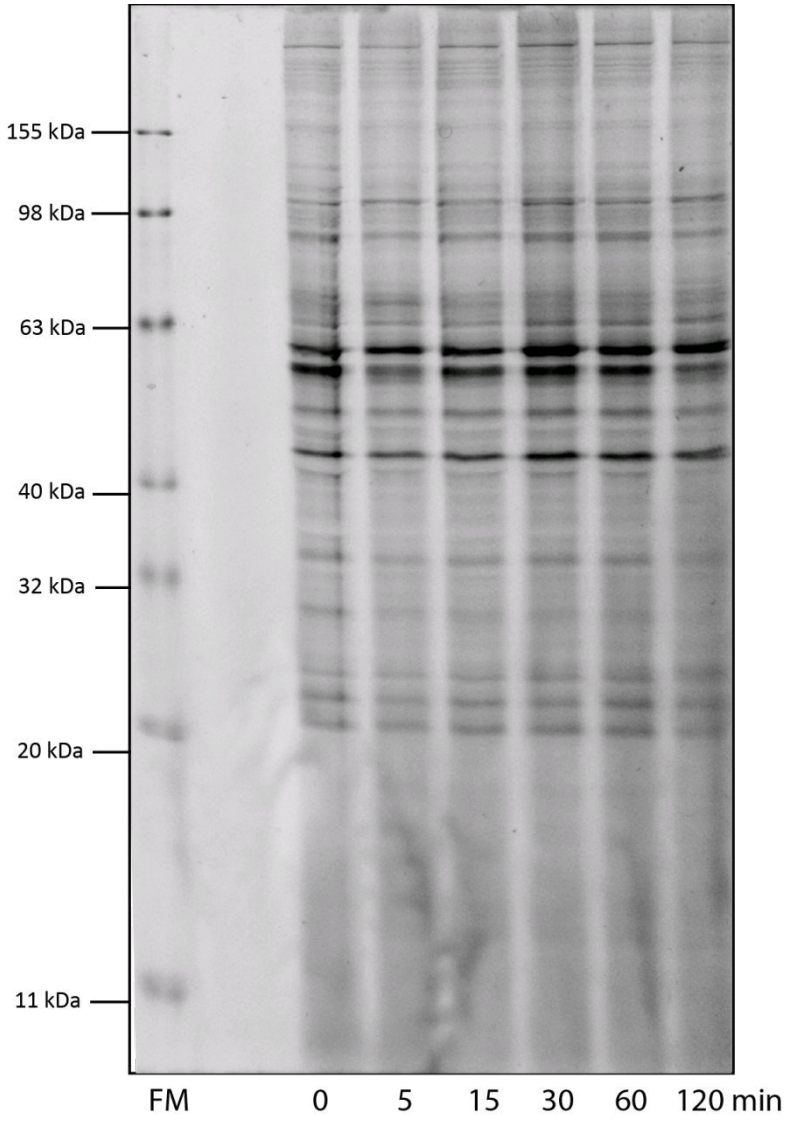

Supporting Figure 4: Time dependent *in situ* labeling: varying preincubation time of living Hela cells with compound **4** (10 µM) before UV irradiation (1 h).

	Score	Coverage	# Peptides	# PSM	Peak Area
H460 +	73.99	50.34	14	20	4.338E8
H460 -	8.10	6.29	2	3	3.134E7
Hela +	39.19	25.17	9	12	6.602E7
Hela -		0.00			0.000E0
Jurkat +	92.40	45.17	13	26	5.553E8
Jurkat -		0.00			5.069E7
MDA-MB +	53.82	44.27	13	14	1.823E8
MDA-MB -		0.00			0.000E0

Supporting Table 1: Mass spec data for tubulin, beta, 2 [Homo sapiens] (5174735;IPI00007752.1) selectively enriched and identified in different cell lines, Peak Areas calculated via Precursor Ions Area Detector of Thermo Proteome Discoverer 1.3, + Sample labeled with UV probe prior to biotin enrichment, - Sample NOT labeled with UV probe prior to biotin enrichment.

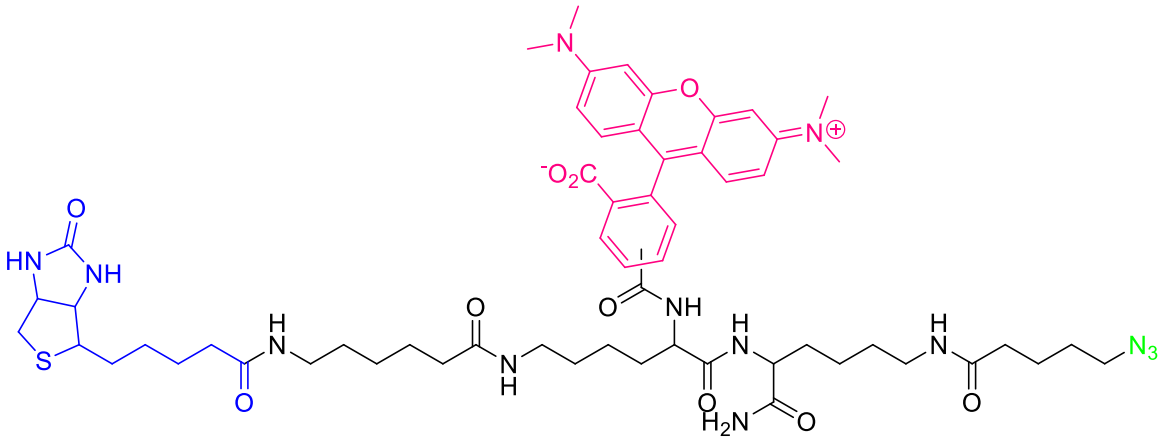

biotin-rhodamine-azide **15**

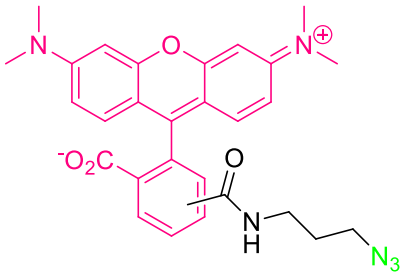

rhodamine-azide

Supporting Scheme 1: Molecular structure of Rhodamine Azide (RhN_3) used for in-gel fluorescent scanning and fluorescent microscopy and the Trifunctional Linker **15** (biotin-rhodamine- (alkyl)azide) used for biotin avidin enrichment.

Trifunctional linker **15** was synthesized according to standard solid phase peptide synthesis (SPPS) protocols[1] *via* Fmoc/tBu strategy[2] starting on Fmoc-Rink Amid MBHA resin[3]. The protected building blocks were deprotected via TFA (2 % in DCM) and were coupled by means of TBTU[4]/HOBt[5] and DIPEA[6] in following order: a) Fmoc-Lys(MTT)-OH[7] b) 5-Azido-pentanoic acid[8] c) Fmoc-Lys(biotinyl-ε-aminocaproyl)-OH[7] d) 5-(and-6)-carboxytetramethylrhodamine succinimidyl ester[9]. The peptidic compound was cleaved from the solid support with TFA (95 % in H_2O, 2 h at ambient temperature) and was precipitated in cold diethyl ether at -20 °C. The solid residue was purified *via* RP-HPLC (XBridge BEH C18 5 µm 30 x 150 mm, linear gradient 2 % - 98 % acetonitrile / H_2O with 0.1 % TFA in 30 min, UV-Vis detection at 550 nm, RT 10.2 – 10.8 min) and yielded after lyophilisation 59.6 mg purple powder (51.8 µmol, 24 % overall yield).

HRMS (ESI)	calculated	found
$[M+H]^+ = C_{85}H_{80}N_{13}O_{10}S^+$	1150.5866	1150.5850
$[M+2H]^{2+} = C_{85}H_{81}N_{13}O_{10}S^{2+}$	575.7970	575.7965

Synthetic procedures

(*S*)-methyl 3-(4-benzoylphenyl)-2-(*tert*-butoxycarbonylamino)propanoate (7)

A solution of Boc-protected iodophenylalanine methylester **6** (785 mg, 2.07 mmol), K_2CO_3 (857 mg, 6.21 mmol), *bis*(triphenylphosphine)palladium(II) dichloride (73 mg, 0.10 mmol) and phenylboronic acid (278 mg, 2.28 mmol) in anisole (20 mL) was stirred under CO-atmosphere at 80°C for 19 h. After cooling to room temperature the reaction mixture was diluted with diethyl ether (80 mL), washed with water and brine, dried with Na_2SO_4, and concentrated. The crude product was purified by flash chromatography (hexanes/ethyl acetate, 9:1, 7:3) to yield **7** (686 mg, 1.79 mmol, 83%) as a yellowish oil.

[tlc: hexanes/ethyl acetate = 8:2, R_f(**7**) = 0.14]

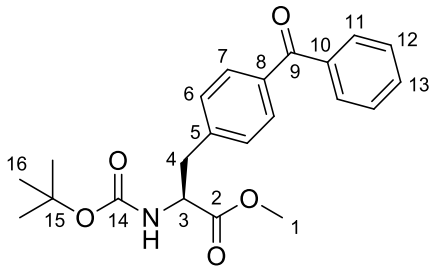

7

^{1}H-NMR ($CDCl_3$, 400 MHz): δ = 1.42 (s, 9 H, 16-H), 3.11 (dd, $^2J_{4a,4b}$ = 13.5 Hz, $^3J_{4a,3}$ = 6.1 Hz, 1 H, 4-H_a), 3.23 (dd, $^2J_{4b,4a}$ = 13.6 Hz, $^3J_{4b,3}$ = 5.6 Hz, 1 H, 4-H_b), 3.74 (s, 3 H, 1-H), 4.64 (m, 1 H, 3-H), 5.03 ($^3J_{NH,3}$ = 7.5 Hz, 1 H, NH), 7.25 (d, $^3J_{6,7}$ = 8.1 Hz, 2 H, 6-H), 7.48 (dd, $^3J_{12,11}$ = $^3J_{12,13}$ = 7.6 Hz, 2 H, 12-H), 7.59 (tt, $^3J_{13,12}$ = 7.4 Hz, $^4J_{13,11}$ = 1.3 Hz, 1 H, 13-H), 7.75 (d, $^3J_{7,6}$ = 8.2 Hz, 2 H, 7-H), 7.77 (dd, $^3J_{11,12}$ = 8.4 Hz, $^4J_{11,13}$ = 1.4 Hz, 2 H, 11-H).

^{13}C-NMR ($CDCl_3$, 100 MHz): δ = 28.3 (q, C-16), 38.4 (t, C-4), 52.4 (q, C-1), 54.2 (d, C-3), 80.1 (s, C-15), 128.3 (d, C-12), 129.3 (d, C-6), 129.9 (d, C-11), 130.3 (d, C-7), 132.4 (d, C-13), 136.3 (s, C-8), 137.6 (s, C-10), 141.1 (s, C-5), 155.0 (s, C-14), 172.0 (s, C-2), 196.3 (s, C-9).

optical rotation: $[\alpha]^{20}_D$ = +50.3° (c = 2.0, $CHCl_3$) [Lit.: $[\alpha]^{20}_D$ = +51.0° (c = 2.0, $CHCl_3$)[10]

(*S*,*E*)-ethyl 4-(*tert*-butoxycarbonylamino)-5-(4-iodophenyl)-2-methylpent-2-enoate (9)

A solution of DIBALH (1 M) in hexane (4.20 mL, 4.20 mmol) was added dropwise at –78°C to a solution of Boc-protected iodophenylalanine methylester **6** (850 mg, 2.10 mmol) in dry dichloromethane (12 mL). After stirring the reaction mixture for 1 h at –78°C, phosphonium salt **8** (1.02 g, 2.31 mmol) and KO*t*Bu (259 mg, 2.31 mmol) were added and the reaction mixture was warmed to room temperature overnight. The reaction mixture was poured into 10% aqueous tartaric acid (100 mL) and vigorously stirred for 30 min. After separation of the layers, the aqueous layer was extracted thrice with EtOAc. The combined organic layers were washed with water and brine, dried with Na_2SO_4, and concentrated. The crude product was purified by flash chromatography (hexanes/ethyl acetate, 8:2) to yield **9** (805 mg, 1.75 mmol, 83%) as a white solid, m.p. 112–113°C.

[tlc: hexanes/ethyl acetate = 8:2, R_f(**9**) = 0.28]

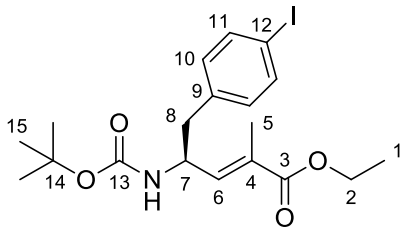

9

^{1}H-NMR ($CDCl_3$, 400 MHz): δ = 1.28 (t, $^3J_{1,2}$ = 7.1 Hz, 1-H), 1.40 (s, 9 H, 15-H), 1.71 (d, $^4J_{5,6}$ = 1.3 Hz, 3 H, 5-H), 2.72 (dd, $^2J_{8a,8b}$ = 13.5 Hz, $^3J_{8a,7}$ = 7.0 Hz, 1 H, 8-H_a), 2.86 (dd, $^2J_{8b,8a}$ = 13.3 Hz, $^3J_{8b,7}$ = 5.5 Hz, 1 H, 8-H_b), 4.18 (q, $^3J_{2,1}$ = 7.1 Hz, 2 H, 2-H), 4.50–4.66 (m, 2 H, 7-H, NH), 6.47 (dq, $^3J_{6,7}$ = 9.0 Hz, $^4J_{6,5}$ = 1.4 Hz, 1 H, 6-H), 6.92 (d, $^3J_{10,11}$ = 8.2 Hz, 2 H, 10-H), 7.60 (d, $^3J_{11,10}$ = 8.2 Hz, 1 H, 11-H).

^{13}C-NMR ($CDCl_3$, 100 MHz): δ = 12.7 (q, C-5), 14.2 (q, C-1), 28.3 (q, C-15), 40.7 (t, C-8), 49.9 (d, C-7), 60.8 (t, C-2), 79.8 (s, C-14), 92.0 (d, C-12), 129.8 (s, C-4), 131.5 (d, C-19), 136.4 (s, C-9), 137.5 (d, C-11), 139.5 (s, C-6), 154.9 (s, C-13), 167.6 (s, C-3).

optical rotation: $[\alpha]^{21}_D$ = +21.8° (c = 0.9, >95% *E,* $CHCl_3$)

HRMS (CI)	calculated	found
$C_{19}H_{27}NO_4I$ $[M+H]^+$	460.0985	460.0993

elemental analysis:

$C_{19}H_{26}NO_4I$	calculated	C 49.68	H 5.71	N 3.05
(459.32)	found	C 50.12	H 5.64	N 2.74

(*S*,*E*)-ethyl 5-(4-benzoylphenyl)-4-(*tert*-butoxycarbonylamino)-2-methylpent-2-enoate (10)

A solution of **9** (88 mg, 0.19 mmol), K_2CO_3 (79 mg, 0.57 mmol), *bis*(triphenylphosphine)palladium(II) dichloride (7 mg, 10 µmol) and phenylboronic acid (27 mg, 0.22 mmol) in anisole (2 mL) was stirred under CO-atmosphere at 80°C for 17 h. After cooling to room temperature the reaction mixture was diluted with diethyl ether (80 mL), washed with water and brine, dried with Na_2SO_4, and concentrated. The crude product was purified by flash chromatography (hexanes/ethyl acetate, 8:2) to yield **10** (81 mg, 0.19 mmol, 97%) as a reddish solid, m.p. 76–78°C.

[tlc: hexanes/ethyl acetate = 8:2, R_f(**10**) = 0.13]

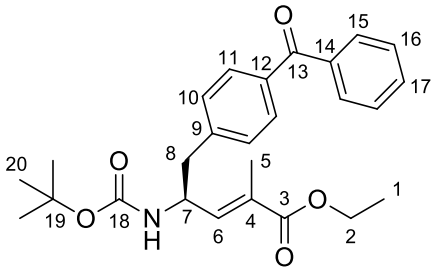

10

^{1}H-NMR ($CDCl_3$, 400 MHz): δ = 1.28 (t, $^3J_{1,2}$ = 7.1 Hz, 3 H, 1-H), 1.40 (s, 9 H, 15-H), 1.73 (d, $^4J_{5,6}$ = 1.4 Hz, 3 H, 5-H), 2.87 (dd, $^2J_{8a,8b}$ = 13.3 Hz, $^3J_{8a,7}$ = 7.0 Hz, 1 H, 8-H_a), 3.02 (dd, $^2J_{8b,8a}$ = 13.0 Hz, $^3J_{8b,7}$ = 5.7 Hz, 1 H, 8-H_b), 4.18 (q, $^3J_{2,1}$ = 7.1 Hz, 2 H, 2-H), 4.60–4.76 (m, 2 H, 7-H, NH), 6.53 (dq, $^3J_{6,7}$ = 9.0 Hz, $^4J_{6,5}$ = 1.4 Hz, 1 H, 6-H), 7.29 (d, $^3J_{10,11}$ = 8.2 Hz, 2 H, 10-H), 7.47 (dd, $^3J_{16,15}$ = $^3J_{16,17}$ = 7.6 Hz, 2 H, 16-H), 7.58 (tt, $^3J_{17,16}$ = 7.4 Hz, $^4J_{17,15}$ = 1.3 Hz, 1 H, 17-H), 7.74 (d, $^3J_{11,10}$ = 8.2 Hz, 2 H, 11-H), 7.77 (dd, $^3J_{15,16}$ = 8.4 Hz, $^4J_{15,17}$ = 1.4 Hz, 2 H, 15-H).

^{13}C-NMR ($CDCl_3$, 100 MHz): δ = 12.7 (q, C-5), 14.2 (q, C-1), 28.3 (q, C-20), 41.3 (t, C-8), 50.0 (d, C-7), 60.8 (t, C-2), 80.0 (s, C-19), 128.2 (d, C-16), 129.5 (d, C-10), 129.9 (s, d, C-4, C-15), 130.3 (d, C-11), 132.3 (d, C-17), 136.0 (s, C-12), 137.6 (s, C-14), 139.5 (s, C-6), 141.8 (s, C-9), 155.0 (s, C-18), 172.0 (s, C-3), 196.3 (s, C-13).

optical rotation: $[\alpha]^{21}_D$ = +25.4° (c = 1.1, $CHCl_3$)

HRMS (CI)	calculated	found
$C_{22}H_{24}NO_5$ $[M–C_4H_8+H]^+$	382.1654	382.1667

elemental analysis:

$C_{26}H_{31}NO_5$	calculated	C 71.37	H 7.14	N 3.20
(437.53)	found	C 70.75	H 7.15	N 2.85

(*S*)-methyl 3-(4-benzoylphenyl)-2-(2-((*R*)-3-(*tert*-butoxycarbonyl(methyl)amino)-4-methylpentyl)thiazole-4-carboxamido)propanoate (11a)

HCl in dioxane (1.28 mL, 5.10 mmol, 4 M) was added at 0°C to **7** (196 mg, 0.51 mmol). The solvent was evaporated in vacuum after complete deprotection (30 min, tlc monitoring) and the hydrochloride salt was dried in high vacuum.

Isobutyl chloroformate (68 µL, 0.51 mmol) was added dropwise at –20°C to a solution of Boc-protected tubuvaline **BocTuvOH**[11] (157 mg, 0.46 mmol) and NMM (127 µL, 1.15 mmol) in dry THF (5 mL). After 20 min, *N*-deprotected **7** was added and the mixture was allowed to warm to room temperature overnight. Water was added and the mixture was extracted with ethyl acetate (3x). The combined organic layers were washed with aqueous HCl (1 M), water, saturated aqueous $NaHCO_3$, water and brine, dried over Na_2SO_4 and concentrated in vacuum. The crude product was purified by flash chromatography (SiO_2, hexanes/ethyl acetate = 6:4) to yield dipeptide **11a** (238 mg, 0.39 mmol, 85% over 2 steps) as colourless oil and a mixture of rotamers.

[tlc: hexanes/ethyl acetate = 1:1, R_f(**11a**) = 0.25]

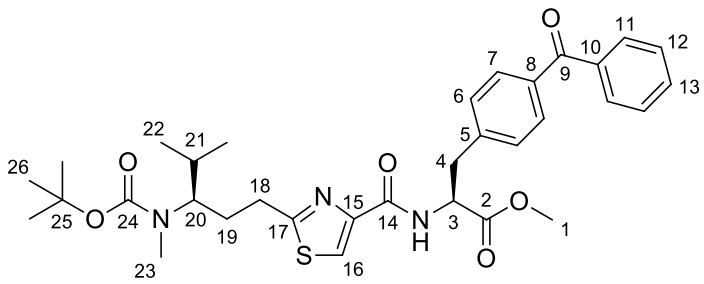

11a

major rotamer

^{1}H-NMR ($CDCl_3$, 400 MHz): δ = 0.81 (d, $^3J_{22,21}$ = 6.5 Hz, 3 H, 22-H), 0.83 (d, $^3J_{22',21}$ = 6.5 Hz, 3 H, 22'-H), 1.38 (s, 9 H, 26-H), 1.65 (m, 1 H, 21-H), 1.78 (m, 1 H, 19-H_a), 2.14 (m, 1 H, 19-H_b), 2.63 (s, 3 H, 23-H), 2.88 (m, 2 H, 18-H), 3.27 (dd, $^2J_{4a,4b}$ = 13.9 Hz, $^3J_{4a,3}$ = 6.4 Hz, 1 H, 4-H_a), 3.36 (dd, $^2J_{4b,4a}$ = 13.9 Hz, $^3J_{4b,3}$ = 6.4 Hz, 1 H, 4-H_b), 3.74 (s, 3 H, 1-H), 3.82 (m, 1 H, 20-H), 5.09 (m, 1 H, 3-H), 7.30 (d, $^3J_{6,7}$ = 8.1 Hz, 2 H, 6-H), 7.46 (dd, $^3J_{12,11}$ = $^3J_{12,13}$ = 7.6 Hz, 2 H, 12-H), 7.57 (t, $^3J_{13,12}$ = 7.4 Hz, 13-H), 7.73 (d, $^3J_{7,6}$ = 8.3 Hz, 2 H, 7-H), 7.75 (m, 2 H, 11-H), 7.79 ($^3J_{NH,3}$ = 8.0 Hz, 1 H, NH), 7.40 (s, 1 H, 16-H).

^{13}C-NMR ($CDCl_3$, 100 MHz): δ = 19.6 (q, C-22), 19.9 (q, C-22'), 28.2 (q, C-23), 28.4 (q, C-26), 29.5 (t, C-19), 30.1 (t, C-18), 30.5 (d, C-21), 38.1 (t, C-4), 52.4 (q, C-1), 53.0 (d, C-3), 60.3 (d, C-20), 79.2 (s, C-25), 123.1 (d, C-16), 128.2 (d, C-12), 129.2 (d, C-6), 129.9 (d, C-11), 130.4 (d, C-7), 132.3 (d, C-13), 136.2 (s, C-8), 137.6 (s,

C-10), 141.1 (s, C-5), 148.7 (s, C-15), 156.4 (s, C-24), 160.6 (s, C-14), 170.8 (s, C-17), 171.4 (s, C-2), 196.2 (s, C-9).

minor rotamer (selected signals)

^{1}H-NMR ($CDCl_3$, 400 MHz): δ = 0.91 (d, $^{3}J_{22,21}$ = 6.5 Hz, 3 H, 22-H), 0.93 (d, $^{3}J_{22',21}$ = 6.5 Hz, 3 H, 22'-H), 1.44 (s, 9 H, 26-H), 2.66 (s, 3 H, 23-H), 3.28 (dd, $^{2}J_{4a,4b}$ = 13.7 Hz, $^{3}J_{4a,3}$ = 6.2 Hz, 1 H, 4-H_a), 3.64 (bs, 1 H, 20-H), 7.96 (s, 1 H, 16-H).

^{13}C-NMR ($CDCl_3$, 100 MHz): δ = 20.1 (q, C-22), 20.3 (q, C-22'), 28.4 (q, C-23), 29.1 (t, C-19), 30.3 (t, C-18), 30.7 (d, C-21), 38.2 (t, C-4), 53.0 (d, C-3), 79.5 (s, C-25), 129.2 (d, C-6), 129.9 (d, C-11), 136.2 (s, C-8), 141.1 (s, C-5), 148.8 (s, C-15), 156.6 (s, C-24), 160.7 (s, C-14), 171.0 (s, C-17), 171.5 (s, C-2), 196.2 (s, C-9).

optical rotation: $[\alpha]^{21}_{D}$ = +9.4° (c = 0.6, $CHCl_3$)

HRMS (CI)	calculated	found
$C_{33}H_{42}N_3O_6S$ $[M+H]^+$	608.2794	608.2751

(*S*,*E*)-ethyl 5-(4-benzoylphenyl)-4-(2-((*R*)-3-(*tert*-butoxycarbonyl(methyl)amino)-4-methylpentyl)thiazole-4-carboxamido)-2-methylpent-2-enoate (11b)

HCl in dioxane (1.63 mL, 6.50 mmol, 4 M) was added at 0°C to **10** (284 mg, 0.65 mmol). The solvent was evaporated in vacuum after complete deprotection (30 min, tlc monitoring) and the hydrochloride salt was dried in high vacuum.

Isobutyl chloroformate (86 µL, 0.65 mmol) was added dropwise at –20°C to a solution of Boc-protected tubuvaline **Boc-TuvOH**[11] (223 mg, 0.65 mmol) and NMM (180 µL, 1.63 mmol) in dry THF (6 mL). After 20 min, *N*-deprotected **10** was added and the mixture was allowed to warm to room temperature overnight. Water was added and the mixture was extracted with ethyl acetate (3x). The combined organic layers were washed with aqueous HCl (1 M), water, saturated aqueous $NaHCO_3$, water and brine, dried over Na_2SO_4 and concentrated in vacuum. The crude product was purified by flash chromatography (SiO_2, petroleum ether/ethyl acetate = 7:3, 6:4) to yield dipeptide **11b** (394 mg, 0.60 mmol, 92% over 2 steps) as a white solid and a mixture of rotamers, m.p. 49–52°C.

[tlc: petroleum ether/ethyl acetate = 6:4, R_f(**11b**) = 0.19]

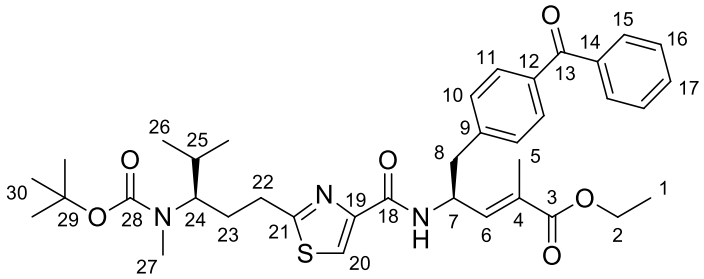

11b

major rotamer

^{1}H-NMR ($CDCl_3$, 400 MHz): δ = 0.84 (d, $^3J_{26,25}$ = 6.5 Hz, 6 H, 26-H), 1.27 (t, $^3J_{1,2}$ = 7.1 Hz, 3 H, 1-H), 1.40 (s, 9 H, 30-H), 1.67 (m, 1 H, 25-H), 1.77 (d, $^4J_{5,6}$ = 1.1 Hz, 3 H, 5-H), 1.81 (m 1 H, 23-H_a), 2.11 (m, 1 H, 23-H_b), 2.65 (s, 3 H, 27-H), 2.85 (m, 2 H, 22-H), 3.00 (dd, $^2J_{8a,8b}$ = 13.2 Hz, $^3J_{8a,7}$ = 7.8 Hz, 1 H, 8-H_a), 3.20 (dd, $^2J_{8b,8a}$ = 13.4 Hz, $^3J_{8b,7}$ = 6.2 Hz, 1 H, 8-H_b), 3.79 (m, 1 H, 24-H), 4.18 (q, $^3J_{2,1}$ = 7.1 Hz, 2 H, 2-H), 5.20 (m, 1 H, 7-H), 6.67 (dq, $^3J_{6,7}$ = 9.0 Hz, $^4J_{6,5}$ = 1.4 Hz, 1 H, 6-H), 7.35 (d, $^3J_{10,11}$ = 8.1 Hz, 2 H, 10-H), 7.46 (dd, $^3J_{16,15}$ = $^3J_{16,17}$ = 7.6 Hz, 2 H, 16-H), 7.52 (d $^3J_{NH,7}$ = 8.2 Hz, 1 H, NH), 7.57 (t, $^3J_{17,16}$ = 7.4 Hz, 1 H, 17-H), 7.73 (d, $^3J_{11,10}$ = 8.3 Hz, 2 H, 11-H), 7.75 (d, $^3J_{15,16}$ = 7.8 Hz, 2 H, 15-H), 7.92 (s, 1 H, 20-H).

^{13}C-NMR ($CDCl_3$, 100 MHz): δ = 12.9 (q, C-5), 14.2 (q, C-1), 19.6 (q, C-26), 19.9 (q, C-26‘), 28.2 (q, C-27), 28.4 (q, C-30), 29.7 (t, C-23), 30.2 (t, C-22), 30.5 (d, C-25), 41.0 (t, C-8), 48.6 (d, C-7), 60.1 (d, C-24), 60.8 (t, C-2), 79.2 (s, C-29), 122.8 (d,

C-20), 128.2 (d, C-16), 129.4 (d, C-10), 129.9 (d, C-15), 130.3 (d, C-11), 130.8 (s, C-4), 132.3 (d, C-17), 136.0 (s, C-12), 137.7 (s, C-14), 138.5 (s, C-6), 141.8 (s, C-9), 149.0 (s, C-19), 156.5 (s, C-28), 160.2 (s, C-18), 167.5 (s, C-21), 170.9 (s, C-3), 196.3 (s, C-13).

minor rotamer (selected signals)

^{1}H-NMR ($CDCl_3$, 400 MHz): δ = 0.95 (d, $^{3}J_{26,25}$ = 6.5 Hz, 6 H, 26-H), = 0.97 (d, $^{3}J_{26',25}$ = 6.5 Hz, 6 H, 26'-H), 1.46 (s, 9 H, 30-H), 1.79 (d, $^{4}J_{5,6}$ = 1.1 Hz, 3 H, 5-H), 3.01 (dd, $^{2}J_{8a,8b}$ = 13.2 Hz, $^{3}J_{8a,7}$ = 7.8 Hz, 1 H, 8-H_a), 3.21 (dd, $^{2}J_{8b,8a}$ = 13.4 Hz, $^{3}J_{8b,7}$ = 6.2 Hz, 1 H, 8-H_b), 3.65 (bs, 1 H, 24-H), 4.19 (q, $^{3}J_{2,1}$ = 7.1 Hz, 2 H, 2-H), 6.68 (dq, $^{3}J_{6,7}$ = 9.0 Hz, $^{4}J_{6,5}$ = 1.4 Hz, 1 H, 6-H), 7.35 (d, $^{3}J_{10,11}$ = 8.1 Hz, 2 H, 10-H), 7.52 (d $^{3}J_{NH,7}$ = 8.4 Hz, 1 H, NH), 7.94 (s, 1 H, 20-H).

^{13}C-NMR ($CDCl_3$, 100 MHz): δ = 20.1 (q, C-26), 20.3 (q, C-26'), 29.4 (t, C-23), 30.2 (t, C-22), 30.7 (d, C-25), 41.0 (t, C-8), 48.7 (d, C-7), 79.5 (s, C-29), 129.4 (d, C-10), 130.8 (s, C-4), 149.2 (s, C-19), 156.6 (s, C-28), 160.3 (s, C-18), 167.6 (s, C-21), 171.1 (s, C-3).

optical rotation: $[\alpha]^{21}_{D}$ = +8.6° (c = 1.1, $CHCl_3$)

HRMS (CI)	calculated	found
$C_{37}H_{47}N_3O_6S$ [M]	661.3186	661.3233

elemental analysis:

$C_{37}H_{47}N_3O_6S$	calculated	C 67.14	H 7.16	N 6.35
(661.85)	found	C 66.36	H 7.17	N 6.04

(*S*)-methyl 3-(4-benzoylphenyl)-2-(2-((*R*)-3-((2*S*,3*S*)-2-(benzyloxycarbonyl-amino)-*N*,3-dimethylpentanamido)-4-methylpentyl)thiazole-4-carboxamido) propanoate (12a)

HCl in dioxane (2.0 mL, 8.0 mmol, 4 M) was added at 0°C to dipeptide **11a** (182 mg, 0.30 mmol). The solvent was evaporated in vacuum after complete deprotection (30 min, tlc monitoring) and the hydrochloride salt was dried in high vacuum.

N-Deprotected **11a**, Cbz-protected L-isoleucine (90 mg, 0.33 mmol) and BEP (90 mg, 0.33 mmol) were dissolved in dry DCM (3 mL) and diisopropyl ethylamine (160 µL, 0.94 mmol) was added dropwise to this solution at –10°C. The cooling bath was removed after 20 min and the reaction mixture was stirred at room temperature for 20 h. The reaction mixture was diluted with DCM and washed with aqueous HCl (1 M), saturated aqueous $NaHCO_3$, water and brine, dried over Na_2SO_4 and concentrated in vacuum. The crude product was purified by flash chromatography (SiO_2, hexanes/ethyl acetate = 1:1) to yield tripeptide **12a** (195 mg, 0.26 mmol, 86% over 2 steps) as a white solid and a mixture of rotamers, m.p. 58–60°C.

[tlc: hexanes/ethyl acetate = 1:1, R_f(**12a**) = 0.18]

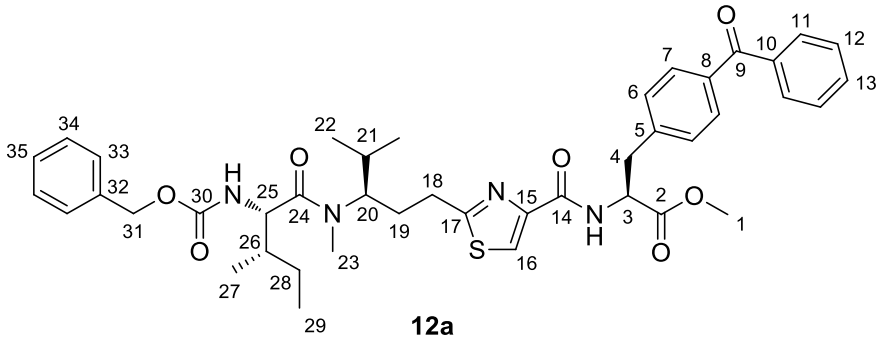

12a

major rotamer

^{1}H-NMR ($CDCl_3$, 400 MHz): δ = 0.75 (d, $^3J_{22,21}$ = 6.6 Hz, 3 H, 22-H), 0.85 (t, $^3J_{29,28}$ = 7.3 Hz, 3 H, 29-H), 0.94 (d, $^3J_{22',21}$ = 6.5 Hz, 3 H, 22'-H), 0.98 (d, $^3J_{27,26}$ = 6.7 Hz, 3 H, 27-H), 1.10 (m, 1 H, 28-H_a), 1.58 (m, 1 H, 28-H_b), 1.67–1.77 (m, 2 H, 21-H, 26-H), 1.84 (m, 1 H, 19-H_a), 2.12 (m, 1 H, 19-H_b), 2.79 (m, 2 H, 18-H), 2.95 (s, 3 H, 23-H), 3.28 (dd, $^2J_{4a,4b}$ = 13.8 Hz, $^3J_{4a,3}$ = 6.5 Hz, 1 H, 4-H_a), 3.35 (dd, $^2J_{4b,4a}$ = 13.8 Hz, $^3J_{4b,3}$ = 6.1 Hz, 1 H, 4-H_b), 3.72 (s, 3 H, 1-H), 4.31 (m, 1 H, 20-H), 4.55 (dd, $^3J_{25,NH}$ = 9.3 Hz, $^3J_{25,26}$ = 6.7 Hz, 1 H, 25-H), 5.04–5.11 (m, 3 H, 3-H, 31-H), 5.52 (d, $^3J_{NH,25}$ = 9.3 Hz, 1 H, NH), 7.20–7.35 (m, 7 H, 6-H, 33-H, 34-H, 35-H), 7.46 (dd, $^3J_{12,11}$ = $^3J_{12,13}$ = 7.6 Hz, 2 H, 12-H), 7.57 (t, $^3J_{13,12}$ = 7.4 Hz, 1 H, 13-H), 7.72 (d, $^3J_{7,6}$ = 8.2 Hz, 2 H, 7-H), 7.76 (m, 2 H, 11-H), 7.85 ($^3J_{NH,3}$ = 8.1 Hz, 1 H, NH), 7.95 (s, 1 H, 16-H).

^{13}C-NMR ($CDCl_3$, 100 MHz): δ = 11.3 (q, C-29), 16.0 (q, C-27), 19.5 (q, C-22), 20.0 (q, C-22'), 23.7 (t, C-28), 29.2 (t, C-19), 29.6 (q, C-23), 30.0 (d, C-21), 30.3 (t, C-18),

37.5 (d, C-26), 38.1 (t, C-4), 52.4 (q, C-1), 53.0 (d, C-3), 55.8 (d, C-25), 58.9 (d, C-20), 66.8 (t, C-32), 123.2 (d, C-16), 127.8, 128.0, 128.3, 128.4 (4 d, C-12, C-33, C-33, C-34), 129.2 (d, C-6), 129.9 (d, C-11), 130.3 (d, C-7), 132.3 (d, C-13), 136.2, 136.4 (2 s, C-8, C-32), 137.5 (s, C-10), 141.1 (s, C-5), 148.8 (s, C-15), 156.4 (s, C-30), 160.6 (s, C-14), 170.2 (s, C-17), 171.5 (s, C-2), 173.2 (s, C-24), 196.2 (s, C-9).

minor rotamer (selected signals)

^{1}H-NMR ($CDCl_3$, 400 MHz): δ = 1.03 (d, $^{3}J_{22,21}$ = 6.7 Hz, 3 H, 22-H), 2.70 (s, 3 H, 23-H), 3.58 (m, 1 H, 20-H), 4.63 (dd, $^{3}J_{25,NH}$ = 9.5 Hz, $^{3}J_{25,26}$ = 6.6 Hz, 1 H, 25-H), 5.63 (d, $^{3}J_{NH,25}$ = 9.7 Hz, 1 H, NH), 7.91 (s, 1 H, 16-H).

^{13}C-NMR ($CDCl_3$, 100 MHz): δ = 11.3 (q, C-29), 16.2 (q, C-27), 20.3 (q, C-22), 20.4 (q, C-22‘), 23.5 (t, C-28), 27.4 (q, C-23), 30.3 (t, C-19), 31.3 (t, C-18), 37.9 (d, C-26), 55.2 (d, C-25), 62.8 (d, C-14), 66.8 (t, C-32), 132.3 (d, C-16), 132.3 (d, C-13), 137.6 (s, C-10), 141.3 (s, C-5), 160.7 (s, C-14), 171.5 (s, C-2).

optical rotation: $[\alpha]^{21}_{D}$ = –1.2° (c = 1.0, $CHCl_3$)

HRMS (CI)	calculated	found
$C_{42}H_{51}N_4O_5S$ $[M+H]^+$	755.3478	755.3440

elemental analysis:

$C_{42}H_{50}N_4O_7S$	calculated	C 66.82	H 6.68	N 7.42
(754.93)	found	C 66.30	H 6.70	N 7.29

(*S*,*E*)-ethyl 5-(4-benzoylphenyl)-4-(2-((*R*)-3-((2*S*,3*S*)-2-(benzyloxycarbonyl-amino)-*N*,3-dimethylpentanamido)-4-methylpentyl)thiazole-4-carboxamido)-2-methylpent-2-enoate (12b)

HCl in dioxane (3.0 mL, 12.0 mmol, 4 M) was added at 0°C to dipeptide **11b** (182 mg, 0.30 mmol). The solvent was evaporated in vacuum after complete deprotection (30 min, tlc monitoring) and the hydrochloride salt was dried in high vacuum.

N-Deprotected **11b**, Cbz-protected L-isoleucine (90 mg, 0.33 mmol) and BEP (90 mg, 0.33 mmol) were dissolved in dry DCM (3 mL) and diisopropyl ethylamine (160 µL, 0.94 mmol) was added dropwise to this solution at –10°C. The cooling bath was removed after 20 min and the reaction mixture was stirred at room temperature for 20 h. The reaction mixture was diluted with DCM and washed with aqueous HCl (1 M), saturated aqueous $NaHCO_3$, water and brine, dried over Na_2SO_4 and concentrated in vacuum. The crude product was purified by flash chromatography (SiO_2, hexanes/ethyl acetate = 1:1) to yield tripeptide **12b** (195 mg, 0.26 mmol, 86% over 2 steps) as a white solid and a mixture of rotamers, m.p. 58–60°C.

[tlc: hexanes/ethyl acetate = 1:1, R_f(**12b**) = 0.27]

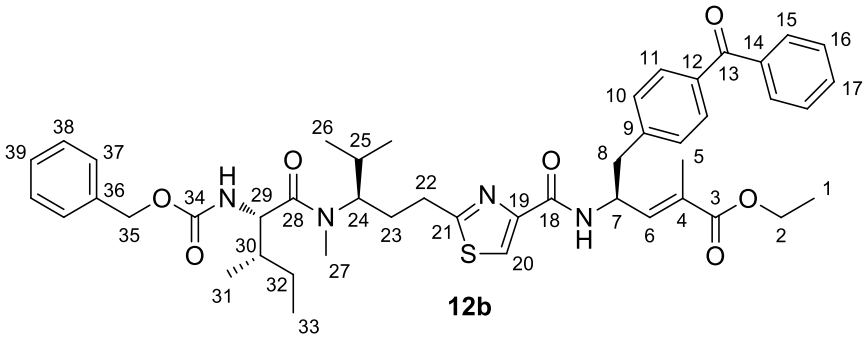

12b

major rotamer

^{1}H-NMR ($CDCl_3$, 400 MHz): δ = 0.78 (d, $^3J_{26,25}$ = 6.6 Hz, 3 H, 26-H), 0.86 (t, $^3J_{33,32}$ = 7.4 Hz, 3 H, 33-H), 0.96 (d, $^3J_{26',25}$ = 6.5 Hz, 3 H, 26'-H), 0.99 (d, $^3J_{31,30}$ = 6.8 Hz, 3 H, 31-H), 1.13 (m, 1 H, 32-H_a), 1.25 (t, $^3J_{1,2}$ = 7.0 Hz, 3 H, 1-H), 1.59 (m, 1 H, 32-H_b), 1.70 (m, 1 H, 25-H), 1.75 (d, $^4J_{5,7}$ = 1.3 Hz, 3 H, 5-H), 1.77–1.92 (m, 2 H, 23-H_a, 30-H), 2.09 (m, 1 H, 23-H_b), 2.81 (t, $^3J_{22,23}$ = 7.6 Hz, 2 H, 22-H), 2.98 (s, 3 H, 27-H), 3.01 (dd, $^2J_{8a,8b}$ = 13.3 Hz, $^3J_{8a,7}$ = 7.7 Hz, 1 H, 8-H_a), 3.20 (dd, $^2J_{8b,8a}$ = 13.4 Hz, $^3J_{8b,7}$ = 5.8 Hz, 1 H, 8-H_b), 4.16 (q, $^3J_{2,1}$ = 7.1 Hz, 2 H, 2-H), 4.39 (m, 1 H, 24-H), 4.56 (dd, $^3J_{29,NH}$ = 9.4 Hz, $^3J_{29,30}$ = 7.1 Hz, 1 H, 29-H), 5.09 (d, $^2J_{35a,35b}$ = 12.4 Hz, 1 H, 35-H_a), 5.11 (d, $^2J_{35b,35a}$ = 12.4 Hz, 1 H, 35-H_b), 5.20 (m, 1 H, 7-H), 5.50 (d, $^3J_{NH,29}$ = 9.4 Hz, 1 H, NH), 6.73 (dq, $^3J_{6,5}$ = 9.4 Hz, $^4J_{6,5}$ = 1.4 Hz, 1 H, 6-H), 7.22–7.37 (m, 7 H, 10-H, 37-H, 38-H, 39-H), 7.47 (dd, $^3J_{16,17}$ = $^3J_{16,15}$ = 7.6 Hz, 2 H, 16-H), 7.57 (t, $^3J_{17,16}$ =

7.4 Hz, 1 H, 17-H), 7.66 (d, $^{3}J_{NH,7}$ = 8.3 Hz, 1 H, NH), 7.72 (d, $^{3}J_{11,10}$ = 8.2 Hz, 1 H, 11-H), 7.76 (m, 1 H, 15-H), 7.92 (s, 1 H, 20-H).

^{13}C-NMR ($CDCl_3$, 100 MHz): δ = 11.2 (q, C-33), 12.8 (q, C-5), 14.2 (q, C-1), 15.9 (q, C-31), 19.5 (q, C-26), 20.1 (q, C-26‘), 23.9 (t, C-32), 29.4 (t, C-23), 29.6 (q, C-27), 29.9 (t, C-22), 30.2 (d, C-25), 37.6 (d, C-30), 41.0 (t, C-8), 48.7 (d, C-7), 55.8 (d, C-29), 58.6 (d, C-24), 60.8 (t, C-2), 66.8 (t, C-35), 122.7 (d, C-20), 127.8, 128.0, 128.2, 128.4 (4 d, C-16, C-37, C-38, C-38), 129.4 (d, C-10), 129.9 (d, C-15), 130.3 (d, C-11), 130.7 (s, C-4), 132.3 (d, C-17), 136.0 (s, C-12), 136.4 (s, C-36), 137.7 (s, C-14), 138.6 (d, C-6), 141.9 (s, C-9), 149.3 (s, C-19), 156.5 (s, C-34), 160.4 (s, C-18), 167.7 (s, C-21), 169.8 (s, C-28), 173.3 (s, C-3), 196.3 (s, C-13).

minor rotamer (selected signals)

^{1}H-NMR ($CDCl_3$, 400 MHz): δ = 0.91 (d, $^{3}J_{26,25}$ = 6.7 Hz, 3 H, 26-H), 1.02 (d, $^{3}J_{26',25}$ = 6.5 Hz, 3 H, 26‘-H), 1.29 (t, $^{3}J_{1,2}$ = 7.6 Hz, 3 H, 1-H), 2.74 (s, 3 H, 27-H), 2.89 (m, 2 H, 22-H), 3.52 (m, 1 H, 24-H), 4.19 (q, $^{3}J_{2,1}$ = 7.0 Hz, 2 H, 2-H), 4.76 (dd, $^{3}J_{29,NH}$ = 9.6 Hz, $^{3}J_{29,30}$ = 5.8 Hz, 1 H, 29-H), 5.60 (d, $^{3}J_{NH,29}$ = 9.6 Hz, 1 H, NH), 7.82 (d, $^{3}J_{NH,7}$ = 8.3 Hz, 1 H, NH), 7.93 (s, 1 H, 20-H).

^{13}C-NMR ($CDCl_3$, 100 MHz): δ = 11.3 (q, C-33), 12.8 (q, C-5), 14.2 (q, C-1), 16.3 (q, C-31), 20.3 (q, C-26), 20.4 (q, C-26‘), 23.3 (t, C-32), 27.6 (q, C-27), 37.9 (d, C-30), 55.4 (d, C-29), 60.8 (t, C-2), 66.9 (t, C-35), 123.2 (d, C-20), 128.2 (d, C-16), 132.3 (d, C-17), 149.4 (s, C-19), 167.6 (s, C-21), 170.2 (s, C-28).

optical rotation: $[\alpha]^{21}_{D}$ = +11.2° (c = 1.0, $CHCl_3$)

HRMS (CI)	calculated	found
$C_{46}H_{58}N_4O_7S$ $[M+2H]^{2+}$	810.4026	810.4061

elemental analysis:

$C_{46}H_{56}N_4O_7S$	calculated	C 68.29	H 6.98	N 6.93
(809.02)	found	C 67.73	H 7.07	N 6.73

(*S*)-methyl 3-(4-benzoylphenyl)-2-(2-((*R*)-3-((2*S*,3*S*)-*N*,3-dimethyl-2-((*R*)-1-methylpiperidine-2-carboxamido)pentanamido)-4-methylpentyl)thiazole-4-carboxamido)propanoate (13a)

HBr in HOAc (120 µL, 0.70 mmol, 33 wt.-%) was added at room temperature to tripeptide **12a** (52 mg, 0.30 mmol). After complete deprotection (1 h, tlc monitoring) the reaction mixture was diluted with diethyl ether (5 mL). The hydrobromide salt was filtered off, washed with diethyl ether (3 x 5 mL) and treated with saturated aqueous $NaHCO_3$ (5 mL). The free amine was extracted with DCM and the solvent was removed in vacuum to get the crude amine as a colourless oil.

A solution of *N*-methyl pipecolic acid (21 mg, 0.15 mmol), pentafluorophenol (31 mg, 0.17 mmol) and DCC (35 mg, 0.17 mmol) in dry DCM (2 mL) was stirred at room temperature for 1 day. The urea was filtered off and the filtrate was stirred with *N*-deprotected **12a** for 20 h. The reaction mixture was diluted with DCM and washed with saturated aqueous $NaHCO_3$, water and brine, dried over Na_2SO_4 and concentrated in vacuum. The crude product was purified by flash chromatography (SiO_2, DCM/MeOH = 98:2, 95:5) to yield tetrapeptide **13a** (38 mg, 51 µmol, 74% over 2 steps) as a white solid and a mixture of rotamers, m.p. 64–66°C.

[tlc: DCM/MeOH = 95:5, R_f(**13a**) = 0.21]

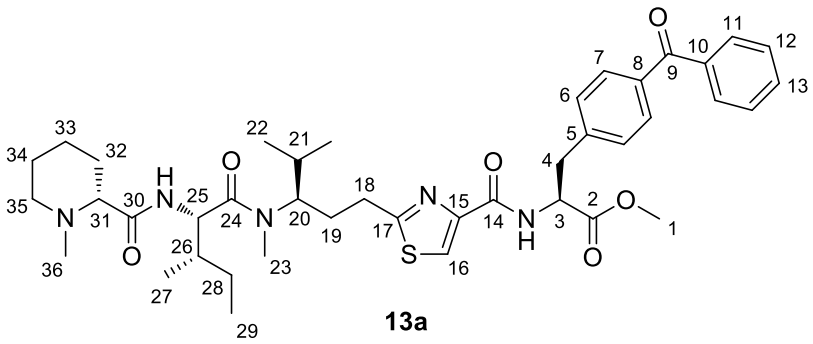

13a

major rotamer

^{1}H-NMR ($CDCl_3$, 400 MHz): δ = 0.74 (d, $^3J_{22,21}$ = 6.6 Hz, 3 H, 22-H), 0.88 (t, $^3J_{29,28}$ = 7.4 Hz, 3 H, 29-H), 0.94 (d, $^3J_{22',21}$ = 6.5 Hz, 3 H, 22'-H), 0.96 (d, $^3J_{27,26}$ = 6.7 Hz, 3 H, 27-H), 1.10–1.24 (m, 2 H, 28-H_a, 33-H_{ax}), 1.34 (m, 1 H, 32-H_{ax}), 1.45–1.73 (m, 5 H, 21-H, 28-H_b, 33-H_{eq}, 34-H), 1.77–1.90 (m, 3 H, 19-H_a, 26-H, 32-H_{eq}), 1.99 (ddd, $^2J_{35ax,35eq}$ = 11.7 Hz, $^3J_{35ax,34ax}$ = 11.7 Hz, $^3J_{35ax,34eq}$ = 2.2 Hz, 1 H, 35-H_{ax}), 2.14 (m, 1 H, 19-H_b), 2.21 (s, 3 H, 36-H), 2.46 (dd, $^3J_{31a,32eq}$ = 10.9 Hz, $^3J_{31,32ax}$ = 2.7 Hz, 1 H, 31-H), 2.77–2.92 (m, 3 H, 18-H, 35-H_{eq}), 2.98 (s, 3 H, 23-H), 3.28 (dd, $^2J_{4a,4b}$ = 13.8 Hz, $^3J_{4a,3}$ = 6.4 Hz, 1 H, 4-H_a), 3.35 (dd, $^2J_{4b,4a}$ = 13.8 Hz, $^3J_{4b,3}$ = 6.0 Hz, 1 H, 4-H_b), 3.74 (s, 3 H, 1-H), 4.33 (m, 1 H, 20-H), 4.76 (dd, $^3J_{25,NH}$ = $^3J_{25,26}$ = 8.8 Hz, 1 H, 25-H), 5.08 (m, 1 H, 3-H), 7.02 (d, $^3J_{NH,25}$ = 9.4 Hz, 1 H, NH), 7.30 (d, $^3J_{6,7}$ = 8.0 Hz,

2 H, 6-H), 7.46 (dd, $^3J_{12,11}$ = $^3J_{12,13}$ = 7.6 Hz, 2 H, 12-H), 7.57 (t, $^3J_{13,12}$ = 7.3 Hz, 1 H, 13-H), 7.72 (d, $^3J_{7,6}$ = 8.1 Hz, 2 H, 7-H), 7.75 (d, $^3J_{11,12}$ = 7.9 Hz, 2 H, 11-H), 7.85 ($^3J_{NH,3}$ = 8.1 Hz, 1 H, NH), 7.94 (s, 1 H, 16-H).

^{13}C-NMR ($CDCl_3$, 100 MHz): δ = 10.9 (q, C-29), 15.9 (q, C-27), 19.5 (q, C-22), 20.1 (q, C-22‘), 23.2 (t, C-28), 24.5 (t, C-32), 25.0 (t, C-34), 29.2 (t, C-19), 29.6 (q, C-23), 30.0 (d, C-21), 30.2 (t, C-18), 30.4 (t, C-32), 37.0 (d, C-26), 38.1 (t, C-4), 44.8 (q, C-36), 52.4 (q, C-1), 53.0 (2 d, C-3, C-25), 53.0 (t, C-35), 58.7 (d, C-20), 69.6 (d, C-31), 123.2 (d, C-16), 128.2 (d, C-12), 129.2 (d, C-6), 129.9 (d, C-11), 130.3 (d, C-7), 132.3 (d, C-13), 136.3 (s, C-8), 137.6 (s, C-10), 141.1 (s, C-5), 148.9 (s, C-15), 160.6 (s, C-14), 170.3 (s, C-17), 171.5 (s, C-2), 173.2 (s, C-24), 174.2 (s, C-30), 196.2 (s, C-9).

minor rotamer (selected signals)

^{1}H-NMR ($CDCl_3$, 400 MHz): δ = 0.96 (d, $^3J_{27,26}$ = 6.4 Hz, 3 H, 27-H), 2.75 (s, 3 H, 23-H), 3.64 (m, 1 H, 20-H), 4.96 (dd, $^3J_{25,NH}$ = 9.4 Hz, $^3J_{25,26}$ = 6.3 Hz, 1 H, 25-H), 7.16 (d, $^3J_{NH,25}$ = 9.7 Hz, 1 H, NH), 7.91 (s, 2 H, 16-H).

^{13}C-NMR ($CDCl_3$, 100 MHz): δ = 11.4 (q, C-29), 16.5 (q, C-27), 20.3 (q, C-22), 20.6 (q, C-22‘), 27.3 (q, C-23), 38.4 (d, C-26), 62.8 (d, C-20), 123.3 (d, C-16), 141.2 (s, C-5), 170.1 (s, C-17), 172.9 (s, C-24).

optical rotation: $[\alpha]^{21}_D$ = +11.8° (c = 1.0, $CHCl_3$)

HRMS (CI)	calculated	found
$C_{41}H_{56}N_5O_6S$ $[M+H]^+$	746.3951	746.3964

elemental analysis:

$C_{41}H_{55}N_5O_6S$	calculated	C 66.01	H 7.43	N 9.39
(745.97)	found	C 65.90	H 7.45	N 9.41

(*S*,*E*)-ethyl 5-(4-benzoylphenyl)-4-(2-((*R*)-3-((2*S*,3*S*)-*N*,3-dimethyl-2-((*R*)-1-methylpiperidine-2-carboxamido)pentanamido)-4-methylpentyl)thiazole-4-carboxamido)-2-methylpent-2-enoate (13b)

HBr in HOAc (0.70 mL, 4.05 mmol, 33 wt.-%) was added at room temperature to tripeptide **12b** (319 mg, 0.39 mmol). After complete deprotection (1 h, tlc monitoring) the reaction mixture was diluted with diethyl ether (10 mL). The hydrobromide salt was filtered off, washed with diethyl ether (3 x 10 mL) and treated with saturated aqueous $NaHCO_3$ (5 mL). The free amine was extracted with DCM and the solvent was removed in vacuum to get the crude amine as a colourless oil.

A solution of *N*-methyl pipecolic acid (112 mg, 0.78 mmol), pentafluorophenol (158 mg, 0.86 mmol) and DCC (177 mg, 0.86 mmol) in dry DCM (8 mL) was stirred at room temperature for 1 day. The urea was filtered off and the filtrate was stirred with *N*-deprotected **12b** for 20 h. The reaction mixture was diluted with DCM and washed with saturated aqueous $NaHCO_3$, water and brine, dried over Na_2SO_4 and concentrated in vacuum. The crude product was purified by flash chromatography (SiO_2, DCM/MeOH = 98:2, 95:5) to yield tetrapeptide **13b** (196 mg, 0.24 mmol, 66% over 2 steps) as a white solid and a mixture of rotamers, m.p. 68–70°C.

[tlc: DCM/MeOH = 95:5, R_f(**13b**) = 0.18]

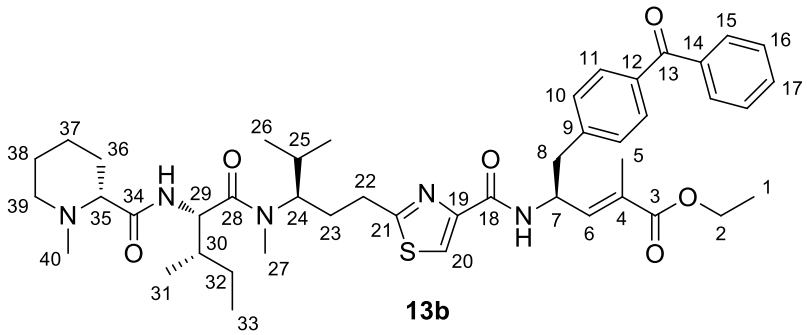

13b

major rotamer

^{1}H-NMR ($CDCl_3$, 400 MHz): δ = 0.79 (d, $^3J_{26,25}$ = 6.6 Hz, 3 H, 26-H), 0.90 (t, $^3J_{33,32}$ = 7.4 Hz, 3 H, 33-H), 0.98 (d, $^3J_{26',25}$ = 6.6 Hz, 3 H, 26'-H), 1.00 (d, $^3J_{31,30}$ = 6.8 Hz, 3 H, 31-H), 1.13–1.22 (m, 1 H, 32-H_a, 37-H_{ax}), 1.29 (t, $^3J_{1,2}$ = 7.1 Hz, 3 H, 1-H), 1.39 (m, 1 H, 36-H_{ax}), 1.51–1.75 (m, 5 H, 25-H, 32-H_b, 37-H_{eq}, 38-H), 1.78 (s, 3 H, 5-H), 1.82–1.92 (m, 3 H, 23-H_a, 30-H, 36-H_{eq}), 2.05 (m, 1 H, 39-H_{ax}), 2.13 (m, 1 H, 23-H_b), 2.24 (s, 3 H, 40-H), 2.50 (m, 1 H, 35-H), 2.85 (t, $^3J_{22,23}$ = 8.0 Hz, 2 H, 22-H), 2.90 (m, 1 H, 39-H_{eq}), 3.03 (s, 3 H, 27-H), 3.04 (dd, $^2J_{8a,8b}$ = 13.2 Hz, $^3J_{8a,7}$ = 7.8 Hz, 1 H, 8-H_a), 3.25 (dd, $^2J_{8b,8a}$ = 13.4 Hz, $^3J_{8b,7}$ = 6.0 Hz, 1 H, 8-H_b), 4.20 (q, $^3J_{2,1}$ = 7.1 Hz, 2 H, 2-H), 4.23 (m 1 H, 24-H), 4.81 (dd, $^3J_{29,NH}$ = 9.3 Hz, $^3J_{29,30}$ = 8.2 Hz, 1 H, 29-H), 5.23 (m, 1 H, 7-H), 6.74 (d, $^3J_{6,7}$ = 9.3 Hz, 1 H, 6-H), 7.07 (d, $^3J_{NH,29}$ = 9.2 Hz, 1 H, NH), 7.37

(d, $^{3}J_{10,11}$ = 8.2 Hz, 2 H, 10-H), 7.49 (dd, $^{3}J_{16,15}$ = $^{3}J_{16,17}$ = 7.6 Hz, 2 H, 16-H), 7.59 (tt, $^{3}J_{17,16}$ = 7.4 Hz, $^{4}J_{17,15}$ = 1.3 Hz, 1 H, 17-H), 7.68 (d, $^{3}J_{NH,7}$ = 8.4 Hz, 1 H, NH), 7.75 (d, $^{3}J_{11,10}$ = 8.2 Hz, 2 H, 11-H), 7.77 (m, 2 H, 15-H), 7.94 (s, 1 H, 20-H).

^{13}C-NMR ($CDCl_3$, 100 MHz): δ = 10.9 (q, C-33), 12.8 (q, C-5), 14.2 (q, C-1), 15.9 (q, C-31), 19.6 (q, C-26), 20.1 (q, C-26‘), 23.2 (t, C-32), 24.6 (t, C-37), 25.0 (t, C-38), 29.4 (t, C-23), 29.6 (q, C-27), 30.0 (t, C-22), 30.2 (d, C-25), 30.4 (t, C-36), 37.1 (d, C-30), 41.0 (t, C-8), 44.8 (q, C-40), 48.6 (d, C-7), 53.0 (d, C-29), 55.4 (t, C-39), 60.8 (t, C-2), 62.7 (d, C-24), 69.6 (d, C-35), 122.7 (d, C-20), 128.2 (d, C-16), 129.4 (d, C-10), 129.9 (d, C-15), 130.3 (d, C-11), 130.5 (s, C-4), 132.3 (d, C-17), 135.9 (s, C-12), 137.6 (s, C-14), 138.7 (d, C-6), 141.9 (s, C-9), 149.3 (s, C-19), 160.4 (s, C-18), 167.7 (s, C-21), 169.9 (s, C-28), 173.2 (s, C-3), 174.2 (s, C-34), 196.3 (s, C-13).

minor rotamer (selected signals)

^{1}H-NMR ($CDCl_3$, 400 MHz): δ = 0.91 (t, $^{3}J_{33,32}$ = 7.1 Hz, 3 H, 33-H), 1.06 (d, $^{3}J_{26,25}$ = 6.5 Hz, 3 H, 26-H), 2.79 (s, 3 H, 27-H), 3.63 (m 1 H, 24-H), 5.08 (dd, $^{3}J_{29,NH}$ = 9.6 Hz, $^{3}J_{29,30}$ = 5.7 Hz, 1 H, 29-H), 7.23 (d, $^{3}J_{NH,29}$ = 9.6 Hz, 1 H, NH), 7.93 (s, 1 H, 20-H).

^{13}C-NMR ($CDCl_3$, 100 MHz): δ = 11.4 (q, C-33), 16.6 (q, C-31), 20.4 (q, C-26), 20.5 (q, C-26‘), 27.4 (q, C-27), 38.4 (d, C-30), 44.9 (q, C-40), 58.4 (d, C-24), 60.6 (t, C-2), 123.0 (d, C-22), 135.9 (d, s, C-12), 137.6 (s, C-14), 142.0 (s, C-9), 170.0 (s, C-28), 172.9 (s, C-3).

optical rotation: $[\alpha]^{21}_{D}$ = +27.5° (c = 0.8, $CHCl_3$)

HRMS (CI)	calculated	found
$C_{31}H_{50}N_5O_5S$ $[M–C_{14}H_{11}O+H]^+$	604.3533	604.3530

elemental analysis

$C_{45}H_{61}N_5O_6S$	calculated	C 67.56	H 7.68	N 8.44
(800.06)	found	C 66.96	H 7.94	N 8.44

(*S*)-3-(4-benzoylphenyl)-2-(2-((*R*)-3-((2*S*,3*S*)-*N*,3-dimethyl-2-((*R*)-1-methyl-piperidine-2-carboxamido)pentanamido)-4-methylpentyl)thiazole-4-carbox-amido)propanoic acid-TFA-salt (14a)

A mixture of *N*-methylated tetrapeptide **13a** (50 mg, 67 µmol) and 1 M NaOH (140 µL, 140 µmol) in dioxane (1 mL) was stirred at 80°C until complete saponification occurred (6 h). The solvent was removed in vacuum and the residue was dissolved in water, acidified to pH 1 with trifluoroacetic acid, and extracted thrice with EtOAc. The combined organic layers were dried with Na_2SO_4 and the solvent was evaporated in vacuum. Purification by flash chromatography (DCM/ MeOH, 9:1) provided the TFA salt of **14a** (52 mg, 61 µmol, 92%) as a white solid and a mixture of rotamers; m.p. 186–188°C.

[tlc: DCM/MeOH = 9:1, R_f(**14a**) = 0.11]

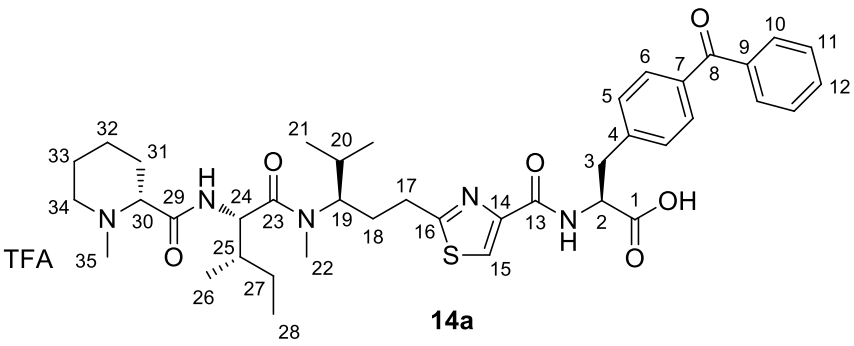

14a

major rotamer

^{1}H-NMR ($CDCl_3$, 400 MHz): δ = 0.74 (d, $^3J_{21,20}$ = 6.6 Hz, 3 H, 21-H), 0.88 (t, $^3J_{28,27}$ = 7.4 Hz, 3 H, 28-H), 0.91 (d, $^3J_{21',20}$ = 6.3 Hz, 3 H, 21'-H), 0.97 (d, $^3J_{26,25}$ = 6.7 Hz, 3 H, 26-H), 1.18 (m, 1 H, 27-H_a), 1.52 (m, 1 H, 32-H_{ax}), 1.62 (m, 1 H, 27-H_b), 1.68–1.78 (m, 3 H, 20-H, 32-H_{eq}, 33-H_{ax}), 1.80–1.95 (4 H, 18-H_a, 25-H, 31-H_{ax}, 33-H_{eq}), 2.01 (m, 1 H, 31-H_{eq}), 2.17 (m, 1 H, 18-H_b), 2.54 (s, 3 H, 35-H), 2.73 (m, 1 H, 34-H_{ax}), 2.85 (m, 2 H, 17-H), 3.04 (s, 3 H, 22-H), 3.25–3.30 (m, 2 H, 3-H_a, 34-H_{eq}), 3.38 (m, 1 H, 30-H), 3.44 (dd, $^2J_{3b,3a}$ = 13.6 Hz, $^3J_{3b,2}$ = 5.1 Hz, 1 H, 3-H_b), 4.17 (bs, 1 H, 19-H), 4.72 (d, $^3J_{24,NH}$ = 7.9 Hz, 1 H, 24-H), 4.77 (t, $^3J_{2,3}$ = 5.7 Hz, 1 H, 2-H), 7.40 (d, $^3J_{5,6}$ = 8.1 Hz, 2 H, 5-H), 7.50 (dd, $^3J_{11,10}$ = $^3J_{11,12}$ = 7.6 Hz, 2 H, 11-H), 7.61–7.64 (m, 3 H, 6-H, 12-H), 7.71 (d, $^3J_{10,11}$ = 7.7 Hz, 2 H, 10-H), 8.04 (s, 1 H, 15-H).

^{13}C-NMR ($CDCl_3$, 100 MHz): δ = 11.4 (q, C-28), 16.3 (q, C-26), 20.3 (q, C-21), 20.6 (q, C-21'), 23.0 (t, C-27), 24.8 (t, C-32), 25.5 (t, C-33), 30.1 (t, C-18), 30.5 (q, C-22), 30.7 (t, C-31), 31.1 (t, d, C-17, C-20), 37.6 (d, C-25), 39.1 (t, C-3), 43.5 (q, C-35), 55.8 (d, C-24), 56.4 (t, C-34), 56.8 (d, C-19), 69.0 (d, C-30), 124.5 (d, C-15), 129.5 (d, C-11), 130.9 (2 d, C-5, C-10), 131.1 (d, C-6), 133.7 (d, C-12), 136.9 (s, C-7),

139.0 (s, C-9), 145.0 (s, C-4), 150.4 (s, C-14), 162.7 (s, C-13), 171.4 (s, C-16), 172.1 (s, C-23), 174.5 (s, C-29), 177.9 (s, C-1), 198.2 (s, C-8).

minor rotamer (selected signals)

^{1}H-NMR ($CDCl_3$, 400 MHz): δ = 1.06 (d, $^{3}J_{26,25}$ = 6.4 Hz, 3 H, 26-H), 2.50 (s, 3 H, 35-H), 2.61 (s, 3 H, 22-H), 3.68 (m, 1 H, 19-H), 4.72 (d, $^{3}J_{24,NH}$ = 5.4 Hz, 1 H, 24-H), 7.97 (s, 1 H, 16-H).

^{13}C-NMR ($CDCl_3$, 100 MHz): δ = 11.8 (q, C-28), 16.7 (q, C-26), 21.0 (q, C-21), 28.3 (q, C-22), 38.0 (d, C-25), 39.3 (t, C-3), 43.5 (q, C-35), 150.5 (s, C-14).

optical rotation: $[\alpha]^{21}_{D}$ = +7.9° (c = 0.6, MeOH)

HRMS (ESI)	calculated	found
$C_{40}H_{54}N_5O_6S$ $[M+H]^+$	732.3795	732.3769

(*S*,*E*)-5-(4-benzoylphenyl)-4-(2-((*R*)-3-((2*S*,3*S*)-*N*,3-dimethyl-2-((*R*)-1-methylpiperidine-2-carboxamido)pentanamido)-4-methylpentyl)thiazole-4-carboxamido)-2-methylpent-2-enoic acid-TFA-salt (14b)

A mixture of *N*-methylated tetrapeptide **13b** (50 mg, 62 µmol) and 1 M NaOH (180 µL, 180 µmol) in dioxane (1 mL) was stirred at 80°C until complete saponification occurred (7 h). The solvent was removed in vacuum and the residue was dissolved in water, acidified to pH 1 with trifluoroacetic acid, and extracted thrice with EtOAc. The combined organic layers were dried with Na_2SO_4 and the solvent was evaporated in vacuum. Purification by flash chromatography (DCM/ MeOH, 9:1) provided the TFA salt of **14b** (53 mg, 60 µmol, 97%) as a white solid and a mixture of rotamers; m.p. 158–160°C.

[tlc: DCM/MeOH = 9:1, R_f(**14b**) = 0.27]

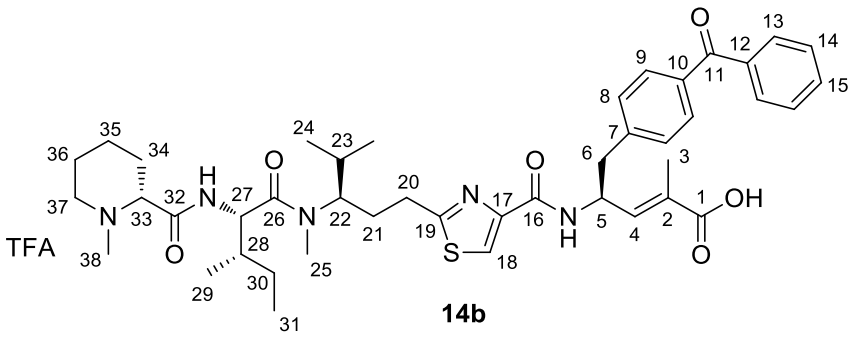

14b

major rotamer

^{1}H-NMR ($CDCl_3$, 400 MHz): δ = 0.65 (d, $^3J_{24,23}$ = 6.6 Hz, 3 H, 24-H), 0.80 (t, $^3J_{31,30}$ = 7.4 Hz, 3 H, 31-H), 0.83 (d, $^3J_{24',23}$ = 6.5 Hz, 3 H, 24'-H), 0.90 (d, $^3J_{29,28}$ = 6.8 Hz, 3 H, 29-H), 1.13 (m, 1 H, 30-H_a), 1.38 (m, 1 H, 35-H_{ax}), 1.48 (m, 1 H, 30-H_b), 1.57–1.76 (m, 8 H, 3-H, 23-H, 34-H_{ax}, 35-H_{eq}, 36-H), 1.79–1.92 (m, 3 H, 21-H_a, 28-H, 34-H_{eq}), 2.03 (m, 1 H, 21-H_b), 2.45 (s, 3 H, 38-H), 2.66 (ddd, $^2J_{37ax,37eq}$ = 12.5 Hz, $^3J_{37ax,36ax}$ = 12.5 Hz, $^3J_{37ax,36eq}$ = 2.9 Hz, 1 H, 37-H_{ax}), 2.75 (m, 1 H, 20-H_a), 2.85 (m, 1 H, 20-H_b), 2.94 (dd, $^2J_{6a,6b}$ = 13.0 Hz, $^3J_{6a,5}$ = 7.5 Hz, 1 H, 6-H_a), 2.98 (s, 3 H, 25-H), 3.09 (dd, $^2J_{6b,6a}$ = 13.3 Hz, $^3J_{6b,5}$ = 6.9 Hz, 1 H, 6-H_b), 3.19 (m, 1 H, 37-H_{eq}), 3.33 (dd, $^2J_{33,34eq}$ = 11.5 Hz, $^3J_{33,34ax}$ = 2.4 Hz, 1 H, 33-H), 4.18 (m, 1 H, 22-H), 4.61 (d, $^3J_{27,28}$ = 8.6 Hz, 1 H, 27-H), 5.05 (m, 1 H, 5-H), 6.60 (dq, $^3J_{4,5}$ = 9.2 Hz, $^4J_{4,3}$ = 1.0 Hz, 1 H, 4-H), 7.31 (d, $^3J_{8,9}$ = 8.1 Hz, 2 H, 8-H), 7.39 (dd, $^3J_{14,15}$ = $^3J_{14,13}$ = 7.6 Hz, 2 H, 14-H), 7.51 (t, $^3J_{15,14}$ = 7.5 Hz, 1 H, 15-H), 7.56 (d, $^3J_{9,8}$ = 8.2 Hz, 2 H, 9-H), 7.60 (m, 2 H, 13-H), 7.91 (s, 1 H, 18-H).

^{13}C-NMR ($CDCl_3$, 100 MHz): δ = 11.2 (q, C-31), 13.9 (q, C-29), 16.0 (q, C-3), 20.3 (q, C-24), 20.6 (q, C-24'), 23.0 (t, C-30), 24.7 (t, C-35), 25.7 (t, C-36), 30.3 (q, C-25), 30.5 (t, C-21), 30.6 (t, C-34), 31.0 (t, C-20), 31.4 (d, C-23), 37.7 (d, C-28), 41.9 (t,

C-6), 43.4 (q, C-38), 50.8 (d, C-5), 55.6 (d, C-27), 56.3 (t, C-37), 60.2 (d, C-22), 69.0 (d, C-33), 118.2 (q, $^{2}J_{C,F}$ = 291 Hz, $\underline{C}F_3COOH$), 124.5 (d, C-18), 129.5 (d, C-14), 130.9 (2 d, C-8, C-13), 130.9 (d, C-9), 133.7 (d, C-15), 137.0, 137.1 (d, s, C-4, C-10), 139.0 (s, C-12), 144.5 (s, C-7), 150.4 (s, C-17), 162.7 (s, C-16), 163.2 (q, $^{3}J_{C,F}$ = 34.6 Hz, $CF_3\underline{C}OOH$), 171.2 (s, C-19), 171.9 (s, C-26), 174.8 (s, C-32), 175.6 (s, C-19), 198.2 (s, C-11).

minor rotamer

^{1}H-NMR ($CDCl_3$, 400 MHz): δ = 0.98 (d, $^{3}J_{24,23}$ = 6.5 Hz, 3 H, 24-H), 2.35 (s, 3 H, 38-H), 2.55 (s, 3 H, 25-H), 4.67 (d, $^{3}J_{27,28}$ = 8.9 Hz, 1 H, 27-H), 7.88 (s, 1 H, 18-H).

^{13}C-NMR ($CDCl_3$, 100 MHz): δ = 11.9 (q, C-31), 16.5 (q, C-3), 20.7 (q, C-24), 20.9 (q, C-24‘), 28.3 (q, C-25), 38.5 (d, C-28), 43.6 (q, C-38), 64.7 (d, C-22).

optical rotation: $[\alpha]^{21}_{D}$ = –4.5° (c = 0.9, MeOH)

HRMS (ESI)	calculated	found
$C_{43}H_{58}N_5O_6S$ $[M+H]^+$	772.4108	772.4082

_N_-((_S_)-3-(4-Benzoylphenyl)-1-oxo-1-(prop-2-ynylamino)propan-2-yl)-2-((_R_)-3-((2_S_,3_S_)-_N_,3-dimethyl-2-((_R_)-1-methyl-piperidine-2-carboxamido)pentanamido)-4-methylpentyl)thiazole-4-carbox-amide (4)

At –20°C isobutylchloroformiate (3 µl, 23.1 µmol) was added dropwise to a solution of benzophenon pretubulysin derivative **14a** (16.7 mg, 19.7 µmol) and *N*-methylmorpholine (9 µl, 81.9 µmol) in dry THF/DMF (2:1, 600 µl). After 10 min propargylamine hydrochloride (3 mg, 31.1 µmol) was added and the reaction mixture was stirred overnight. The solvents were evaporated and the residue was dissolved in ethyl acetate and washed with saturated $NaHCO_3$ solution. The aqueous layer was extracted twice with ethyl acetate and the combined organic layers were dried over Na_2SO_4. The crude product was purified by flash chromatography (DCM/MeOH 98:2 – 9:1) to yield the propargylamide ***4*** (8 mg, 10.4 µmol, 53 %) as a pale yellow solid and a mixture of rotamers; m.p.85 °C.

[tlc: DCM/MeOH = 9:1, R_f(**4**) = 0.18]

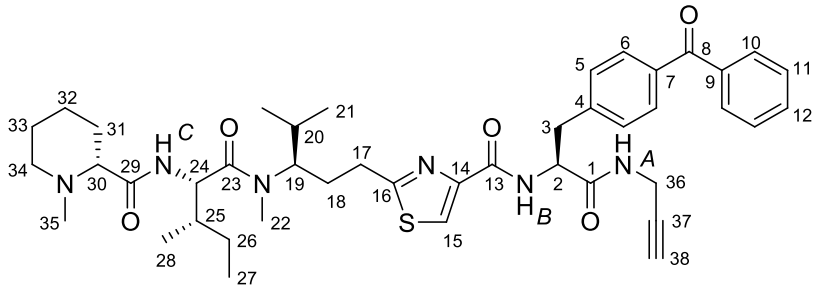

major rotamer

^{1}H-NMR ($CDCl_3$, 400 MHz): δ = 0.74 (d, $^3J_{21,20}$ = 6.6 Hz, 3 H, 21-H), 0.86 (t, $^3J_{27,26}$ = 7.4 Hz, 3 H, 27-H), 0.92 (d, $^3J_{21',20}$ = 6.6 Hz, 3 H, 21'-H), 0.97 (d, $^3J_{28,25}$ = 6.7 Hz, 3 H, 28-H), 1.08-1.70 (m, 9 H, 20-H, 26-H, 31-H_{ax}, 32-H, 33-H), 1.74-1.91 (m, 3 H, 18-H_a, 25-H, 31-H_{eq}), 1.93-2.13 (m, 2 H, 18-H_b, 34-H_{ax}), 2.17 (dd, $^4J_{38,36a}$ = $^4J_{38,36b}$ = 2.5 Hz, 1 H, 38-H), 2.20 (s, 3 H, 35-H), 2.47 (dd, $^3J_{30,31ax}$ = 11.0 Hz, $^3J_{30,31eq}$ = 3.0 Hz, 1 H, 30-H), 2.72-2.99 (m, 3 H, 17-H, 34-H_{eq}), 3.00 (s, 3 H, 22-H), 3.22 (dd, $^2J_{3a,3b}$ = 13.9 Hz, $^3J_{3a,2}$ = 7.5 Hz, 1 H, 3-H_a), 3.38 (dd, $^2J_{3b,3a}$ = 13.9 Hz, $^3J_{3b,2}$ = 6.8 Hz, 1 H, 3-H_b), 3.95 (ddd, $^2J_{36a,36b}$ = 17.5 Hz, $^3J_{36a,NH\ A}$ = 5.1 Hz, $^4J_{36a,38}$ = 2.5 Hz, 1 H, 36-H_a), 4.04 (ddd, $^2J_{36b,36a}$ = 17.5 Hz, $^3J_{36b,NH\ A}$ = 5.6 Hz, $^4J_{36b,38}$ = 2.6 Hz, 1 H, 36-H_a), 4.32 (bs, 1 H, 19-H), 4.76 (dd, $^3J_{24,NH\ C} \approx {}^3J_{24,25} \approx$ 8.9 Hz, 1 H, 24-H), 4.90 (ddd, $^3J_{2,NH\ B} \approx {}^3J_{2,3a} \approx {}^3J_{2,3b} \approx$7.7 Hz, 1 H, 2-H), 6.63 (dd, $^3J_{NH\ A,36a} \approx {}^3J_{NH\ A,36b} \approx$ 5.3 Hz, 1 H, NH_A), 7.01 (d, $^3J_{NH\ C,24}$ = 9.6 Hz, 1 H, NH_C), 7.37 (d, $^3J_{5,6}$ = 8.2 Hz, 2 H, 5-H), 7.44 (dd, $^3J_{11,10} \approx {}^3J_{11,12} \approx$ 7.5 Hz, 2 H, 11-H), 7.56 (tt, $^3J_{12,11}$ = 7.4 Hz, $^4J_{12,10}$ = 1.3 Hz, 1 H, 12-H), 7.71 (d, $^3J_{6,5}$ = 8.3 Hz,

2 H, 6-H), 7.74 (dd, $^{3}J_{10,11}$ = 8.3 Hz, $^{4}J_{10,12}$ = 1.3 Hz, 2 H, 10-H), 7.92 (s, 1 H, 15-H), 7.93 (m, 1 H, NH_B).**^{13}C-NMR** ($CDCl_3$, 100 MHz, selected signals, according to HSQC): δ = 10.9 (q, C-27), 15.9 (q, C-28), 19.6 (q, C-21), 20.1 (q, C-21'), 23.3 (t, C-26), 24.7 (t, C-32), 29.2 (t, C-36), 29.4 (t, C-18), 30.0 (t, C-17), 30.2 (d, C-20), 37.1 (d, C-25), 38.1 (t, C-3), 44.9 (q, C-35), 53.4 (d, C-24), 54.2 (d, C-2), 55.4 (t, C-34), 69.7 (d, C-30), 71.7 (d, C-38), 123.5 (d, C-15), 128.3 (d, C-11), 129.2 (d, C-5), 130.0 (d, C-10), 130.5 (d, C-6), 132.4 (d, C-12), 170.2 (s, C-16).

HRMS (CI)	calculated	found
$C_{43}H_{57}N_6O_5S$ $[M+H]^+$	769.4111	769.4073

_N_-((_S_,_E_)-5-(4-Benzoylphenyl)-1-oxo-1-(prop-2-ynylamino)pent-2-en-4-yl)-2-((_R_)-3-((2_S_,3_S_)-_N_,3-dimethyl-2-((_R_)-1-methyl-piperidine-2-carboxamido)pentanamido)-4-methylpentyl)thiazole-4-carbox-amide (5)

At –20°C isobutylchloroformiate (3 µl, 23.1 µmol) was added dropwise to a solution of benzophenon pretubulysin derivative **14b** (17.4 mg, 19.6 µmol) and *N*-methyl-morpholine (9 µl, 81.9 µmol) in dry THF (400 µl). After 10 min propargylamine hydrochloride (3 mg, 31.1 µmol) was added and the reaction mixture was stirred overnight. The solvent was evaporated and the residue was dissolved in ethyl acetate and washed with saturated $NaHCO_3$ solution. The aqueous layer was extracted twice with ethyl acetate and the combined organic layers were dried over Na_2SO_4. The crude product was purified by flash chromatography (DCM/MeOH 97:3 – 9:1) to yield the propargylamide ***5*** (11 mg, 13.6 µmol, 69 %) as a colorless glassy solid and a mixture of rotamers; m.p.82 °C.

[tlc: DCM/MeOH = 9:1, R_f(**5**) = 0.26]

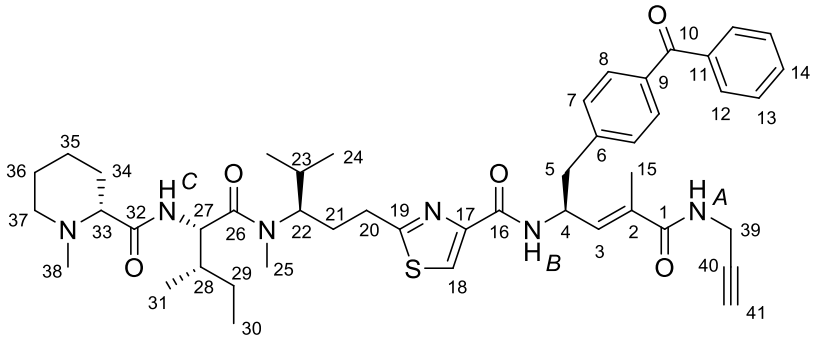

major rotamer

^{1}H-NMR ($CDCl_3$, 400 MHz): δ = 0.75 (d, $^3J_{24,23}$ = 6.6 Hz, 3 H, 24-H), 0.86 (t, $^3J_{30,29}$ = 7.4 Hz, 3 H, 30-H), 0.93 (d, $^3J_{24',23}$ = 6.5 Hz, 3 H, 24'-H), 0.97 (d, $^3J_{31,28}$ = 6.7 Hz, 3 H, 31-H), 1.15 (m, 1 H, 29-H_a), 1.37 (m, 1 H, 34-H_{ax}), 1.42-1.93 (m, 12 H, 15-H, 21-H_a, 23-H, 28-H, 29-H_b, 34-H_{eq}, 35-H, 36-H), 1.98 (ddd, $^2J_{37ax,37eq} \approx {}^3J_{37ax,36ax} \approx$ 11.6 Hz, $^3J_{37ax,36eq}$ = 2.5 Hz, 1 H, 37-H_{ax}), 2.08 (m, 1 H, 21-H_b), 2.20 (s, 3 H, 38-H), 2.20 (m, 1 H, 41-H), 2.48 (dd, $^3J_{33,34ax}$ = 10.8 Hz, $^3J_{33,34eq}$ = 2.4 Hz, 1 H, 33-H), 2.78-2.89 (m, 3 H, 20-H, 37-H_{eq}), 2.99 (m, 1 H, 5-H_a), 3.00 (3 H, 25-H), 3.23 (dd, $^2J_{5b,5a}$ = 13.3 Hz, $^3J_{5b,4}$ = 5.8 Hz, 1-H, 5-H_b), 4.06 (dd, $^3J_{39,NH\ A}$ = 5.2 Hz, $^4J_{39,41}$ = 2.5 Hz, 1 H, 39-H), 4.35 (bs, 1 H, 22-H), 4.77 (dd, $^3J_{27,NH\ C}$ = 9.3 Hz, $^3J_{27,28}$ = 8.3 Hz, 1 H, 27-H), 5.15 (m, 1 H, 4-H), 5.95 (t, $^3J_{NH\ A,39}$ = 4.9 Hz, 1 H, NH_A), 6.47 (d, $^3J_{3,4}$ = 9.6 Hz, 1 H, 3-H), 7.06 (d, $^3J_{NH\ C,27}$ = 9.4 Hz, 1 H, NH_C), 7.34 (d, $^3J_{7,8}$ = 8.2 Hz, 2 H, 7-H), 7.45 (dd,

$^{3}J_{13,12} \approx {}^{3}J_{13,14} \approx 7.5$ Hz, 2 H, 13-H), 7.56 (tt, $^{3}J_{14,13} = 7.4$ Hz, $^{4}J_{14,12} = 1.2$ Hz, 1 H, 14-H), 7.67 (d, $^{3}J_{NH\,B,4} = 8.2$ Hz, 1 H, NH_B), 7.72 (d, $^{3}J_{8,7} = 8.2$ Hz, 2 H, 8-H), 7.74 (m, 2 H, 12-H), 7.90 (s, 1 H, 18-H).

^{13}C-NMR ($CDCl_3$, 100 MHz): δ = 11.0 (q, C-30), 13.1 (q, C-15), 15.9 (q, C-31), 19.7 (q, C-24), 20.1 (q, C-24'), 23.3 (t, C-29), 24.6 (t, C-35), 25.1 (t, C-36), 29.5 (tq, C-21, C-25), 29.6 (t, C-39), 30.0 (t, C-20), 30.3 (d, C-23), 30.5 (t, C-34), 37.2 (d, C-28), 41.2 (t, C-5), 44.9 (q, C-38), 48.6 (d, C-4), 53.1 (d, C-27), 55.4 (t, C-37), 69.7 (d, C-33), 71.8 (d, C-41), 79.4 (s, C-40), 122.7 (d, C-18), 128.3 (d, C-13), 129.4 (d, C-7), 129.9 (d, C-12), 130.4 (d, C-8), 132.4 (d, C-14), 134.6 (d, C-3), 136.0, 137.6 (2s, C-9, C-11), 142.0 (s, C-6), 149.2 (s, C-17), 160.4 (s, C-16), 167.9 (s, C-1), 169.9 (s, C-19), 173.4, 174.2 (2s, C-26, C-32), 196.3 (s, C-10).

Not observable: C-2, C-22

optical rotation: $[\alpha]^{20}_{D} = +25°$ (c = 0.23, $CHCl_3$)

HRMS (CI)	calculated	found
$C_{46}H_{61}N_6O_5S$ $[M+H]^+$	809.4424	809.4385

1. R. B. Merrifield, *J. Am. Chem. Soc.* **1963,** *85,* 2149.
2. L.A. Carpino, G. Y. Han, *J. Am. Chem. Soc.* **1970,** *92,* 5748.
3. C. Boussard, V. E. Doyle, N. Mahmood, T. Klimkait, M. Pritchard, I. H. Gilbert, *European Journal of Medicinal Chemistry* **2002,** *37,* 883.
4. R. Knorr, A. Trzeciak, W. Bannwarth, D. Gillessen, *Tetrahedron Lett.* **1989,** *30,* 1927.
5. W. König, R. Geiger, *Chem. Ber.* **1970,** *103,* 788.
6. F. Albericio, R. Chincilla, d. J. Dodsworth, *Org. Prep. And Proced. Int.* **2001,** *33,* 203.
7. Purchased from Novabiochem, Merck Schuchardt OHG, Hohenbrunn, Germany.
8. Purchased from PolyPeptide Group, Bachem AG, Bubendorf, Switzerland.
9. Purchased from invitrogen, Eugene, Oregon, USA.
10. E. Morera, G. Ortar, *Biiorg. Med. Chem. Lett.* **2000**, *10*, 1815–1818.
11. A. Ullrich, J. Herrmann, R. Müller, U. Kazmaier, *Eur. J. Org. Chem.* **2009**, 6367–6378.

Supporting information for "*N*-(1-(2-oxo-2-(phenylamino)ethyl)piperidin-4-yl)benzamides as reversible inhibitors of the protein disulfide isomerase

Supporting Table 1

Accession	Description	ΣCoverage	Σ# PSMs	Av Area	enrichemnt factor	MW [kDa]
IPI00010796.1	Protein disulfide-isomerase	74.61	273	1.116E9	26.171	57.1
IPI01012004.1	cDNA PSEC0175 fis, clone OVARC1000169, highly similar to Protein disulfide-isomerase A3	56.46	77	1.618E8	18.367	54.1
IPI00893541.1	14 kDa protein	40.65	13	1.656E8	17.753	13.5
IPI00141318.2	Cytoskeleton-associated protein 4	55.48	77	1.354E8	15.035	66.0
IPI00939219.1	Equilibrative nucleoside transporter 1	24.34	14	2.788E7	12.823	50.2
IPI00910147.1	cDNA FLJ52943, highly similar to Zinc transporter SLC39A7	10.96	3	2.772E7	6.170	39.6
IPI00909449.2	GH3 domain-containing protein isoform 2	22.81	23	2.673E7	6.083	53.5
IPI00335161.4	Isoform 2 of All-trans-retinol 13,14-reductase	10.19	5	2.221E7	6.015	52.4
IPI00103756.1	Isoform 4 of Chloride channel CLIC-like protein 1	22.13	8	2.076E8	5.860	39.8
IPI00555585.3	Uncharacterized protein	39.47	21	8.568E7	5.371	47.9
IPI00456429.3	Ubiquitin-60S ribosomal protein L40	32.03	6	6.063E7	4.586	14.7
IPI00845345.2	Uncharacterized protein	18.67	14	1.256E8	4.396	45.3
IPI00022275.6	Phosphatidylinositide phosphatase SAC1	41.57	43	8.266E7	4.098	66.9
IPI00030131.3	Isoform Beta of Lamina-associated polypeptide 2, isoforms beta/gamma	47.36	36	1.043E8	3.947	50.6
IPI00983068.1	Isoform 1 of Thioredoxin reductase 1, cytoplasmic	21.42	9	1.420E7	3.489	70.8
IPI00179473.9	Isoform 1 of Sequestosome-1	15.23	13	1.009E8	3.406	47.7
IPI00747361.3	aladin isoform 2	21.83	8	2.341E7	3.124	55.8
IPI00024642.2	Isoform 1 of Coiled-coil domain-containing protein 47	13.04	15	4.161E7	2.996	55.8
IPI00386755.2	ERO1-like protein alpha	25.43	18	4.365E7	2.914	54.4
IPI00292135.1	Lamin-B receptor	30.73	55	2.284E8	2.913	70.7
IPI00005751.1	Serine palmitoyltransferase 2	15.48	7	2.605E7	2.888	62.9
IPI00984224.1	Uncharacterized protein	4.58	1	6.416E5	2.885	34.2
IPI00218343.4	Tubulin alpha-1C chain	12.47	9	3.115E7	2.648	49.9
IPI00254338.2	Protein FAM134C	15.45	5	1.692E7	2.334	51.4
IPI00007074.5	Tyrosyl-tRNA synthetase, cytoplasmic	22.73	12	3.276E7	2.289	59.1
IPI00479186.7	Isoform M2 of Pyruvate kinase isozymes M1/M2	69.68	141	3.807E8	2.120	57.9
IPI00644576.1	Uncharacterized protein	2.72	7	1.834E7	2.087	276.4
IPI01015575.1	YME1-like 1	10.27	11	5.121E7	2.074	82.6
IPI00290566.1	T-complex protein 1 subunit alpha	60.07	69	8.812E7	1.931	60.3
IPI00554777.2	Asparagine synthetase [glutamine-hydrolyzing]	12.12	6	1.036E7	1.930	64.3
IPI00915282.1	Isoform 2 of Anaphase-promoting complex subunit 7	6.33	3	4.093E7	1.912	60.0
IPI00554737.3;P3015	Serine/threonine-protein phosphatase 2A 65 kDa regulatory subunit A alpha isoform	39.22	37	6.431E7	1.891	65.3
IPI00303292.2	Importin subunit alpha-1	15.06	6	2.033E7	1.884	60.2
IPI00902909.1	cDNA FLJ16112 fis, clone 3NB692001853, highly similar to NUCLEOSOME ASSEMBLY PROTEIN 1-l	23.22	16	5.939E7	1.883	37.3
IPI00216049.1	Isoform 1 of Heterogeneous nuclear ribonucleoprotein K	53.78	63	2.069E8	1.883	50.9
IPI01015268.1	Importin subunit alpha-7	6.72	10	4.334E7	1.860	60.0
IPI00553185.2	T-complex protein 1 subunit gamma	53.94	54	1.032E8	1.804	60.5
IPI00018465.1	T-complex protein 1 subunit eta	47.33	41	6.650E7	1.804	59.3

IPI00964079.1	Uncharacterized protein	54.62	51	9.238E7	1.795	57.1
IPI01014604.2	T-complex protein 1 subunit delta	28.49	25	4.335E7	1.785	54.7
IPI00306398.8	Isoform 2 of NudC domain-containing protein 1	13.00	6	8.353E7	1.779	63.5
IPI01013273.1	cDNA, FLJ79129, highly similar to T-complex protein 1 subunit zeta	58.00	63	1.231E8	1.770	54.8
IPI00017184.2	EH domain-containing protein 1	66.85	47	8.379E7	1.765	60.6
IPI00012578.1	Importin subunit alpha-4	9.60	7	1.292E7	1.738	57.9
IPI00329625.5	cDNA FLJ56153, highly similar to Homo sapiens transforming growth factor beta regulator 4 (TBR(	16.67	16	8.460E7	1.691	71.8
IPI00329692.3	Isoform Long of Glycylpeptide N-tetradecanoyltransferase 1	12.90	11	6.266E7	1.632	56.8
IPI00003269.1	Beta-actin-like protein 2	14.10	6	2.926E7	1.631	42.0
IPI00981943.1	Uncharacterized protein	15.31	9	8.503E7	1.616	68.8
IPI00867509.1	Coronin-1C_i3 protein	32.45	27	4.511E7	1.615	58.9
IPI00024403.1	Copine-3	16.39	14	3.454E7	1.604	60.1
IPI00302925.4	59 kDa protein	58.14	63	1.485E8	1.599	59.4
IPI00099311.3	Isoform 1 of tRNA (adenine-N(1)-)-methyltransferase non-catalytic subunit TRM6	8.85	4	2.921E7	1.556	55.8
IPI00289601.10	Histone deacetylase 2	28.18	21	6.567E7	1.556	65.5
IPI00402182.2	Isoform 2 of Heterogeneous nuclear ribonucleoprotein Q	16.67	9	2.930E7	1.536	65.6
IPI00939917.1	Isoform 3 of SWI/SNF-related matrix-associated actin-dependent regulator of chromatin subfamily	4.14	1	8.587E6	1.516	55.2
IPI00383680.3	dolichyl-diphosphooligosaccharide--protein glycosyltransferase subunit 2 isoform 2 precursor	29.27	18	5.078E7	1.487	67.7
IPI00555572.1	Isoform 1 of Apoptosis inhibitor 5	5.29	5	4.412E8	1.472	57.5
IPI00830039.1	Isoform 2 of Splicing factor U2AF 65 kDa subunit	19.32	16	1.235E8	1.457	53.1
IPI00020599.1	Calreticulin	58.03	32	1.273E8	1.440	48.1
IPI00383581.4	cDNA FLJ61290, highly similar to Neutral alpha-glucosidase AB	17.79	12	1.681E8	1.437	112.9
IPI00915422.1	coatomer subunit delta isoform 2	17.73	11	5.287E7	1.414	47.2
IPI00917016.2	copine-1 isoform c	19.78	8	1.014E8	1.394	58.9
IPI00297492.2	Dolichyl-diphosphooligosaccharide--protein glycosyltransferase subunit STT3A	9.79	9	1.895E8	1.386	80.5
IPI01015522.1	cDNA FLJ55253, highly similar to Actin, cytoplasmic 1	35.73	12	3.161E8	1.294	38.6
IPI00784154.1	60 kDa heat shock protein, mitochondrial	80.80	134	2.863E8	1.271	61.0
IPI00220834.8	X-ray repair cross-complementing protein 5	3.55	1	7.230E5	1.202	82.7
IPI00304596.3	Non-POU domain-containing octamer-binding protein	43.95	77	1.308E8	1.188	54.2

Supporting Table 2

Accession	Description	ΣCoverage	Σ# PSMs	Av Area	enrichemnt factor	MW [kDa]
IPI00010796.1;P0723	Protein disulfide-isomerase	50.39	114	3.445E8	65.77	57.1
IPI00007676.3	Estradiol 17-beta-dehydrogenase 12	24.68	16	2.551E7	65.29	34.3
IPI00156689.3;Q9953	Synaptic vesicle membrane protein VAT-1 homolog	48.35	59	1.114E8	60.46	41.9
IPI00298289.1	Isoform 2 of Reticulon-4	31.37	22	1.346E8	47.38	40.3
IPI00009904.1;P1366	Protein disulfide-isomerase A4	34.42	88	9.593E7	39.48	72.9
IPI00141318.2;Q0706	Cytoskeleton-associated protein 4	38.04	63	6.319E7	37.72	66.0
IPI00303954.3	cytochrome b5 type B precursor	43.33	3	3.043E7	22.44	16.7
IPI00983110.1	Conserved hypothetical protein	16.67	3	8.765E6	21.27	24.6
IPI00218200.8	B-cell receptor-associated protein 31	22.36	9	6.088E7	20.69	28.0
IPI00966408.1	Estradiol 17-beta-dehydrogenase 11	12.89	4	4.568E6	18.81	28.1
IPI00339384.5	Isoform 1 of Retinol dehydrogenase 11	12.26	10	1.951E7	17.73	35.4
IPI00644989.2;Q1508	Isoform 1 of Protein disulfide-isomerase A6	29.77	42	5.158E7	17.63	48.1
IPI01010177.1	cDNA FLJ51879, highly similar to Prenylcysteine oxidase	11.48	6	1.082E7	17.47	48.3
IPI00026824.2	Heme oxygenase 2	12.97	8	3.000E7	17.46	41.6
IPI00031522.2	Trifunctional enzyme subunit alpha, mitochondrial	18.74	25	7.501E6	17.33	82.9
IPI00007940.6	erlin-1	10.92	9	1.357E7	16.22	39.1
IPI01012004.1	cDNA PSEC0175 fis, clone OVARC1000169, highly similar to Protein disulfide-isomerase A3	37.08	53	7.450E7	14.30	54.1
IPI00006666.1	Monocarboxylate transporter 4	4.52	8	2.370E7	12.81	49.4
IPI00019407.1	Sterol-4-alpha-carboxylate 3-dehydrogenase, decarboxylating	6.43	2	3.592E6	12.43	41.9
IPI01020664.1	Uncharacterized protein	12.88	2	2.740E7	12.05	32.4
IPI00939560.1	thioredoxin domain-containing protein 5 isoform 3	5.56	2	6.204E7	11.83	36.2
IPI00152441.3;Q8TC	Isoform 1 of Minor histocompatibility antigen H13	12.20	16	4.233E7	11.77	41.5
IPI01015801.1	cDNA FLJ16138 fis, clone BRALZ2017531, highly similar to Glutamate dehydrogenase 1, mitochondri	18.16	9	2.449E7	11.37	42.9
IPI00395887.4	Thioredoxin-related transmembrane protein 1	18.93	9	3.346E7	11.09	31.8
IPI00177817.4	Isoform 2 of Sarcoplasmic/endoplasmic reticulum calcium ATPase 2	17.55	30	2.794E7	11.08	109.6
IPI00893541.1	14 kDa protein	38.21	21	7.041E7	10.89	13.5
IPI00015842.1	Reticulocalbin-1	15.41	5	1.264E7	10.31	38.9
IPI00216026.2;P4588	Isoform 3 of Voltage-dependent anion-selective channel protein 2	29.25	23	4.318E7	10.02	31.5
IPI00030131.3	Isoform Beta of Lamina-associated polypeptide 2, isoforms beta/gamma	16.74	7	2.452E7	9.86	50.6
IPI00334174.3	Isoform 2 of Ras-related protein Rab-1A	19.15	7	1.185E7	9.02	15.3
IPI00002230.6	neutral cholesterol ester hydrolase 1 isoform b	14.09	12	1.285E7	8.19	49.0
IPI00178744.5	Isoform 2 of Very long-chain specific acyl-CoA dehydrogenase, mitochondrial	4.27	4	3.501E6	8.18	68.0
IPI00219301.7	Myristoylated alanine-rich C-kinase substrate	9.04	2	5.830E6	6.25	31.5
IPI00216308.5;P2179	Voltage-dependent anion-selective channel protein 1	33.92	20	1.751E7	5.86	30.8
IPI00655812.1	Uncharacterized protein	13.55	6	1.399E7	5.78	55.6
IPI00292135.1	Lamin-B receptor	6.18	5	4.680E6	5.77	70.7
IPI00032140.4	Serpin H1	23.68	15	7.930E6	5.54	46.4
IPI00025086.4	Cytochrome c oxidase subunit 5A, mitochondrial	16.00	2	5.414E6	5.32	16.8

IPI00008986.1	Large neutral amino acids transporter small subunit 1	6.71	2	1.638E7	5.20	55.0
IPI01013280.1	cDNA FLJ54090, highly similar to 4F2 cell-surface antigen heavy chain	17.42	21	1.952E7	5.10	55.9
P08670;IPI00418471.	Vimentin OS=Homo sapiens GN=VIM PE=1 SV=4 - [VIME_HUMAN]	25.32	24	2.108E7	5.01	53.6
IPI00645646.1	17 kDa protein	27.22	12	8.742E6	4.59	17.3
IPI00642042.3	Putative uncharacterized protein DKFZp686J1372	19.40	7	2.737E7	4.55	27.2
IPI00220194.6	Solute carrier family 2, facilitated glucose transporter member 1	11.99	12	1.402E7	4.52	54.0
IPI00025874.2	Dolichyl-diphosphooligosaccharide--protein glycosyltransferase subunit 1 precursor	9.60	12	7.584E6	4.51	72.7
IPI00977640.1	sodium/potassium-transporting ATPase subunit alpha-1 isoform d	11.90	19	1.380E7	4.50	109.5
IPI00656071.1	Isoform 1 of Mitochondrial import inner membrane translocase subunit TIM50	7.65	3	1.060E6	4.48	39.6
IPI00855957.3	Isoform 2 of Far upstream element-binding protein 2	5.21	5	1.240E7	3.66	72.9
IPI00007188.6	ADP/ATP translocase 2	18.12	20	1.727E7	3.65	32.8
IPI00941747.1	Calnexin	11.99	7	2.971E7	3.61	67.5
IPI00910322.1	cDNA FLJ52936, weakly similar to Tropomyosin alpha-4 chain	22.08	4	2.428E7	3.55	17.6
IPI00374151.1	thioredoxin-dependent peroxide reductase, mitochondrial isoform b	10.92	2	5.637E5	3.46	25.8
IPI00100656.3	Isoform 1 of Trans-2,3-enoyl-CoA reductase	11.04	5	5.880E6	3.20	36.0
IPI01022950.1	Uncharacterized protein	8.02	8	9.403E7	3.12	36.1
IPI00019472.4	Neutral amino acid transporter B(0)	5.73	4	1.050E6	3.06	56.6
IPI00003362.3	78 kDa glucose-regulated protein	27.68	40	4.159E7	2.91	72.3
IPI00027230.3	Endoplasmin	15.44	26	3.473E7	2.73	92.4
IPI00644224.2	cDNA FLJ54020, highly similar to Heterogeneous nuclear ribonucleoprotein U	11.61	10	7.672E6	2.72	86.8
IPI00514561.1	cDNA FLJ54552, highly similar to Heterogeneous nuclear ribonucleoprotein K	19.16	9	7.241E6	2.62	47.5
IPI00021812.2	Neuroblast differentiation-associated protein AHNAK	7.45	18	2.741E7	2.53	628.7
IPI00966238.2	cDNA FLJ51907, highly similar to Stress-70 protein, mitochondrial	18.80	21	1.253E7	2.41	72.4
IPI00917575.2	cDNA FLJ51046, highly similar to 60 kDa heat shock protein, mitochondrial	16.44	13	1.321E7	2.37	55.0
IPI00028481.1	Ras-related protein Rab-8A	12.08	4	1.133E7	2.29	23.7
IPI00646304.4	Peptidyl-prolyl cis-trans isomerase B	17.13	5	4.132E6	2.24	23.7
IPI01012829.1	Uncharacterized protein	16.42	3	2.037E7	2.06	22.9
IPI00000861.1	Isoform 1 of LIM and SH3 domain protein 1	14.56	3	9.862E6	2.00	29.7
IPI00797148.1	Isoform 2 of Heterogeneous nuclear ribonucleoprotein A1	22.10	8	1.285E7	1.94	29.4
IPI00010740.1	Isoform Long of Splicing factor, proline- and glutamine-rich	4.38	2	1.083E7	1.90	76.1
IPI00444262.3	cDNA FLJ45706 fis, clone FEBRA2028457, highly similar to Nucleolin	8.96	8	2.138E7	1.76	65.9
IPI01021460.1	Uncharacterized protein	22.31	2	1.684E7	1.76	14.4
IPI00908662.3	cDNA FLJ50994, moderately similar to 60S ribosomal protein L4	10.88	3	6.962E6	1.74	27.0
IPI00414676.6;P0823	Heat shock protein HSP 90-beta	23.90	58	6.121E7	1.72	83.2
IPI00984887.1	Uncharacterized protein	16.46	4	1.158E6	1.66	17.4
IPI00658013.1	nucleophosmin isoform 3	20.46	6	2.254E7	1.62	28.4
IPI00455315.4;P0735	Isoform 1 of Annexin A2	36.87	77	8.532E7	1.60	38.6
IPI00645201.1	Uncharacterized protein	20.74	5	4.160E6	1.52	21.9
IPI00396378.3	Isoform B1 of Heterogeneous nuclear ribonucleoproteins A2/B1	24.08	11	1.811E7	1.49	37.4

IPI01021193.1	Uncharacterized protein	23.27	8	8.997E6	1.39	18.1
IPI00396485.3	Elongation factor 1-alpha 1	17.53	41	5.670E7	1.37	50.1
IPI00010896.3	Chloride intracellular channel protein 1	12.45	2	1.838E7	1.31	26.9
IPI01019113.1;Q2KJI	Tubulin beta chain	27.25	50	4.121E7	1.28	49.6
IPI00847989.3	Pyruvate kinase	24.45	25	1.596E7	1.27	50.0
IPI00003865.1;A2Q02	Isoform 1 of Heat shock cognate 71 kDa protein	31.89	55	4.385E7	1.27	70.9
IPI00784295.2;P0790	Isoform 1 of Heat shock protein HSP 90-alpha	16.12	44	5.771E7	1.26	84.6
IPI00007752.1	Tubulin beta-2C chain	20.00	28	3.160E7	1.25	49.8
IPI00217465.5	Histone H1.2	10.80	2	1.354E7	1.22	21.4
IPI00021263.3;P6310	14-3-3 protein zeta/delta	22.45	13	1.870E7	0.99	27.7
IPI00299402.1;P1149	Pyruvate carboxylase, mitochondrial	10.53	17	1.216E7	0.89	129.6
IPI00216691.5	Profilin-1	20.00	2	1.139E7	0.77	15.0
IPI00795257.3	Glyceraldehyde-3-phosphate dehydrogenase	9.90	4	1.425E7	0.73	31.5
IPI00217966.9;P0033	Isoform 1 of L-lactate dehydrogenase A chain	13.55	5	2.549E7	0.69	36.7
IPI00465439.5	Fructose-bisphosphate aldolase A	9.89	2	2.125E6	0.62	39.4

Supporting Table 3

Accession	Description	ΣCoverage	Σ# PSMs	av area	enrichemnt factor	MW [kDa]
IPI00010796.1	Protein disulfide-isomerase	61.61	236	1.359E9	38.32	57.1
IPI01012004.1	cDNA PSEC0175 fis, clone OVARC1000169, highly similar to Protein disulfide-isomerase A3	32.92	41	1.271E8	10.32	54.1
IPI00939219.1	Equilibrative nucleoside transporter 1	15.13	8	5.366E7	9.99	50.2
IPI00893541.1	14 kDa protein	28.46	14	1.104E8	8.47	13.5
IPI00064193.3	Isoform 1 of Protein disulfide-isomerase TMX3	15.42	8	4.447E7	5.14	51.8
IPI00141318.2	Cytoskeleton-associated protein 4	43.52	73	2.572E8	4.11	66.0
IPI00009904.1	Protein disulfide-isomerase A4	19.53	18	6.740E7	3.02	72.9
IPI00296157.6	Isoform 1 of All-trans-retinol 13,14-reductase	21.15	22	7.851E7	2.73	66.8
IPI01021659.1	23 kDa protein	14.14	2	1.313E7	2.27	23.4
IPI00443485.2	Isoform 2 of CDK5 regulatory subunit-associated protein 1-like 1	7.99	3	2.918E7	2.01	54.6
IPI00845345.2	Uncharacterized protein	17.44	10	3.680E7	1.96	45.3
IPI00642042.3	Putative uncharacterized protein DKFZp686J1372	15.09	3	1.203E7	1.83	27.2
IPI00031804.1	Isoform 1 of Voltage-dependent anion-selective channel protein 3	7.42	3	3.070E7	1.72	30.6
IPI01015565.1	Uncharacterized protein	33.56	6	5.910E7	1.67	16.8
IPI00455167.4	Uncharacterized protein	9.09	2	7.940E6	1.65	24.9
IPI00022275.6	Phosphatidylinositide phosphatase SAC1	25.38	31	7.855E7	1.57	66.9
IPI00215893.8	Heme oxygenase 1	12.15	2	8.121E6	1.56	32.8
IPI01010050.1	cDNA, FLJ78818, highly similar to Voltage-dependent anion-selective channel protein 2	25.49	5	4.457E7	1.56	27.5
IPI00179473.9	Isoform 1 of Sequestosome-1	18.41	11	5.497E7	1.55	47.7
IPI00004668.1	Isoform 1 of Alpha-(1,6)-fucosyltransferase	27.13	27	5.591E7	1.51	66.5
IPI00178744.5	Isoform 2 of Very long-chain specific acyl-CoA dehydrogenase, mitochondrial	51.50	102	2.974E8	1.49	68.0
IPI00021840.1	40S ribosomal protein S6	22.09	10	9.622E7	1.48	28.7
IPI00013860.3	3-hydroxyisobutyrate dehydrogenase, mitochondrial	14.58	3	4.840E6	1.48	35.3
IPI00386755.2	ERO1-like protein alpha	42.74	38	1.013E8	1.43	54.4
IPI00027230.3	Endoplasmin	3.24	2	1.660E7	1.41	92.4
IPI00402109.4	Isoform 2 of Phosphatidylinositol glycan anchor biosynthesis class U protein	8.43	2	4.034E6	1.41	47.6
IPI00007676.3	Estradiol 17-beta-dehydrogenase 12	11.54	3	1.377E7	1.37	34.3
IPI00644079.4	cDNA FLJ44920 fis, clone BRAMY3011501, highly similar to Heterogeneous nuclear ribonucleoprotein U	4.00	3	1.598E7	1.35	83.0
IPI00216308.5	Voltage-dependent anion-selective channel protein 1	35.69	12	8.067E7	1.34	30.8
IPI00642256.2	Isoform 2 of F-actin-capping protein subunit beta	21.32	4	1.057E7	1.32	30.6
IPI00419880.6	40S ribosomal protein S3a	33.71	12	4.668E7	1.32	29.9
IPI00030243.1	Isoform 1 of Proteasome activator complex subunit 3	24.41	6	4.918E7	1.31	29.5
IPI00296528.4	Annexin A10	10.19	3	1.067E7	1.30	37.3
IPI00607732.1	Isoform 2 of Nicalin	4.27	2	7.094E6	1.30	62.8
IPI00976899.1	Uncharacterized protein	28.29	5	2.264E7	1.30	22.4
IPI00011253.3	40S ribosomal protein S3	50.62	14	1.206E8	1.30	26.7
IPI01021739.1	Protein	23.39	2	5.660E6	1.28	14.1
IPI00979595.1	Uncharacterized protein	37.02	11	1.355E8	1.27	25.2

IPI01012528.1	Uncharacterized protein	27.39	6	1.621E7	1.27	17.4
IPI00848226.1	Guanine nucleotide-binding protein subunit beta-2-like 1	57.41	23	1.151E8	1.27	35.1
IPI01017942.1	34 kDa protein	34.34	8	2.514E7	1.26	34.1
IPI00014230.1	Complement component 1 Q subcomponent-binding protein, mitochondrial	12.06	3	4.884E7	1.25	31.3
IPI00910902.1	cDNA FLJ50573, highly similar to Homo sapiens NAD(P)H dehydrogenase, quinone 1 (NQO1), transcrip	25.25	9	5.428E7	1.25	22.8
IPI00410017.1	Isoform 2 of Polyadenylate-binding protein 1	10.42	4	2.189E7	1.25	61.1
IPI00759824.2	Isoform 2 of Acidic leucine-rich nuclear phosphoprotein 32 family member B	13.85	2	1.139E7	1.25	22.3
IPI00974544.1	Isoform SV of 14-3-3 protein epsilon	9.01	2	1.281E7	1.25	26.5
IPI00010896.3	Chloride intracellular channel protein 1	28.63	4	2.822E7	1.24	26.9
IPI00299573.12	60S ribosomal protein L7a	22.56	10	3.314E7	1.24	30.0
IPI00895865.1	electron transfer flavoprotein subunit alpha, mitochondrial isoform b	19.72	4	1.493E7	1.22	30.0
IPI00220637.5	Seryl-tRNA synthetase, cytoplasmic	4.67	2	2.981E6	1.22	58.7
IPI00872780.2	cDNA FLJ51794, highly similar to Annexin A4	10.70	2	1.017E7	1.19	33.5
IPI00295386.7	Carbonyl reductase [NADPH] 1	14.44	4	1.087E7	1.19	30.4
IPI00427502.1	Isoform 2 of GH3 domain-containing protein	9.49	4	5.448E6	1.18	51.4
IPI00024642.2	Isoform 1 of Coiled-coil domain-containing protein 47	27.74	26	4.893E7	1.17	55.8
IPI00921824.1	cDNA FLJ58226, highly similar to Polypeptide N-acetylgalactosaminyltransferase 2	8.30	2	1.438E7	1.16	30.2
IPI00329801.12	Annexin A5	20.31	6	1.364E7	1.15	35.9
IPI00003833.3	Mitochondrial carrier homolog 2	26.40	5	2.588E7	1.15	33.3
IPI00789337.4	cDNA, FLJ79516, highly similar to 14-3-3 protein zeta/delta	13.10	2	6.447E6	1.15	19.1
IPI00339384.5	Isoform 1 of Retinol dehydrogenase 11	12.58	3	1.390E7	1.14	35.4
IPI00910650.1	cDNA FLJ54979, highly similar to Homo sapiens cyclin-dependent kinase 2 (CDK2), transcript variant 2	13.87	3	1.382E7	1.13	27.1
IPI00254338.2	Protein FAM134C	6.44	6	4.738E7	1.13	51.4
IPI00923547.1	60 kDa chaperonin (Fragment)	11.35	6	1.165E8	1.13	19.8
IPI00795257.3	Glyceraldehyde-3-phosphate dehydrogenase	15.36	3	4.249E7	1.13	31.5
IPI00003362.3	78 kDa glucose-regulated protein	8.56	10	5.909E7	1.13	72.3
IPI00027834.3	Heterogeneous nuclear ribonucleoprotein L	12.05	5	1.043E7	1.11	64.1
IPI01022070.1	Uncharacterized protein	7.16	6	1.896E8	1.10	43.7
IPI00871418.1	Uncharacterized protein	12.81	6	2.851E7	1.09	53.1
IPI00478410.2	Isoform Liver of ATP synthase subunit gamma, mitochondrial	7.72	3	1.605E7	1.07	33.0
IPI00152981.1	Acyl-CoA dehydrogenase family member 9, mitochondrial	19.00	15	2.424E7	1.07	68.7
IPI00946316.1	19 kDa protein	18.24	2	3.038E7	1.05	18.9
IPI00513860.2	cDNA FLJ58153, highly similar to ATP-dependent metalloprotease YME1L1	11.13	9	3.991E7	1.05	75.9
IPI00020599.1	Calreticulin	44.36	77	4.430E8	1.04	48.1
IPI00964643.1	Uncharacterized protein	25.69	3	1.080E7	1.04	16.5
IPI00784154.1	60 kDa heat shock protein, mitochondrial	76.44	480	1.090E9	1.04	61.0
IPI00843975.1	Ezrin	8.19	10	5.861E7	1.03	69.4
IPI01015738.1	Uncharacterized protein	3.18	9	2.180E7	1.03	79.9
IPI00943173.1	Coronin-1C	17.09	13	4.694E7	1.02	53.2

IPI00793589.2	cDNA FLJ51740, highly similar to Dolichyl-diphosphooligosaccharide--proteinglycosyltransferase 67 kDa	7.75	7	2.844E7	1.01	65.8
IPI00554541.2	Isoform 1 of Acetolactate synthase-like protein	20.41	9	6.021E7	1.01	67.8
IPI00383680.3	dolichyl-diphosphooligosaccharide--protein glycosyltransferase subunit 2 isoform 2 precursor	45.69	112	4.112E8	0.99	67.7
IPI00972999.1	Histone deacetylase	18.12	21	9.346E7	0.99	52.0
IPI00169283.1	Isoform 1 of Motile sperm domain-containing protein 2	6.18	4	1.099E7	0.98	59.7
IPI00939917.1	Isoform 3 of SWI/SNF-related matrix-associated actin-dependent regulator of chromatin subfamily D m	19.88	13	4.258E7	0.97	55.2
IPI00909509.1	cDNA FLJ59138, highly similar to Annexin A2	21.13	5	2.799E7	0.97	21.7
IPI00396485.3	Elongation factor 1-alpha 1	20.56	18	7.118E7	0.96	50.1
IPI01022950.1	Uncharacterized protein	34.26	14	1.378E8	0.96	36.1
IPI00304596.3	Non-POU domain-containing octamer-binding protein	32.70	29	5.274E7	0.96	54.2
IPI00010154.3	Rab GDP dissociation inhibitor alpha	6.04	2	1.854E7	0.96	50.6
IPI00916535.1	prolyl 4-hydroxylase subunit alpha-1 isoform 3 precursor	23.64	37	8.428E7	0.94	58.9
IPI00514561.1	cDNA FLJ54552, highly similar to Heterogeneous nuclear ribonucleoprotein K	47.90	113	6.788E8	0.93	47.5
IPI00218547.1	Isoform Short of Delta-1-pyrroline-5-carboxylate synthase	3.03	2	1.456E6	0.93	87.0
IPI00910934.2	Isoform 5 of Putative oxidoreductase GLYR1	10.38	10	1.597E7	0.93	51.5
IPI00024403.1	Copine-3	16.20	16	4.031E7	0.92	60.1
IPI00216952.1	Isoform C of Prelamin-A/C	61.71	227	4.948E8	0.92	65.1
IPI00012585.1	Beta-hexosaminidase subunit beta	3.78	2	1.149E7	0.92	63.1
IPI01021618.1	Uncharacterized protein	9.03	2	1.592E7	0.91	30.3
IPI00300659.4	Parafibromin	12.24	7	1.376E7	0.90	60.5
IPI01013155.1	cDNA FLJ54614, highly similar to Vacuolar protein sorting-associated protein 45	5.62	2	2.424E6	0.89	50.4
IPI00383581.4	cDNA FLJ61290, highly similar to Neutral alpha-glucosidase AB	16.98	38	6.305E7	0.89	112.9
IPI00219365.3	Moesin	10.40	11	5.873E7	0.88	67.8
IPI01011799.1	cDNA FLJ61680, highly similar to GPI transamidase component PIG-T	22.47	7	1.532E7	0.88	36.0
IPI00966238.2	cDNA FLJ51907, highly similar to Stress-70 protein, mitochondrial	23.76	32	8.830E7	0.87	72.4
IPI00295992.4	Isoform 2 of ATPase family AAA domain-containing protein 3A	42.49	118	2.860E8	0.87	66.2
IPI00976467.1	cDNA FLJ45269 fis, clone BRHIP2029529, highly similar to TFIIH basal transcription factor complex p6	6.48	2	1.282E7	0.87	48.7
IPI00915282.1	Isoform 2 of Anaphase-promoting complex subunit 7	6.15	2	7.209E6	0.86	60.0
IPI00965308.1	Uncharacterized protein	7.08	2	2.698E7	0.86	47.3
IPI00893179.1	X-ray repair complementing defective repair in Chinese hamster cells 6	12.93	12	2.056E7	0.85	64.0
IPI00400849.2	Isoform 3 of Phosphatidylinositol-binding clathrin assembly protein	16.39	23	5.558E7	0.85	66.4
IPI00003865.1	Isoform 1 of Heat shock cognate 71 kDa protein	33.28	54	1.003E8	0.83	70.9
IPI00945733.1	Uncharacterized protein	11.89	3	7.736E6	0.83	36.8
IPI01011344.1	Uncharacterized protein	36.34	39	3.310E8	0.82	37.4
IPI00946351.1	Uncharacterized protein	3.98	2	4.181E7	0.82	65.3
IPI01013230.1	cDNA FLJ51319, highly similar to tRNA (adenine-N(1)-)-methyltransferase non-catalytic subunit TRM6	24.46	25	3.672E7	0.82	36.4
IPI01014338.1	cDNA FLJ52118, highly similar to 14-3-3 protein theta	10.48	2	5.340E6	0.81	23.8
IPI00218830.1	Isoform Short of Glycylpeptide N-tetradecanoyltransferase 1	22.36	15	4.550E7	0.81	48.1
IPI00830039.1	Isoform 2 of Splicing factor U2AF 65 kDa subunit	24.84	39	1.110E8	0.80	53.1

IPI00010720.1	T-complex protein 1 subunit epsilon	48.61	85	2.516E8	0.80	59.6
IPI00915274.1	H/ACA ribonucleoprotein complex subunit 4 isoform 2	4.72	2	3.476E6	0.80	57.0
IPI00746165.2	Isoform 1 of WD repeat-containing protein 1	28.88	24	8.399E7	0.80	66.2
IPI00645452.1	Uncharacterized protein	30.05	14	4.296E7	0.80	47.7
IPI00395775.6	Isoform 2 of Paraspeckle component 1	26.72	32	1.377E8	0.80	45.5
IPI00916869.2	cDNA FLJ59519, highly similar to U4/U6.U5 tri-snRNP-associated protein 2	10.82	5	2.606E7	0.79	53.5
IPI00329625.5	cDNA FLJ56153, highly similar to Homo sapiens transforming growth factor beta regulator 4 (TBRG4),	34.27	52	1.004E8	0.78	71.8
IPI00290566.1	T-complex protein 1 subunit alpha	56.65	95	2.784E8	0.78	60.3
IPI00027626.3	T-complex protein 1 subunit zeta	47.65	133	3.458E8	0.78	58.0
IPI00784090.2	T-complex protein 1 subunit theta	48.18	67	1.569E8	0.77	59.6
IPI00479186.7	Isoform M2 of Pyruvate kinase isozymes M1/M2	64.78	401	1.834E9	0.77	57.9
IPI00788826.1	Isoform 4 of Poly(U)-binding-splicing factor PUF60	16.43	11	4.326E7	0.77	54.0
IPI00414676.6	Heat shock protein HSP 90-beta	20.58	26	1.092E8	0.77	83.2
IPI00797537.3	Isoform 1 of NudC domain-containing protein 1	17.67	12	4.347E7	0.77	66.7
IPI00013894.1	Stress-induced-phosphoprotein 1	36.10	57	2.354E8	0.76	62.6
IPI00514053.1	Coatomer subunit delta	38.94	42	1.343E8	0.76	57.2
IPI00514530.5	Uncharacterized protein	25.95	23	2.403E8	0.76	32.3
IPI00930688.1	Tubulin alpha-1B chain	35.48	45	2.028E8	0.76	50.1
IPI00983581.1	SYNCRIP protein (Fragment)	10.60	6	2.320E7	0.76	50.6
IPI01014074.1	cDNA FLJ53296, highly similar to Serine/threonine-protein phosphatase 2A 65 kDa regulatory subunit A	51.64	85	3.420E8	0.75	64.1
IPI01011335.1	cDNA FLJ60435, highly similar to Heterogeneous nuclear ribonucleoprotein M	6.83	2	7.418E6	0.75	39.2
IPI00553185.2	T-complex protein 1 subunit gamma	57.43	97	4.095E8	0.75	60.5
IPI00419979.3	Serine/threonine-protein kinase PAK 2	11.62	5	3.032E7	0.73	58.0
IPI00604652.1	NEDD8-activating enzyme E1 regulatory subunit isoform c	10.34	6	1.038E7	0.72	50.6
IPI00910719.1	cDNA FLJ55705, highly similar to Threonyl-tRNA synthetase, cytoplasmic	5.65	6	8.713E6	0.72	70.3
IPI00299402.1	Pyruvate carboxylase, mitochondrial	5.43	5	1.258E7	0.71	129.6
IPI00984387.1	cDNA FLJ53166, highly similar to Dihydropyrimidinase-related protein 2	29.48	26	6.433E7	0.70	58.1
IPI00412880.2	Isoform 1 of Histone-arginine methyltransferase CARM1	8.38	12	6.143E7	0.70	63.4
IPI00798375.2	cDNA FLJ59357, highly similar to Probable ATP-dependent RNA helicase DDX5	14.34	15	7.601E7	0.69	61.5
IPI00007074.5	Tyrosyl-tRNA synthetase, cytoplasmic	21.40	19	4.204E7	0.68	59.1
IPI00940673.2	cDNA FLJ36348 fis, clone THYMU2007025, highly similar to TRANSKETOLASE	8.70	3	2.593E7	0.67	58.9
IPI00925572.1	asparagine synthetase [glutamine-hydrolyzing] isoform b	21.67	28	7.616E7	0.67	62.1
IPI00911039.1	cDNA FLJ54408, highly similar to Heat shock 70 kDa protein 1	8.70	11	5.633E7	0.66	63.9
IPI00005578.1	EH domain-containing protein 4	9.24	10	9.722E7	0.66	61.1
IPI00017184.2	EH domain-containing protein 1	65.92	156	4.127E8	0.65	60.6
IPI01015295.1	Uncharacterized protein	42.80	59	1.806E8	0.65	59.7
IPI00219526.6	Isoform 1 of Phosphoglucomutase-1	38.08	38	6.857E7	0.65	61.4
IPI00917016.2	copine-1 isoform c	23.51	44	1.407E8	0.64	58.9
IPI00965314.1	Uncharacterized protein	6.89	3	1.137E7	0.64	47.0

IPI00465436.4	Catalase	29.22	17	4.810E7	0.63	59.7
IPI00925601.1	Uncharacterized protein	63.62	87	2.164E8	0.62	64.5
IPI00103483.1	Negative elongation factor B	3.45	3	4.457E6	0.61	65.7
IPI00306960.3	Asparaginyl-tRNA synthetase, cytoplasmic	31.02	23	5.166E7	0.59	62.9
IPI00945725.1	cDNA FLJ58035, highly similar to Homo sapiens eukaryotic translation initiation factor (eIF) 2A (eIF2A)	6.61	2	8.879E6	0.59	62.2
IPI00925990.1	Uncharacterized protein	25.95	4	6.467E6	0.56	20.3
IPI00640357.1	ubiquitin carboxyl-terminal hydrolase 14 isoform b	10.02	3	2.797E7	0.54	52.4
IPI00910422.2	cDNA FLJ52802, highly similar to Eukaryotic translation initiation factor 3subunit 6-interacting protein	32.36	14	3.992E7	0.53	61.0
IPI00789582.2	cDNA FLJ51552, highly similar to Eukaryotic translation initiation factor 3 subunit 7	8.42	4	1.326E7	0.51	58.1
IPI00917117.1	FAM129B protein (Fragment)	7.34	5	1.381E8	0.50	35.2
IPI00184821.1	Isoform 1 of Bifunctional coenzyme A synthase	4.79	2	3.476E6	0.49	62.3
IPI00180983.1	Isoform 2 of Insulin-like growth factor 2 mRNA-binding protein 2	12.77	6	2.966E7	0.49	61.8
IPI00219762.5	Uncharacterized protein	5.14	3	6.002E6	0.48	103.8
IPI01011685.1	Uncharacterized protein	10.56	2	2.433E7	0.48	31.4
IPI00759806.1	Isoform MBP-1 of Alpha-enolase	10.56	2	8.643E6	0.47	36.9
IPI00030009.4	Isoform A of Bifunctional 3'-phosphoadenosine 5'-phosphosulfate synthase 2	12.87	5	1.729E7	0.37	69.5
IPI00645078.1	Ubiquitin-like modifier-activating enzyme 1	3.40	2	7.529E6	0.37	117.8
IPI00479201.3	Isoform 2 of Putative adenosylhomocysteinase 2	4.35	2	8.923E6	0.35	53.7

Supporting Table 4

Accession	Description	ΣCoverage	Σ# PSMs	Av Area	enrichemnt factor	MW [kDa]
IPI00010796.1	Protein disulfide-isomerase	61.22	290	2.188E9	43.238	57.1
IPI01012004.1	cDNA PSEC0175 fis, clone OVARC1000169, highly similar to Protein disulfide-isomerase A3	38.54	45	2.486E8	17.923	54.1
IPI00893541.1	14 kDa protein	38.21	10	2.384E8	14.993	13.5
IPI00141318.2	Cytoskeleton-associated protein 4	38.70	40	1.714E8	6.640	66.0
IPI00555585.3	Protein disulfide-isomerase TMX3	15.31	13	7.745E7	6.452	47.9
IPI00009904.1	Protein disulfide-isomerase A4	4.65	2	4.887E7	5.256	72.9
IPI00030131.3	Isoform Beta of Lamina-associated polypeptide 2, isoforms beta/gamma	14.98	7	4.127E7	4.757	50.6
IPI00909005.1	cDNA FLJ54014, highly similar to All-trans-retinol 13,14-reductase	15.85	20	1.011E8	3.546	60.6
IPI01015565.1	Polyubiquitin-C	33.56	2	4.462E7	3.452	16.8
IPI00441550.4	Isoform 2 of Beta-galactosidase	4.58	2	3.230E7	3.113	60.5
IPI00292135.1	Lamin-B receptor	10.89	14	5.890E7	2.818	70.7
IPI00607732.1	Isoform 2 of Nicalin	4.80	4	1.470E7	2.513	62.8
IPI00845345.2	Regulator of microtubule dynamics protein 3	16.71	4	3.467E7	2.322	45.3
IPI00215828.1	Isoform 2 of Alpha-(1,6)-fucosyltransferase	7.14	2	4.577E7	2.234	35.8
IPI00386755.2	ERO1-like protein alpha	12.61	11	4.170E7	2.171	54.4
IPI01022604.1	Mutant Allgrove syndrome protein	7.35	2	1.418E7	2.124	45.6
IPI00022275.6	Phosphatidylinositide phosphatase SAC1	27.26	36	1.502E8	2.111	66.9
IPI00941685.1	LEM domain-containing protein 2 isoform 2	12.44	2	3.521E6	2.104	23.5
IPI00178744.5	Isoform 2 of Very long-chain specific acyl-CoA dehydrogenase, mitochondrial	23.70	27	8.651E7	1.986	68.0
IPI00909509.1	cDNA FLJ59138, highly similar to Annexin A2	10.82	2	3.662E7	1.974	21.7
IPI01015427.1	cDNA FLJ58247, highly similar to 26S protease regulatory subunit 4	6.54	2	6.059E6	1.780	41.1
IPI00910507.1	cDNA FLJ59352, highly similar to Brain-specific angiogenesis inhibitor1-associated protein 2	4.60	2	4.084E7	1.765	54.8
IPI00554786.5	Isoform 5 of Thioredoxin reductase 1, cytoplasmic	37.27	18	6.589E7	1.715	54.7
IPI00910934.2	Isoform 5 of Putative oxidoreductase GLYR1	6.78	8	2.342E7	1.535	51.5
IPI00743775.1	Isoform 2 of Coiled-coil domain-containing protein 47	27.50	27	7.601E7	1.532	55.3
IPI00915950.1	Isoform 4 of Mitochondrial ribonuclease P protein 3	4.71	2	3.237E6	1.531	56.5
IPI00152981.1	Acyl-CoA dehydrogenase family member 9, mitochondrial	20.45	13	2.838E7	1.493	68.7
IPI00513860.2	cDNA FLJ58153, highly similar to ATP-dependent metalloprotease YME1L1	9.37	9	3.456E7	1.438	75.9
IPI00024403.1	Copine-3	21.23	22	7.099E7	1.413	60.1
IPI00784104.1	Isoform 2 of Sequestosome-1	16.85	8	1.105E8	1.364	38.6
IPI00784154.1	60 kDa heat shock protein, mitochondrial	67.19	475	1.227E9	1.338	61.0
IPI00011454.1	Isoform 2 of Neutral alpha-glucosidase AB	6.31	11	5.540E7	1.306	109.4
IPI00028635.5	Dolichyl-diphosphooligosaccharide--protein glycosyltransferase subunit 2	46.59	97	3.701E8	1.299	69.2
IPI00329625.5	cDNA FLJ56153, highly similar to Homo sapiens transforming growth factor beta regulator	31.62	58	1.403E8	1.297	71.8
IPI00916535.1	prolyl 4-hydroxylase subunit alpha-1 isoform 3 precursor	21.51	26	7.143E7	1.294	58.9
IPI00295992.4	Isoform 2 of ATPase family AAA domain-containing protein 3A	23.72	29	1.063E8	1.288	66.2
IPI01011639.1	cDNA FLJ50809, highly similar to Dolichyl-diphosphooligosaccharide--protein glycosyltransf	11.72	7	2.799E7	1.274	49.9
IPI00922694.2	Uncharacterized protein	5.54	6	4.804E7	1.270	69.9

IPI00020599.1	Calreticulin	51.80	85	6.236E8	1.266	48.1
IPI00030380.1	General transcription factor IIH subunit 1	4.01	2	1.809E7	1.266	62.0
IPI00300659.4	Parafibromin	12.05	12	2.252E7	1.164	60.5
IPI00465436.4	Catalase	35.48	31	8.485E7	1.163	59.7
IPI00797537.3	Isoform 1 of NudC domain-containing protein 1	17.15	10	4.424E7	1.139	66.7
IPI00972999.1	Histone deacetylase	16.81	28	1.004E8	1.120	52.0
IPI00220637.5	Seryl-tRNA synthetase, cytoplasmic	17.70	13	4.936E7	1.097	58.7
IPI00303292.2	Importin subunit alpha-1	19.70	12	3.465E7	1.088	60.2
IPI00939917.1	Isoform 3 of SWI/SNF-related matrix-associated actin-dependent regulator of chromatin su	25.67	24	6.830E7	1.071	55.2
IPI00299033.1	Importin subunit alpha-3	7.10	9	6.228E7	1.059	57.8
IPI01021659.1	23 kDa protein	19.19	8	8.841E7	1.056	23.4
IPI00983309.1	Uncharacterized protein	4.89	2	3.973E6	1.036	69.5
IPI00012578.1	Importin subunit alpha-4	8.64	14	7.211E7	1.012	57.9
IPI00182373.2	Isoform IIa of Prolyl 4-hydroxylase subunit alpha-2	4.69	2	2.713E6	0.998	60.6
IPI00216049.1	Isoform 1 of Heterogeneous nuclear ribonucleoprotein K	48.16	68	6.398E8	0.993	50.9
IPI00013981.4	Tyrosine-protein kinase Yes	3.50	2	5.983E6	0.975	60.8
IPI01015580.1	Uncharacterized protein	6.98	11	7.236E7	0.974	76.2
IPI00010720.1	T-complex protein 1 subunit epsilon	63.96	112	5.071E8	0.969	59.6
IPI00304596.3	Non-POU domain-containing octamer-binding protein	35.46	41	1.411E8	0.966	54.2
IPI00290566.1	T-complex protein 1 subunit alpha	70.32	111	4.727E8	0.965	60.3
IPI00167198.6	Isoform 2 of U4/U6 small nuclear ribonucleoprotein Prp31	5.22	2	1.518E7	0.948	40.8
IPI00377261.1	Isoform 1 of Far upstream element-binding protein 3	7.34	2	5.301E7	0.944	61.6
IPI00479186.7	Isoform M2 of Pyruvate kinase isozymes M1/M2	64.78	533	3.120E9	0.943	57.9
IPI00640357.1	ubiquitin carboxyl-terminal hydrolase 14 isoform b	23.09	17	8.107E7	0.919	52.4
IPI00784090.2	T-complex protein 1 subunit theta	61.86	104	4.447E8	0.915	59.6
IPI00021439.1	Actin, cytoplasmic 1	31.73	16	1.254E8	0.915	41.7
IPI00930688.1	Tubulin alpha-1B chain	39.47	45	2.284E8	0.911	50.1
IPI00027626.3	T-complex protein 1 subunit zeta	49.53	179	5.823E8	0.910	58.0
IPI00010080.2	Serine/threonine-protein kinase OSR1	18.79	12	5.943E7	0.906	58.0
IPI00218830.1	Isoform Short of Glycylpeptide N-tetradecanoyltransferase 1	25.24	24	5.265E7	0.905	48.1
IPI00007074.5	Tyrosyl-tRNA synthetase, cytoplasmic	45.27	39	1.190E8	0.900	59.1
IPI00412880.2	Isoform 1 of Histone-arginine methyltransferase CARM1	16.24	16	9.897E7	0.887	63.4
IPI00216952.1	Isoform C of Prelamin-A/C	41.78	49	2.077E8	0.881	65.1
IPI00925572.1	asparagine synthetase [glutamine-hydrolyzing] isoform b	27.59	31	1.377E8	0.880	62.1
IPI01014074.1	cDNA FLJ53296, highly similar to Serine/threonine-protein phosphatase 2A 65 kDa regulato	44.91	94	4.056E8	0.876	64.1
IPI00647896.1	Uncharacterized protein	18.28	6	3.825E7	0.859	41.7
IPI00514053.1	Coatomer subunit delta	18.20	26	1.261E8	0.852	57.2
IPI00788826.1	Isoform 4 of Poly(U)-binding-splicing factor PUF60	17.03	12	9.478E7	0.829	54.0
IPI00553185.2	T-complex protein 1 subunit gamma	52.11	64	3.811E8	0.823	60.5

IPI00257882.7	Xaa-Pro dipeptidase	16.23	13	5.892E7	0.815	54.5
IPI00099311.3	Isoform 1 of tRNA (adenine-N(1)-)-methyltransferase non-catalytic subunit TRM6	30.18	30	8.841E7	0.811	55.8
IPI00830039.1	Isoform 2 of Splicing factor U2AF 65 kDa subunit	33.97	40	1.997E8	0.811	53.1
IPI01015295.1	Uncharacterized protein	19.39	15	7.224E7	0.807	59.7
IPI00798375.2	cDNA FLJ59357, highly similar to Probable ATP-dependent RNA helicase DDX5	16.18	13	9.793E7	0.800	61.5
IPI00783097.4	Glycyl-tRNA synthetase	4.60	4	3.995E7	0.792	83.1
IPI00642416.1	60 kDa SS-A/Ro ribonucleoprotein isoform 4	4.63	2	2.167E7	0.791	58.4
IPI00008223.3	UV excision repair protein RAD23 homolog B	13.20	5	3.305E7	0.784	43.1
IPI01009339.1	27 kDa protein	20.56	9	5.512E7	0.782	27.3
IPI00400849.2	Isoform 3 of Phosphatidylinositol-binding clathrin assembly protein	10.16	7	3.284E7	0.768	66.4
IPI00465248.5	Isoform alpha-enolase of Alpha-enolase	9.68	4	2.847E6	0.764	47.1
IPI00514530.5	Uncharacterized protein	15.92	10	1.702E8	0.763	32.3
IPI00917117.1	FAM129B protein (Fragment)	7.34	7	1.939E8	0.762	35.2
IPI00003865.1	Isoform 1 of Heat shock cognate 71 kDa protein	19.97	16	7.497E7	0.751	70.9
IPI00219526.6	Isoform 1 of Phosphoglucomutase-1	22.60	21	5.262E7	0.749	61.4
IPI00917016.2	copine-1 isoform c	15.30	23	9.648E7	0.746	58.9
IPI00013894.1	Stress-induced-phosphoprotein 1	12.89	18	1.218E8	0.742	62.6
IPI00017184.2	EH domain-containing protein 1	76.59	205	8.618E8	0.729	60.6
IPI00410017.1	Isoform 2 of Polyadenylate-binding protein 1	20.11	12	5.163E7	0.711	61.1
IPI00975868.1	Annexin family protein	6.02	2	7.686E6	0.700	58.4
IPI00911039.1	cDNA FLJ54408, highly similar to Heat shock 70 kDa protein 1	11.43	6	4.386E7	0.692	63.9
IPI00943173.1	Coronin-1C	24.68	23	1.089E8	0.691	53.2
IPI00746165.2	Isoform 1 of WD repeat-containing protein 1	19.97	11	7.173E7	0.685	66.2
IPI00965308.1	Uncharacterized protein	7.08	3	1.954E7	0.679	47.3
IPI00010154.3	Rab GDP dissociation inhibitor alpha	40.27	27	5.803E7	0.675	50.6
IPI00396485.3	Elongation factor 1-alpha 1	11.04	13	7.105E7	0.663	50.1
IPI00792478.1	tubulin alpha-8 chain isoform 2	28.46	23	1.360E8	0.638	42.9
IPI00925601.1	Uncharacterized protein	32.66	37	1.561E8	0.636	64.5
IPI01015917.1	T-complex protein 1 subunit delta	5.91	2	3.589E7	0.619	42.3
IPI00414676.6	Heat shock protein HSP 90-beta	13.54	23	1.195E8	0.612	83.2
IPI00893179.1	X-ray repair complementing defective repair in Chinese hamster cells 6	6.46	2	1.030E7	0.600	64.0
IPI01012685.1	Uncharacterized protein	12.57	8	2.309E7	0.590	59.6
IPI01015738.1	Uncharacterized protein	4.77	4	1.565E7	0.581	79.9
IPI00985384.1	ATP-dependent RNA helicase DDX3X isoform 3	3.56	2	1.474E7	0.561	71.3
IPI00642944.1	Uncharacterized protein	11.38	8	4.935E7	0.554	67.9
IPI00441992.1	cDNA FLJ16815 fis, clone THYMU3044175, highly similar to Adenosylhomocysteinase	6.62	2	1.257E7	0.520	35.3
IPI00903145.1	Radixin	8.23	5	5.570E7	0.516	68.5
IPI00984387.1	cDNA FLJ53166, highly similar to Dihydropyrimidinase-related protein 2	16.04	8	2.683E7	0.509	58.1
IPI00217966.9	Isoform 1 of L-lactate dehydrogenase A chain	12.65	3	1.004E7	0.505	36.7

IPI01013382.1	cDNA FLJ53335, highly similar to Cytosolic purine 5'-nucleotidase	11.28	8	1.467E7	0.496	61.4
IPI00465225.1	heterogeneous nuclear ribonucleoprotein L isoform b	5.04	2	2.263E7	0.473	50.5
IPI00419979.3	Serine/threonine-protein kinase PAK 2	15.81	6	4.744E7	0.472	58.0
IPI00184821.1	Isoform 1 of Bifunctional coenzyme A synthase	7.62	5	8.948E6	0.472	62.3
IPI00983581.1	SYNCRIP protein (Fragment)	14.57	5	4.427E7	0.465	50.6
IPI00940673.2	cDNA FLJ36348 fis, clone THYMU2007025, highly similar to TRANSKETOLASE	12.22	5	3.961E7	0.459	58.9
IPI00604652.1	NEDD8-activating enzyme E1 regulatory subunit isoform c	6.97	2	1.238E7	0.457	50.6
IPI00789134.5	Glyceraldehyde-3-phosphate dehydrogenase	11.15	2	2.207E7	0.450	27.9
IPI00784295.2	Isoform 1 of Heat shock protein HSP 90-alpha	8.61	14	1.100E8	0.404	84.6
IPI00967118.1	Uncharacterized protein	15.24	2	7.587E6	0.392	23.4
IPI00910422.2	cDNA FLJ52802, highly similar to Eukaryotic translation initiation factor 3subunit 6-interact	24.61	9	3.875E7	0.374	61.0
IPI00789582.2	cDNA FLJ51552, highly similar to Eukaryotic translation initiation factor 3 subunit 7	8.42	3	1.312E7	0.367	58.1
IPI00306960.3	Asparaginyl-tRNA synthetase, cytoplasmic	8.94	4	1.906E7	0.339	62.9
IPI00852780.1	Protein	13.54	2	6.281E6	0.322	25.8
IPI00910719.1	cDNA FLJ55705, highly similar to Threonyl-tRNA synthetase, cytoplasmic	3.49	2	4.421E6	0.318	70.3

Curriculum Vitae

Jürgen Eirich

Klopstockstr. 8

80804 München

geboren am 1984-10-13 in Lohr am Main

Bildung

2010 – heute	Technische Universität München (TUM)
	Lehrstuhl für Organische Chemie II
2009-04 – 2010-10	Ludwig-Maximilians-Universität (LMU), München
	Master of Science "Biochemistry"
2005-10 – 2009-04	Ludwig-Maximilians-Universität
	Bachelor of Science "Chemistry and Biochemistry"
1995-09 – 2004-05	Johann-Schöner-Gymnasium, Karlstadt am Main
	Abitur
1991-09 – 1995-07	Grundschule Karlstadt-Wiesenfeld